



Autopilot Project

Authors:

Abdelateef Khaled 20201344,
Alia Elhalawani 202000292,
Aya Atya 202000247,
Seif Raslan 202000797

Under the supervision of: Dr. Mohanned Draz

Contents

| | |
|---|-----------|
| 1 Research Questions | 10 |
| 1.1 Autopilot definition | 10 |
| 1.2 The first successful autopilot invented | 10 |
| 1.3 Inputs and outputs of autopilot system | 10 |
| 1.4 Pilots job in the presence of autopilot systems | 11 |
| 1.5 difference between an Autopilot SAS (stability augmentation system) | 11 |
| 1.6 The role of the onboard sensors | 12 |
| 1.7 How to measure a state that is not directly measured by a sensor | 12 |
| 1.8 Fly-by-wire control system | 13 |
| 1.9 open-source autopilots for UAVs | 13 |
| 2 Flight Mechanics Review | 14 |
| 2.1 General rigid body dynamics (RBD) equations in 3D space | 14 |
| 2.2 Classification of Equations into Kinematics and Kinetics | 15 |
| 2.3 Assumptions | 16 |
| 2.4 The set of equations added to the (RBD) equations to form the Fixed Wing Airplanes (EOM) | 16 |
| 2.5 Aircraft's EOM Mathematical Classification. | 18 |
| 2.6 The difference between the (Body axes) and the (earth or inertial axes) | 19 |
| 2.7 Difference between the pitch angle (θ) and the angle of attack (α), and between the sideslip angle (β) and the heading angle (ψ) | 19 |
| 2.8 Different attitude representations | 20 |
| 3 Numerical Solution of ODEs | 21 |
| 3.1 Numerical Solving Algorithms for ODEs | 21 |
| 3.2 Algorithm for Solving the Airplane's EOM | 21 |
| 3.3 The solution of first order system of ODEs | 22 |
| 3.3.1 Solution Algorithm | 22 |
| 3.3.2 Solution Results and Validation | 23 |
| 4 Airplane Simulator Part I | 23 |
| 4.1 Initial Conditions Configuration | 23 |
| 4.2 Airplane Equations of Motion | 24 |
| 4.3 Evaluation of Rigid Body Dynamics Solutions: A Simulink and MATLAB Comparison | 25 |
| 5 Airplane Simulator Part II | 27 |
| 5.1 Forces and Moments Calculation | 27 |
| 5.1.1 Stability and Control Derivatives | 27 |
| 5.1.2 Perturbation from Trim Condition | 28 |
| 5.1.3 Moment Calculations | 28 |
| 5.1.4 Absolute Force and Moment Calculation | 28 |
| 5.1.5 Gravitational Forces | 29 |
| 5.2 Integration with RBD Solver | 29 |
| 5.2.1 Total Forces Acting on the Airplane | 29 |
| 5.2.2 Equations of Motion for Translation | 30 |
| 5.2.3 Equations of Motion for Rotation | 30 |
| 5.2.4 Integration Using Runge-Kutta 4th Order (RK4) Method | 30 |
| 5.2.5 Converting Between Body-Fixed and Inertial Frames | 30 |
| 5.3 Validation | 30 |
| 5.3.1 Validation Using Benchmark Test Data | 31 |
| 5.3.2 Validation with Matlab Code | 31 |
| 5.3.3 Validation with Simulink | 40 |
| 5.4 B747-FC3 flight Condition | 49 |

| | |
|---|------------|
| 6 Linearization and approximation | 58 |
| 6.1 Steps | 58 |
| 6.2 Lateral linearization | 58 |
| 6.2.1 | |
| $Y = mg \cos(\theta) \sin(\phi) = m(\dot{\nu} + ru - pw)$ | 58 |
| 6.2.2 | |
| $r = \dot{\psi} \cos(\theta) \cos(\phi) - \dot{\theta} \sin(\phi)$ | 59 |
| 6.3 Longitudinal linearization | 61 |
| 6.3.1 | |
| $X - mg \sin(\theta_0) = m(\dot{u}_0 + q_0 w_0 - r_0 \nu_0)$ | 61 |
| 6.3.2 | |
| $Z + mg \cos(\theta) \cos(\phi) = m(\dot{w} + p\nu - qu)$ | 61 |
| 6.3.3 | |
| $M = I_y \dot{q} + rq(I_x - I_z) + I_{xz}(p^2 - r^2)$ | 62 |
| 6.3.4 | |
| $q = \dot{\theta} \cos \phi + \dot{\psi} \cos \theta \sin \phi$ | 63 |
| 6.4 Longitudinal approximations | 63 |
| 6.4.1 Short-period appoximation | 63 |
| 6.4.2 Long-period approximation | 64 |
| 6.5 Lateral-approximations | 65 |
| 6.5.1 3-DOF spiral approximation | 65 |
| 6.5.2 3-DOF Dutch-roll approximations | 65 |
| 6.5.3 2-DOF Dutch-roll approximations | 65 |
| 6.5.4 1-DOF Dutch-roll | 65 |
| 6.6 applying on B747-FC3 Flight Condition | 66 |
| 6.6.1 Longitudinal Step Response | 68 |
| 6.6.2 Transfer Functions and Root Locus & Bode Plot for Each Input and Output State For Longitudinal Mode | 73 |
| 6.6.3 Lateral Step Response | 81 |
| 6.6.4 Transfer Functions and Root Locus & Bode Plot for Each Input and Output State For Lateral Mode | 89 |
| 6.7 Longitudinal autopilot | 99 |
| 6.7.1 Pitch control | 99 |
| 6.7.2 Altitude Controller | 105 |
| 6.8 Velocity Control | 108 |
| 6.9 Lateral Autopilot | 112 |
| 6.9.1 Yaw Damper Control | 112 |
| 6.9.2 Roll control | 116 |
| 6.9.3 Heading controller design | 118 |
| 7 Nonlinear Simulation and Mission | 122 |
| 7.1 Developing the Test Loop | 122 |
| 7.2 Simulation of Linear and Non-Linear Models | 123 |
| 7.2.1 Pitch Controller Test | 123 |
| 7.2.2 Pitch Controller and Velocity Controller Test | 125 |
| 7.2.3 Altitude Hold Controller Test | 128 |
| 7.2.4 Lateral Controller Test | 131 |
| 7.2.5 Lateral Controller and Altitude Hold Controller Test | 134 |

| | | |
|-----------|--|------------|
| 7.2.6 | Complete Autonomous Mission | 138 |
| 7.3 | Flight Gear Simulation | 140 |
| 8 | References | 141 |
| 9 | Appendix | 142 |
| 9.1 | Appendix A Matlab Codes | 142 |
| 9.1.1 | MATLAB Code for Solving the System of ODEs Using the RK4 Method | 142 |
| 9.1.2 | MATLAB Code for Solving Airplane EOM | 142 |
| 9.1.3 | MATLAB Code for calculating forces and moments | 144 |
| 9.1.4 | MATLAB Code for transforming lateral derivatives | 144 |
| 9.1.5 | MATLAB Code for RK4 modified | 145 |
| 9.1.6 | MATLAB Code for calculating the states of airplane | 145 |
| 9.1.7 | MATLAB Code Longitudinal Lateral stability analysis | 148 |
| 9.1.8 | MATLAB Code for Autopilot Longitudinal Control | 163 |
| 9.1.9 | MATLAB Code for Autopilot Lateral Control | 165 |
| 9.1.10 | MATLAB Code for Simulation to Complete Linear and Non-Linear model | 168 |
| 9.2 | Appendix B Simulink Models | 192 |
| 9.2.1 | 6DOF Euler Angles Simulink Model | 192 |
| 9.2.2 | Calculation of states Simulink Model | 192 |
| 9.2.3 | Autopilot Pitch and altitude control | 194 |
| 9.2.4 | Simulation Model for Linear and Non-Linear | 196 |
| 10 | Bonus | 200 |
| 10.1 | Task2 Bonus | 200 |
| 10.2 | Task4 Bouns | 202 |
| 10.2.1 | Model Linearizer for Longitudinal Mode | 202 |
| 10.2.2 | Model Linearizer for Lateral Mode | 203 |
| 10.2.3 | Comparisons with Manual Linearization | 205 |

List of Figures

| | | |
|----|---|----|
| 1 | First successful autopilot mission | 10 |
| 2 | Fly-By-Wire system | 13 |
| 3 | Numerical Solution of the ODE System Using RK4 and Validation with ode45 | 23 |
| 4 | Comparison of aircraft velocity components (u, v, w) between MATLAB and Simulink results | 25 |
| 5 | Comparison of aircraft orientation angles (ϕ, θ, ψ) between MATLAB and Simulink results. | 26 |
| 6 | Comparison of aircraft angular velocity components (p, q, r) between MATLAB and Simulink results | 26 |
| 7 | Comparison of aircraft position components (x, y, z) between MATLAB and Simulink results. | 27 |
| 8 | Matlab Simulator's plot | 31 |
| 9 | Matlab Simulator's Plots | 31 |
| 10 | Reference (Benchmark) Trajectory Plot | 31 |
| 11 | Reference Plots | 31 |
| 12 | Simulator's Trajectory plot | 32 |
| 13 | Simulator's Plots | 32 |
| 14 | Reference (Benchmark) Trajectory Plot | 32 |
| 15 | Reference Plots | 32 |
| 16 | Simulator's Trajectory plot | 33 |
| 17 | Simulator's Plots | 33 |
| 18 | Reference (Benchmark) Trajectory Plot | 33 |
| 19 | Reference Plots | 33 |
| 20 | Simulator's Trajectory plot | 34 |
| 21 | Simulator's Plots | 34 |
| 22 | Reference (Benchmark) Trajectory Plot | 34 |
| 23 | Reference Plots | 34 |
| 24 | Simulator's Trajectory plot | 35 |
| 25 | Simulator's Plots | 35 |
| 26 | Reference (Benchmark) Trajectory Plot | 35 |
| 27 | Reference Plots | 35 |
| 28 | Simulator's Trajectory plot | 36 |
| 29 | Simulator's Plots | 36 |
| 30 | Reference (Benchmark) Trajectory Plot | 36 |
| 31 | Reference Plots | 36 |
| 32 | Simulator's Trajectory plot | 37 |
| 33 | Simulator's Plots | 37 |
| 34 | Reference (Benchmark) Trajectory Plot | 37 |
| 35 | Reference Plots | 37 |
| 36 | Simulator's Trajectory plot | 38 |
| 37 | Simulator's Plots | 38 |
| 38 | Reference (Benchmark) Trajectory Plot | 38 |
| 39 | Reference Plots | 38 |
| 40 | Simulator's Trajectory plot | 39 |
| 41 | Simulator's Plots | 39 |
| 42 | Reference (Benchmark) Trajectory Plot | 39 |
| 43 | Reference Plots | 39 |
| 44 | Simulink Simulator's plot | 40 |
| 45 | Simulink Simulator's Plots | 40 |
| 46 | Reference (Benchmark) Trajectory Plot | 40 |
| 47 | Reference Plots | 40 |
| 48 | Simulink Simulator's Trajectory plot | 41 |
| 49 | Simulink Simulator's Plots | 41 |
| 50 | Reference (Benchmark) Trajectory Plot | 41 |
| 51 | Reference Plots | 41 |
| 52 | Simulink Simulator's Trajectory plot | 42 |
| 53 | simulink Simulator's Plots | 42 |
| 54 | Reference (Benchmark) Trajectory Plot | 42 |
| 55 | Reference Plots | 42 |

| | | |
|-----|---|----|
| 56 | Simulink Simulator's Trajectory plot | 43 |
| 57 | Simulink Simulator's Plots | 43 |
| 58 | Reference (Benchmark) Trajectory Plot | 43 |
| 59 | Reference Plots | 43 |
| 60 | Simulink Simulator's Trajectory plot | 44 |
| 61 | Simulink Simulator's Plots | 44 |
| 62 | Reference (Benchmark) Trajectory Plot | 44 |
| 63 | Reference Plots | 44 |
| 64 | Simulink Simulator's Trajectory plot | 45 |
| 65 | Simulink Simulator's Plots | 45 |
| 66 | Reference (Benchmark) Trajectory Plot | 45 |
| 67 | Reference Plots | 45 |
| 68 | Simulink Simulator's Trajectory plot | 46 |
| 69 | Simulink Simulator's Plots | 46 |
| 70 | Reference (Benchmark) Trajectory Plot | 46 |
| 71 | Reference Plots | 46 |
| 72 | Simulator's Trajectory plot | 47 |
| 73 | Simulator's Plots | 47 |
| 74 | Reference (Benchmark) Trajectory Plot | 47 |
| 75 | Reference Plots | 47 |
| 76 | Simulator's Trajectory plot | 48 |
| 77 | Simulator's Plots | 48 |
| 78 | Reference (Benchmark) Trajectory Plot | 48 |
| 79 | Reference Plots | 48 |
| 80 | Simulink Trajectory Plot | 49 |
| 81 | Simulink States Plots | 49 |
| 82 | Matlab Trajectory Plot | 49 |
| 83 | Matlab States Plots | 49 |
| 84 | Simulink Trajectory Plot | 50 |
| 85 | Simulink States Plots | 50 |
| 86 | Matlab Trajectory Plot | 50 |
| 87 | Matlab States Plots | 50 |
| 88 | Simulink Trajectory Plot | 51 |
| 89 | Simulink States Plots | 51 |
| 90 | Matlab Trajectory Plot | 51 |
| 91 | Matlab States Plots | 51 |
| 92 | Simulink Trajectory Plot | 52 |
| 93 | Simulink States Plots | 52 |
| 94 | Matlab Trajectory Plot | 52 |
| 95 | Matlab States Plots | 52 |
| 96 | Simulink Trajectory Plot | 53 |
| 97 | Simulink States Plots | 53 |
| 98 | Matlab Trajectory Plot | 53 |
| 99 | Matlab States Plots | 53 |
| 100 | Simulink Trajectory Plot | 54 |
| 101 | Simulink States Plots | 54 |
| 102 | Matlab Trajectory Plot | 54 |
| 103 | Matlab States Plots | 54 |
| 104 | Simulink Trajectory Plot | 55 |
| 105 | Simulink States Plots | 55 |
| 106 | Matlab Trajectory Plot | 55 |
| 107 | Matlab States Plots | 55 |
| 108 | Simulink Trajectory Plot | 56 |
| 109 | Simulink States Plots | 56 |
| 110 | Matlab Trajectory Plot | 56 |
| 111 | Matlab States Plots | 56 |

| | | |
|-----|--|-----|
| 112 | Simulink Trajectory Plot | 57 |
| 113 | Simulink States Plots | 57 |
| 114 | Matlab Trajectory Plot | 57 |
| 115 | Matlab States Plots | 57 |
| 116 | Step response with $\delta_e = 1^\circ$ | 68 |
| 117 | Step response with $\delta_e = 5^\circ$ | 69 |
| 118 | Step response with $\delta_e = 10^\circ$ | 69 |
| 119 | Step response with $\delta_e = 25^\circ$ | 70 |
| 120 | Step response with thrust $T = 2000$ | 71 |
| 121 | Step response with thrust $T = 6000$ | 71 |
| 122 | Step response with thrust $T = 10000$ | 72 |
| 123 | Root Locus and Bode plot for Δ elevator (De) to linear velocity (u) | 73 |
| 124 | Root Locus and Bode plot for Δ elevator (De) to vertical velocity (w) | 74 |
| 125 | Root Locus and Bode plot for Δ elevator (De) to pitch rate (q) | 75 |
| 126 | Root Locus and Bode plot for Δ elevator (De) to pitch angle (θ) | 76 |
| 127 | Root Locus and Bode plot for Thrust (Th) to linear velocity (u) | 77 |
| 128 | Root Locus and Bode plot for Thrust (Th) to vertical velocity (w) | 78 |
| 129 | Root Locus and Bode plot for Thrust (Th) to pitch rate (q) | 79 |
| 130 | Root Locus and Bode plot for Thrust (Th) to pitch angle (θ) | 80 |
| 131 | Step responses for $\delta_a = 1^\circ$ | 81 |
| 132 | Step responses for $\delta_a = 5^\circ$ | 82 |
| 133 | Step responses for $\delta_a = 10^\circ$ | 83 |
| 134 | Step responses for $\delta_a = 25^\circ$ | 84 |
| 135 | Step responses for $\delta_r = 1^\circ$ | 85 |
| 136 | Step responses for $\delta_r = 5^\circ$ | 86 |
| 137 | Step responses for $\delta_r = 10^\circ$ | 87 |
| 138 | Step responses for $\delta_r = 25^\circ$ | 88 |
| 139 | Root Locus and Bode plot for Δ aileron (Da) to side velocity (v) | 89 |
| 140 | Root Locus and Bode plot for Δ aileron (Da) to roll rate (p) | 90 |
| 141 | Root Locus and Bode plot for Δ aileron (Da) to yaw rate (r) | 91 |
| 142 | Root Locus and Bode plot for Δ aileron (Da) to roll angle (phi) | 92 |
| 143 | Root Locus and Bode plot for Δ aileron (Da) to yaw angle (epsi) | 93 |
| 144 | Root Locus and Bode plot for Δ rudder (Dr) to side velocity (v) | 94 |
| 145 | Root Locus and Bode plot for Δ rudder (Dr) to roll rate (p) | 95 |
| 146 | Root Locus and Bode plot for Δ rudder (Dr) to yaw rate (r) | 96 |
| 147 | Root Locus and Bode plot for Δ aileron (Dr) to roll angle (phi) | 97 |
| 148 | Root Locus and Bode plot for Δ aileron (Dr) to yaw angle (epsi) | 98 |
| 149 | Control loop block diagram | 99 |
| 150 | Open loop short period | 100 |
| 151 | Open loop Long period | 100 |
| 152 | Open Loop Step Response | 101 |
| 153 | Closed loop root locus with control | 102 |
| 154 | Closed loop step response | 102 |
| 155 | Step Response when $\theta = 15^\circ$ | 103 |
| 156 | Altitude vs. time when $\theta = 15^\circ$ | 104 |
| 157 | Velocity vs. time when $\theta = 15^\circ$ | 104 |
| 158 | Control loop block diagram for the altitude controller. | 105 |
| 159 | Open-loop step response and root locus analysis. | 106 |
| 160 | Closed-loop step response and root locus analysis. | 107 |
| 161 | Simulink model output showing the altitude response to a step input of 200 feet. | 108 |
| 162 | Simulink model output showing the pitch angle response (θ) to a step input of 200 feet. | 108 |
| 163 | Root locus and step response plots for the untuned velocity control system. | 109 |
| 164 | Root locus and step response plots for the untuned velocity control system. | 110 |
| 165 | Velocity response: The red curve represents the desired velocity ($u = 5$), and the brown curve shows the system's performance in tracking the desired velocity. | 111 |

| | | |
|-----|--|-----|
| 166 | Altitude response: The altitude gained by the aircraft over time, showing steady and consistent climb performance. | 111 |
| 167 | Throttle response: The throttle input used by the controller to achieve the desired velocity ($u = 5$) | 112 |
| 168 | Yaw Damper controller | 112 |
| 169 | Root locus of closed-loop transfer function | 113 |
| 170 | Yaw Damper Closed-Loop Impulse Response | 114 |
| 171 | Control Surfaces Behavior | 115 |
| 172 | Control Surfaces Responses | 115 |
| 173 | Angles and Rates Response | 116 |
| 174 | Roll Damper controller | 116 |
| 175 | Root locus of open loop TF | 117 |
| 176 | Impulse response of open loop TF $\phi/(\delta_a)$. | 117 |
| 177 | free body diagram of the airplane during turn. | 118 |
| 178 | Control Surfaces Behavior from Lateral Autopilot | 119 |
| 179 | Lateral Autopilot's states responses. | 120 |
| 180 | Flowchart of flight Controller closed loop | 122 |
| 181 | θ Response for Pitch Controller for linear and nonlinear models | 123 |
| 182 | U Response for Pitch Controller for linear and nonlinear models | 123 |
| 183 | γ Response for Pitch Controller for linear and nonlinear models | 124 |
| 184 | H Response for Pitch Controller for linear and nonlinear models | 124 |
| 185 | δ_e Response for Pitch Controller for linear and nonlinear models | 125 |
| 186 | θ Response for Pitch and Velocity Controller for linear and nonlinear models | 125 |
| 187 | u Response for Pitch and Velocity Controller for linear and nonlinear models | 126 |
| 188 | γ Response for Pitch and Velocity Controller for linear and nonlinear models | 126 |
| 189 | H Response for Pitch and Velocity Controller for linear and nonlinear models | 127 |
| 190 | (δ_e) Response for Pitch and Velocity Controller for linear and nonlinear models | 127 |
| 191 | (δ_{th}) Response for Pitch and Velocity Controller for linear and nonlinear models | 128 |
| 192 | θ Response for Altitude Hold Controller for linear and nonlinear models | 128 |
| 193 | u Response for Altitude Hold Controller for linear and nonlinear models | 129 |
| 194 | γ Response for Altitude Hold Controller for linear and nonlinear models | 129 |
| 195 | H Response for Altitude Hold Controller for linear and nonlinear models | 130 |
| 196 | (δ_e) Response for Altitude Hold Controller for linear and nonlinear models | 130 |
| 197 | (δ_{th}) Response for Altitude Hold Controller for linear and nonlinear models | 131 |
| 198 | β Response for Lateral Controller for linear and nonlinear models | 131 |
| 199 | ϕ Response for Lateral Controller for linear and nonlinear models | 132 |
| 200 | ψ Response for Lateral Controller for linear and nonlinear models | 132 |
| 201 | H Response for Lateral Controller for linear and nonlinear models | 133 |
| 202 | (δ_r) Response for Lateral Controller for linear and nonlinear models | 133 |
| 203 | (δ_a) Response for Lateral Controller for linear and nonlinear models | 134 |
| 204 | β Response for Lateral and Altitude Hold Controller for linear and nonlinear models | 134 |
| 205 | ϕ Response for Lateral and Altitude Hold Controller for linear and nonlinear models | 135 |
| 206 | ψ Response for Lateral and Altitude Hold Controller for linear and nonlinear models | 135 |
| 207 | H Response for Lateral and Altitude Hold Controller for linear and nonlinear models | 136 |
| 208 | (δ_r) Response for Lateral and Altitude Hold Controller for linear and nonlinear models | 136 |
| 209 | (δ_a) Response for Lateral and Altitude Hold Controller for linear and nonlinear models | 137 |
| 210 | (δ_e) Response for Lateral and Altitude Hold Controller for linear and nonlinear models | 137 |
| 211 | (δ_{th}) Response for Lateral and Altitude Hold Controller for linear and nonlinear models | 138 |
| 212 | Altitude (H) Response for Mission | 139 |
| 213 | Heading Angle (ψ) Response for Mission | 140 |
| 214 | Simulink Model with 6DOF Euler Angles Block for Solving Airplane EOM | 192 |
| 215 | Main Simulink Model with for calculating the states of airplane | 192 |
| 216 | Control inputs sub-block | 193 |
| 217 | Aircraft Model sub-block | 193 |
| 218 | Rigid Body Dynamics Model sub-block | 194 |
| 219 | Autopilot pitch control loop | 194 |
| 220 | Velocity Controller | 194 |

| | | |
|-----|--|-----|
| 221 | Pitch controller | 195 |
| 222 | Longitudinal state space | 195 |
| 223 | Altitude calculations and display | 195 |
| 224 | Theta θ and velocity (u) displays | 195 |
| 225 | The complete model | 196 |
| 226 | Flight Controller for states | 196 |
| 227 | Longitudinal Controller for states | 196 |
| 228 | Lateral Controller for states | 197 |
| 229 | Plane Non-Linear Model | 197 |
| 230 | Aircraft Model | 197 |
| 231 | Non-Linear Rigid Body Dynamics | 198 |
| 232 | Flight Controller for delta states | 198 |
| 233 | Longitudinal Controller for delta states | 198 |
| 234 | Lateral Controller for delta states | 199 |
| 235 | Airplane Linear Model | 199 |
| 236 | Delta States to States Calculations | 199 |
| 237 | Gamma and H Calculations | 200 |
| 238 | Send Data to Flight Gear | 200 |
| 239 | Logging and Visualization | 200 |
| 240 | State-space representation of the longitudinal mode using the Model Linearizer | 202 |
| 241 | Transfer function of the longitudinal mode using the Model Linearizer | 203 |
| 242 | State-space representation of the lateral mode using the Model Linearizer | 204 |
| 243 | Transfer function of the lateral mode using the Model Linearizer | 205 |

List of Tables

| | | |
|---|--|-----|
| 1 | Comparison of Autopilot and Stability Augmentation System (SAS) | 11 |
| 2 | Overview of sensors, functions, and sample rates used in aircraft. | 12 |
| 3 | Body Axes, Velocities, Forces, Angular Velocities, and Moments | 14 |
| 4 | Mission segments points. | 139 |

1 Research Questions

1.1 Autopilot definition

Autopilot is a system used to guide and control the airplane through its mission without the need for the direct control of a human. Its main objective is to lessen the workload on the crew during cruising, long flights, or adverse weather conditions; and to maintain control of altitude, heading, speed, and other parameters.

1.2 The first successful autopilot invented

After the development of the first human-carrying airplane by the Wright Brothers, the autopilot systems were developed with the first successful system built in 1912 by the Sperry brothers. The system was able to maintain heading, roll, and pitch angles. In order to test their design, one of the brothers, Lawrence Sperry, trimmed the airplane at a steady level flight and then activated the autopilot. He started creating some sort of disturbance by standing in the cockpit with his hands above his head, and his mechanic started walking along the wings to see if the autopilot would be able to go back to equilibrium. The autopilot was able to maintain the equilibrium by giving commands to change the aileron, rudder, and elevator deflections. Attached is a photo of the airplane tested with Lawrence Sperry and his mechanic inside of it.[1]

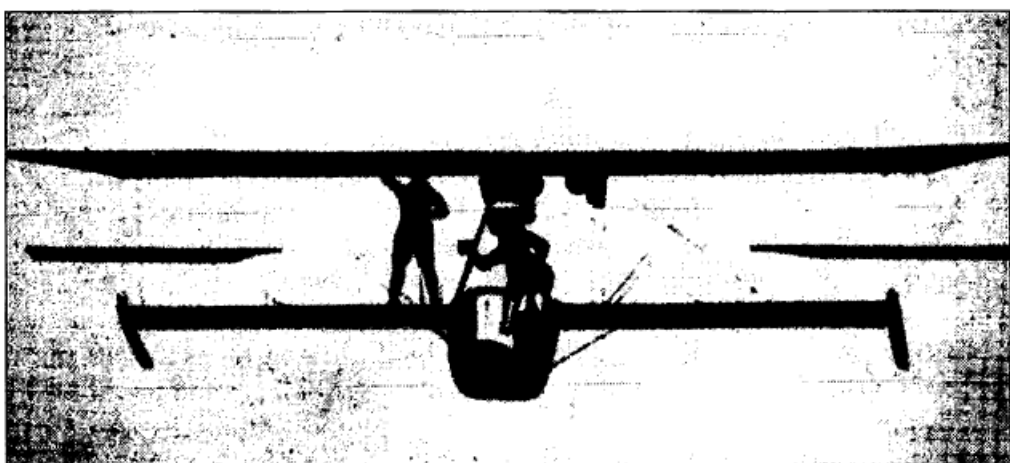


Figure 1: First successful autopilot mission

1.3 Inputs and outputs of autopilot system

Inputs:

- Control inputs: control surfaces (ailerons, rudder, elevator) positions to get feedback about how the deflection is changing.
- Navigation and performance data: coming from sensors such as GPS, Gyroscopes, and IMUs to detect the aircraft and wind speed, altitude, and heading.

Outputs:

- Control surface commands to maintain the desired orientation and direction.
- Flight path adjustments

1.4 Pilots job in the presence of autopilot systems

Pilots continuously monitor aircraft's systems such as engine performance, navigation, and altitude, to ensure that everything is operating properly. After all, the autopilot system is a world of human beings and it can be subjected to failure so in case that happens, the pilot must be there to ensure a safe flight. In addition, the pilots must be aware of the surroundings and keep track of any sudden changes in the environment or in the flight path. [2] Moreover, in normal cases, takeoff and landing is usually done by the pilot if the visibility is okay.

1.5 difference between an Autopilot SAS (stability augmentation system)

| System | Autopilot | SAS |
|-------------|---|---|
| Objective | Automatic control of the flight by adjusting and maintaining flight parameters such as heading, altitude, navigation, and speed | Designed to mainly improve stability by damping the unwanted disturbances or oscillations caused during the flight and smoothing the flight route. However, it doesn't provide control for the aircraft by itself. It makes it easier to control the aircraft but doesn't replace the pilot control[?] |
| System | Control inputs usually connect to the aircraft control surfaces. It uses complex feedback loops with sensor inputs such as GPS and IMU. Typically has several subsystems and multiple modes of operation to account for every flight condition. | Limited to specific inputs. For example, a common type of SAS is the yaw damper which is used to reduce the Dutch roll. Sometimes the SAS systems, such as the yaw damper, can be part of the Autopilot system and sometimes they are standalone systems[?]. The system is usually much simpler than autopilot, with faster and more frequent feedback loops. |
| Application | Commonly used in civil and military aircraft. | Commonly used in helicopters, UAVs, and some modern jets. |

Table 1: Comparison of Autopilot and Stability Augmentation System (SAS)

1.6 The role of the onboard sensors

| Sensor | Function | Sample Rate |
|---------------------|--|--|
| GPS | Determines the plane's position in space using satellites in its network to calculate its distance from it. | 1570 1100 MHz |
| Gyroscopes | Provides stability and heading, and helps maintain the attitude. Their working principle depends on rotational inertia, so they resist changes to their orientation when spinning. This resistance can be used to measure changes in orientation. | 400 750 Hz |
| Accelerometers | Detects changes in velocity by measuring the force exerted on an internal mass whilst the airplane is moving. | Low-frequency accelerometers: 0.1 500 Hz High-frequency accelerometers: 10 10 kHz |
| Altimeters | Measures the height of the aircraft above a certain reference point, usually sea level. It works by either measuring the ambient pressure or the time delay of a reflected wave. | 4.2–4.4 GHz |
| Compasses | Determines the aircraft heading relative to Earth's magnetic poles. | — |
| Airspeed Indicators | Measures the aircraft's speed relative to air. | 1 100 Hz |
| IMUs | Mainly consists of accelerometers and gyroscopes (sometimes magnetometers to provide additional information about the aircraft's heading). It is used to measure attitude (roll, pitch, yaw), velocity, altitude, and changes in gravitational forces. | 100 1000 Hz |

Table 2: Overview of sensors, functions, and sample rates used in aircraft.

1.7 How to measure a state that is not directly measured by a sensor

1. **By calculating it using other states:** for example, dynamic pressure is not directly sensed, but it is calculated using the data of airspeed measure from the pitot tube.
2. **Using some estimation technique:** such as the Kalman Filter which uses a series of observed noisy measurements over time, and produces estimates of unknown variables. For example, it can estimate the position and angular velocity of an aircraft by combining data from GPS, and inertial sensors such as accelerometers.[4]
3. **Observers:** An observer is a mathematical model that estimates the internal states of a system based on measured outputs and known inputs.

1.8 Fly-by-wire control system

As seen in Figure 2 It is a semi-automatic flight control system that is regulated using computers. The system basically uses computers to process control input whether made by the autopilot or the pilot himself, and then it sends electrical signals that correspond to these inputs to the control surface actuators in order to adjust them automatically. [6]

The traditional mechanical systems use levers and cables which the pilot moves to adjust the control surfaces. Although this might give the pilot a direct sense of how every control surface is adjusted, it is complicated and needs consistent monitoring.[7] Its main advantage is that it replaces the direct mechanical linkage making the linkage much lighter, and improves safety and maneuverability.

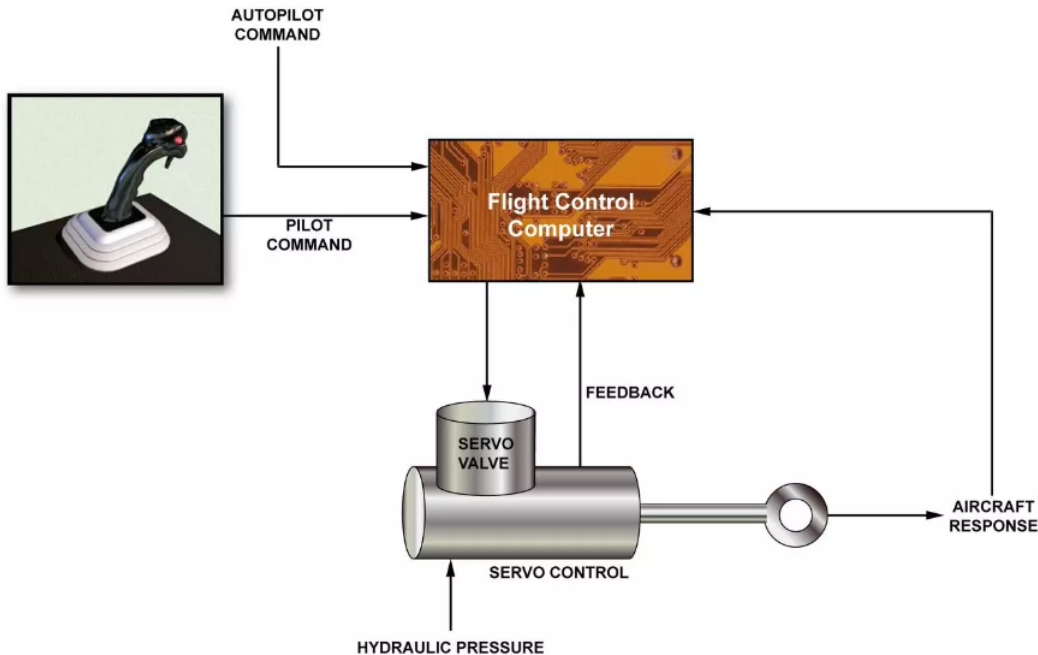


Figure 2: Fly-By-Wire system

1.9 open-source autopilots for UAVs

Pixhawk: used in a wide range of applications from drones and UAVs to industrial applications. [8]

ArduPilot: With the first autopilot open code created in 2009 it now supports many vehicle types: multi-copters, traditional helicopters, fixed-wing aircraft, VTOLs, and others. It is constantly developed and enhanced based on the feedback of users.[9]

Cube Orange+: Advanced open-source autopilot for UAVs. [10]

2 Flight Mechanics Review

2.1 General rigid body dynamics (RBD) equations in 3D space

In 3D space, the equations can be classified as translational or rotational motion.

| Body Axes | Linear Velocities | Forces | Angular Velocities | Moments |
|-----------|-------------------|----------|--------------------|-------------------------|
| x_b | u | $F_x(X)$ | p | \mathcal{L} (rolling) |
| y_b | v | $F_y(Y)$ | q | M (pitching) |
| z_b | w | $F_z(Z)$ | r | N (yawing) |

Table 3: Body Axes, Velocities, Forces, Angular Velocities, and Moments

Translational Motion: Governed by Newton's second law:

$$F = ma$$

$$F = ma = \frac{d}{dt}(m\vec{V}) = m\frac{d\vec{V}}{dt}, \text{ where } \frac{d\vec{V}}{dt} \text{ is } \dot{\vec{V}} + \vec{W} \times \vec{V}$$

Where:

- \vec{F} = sum of external forces acting on the aircraft.
- m = mass of the aircraft.
- a = acceleration of the aircraft.
- \vec{V} and \vec{W} are the velocity and angular velocity vectors, respectively.

Thus in matrix form:

$$\begin{pmatrix} F_x \\ F_y \\ F_z \end{pmatrix} = m \left[\begin{pmatrix} \dot{u} \\ \dot{v} \\ \dot{w} \end{pmatrix} + \begin{pmatrix} qw - rv \\ ru - pw \\ pv - qu \end{pmatrix} \right]$$

Rotational Motion: Described by Euler's equations for the rotational dynamics of a rigid body:

$$M = I \frac{d\vec{\omega}}{dt} + \vec{\omega} \times (I\vec{\omega})$$

Where:

- \vec{M} = sum of external moments acting on the aircraft.
- I = Aircraft's Moment of Inertia.
- $\vec{\omega}$ = Angular velocity vector of aircraft.

Thus in matrix form:

$$\begin{bmatrix} \mathcal{L} \\ M \\ N \end{bmatrix} = I \begin{bmatrix} \dot{p} \\ \dot{q} \\ \dot{r} \end{bmatrix} + \begin{bmatrix} p \\ q \\ r \end{bmatrix} \times I \begin{bmatrix} p \\ q \\ r \end{bmatrix}$$

Where:

$$I = \begin{bmatrix} I_{xx} & -I_{xy} & -I_{xz} \\ -I_{yx} & I_{yy} & -I_{yz} \\ -I_{zx} & -I_{zy} & I_{zz} \end{bmatrix}$$

Assumptions to be used:

- **Inertial Frame Assumption:** The equations are derived in an inertial frame (Earth or space-fixed), assuming no rotation or acceleration of the Earth, which simplifies the dynamics.
- **Symmetric Aircraft:** The aircraft is considered to be symmetric about the longitudinal plane, X-Z plane, which simplifies the inertia. (i.e., $I_{xy} = I_{xz} = I_{yz} = I_{zx} \approx 0$).
- **Constant Mass and Inertia:** Fuel consumption and variations in payload are not taken in account to calculate the mass and inertia properties of the aircraft.

thus we get the following:

$$\begin{pmatrix} \mathcal{L} \\ M \\ N \end{pmatrix} = \begin{pmatrix} I_x \dot{p} - I_{xz} \dot{r} \\ I_y \dot{q} \\ I_z \dot{r} - I_{xz} \dot{p} \end{pmatrix} + \begin{pmatrix} qr(I_z - I_y) - I_{xz} pq \\ pr(I_x - I_z) + I_{xz}(p^2 - r^2) \\ pq(I_y - I_x) + I_{xz} qr \end{pmatrix}$$

Euler rates and Euler angles could be presented by the following steps respectively:

- we could use **Rotation Matrices** To convert from inertial frame (I) to the body frame (B):

$$\begin{pmatrix} X \\ Y \\ Z \end{pmatrix}^{(B)} = [R_\phi^x R_\theta^y R_\psi^z] \begin{pmatrix} X \\ Y \\ Z \end{pmatrix}^{(I)}$$

Where R_{total} is $[R_\phi^x R_\theta^y R_\psi^z]$.

- To get body angular velocities in terms of Euler angles and Euler rates:

$$\begin{pmatrix} p \\ q \\ r \end{pmatrix} = \begin{pmatrix} \dot{\phi} - \dot{\psi} \sin \theta \\ \dot{\theta} \cos \phi + \dot{\psi} \cos \theta \sin \phi \\ \dot{\psi} \cos \theta \cos \phi - \dot{\theta} \sin \phi \end{pmatrix}$$

- To get the time derivatives of Euler angles:

$$\begin{pmatrix} \dot{\phi} \\ \dot{\theta} \\ \dot{\psi} \end{pmatrix} = \begin{pmatrix} p + (q \sin \phi + r \cos \phi) \tan \theta \\ q \cos \phi - r \sin \phi \\ \frac{q \sin \phi + r \cos \phi}{\cos \theta} \end{pmatrix}$$

To express Earth-fixed velocities in terms of body velocities:

$$\begin{pmatrix} \dot{x}_E \\ \dot{y}_E \\ \dot{z}_E \end{pmatrix} = [T]_{EB} \begin{pmatrix} u \\ v \\ w \end{pmatrix}$$

Hence:

$$\begin{pmatrix} \dot{x}_E \\ \dot{y}_E \\ \dot{z}_E \end{pmatrix} = \begin{pmatrix} u^E \cos \theta \cos \psi + v^E (\sin \phi \sin \theta \cos \psi - \cos \phi \sin \psi) + w^E (\cos \phi \sin \theta \cos \psi + \sin \phi \sin \psi) \\ u^E \cos \theta \sin \psi + v^E (\sin \phi \sin \theta \sin \psi + \cos \phi \cos \psi) + w^E (\cos \phi \sin \theta \sin \psi - \sin \phi \cos \psi) \\ -u^E \sin \theta + v^E \sin \phi \cos \theta + w^E \cos \phi \cos \theta \end{pmatrix}$$

2.2 Classification of Equations into Kinematics and Kinetics

- **Kinetics:**

- **Translational equations:** Newton's second law for forces acting on the aircraft.
- **Rotational equations:** Euler's equations for moments and angular accelerations.

- **Kinematics:**

- **Position and orientation:** The position (x, y, z) of the aircraft's center of mass and the Euler angles ϕ (roll), θ (pitch), and ψ (yaw), characterize the aircraft's 3D orientation.
- **Velocity and angular velocity:** Linear velocities u, v, w and angular velocities p, q, r .

2.3 Assumptions

- **Rigid Body Assumption:** The aircraft is considered as a rigid body not deforming under any condition of aerodynamic or inertial force.
- **Inertial Frame Assumption:** The equations are derived in an inertial frame (Earth or space-fixed), assuming no rotation or acceleration of the Earth, which simplifies the dynamics.
- **Small Angle Approximations (for Stability Analysis):** For stability analysis, small angle approximations of the type $\sin(\theta) \approx 0$ and $\cos(\theta) \approx 1$ are normally used while analyzing small perturbations around a trim state (steady flight).
- **Symmetric Aircraft:** The aircraft is considered to be symmetric about the longitudinal plane, X-Z plane, which simplifies the inertia. (i.e., $I_{xy} = I_{xz} = I_{yz} = I_{zx} \approx 0$).
- **Constant Mass and Inertia:** Fuel consumption and variations in payload are not taken in account to calculate the mass and inertia properties of the aircraft.
- **Gravity as a Constant Force:** Gravity is modeled as a constant vertical force, with no variation due to altitude or geographic location.
- **No External Disturbances:** External forces such as wind gusts, atmospheric disturbances, and turbulence are neglected for simplicity.
- **Neglecting Higher-Order Effects:** The non-linearities such as aerodynamic hysteresis or higher order terms of the Taylor series expansion are neglected. Dynamic effects higher than second-order are usually neglected, such as unsteady aerodynamics or large deflections.

2.4 The set of equations added to the (RBD) equations to form the Fixed Wing Airplanes (EOM)

1. Gravitational Forces:

$$\mathbf{F}_g = mg \begin{pmatrix} -\sin \theta \\ \cos \theta \sin \phi \\ \cos \theta \cos \phi \end{pmatrix}$$

2. Body Forces (Aerodynamics, etc.):

$$\mathbf{F} = \begin{pmatrix} F_x \\ F_y \\ F_z \end{pmatrix} = \begin{pmatrix} X \\ Y \\ Z \end{pmatrix}$$

3. Thrust Forces:

The thrust T_x for a jet engine can be approximated as:

$$T_x = \dot{m} \cdot (V_e - V_0) + A_e \cdot (P_e - P_0)$$

Where:

- \dot{m} is the mass flow rate of the air through the engine.
- V_e is the exhaust velocity of the jet.
- V_0 is the velocity of the aircraft (true airspeed).
- A_e is the exit area of the engine.
- P_e is the pressure at the exhaust.
- P_0 is the ambient pressure.

Now, the thrust force vector can be written as:

$$\mathbf{F}_T = \begin{pmatrix} T_x \\ 0 \\ 0 \end{pmatrix}$$

Assuming that Thrust acts in a translational motion (x axis), and there are components in the lateral or vertical directions(as the engine is not tilted at an angle).

2.5 Aircraft's EOM Mathematical Classification.

The equations of motion can be classified into the following based on the mathematical form of the variables involved:

Nonlinear Coupled Differential Equations

The full EOM of an aircraft consists of **nonlinear, coupled, ordinary differential equations** that relate the velocities and accelerations in both the translational and rotational domains. These include:

- **Six degrees of freedom (6-DOF):**
 - **Three translational** equations for motion in the x, y, z directions.
 - **Three rotational** equations for the roll, pitch, and yaw motions.
- **Nonlinearities:**
 - The equations are **nonlinear** due to the coupling terms involving the rotational rates and translational velocities (e.g.: $qr, pr, qw - rv, pv - qu$, etc.).
 - These **coupling** terms introduce **Coriolis effects** and **Gyroscopic effects**, which indicates the influence of rotational motion over translational motion.
 - The dependence of aerodynamic forces and moments on the angle of attack α , sideslip angle β , and control surface deflections, which are nonlinear functions.

Linearized Approximation for Small Disturbances

The nonlinear EOM are **linearized** around a steady-state flight condition. The linearized equations are valid for small perturbations around this equilibrium state and take the form:

$$A\Delta x + B\Delta u = \dot{x}$$

Where:

- x is a state vector, containing small perturbations in velocity, angular rate, etc.
- u is the *input vector*, representing small control inputs.
- A is the *system matrix*, and B is the *input matrix*.

Decoupled Modes:

The linearized equations can often be decoupled into two sets of modes:

Longitudinal modes: Related to pitch, altitude, and speed (involving u, w, q, θ).

- Short-period mode.
- Phugoid mode.

Lateral-directional modes: Related to yaw, roll, and sideslip (involving v, p, r, ϕ, ψ).

- Dutch roll mode.
- Spiral mode.
- Roll subsidence.

2.6 The difference between the (Body axes) and the (earth or inertial axes)

Body Axes System:

- It's fixed to the aircraft and constantly moves and rotates with it.
- It's useful for expressing forces (like aerodynamic forces), moments, and velocities relative to the aircraft itself.

Earth (Inertial) Axes System:

- It's fixed relative to the ground and provides an inertial reference.
- When considering aircraft motion, this frame is typically assumed to be non-rotating and non-accelerating, which simplifies calculations.

2.7 Difference between the pitch angle (θ) and the angle of attack (α), and between the sideslip angle (β) and the heading angle (ψ)

Pitch Angle (θ) vs Angle of Attack (α):

- **Pitch Angle (θ):**
 - The pitch angle is the angle between the aircraft's longitudinal axis and the *local horizontal plane* (horizontal plane in the inertial frame).
 - It represents the nose-up or nose-down attitude of the aircraft relative to the Earth's horizontal plane.
- **Angle of Attack (α):**
 - The angle of attack is the angle between the aircraft's longitudinal axis and the *relative airflow* or *flight path vector*.
 - It also reflects how the aircraft is interacting with the airstream, which is important for lift generation.

Relationship:

$$\alpha = \theta - \gamma$$

Where:

- γ = flight path angle (angle between the velocity vector and the horizontal plane).

Sideslip Angle (β) vs Heading Angle (ψ):

- **Sideslip Angle (β):**
 - The sideslip angle is the angle between the aircraft's longitudinal axis (X-body axis) and the *relative airflow*.
 - It measures the extent to which the aircraft is "sliding" sideways relative to the airflow.
- **Heading Angle (ψ):**
 - The heading angle is the angle between the aircraft's longitudinal axis and *true north* on the horizontal plane. It represents the aircraft's orientation.

2.8 Different attitude representations

There are alternative ways to represent aircraft orientation or attitude other than Euler angles. Each has its advantages and disadvantages.

1. Direction Cosine Matrix (DCM)

A **Direction Cosine Matrix (DCM)** is a 3×3 matrix that transforms vectors from one coordinate frame (e.g., body frame) to another (e.g., Earth frame). It contains the cosine of the angles between each pair of coordinate axes.

- **Advantages:**

- Provides an exact and continuous representation of orientation.
- Directly used to convert vectors between coordinate frames.
- No singularities (unlike Euler angles).

- **Disadvantages:**

- Requires 9 components (matrix elements) to describe orientation, compared to only 3 angles for Euler.
- It is prone to numerical drift (loss of orthogonality) during integration, and orthogonality must be enforced periodically.

2. Quaternions

Quaternions are a compact way to represent orientation using four numbers (scalar + 3-vector). A quaternion can be represented as:

$$q = [q_0, q_1, q_2, q_3] = \left[\cos\left(\frac{\theta}{2}\right), u_x \sin\left(\frac{\theta}{2}\right), u_y \sin\left(\frac{\theta}{2}\right), u_z \sin\left(\frac{\theta}{2}\right) \right]$$

Where θ is the rotation angle and (u_x, u_y, u_z) is the unit vector around which the body rotates.

- **Advantages:**

- No Singularity (*gimbal lock*): Quaternions avoid the singularity problem of Euler angles.
- Compact: Requires only 4 components.
- Efficient: Multiplying quaternions is computationally more efficient than multiplying rotation matrices.

- **Disadvantages:**

- More complex and less intuitive compared to Euler angles.
- Requires normalization during numerical integration to maintain unit magnitude.

3. Axis-Angle Representation

In **axis-angle representation**, orientation is described by a single *rotation axis* and a *rotation angle*. The orientation is given by rotating the body around the unit vector $\mathbf{u} = (u_x, u_y, u_z)$ by an angle θ .

- **Advantages:**

- Simple and intuitive for representing a single rotation.
- Compact (3 numbers: axis + angle).

- **Disadvantages:**

- Similar to quaternions, normalization is needed to keep the unit vector magnitude.
- Not efficient for composing multiple rotations.
- More cumbersome to integrate and use in sequential rotations.

Each representation is suitable for different applications, and in aerospace engineering, **Quaternions** and **DCM** are often preferred for their robustness and lack of singularities.

3 Numerical Solution of ODEs

3.1 Numerical Solving Algorithms for ODEs

Euler's Method: Is a simple and fast numerical method used frequently for its simple and fast approach. The method mainly depends on calculating the next point using the current slope of the point that it is currently on.

$$y_{n+1} = y_n + h f(x_n, y_n)$$

Heun's Method: Similar to Euler's method, It's a second order method that uses the average of the slopes at the beginning and the end of the step.

$$y_{n+1} = y_n + \frac{h}{2} (f(x_n, y_n) + f(x_{n+1}, y_n + h f(x_n, y_n)))$$

Runge-Kutta 2nd Order (RK2): The Runge-Kutta is a method used widely in numerical algorithms. It is a secound order method that uses an intermediate step and has higher accuracy than Euler's method

$$y_{n+1} = y_n + h k_2$$

$$k_2 = f\left(x_n + \frac{h}{2}, y_n + \frac{h}{2} k_1\right)$$

Runge-Kutta 4th Order (RK4): The Runge-Kutta 4th order (RK4) method is a highly accurate algorithm that efficiently estimates solutions with fewer time steps, offering a balance between precision and computational speed.

$$y_{n+1} = y_n + \frac{h}{6} (k_1 + 2k_2 + 2k_3 + k_4)$$

$$k_1 = h \cdot f(x_0, y_0).$$

$$k_2 = h \cdot f\left(x_0 + \frac{h}{2}, y_0 + \frac{k_1}{2}\right).$$

$$k_3 = h \cdot f\left(x_0 + \frac{h}{2}, y_0 + \frac{k_2}{2}\right)$$

$$k_4 = h \cdot f(x_0 + h, y_0 + k_3).$$

3.2 Algorithm for Solving the Airplane's EOM

The most efficient algorithm that can be used in such case we will use the RK4 method. We need to state the initial conditions in order to solve the differential equation. Firstly, we will assume that the mass m and the inertia matrix I are constant so we don't need to include initial states for these states. The initial states can be shown as follows:

Initial Position: (x_0, y_0, z_0)
 Initial Velocity: (u_0, v_0, w_0)
 Initial orientation: $(\phi_0, \theta_0, \psi_0)$
 Initial angular velocity: (p_0, q_0, r_0)

By identifying the initial conditions we are set to use the RK4 method and to achieve this we need to perform a set of iterations in order to identify k_1, k_2, k_3 and k_4 and the following states are needed:

current Position: (x_n, y_n, z_n)
 current Velocity: (u_n, v_n, w_n)
 current orientation: $(\phi_n, \theta_n, \psi_n)$
 current angular velocity: (p_n, q_n, r_n)

The output that will be calculated is the updated states by using the new k_n . Hence, we can list the outputs as follows:

$$k_1 = h \cdot f(x_0, y_0).$$

$$\begin{aligned} k_2 &= h \cdot f \left(x_0 + \frac{h}{2}, y_0 + \frac{k_1}{2} \right), \\ k_3 &= h \cdot f \left(x_0 + \frac{h}{2}, y_0 + \frac{k_2}{2} \right) \\ k_4 &= h \cdot f (x_0 + h, y_0 + k_3). \end{aligned}$$

We will plug the current states in the RK4 formula to determine the new states in which we will compare them with the current states and see if the change is less than a the tolerance we defined then we will stop iterating

$$y_{n+1} = y_n + \frac{h}{6} (k_1 + 2k_2 + 2k_3 + k_4)$$

and for the states:

$$\begin{aligned} \text{New position: } & (x_{n+1}, y_{n+1}, z_{n+1}). \\ \text{New velocity: } & (u_{n+1}, v_{n+1}, w_{n+1}). \\ \text{New orientation (Euler angles): } & (\phi_{n+1}, \theta_{n+1}, \psi_{n+1}). \\ \text{New angular velocity: } & (p_{n+1}, q_{n+1}, r_{n+1}). \end{aligned}$$

3.3 The solution of first order system of ODEs

The system of first-order ordinary differential equations (ODEs) to be solved is given by:

$$\begin{aligned} \frac{dy_1}{dt} &= \sin(t) + \cos(y_1) + \sin(y_2), \\ \frac{dy_2}{dt} &= \cos(t) + \sin(y_2), \end{aligned}$$

with the initial conditions:

$$\text{At } t = 0, \quad \mathbf{y}(0) = \begin{bmatrix} y_1(0) \\ y_2(0) \end{bmatrix} = \begin{bmatrix} -1 \\ 1 \end{bmatrix}.$$

The goal is to solve the system from $t = 0$ to $t = 20$ using 100 time steps (i.e., $n = 100$).

3.3.1 Solution Algorithm

To solve this system of ODEs, we use the fourth-order Runge-Kutta (RK4) method. The Runge-Kutta method is an iterative method that calculates the solution at each time step based on the following equations:

$$\begin{aligned} k_1 &= h \cdot f(t_i, \mathbf{y}_i), \\ k_2 &= h \cdot f \left(t_i + \frac{h}{2}, \mathbf{y}_i + \frac{k_1}{2} \right), \\ k_3 &= h \cdot f \left(t_i + \frac{h}{2}, \mathbf{y}_i + \frac{k_2}{2} \right), \\ k_4 &= h \cdot f (t_i + h, \mathbf{y}_i + k_3), \end{aligned}$$

where h is the time step size, and $f(t, \mathbf{y})$ represents the system of ODEs.

The solution at the next time step \mathbf{y}_{i+1} is then updated as follows:

$$\mathbf{y}_{i+1} = \mathbf{y}_i + \frac{1}{6}(k_1 + 2k_2 + 2k_3 + k_4).$$

We solve the system using the RK4 method with the following parameters:

$$t_0 = 0, \quad t_f = 20, \quad n = 100.$$

The step size is calculated as:

$$h = \frac{t_f - t_0}{n} = \frac{20 - 0}{100} = 0.2.$$

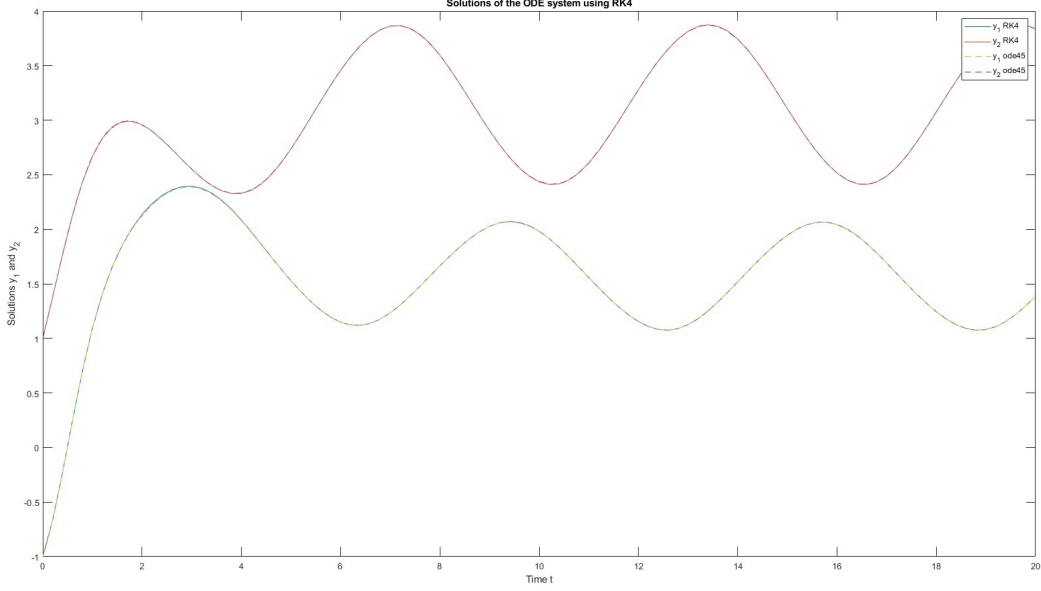


Figure 3: Numerical Solution of the ODE System Using RK4 and Validation with `ode45`

3.3.2 Solution Results and Validation

The MATLAB implementation for this numerical method is shown in Appendix A, and the results of the system of ODEs are plotted in Figure 224.

We validate the solution by comparing it with MATLAB's built-in `ode45` solver. As seen in Figure 224, the RK4 method provides results that closely match those from `ode45`, demonstrating the accuracy and reliability of our implementation.

4 Airplane Simulator Part I

Rigid Body Dynamics (RBD) equations describe the motion of a rigid body under the influence of external forces and moments. These equations are nonlinear, making analytical solutions impractical for most real-world scenarios. To handle this complexity, numerical methods are employed to approximate the solutions. One of the most widely used methods for solving such differential equations is the Runge-Kutta 4th order (RK4) method, known for its accuracy and efficiency.

In this section, we focus on solving the RBD equations for a rigid body subjected to constant external forces and moments. The RK4 method is particularly suitable for this purpose because it provides a good balance between computational cost and precision. By applying RK4, we can simulate the evolution of the rigid body's orientation, angular velocity, and linear velocity over time.

4.1 Initial Conditions Configuration

We aim to solve the Rigid Body Dynamics (RBD) equations for a rigid body under the influence of constant external forces and moments using the Runge-Kutta 4th order (RK4) method. The simulation will be carried out over a time span of 25 seconds, with the following constants:

$$\begin{aligned}
t_{\text{final}} &= 25 \text{ sec}, \\
\text{Forces} &= [10; 5; 3] \text{ N}, \\
\text{Moments} &= [10; 15; 20] \text{ N} \cdot \text{m}, \\
\text{Mass} &= 30 \text{ kg}, \\
I &= \begin{bmatrix} 1 & -2 & -1 \\ -2 & 5 & -4 \\ -1 & -4 & 0.2 \end{bmatrix} \text{ kg} \cdot \text{m}^2
\end{aligned}$$

The initial conditions for the linear and angular velocities, Euler angles, and position are defined as follows:

$$\begin{aligned}
[u, v, w, p, q, r, \phi, \theta, \psi, x, y, z]_{t=0} &= \\
[10, 2, 0, 2 \cdot \frac{\pi}{180}, 1 \cdot \frac{\pi}{180}, 0 \cdot \frac{\pi}{180}, 20 \cdot \frac{\pi}{180}, 15 \cdot \frac{\pi}{180}, 30 \cdot \frac{\pi}{180}, 2, 4, 7]
\end{aligned}$$

Here, u, v, w represent the initial linear velocities along the body-fixed axes, while p, q, r are the initial angular velocities. The Euler angles ϕ, θ, ψ represent the roll, pitch, and yaw angles, respectively, and x, y, z denote the initial position of the rigid body.

Using these initial conditions and the given external forces and moments, the RK4 method will be applied to compute the rigid body's motion over the simulation time.

4.2 Airplane Equations of Motion

The equations of motion for a rigid body are governed by Newton's second law for both translational and rotational motion. The following set of equations describe the dynamics of a rigid body in terms of the forces, moments, and inertial properties. These equations take into account the body's mass and inertia tensor to calculate linear and angular accelerations.

The translational motion is governed by the following equation, where F_x, F_y, F_z are the external forces acting on the body, m is the mass of the body, and u, v, w are the velocities in the body-fixed frame. Additionally, p, q, r represent the angular velocities about the x, y, z -axes:

$$\begin{bmatrix} F_x \\ F_y \\ F_z \end{bmatrix} = m \left(\begin{bmatrix} \dot{u} \\ \dot{v} \\ \dot{w} \end{bmatrix} + \begin{bmatrix} p \\ q \\ r \end{bmatrix} \times \begin{bmatrix} u \\ v \\ w \end{bmatrix} \right)$$

The rotational dynamics are described by the moments acting on the body, L, M, N , and the inertia matrix I :

$$\begin{bmatrix} L \\ M \\ N \end{bmatrix} = I \begin{bmatrix} \dot{p} \\ \dot{q} \\ \dot{r} \end{bmatrix} + \begin{bmatrix} p \\ q \\ r \end{bmatrix} \times I \begin{bmatrix} p \\ q \\ r \end{bmatrix}$$

Where the inertia tensor I is given as:

$$I = \begin{bmatrix} I_{xx} & -I_{xy} & -I_{xz} \\ -I_{yx} & I_{yy} & -I_{yz} \\ -I_{zx} & -I_{zy} & I_{zz} \end{bmatrix}$$

The orientation of the body is described by the Euler angles ϕ (roll), θ (pitch), and ψ (yaw). The rates of change of these angles are related to the angular velocities p, q, r as follows:

$$\begin{bmatrix} \dot{\phi} \\ \dot{\theta} \\ \dot{\psi} \end{bmatrix} = [J] \begin{bmatrix} p \\ q \\ r \end{bmatrix} = \begin{bmatrix} 1 & \sin(\phi) \tan(\theta) & \cos(\phi) \tan(\theta) \\ 0 & \cos(\phi) & -\sin(\phi) \\ 0 & \frac{\sin(\phi)}{\cos(\theta)} & \frac{\cos(\phi)}{\cos(\theta)} \end{bmatrix} \begin{bmatrix} p \\ q \\ r \end{bmatrix}$$

Finally, the translational motion of the body in the inertial frame (x_E, y_E, z_E) is related to the body frame velocities (u, v, w) by the following transformation matrix $[T]_{EB}$:

$$\begin{bmatrix} \dot{x}_E \\ \dot{y}_E \\ \dot{z}_E \end{bmatrix} = [T]_{EB} \begin{bmatrix} u \\ v \\ w \end{bmatrix}$$

Where the transformation matrix is given by:

$$[T]_{EB} = \begin{bmatrix} \cos(\theta) \cos(\psi) & -\cos(\phi) \sin(\psi) + \cos(\psi) \sin(\theta) \sin(\phi) & \sin(\phi) \sin(\psi) + \cos(\phi) \sin(\theta) \cos(\psi) \\ \cos(\theta) \sin(\psi) & \cos(\phi) \cos(\psi) + \sin(\theta) \sin(\phi) \sin(\psi) & -\sin(\phi) \cos(\psi) + \cos(\phi) \sin(\theta) \sin(\psi) \\ -\sin(\theta) & \sin(\phi) \cos(\theta) & \cos(\phi) \cos(\theta) \end{bmatrix}$$

4.3 Evaluation of Rigid Body Dynamics Solutions: A Simulink and MATLAB Comparison

The rigid body dynamics equations were solved using both a Simulink model and a custom MATLAB script that implements the fourth-order Runge-Kutta (RK4) method. The three sets of results—velocities, angles, and angular velocities—show excellent agreement between Simulink and MATLAB outputs, which verifies the accuracy of both approaches.

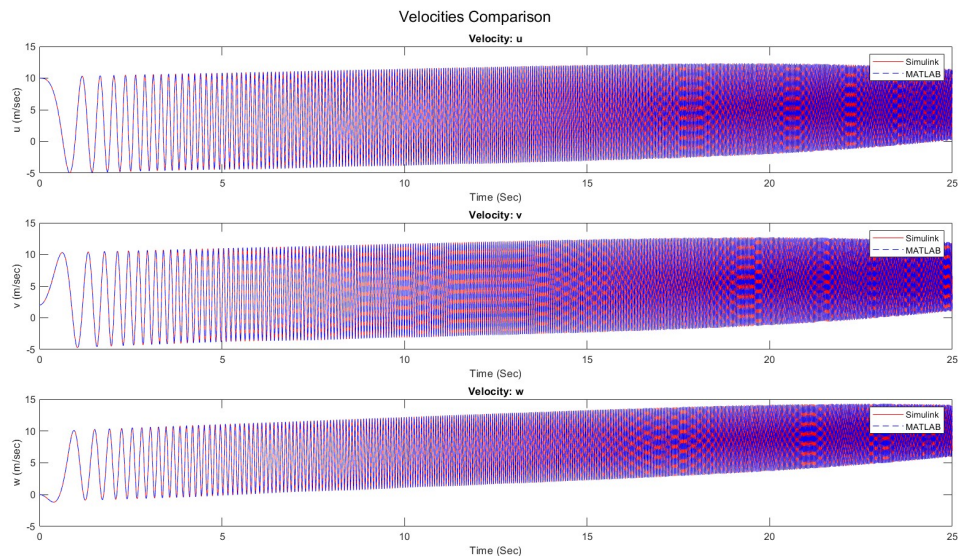


Figure 4: Comparison of aircraft velocity components (u , v , w) between MATLAB and Simulink results

Velocities: The time evolution of the linear velocities u , v , and w is presented in the first plot. Both the Simulink and MATLAB results match closely, showing that all velocity components increase over time. The initial oscillations gradually diminish, leading to smoother behavior as the system stabilizes. This indicates that the dynamic responses of the system are being captured accurately in both simulation environments.

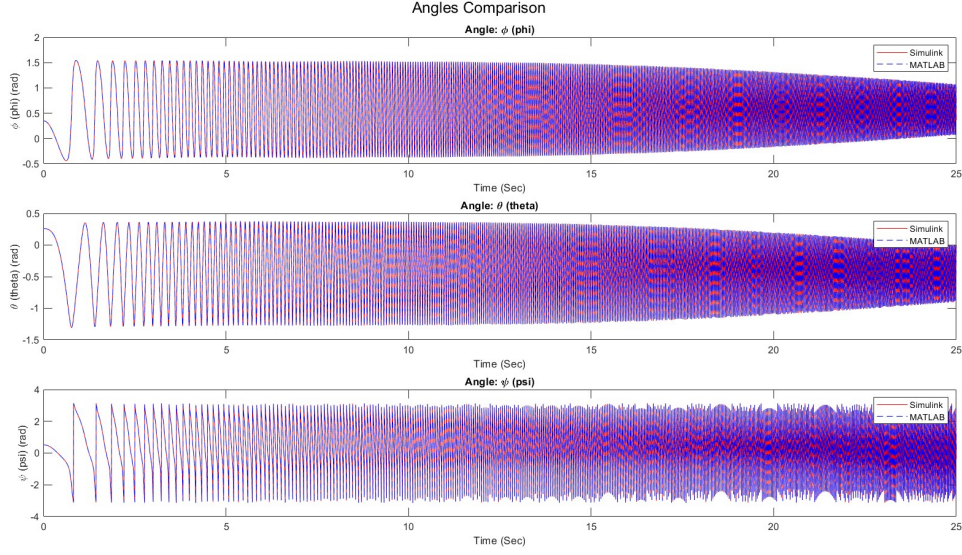


Figure 5: Comparison of aircraft orientation angles (ϕ, θ, ψ) between MATLAB and Simulink results.

Angles: The second plot shows the evolution of the Euler angles ϕ (roll), θ (pitch), and ψ (yaw) over time. The oscillations in the angles during the early phase of the simulation eventually stabilize, reflecting the evolution of the body's rotational dynamics. Once again, the results from both Simulink and MATLAB are in excellent agreement, which validates the correctness of the transformations applied in both methods.

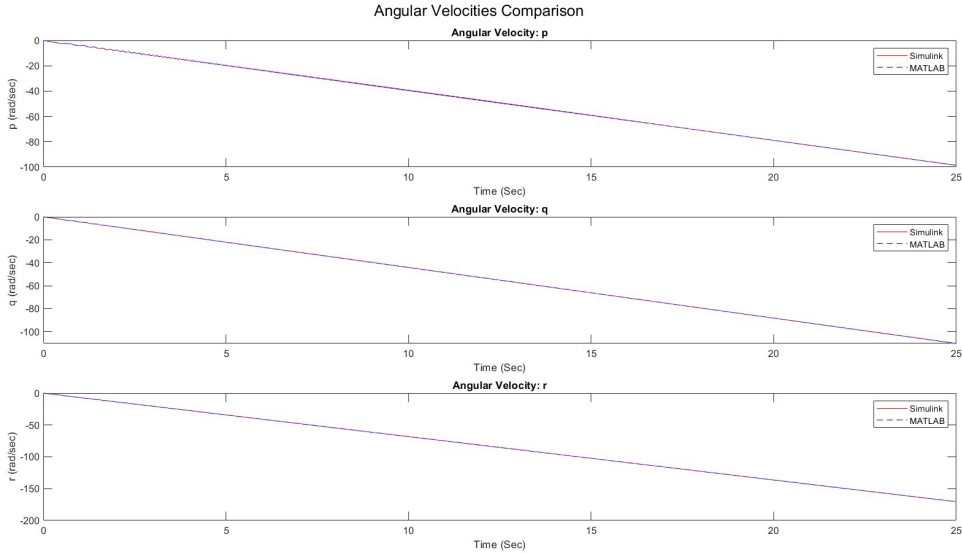


Figure 6: Comparison of aircraft angular velocity components (p, q, r) between MATLAB and Simulink results

Angular Velocities: The third plot depicts the time history of angular velocities p , q , and r . These values decrease over time in a nearly linear fashion. Both Simulink and MATLAB produce identical results, confirming that the inertial dynamics have been properly modeled and integrated using the RK4 method.

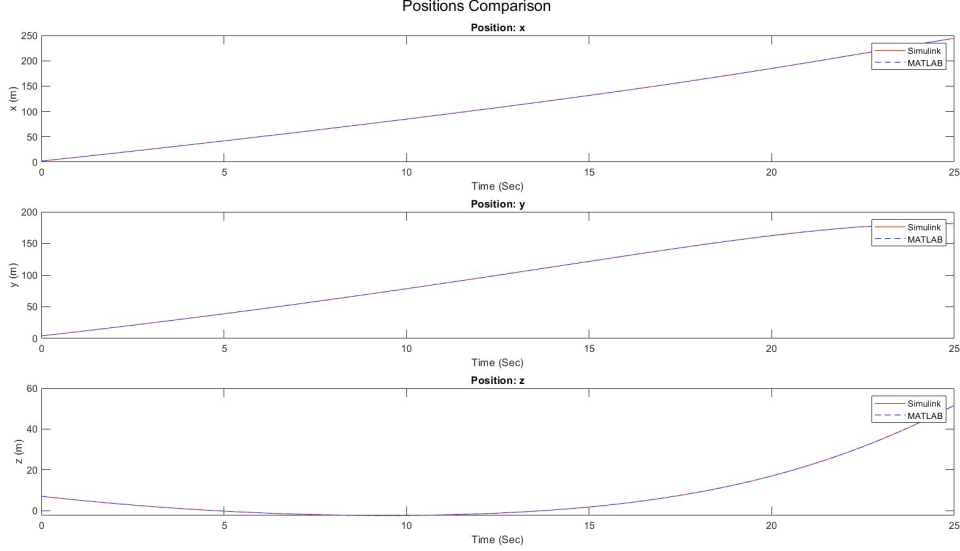


Figure 7: Comparison of aircraft position components (x , y , z) between MATLAB and Simulink results.

Positions: The final plot illustrates the evolution of the position coordinates x , y , and z over time. The positions show a continuous trend, indicating that the body is following a well-defined trajectory.

5 Airplane Simulator Part II

In the continuation of the airplane simulator project, we now focus on incorporating pilot input signals to calculate the aerodynamic and thrust forces and moments acting on the airplane. These calculations will then be used to build the complete non-linear flight simulator by combining them with the Rigid Body Dynamics (RBD) solver developed earlier. The simulator will evaluate the aircraft's behavior in response to control surface deflections and thrust variations.

5.1 Forces and Moments Calculation

The calculation of aerodynamic and thrust forces, as well as moments acting on an airplane, is a critical aspect of the airplane's response to control surface inputs such as aileron, rudder, elevator, and thrust adjustments. These forces and moments result from changes in airflow over the aircraft and engine output, and their effects on the aircraft's dynamics are governed by stability and control derivatives. The stability derivatives describe how small changes in state variables, such as velocity or angular velocity, influence the aerodynamic forces and moments.

5.1.1 Stability and Control Derivatives

The aircraft's response to control inputs is modeled using stability and control derivatives, which are essentially sensitivity factors that describe how the forces and moments change with respect to changes in the aircraft's state or control inputs. These derivatives are usually obtained from wind tunnel tests or flight data and are listed in tables such as those found in the *NASA CR-2144* report.

For example:

- **Stability derivatives** ($\frac{\partial X}{\partial u}$, $\frac{\partial Y}{\partial v}$, etc.) indicate how forces and moments change due to variations in the aircraft's velocities (e.g., longitudinal, lateral, vertical).

- **Control derivatives** ($\frac{\partial X}{\partial \delta_e}$, $\frac{\partial Y}{\partial \delta_r}$, $\frac{\partial Z}{\partial \delta_a}$) show how forces and moments change in response to pilot inputs (e.g., elevator, rudder, and aileron deflections).

5.1.2 Perturbation from Trim Condition

When the aircraft is in steady flight, known as the trim condition, forces and moments are balanced. Any deviation from this steady flight due to control inputs or changes in velocity leads to perturbations in the aerodynamic and thrust forces and moments. These perturbations are calculated using linearized models around the trim point, as follows:

$$\begin{aligned}\Delta X &= \frac{\partial X}{\partial u} \Delta u + \frac{\partial X}{\partial w} \Delta w + \frac{\partial X}{\partial \delta_e} \Delta \delta_e + \frac{\partial X}{\partial \delta_T} \Delta \delta_T \\ \Delta Y &= \frac{\partial Y}{\partial v} \Delta v + \frac{\partial Y}{\partial p} \Delta p + \frac{\partial Y}{\partial r} \Delta r + \frac{\partial Y}{\partial \delta_r} \Delta \delta_r \\ \Delta Z &= \frac{\partial Z}{\partial u} \Delta u + \frac{\partial Z}{\partial w} \Delta w + \frac{\partial Z}{\partial \dot{q}} \Delta \dot{q} + \frac{\partial Z}{\partial q} \Delta q + \frac{\partial Z}{\partial \delta_e} \Delta \delta_e + \frac{\partial Z}{\partial \delta_T} \Delta \delta_T\end{aligned}$$

These equations indicate how the aerodynamic forces in the longitudinal, lateral, and vertical directions change as a result of variations in velocity components (u, v, w) and control surface deflections ($\delta_e, \delta_r, \delta_a, \delta_T$). The perturbation values $\Delta u, \Delta v, \Delta w, \dots$ represent deviations from the values at the trim condition, i.e., the steady flight condition where the forces and moments are balanced.

5.1.3 Moment Calculations

Similar to the aerodynamic forces, the moments acting on the airplane (roll L , pitch M , and yaw N) are calculated as a function of perturbations in the angular velocities (p, q, r) and control surface deflections. These moments determine the rotational behavior of the aircraft and are essential for simulating how the airplane will roll, pitch, or yaw in response to pilot commands.

The equations for the moments are:

$$\begin{aligned}\Delta L &= \frac{\partial L}{\partial v} \Delta v + \frac{\partial L}{\partial p} \Delta p + \frac{\partial L}{\partial r} \Delta r + \frac{\partial L}{\partial \delta_r} \Delta \delta_r + \frac{\partial L}{\partial \delta_a} \Delta \delta_a \\ \Delta M &= \frac{\partial M}{\partial u} \Delta u + \frac{\partial M}{\partial w} \Delta w + \frac{\partial M}{\partial \dot{q}} \Delta \dot{q} + \frac{\partial M}{\partial q} \Delta q + \frac{\partial M}{\partial \delta_e} \Delta \delta_e + \frac{\partial M}{\partial \delta_T} \Delta \delta_T \\ \Delta N &= \frac{\partial N}{\partial v} \Delta v + \frac{\partial N}{\partial p} \Delta p + \frac{\partial N}{\partial r} \Delta r + \frac{\partial N}{\partial \delta_r} \Delta \delta_r + \frac{\partial N}{\partial \delta_a} \Delta \delta_a\end{aligned}$$

In these equations:

- ΔL represents the perturbation in roll moment, influenced by changes in lateral velocity (v), roll rate (p), yaw rate (r), and control inputs such as rudder and aileron deflections.
- ΔM refers to the perturbation in pitch moment, which is driven by longitudinal velocity (u), vertical velocity (w), pitch rate (q), and elevator deflection.
- ΔN captures the perturbation in yaw moment, depending on lateral velocity, roll and yaw rates, and control inputs.

5.1.4 Absolute Force and Moment Calculation

The perturbations in forces and moments calculated above are not the final forces acting on the airplane. These perturbations must be added to the forces and moments at the trim condition (steady flight) to obtain the total forces and moments. For example, the total longitudinal force X is given by:

$$X = X_0 + \Delta X = \Delta X + mg \sin(\theta_0)$$

Here, X_0 is the trim force in the longitudinal direction, and ΔX is the perturbation calculated using the derivatives. Similarly, the lateral and vertical forces are given by:

$$Y = Y_0 + \Delta Y = \Delta Y - mg \cos(\theta_0) \sin(\phi_0)$$

$$Z = Z_0 + \Delta Z = \Delta Z - mg \cos(\theta_0) \cos(\phi_0)$$

The total forces F_x, F_y, F_z acting on the airplane are then fed into the RBD equations to update the airplane's position and orientation at each time step in the simulation.

5.1.5 Gravitational Forces

In addition to the aerodynamic and thrust forces, gravitational forces must be included in the total force calculation. Gravity acts on the airplane in a fixed direction relative to the earth, while the aerodynamic and thrust forces act in the body-fixed frame. Therefore, the gravitational forces are projected into the body frame to compute their contribution to the total force acting on the airplane.

The gravitational forces are given by:

$$F_x = mg \sin(\theta)$$

$$F_y = mg \cos(\theta) \sin(\phi)$$

$$F_z = mg \cos(\theta) \cos(\phi)$$

These gravitational forces are added to the aerodynamic and thrust forces before passing them to the RBD solver.

5.2 Integration with RBD Solver

Once the aerodynamic and thrust forces and moments are calculated, these forces must be integrated with the Rigid Body Dynamics (RBD) solver to simulate the aircraft's motion. The RBD solver uses these forces and moments to determine how the airplane's orientation, velocity, and position evolve over time. The integration of these forces with the RBD solver is essential to accurately model the nonlinear flight dynamics of the airplane.

5.2.1 Total Forces Acting on the Airplane

The total forces acting on the airplane consist of three primary components:

1. **Aerodynamic forces:** These are generated by the airplane's interaction with the airflow, which depend on control surface deflections (e.g., aileron, rudder, elevator) and the aircraft's velocity components (e.g., longitudinal, lateral, vertical).
2. **Thrust force:** This is produced by the aircraft's engines, typically aligned with the longitudinal axis of the airplane. Thrust is influenced by the pilot's throttle input.
3. **Gravitational force:** This is the weight of the airplane acting in the vertical direction relative to the Earth's frame of reference, which changes its direction when projected into the body frame due to the aircraft's orientation.

These total forces are then used to compute the translational motion of the airplane by solving Newton's second law for each axis in the airplane's body frame.

The total forces in the longitudinal (X), lateral (Y), and vertical (Z) directions are given by the following equations:

$$F_x = X - mg \sin(\theta) = \Delta X + mg \sin(\theta_0) - mg \sin(\theta)$$

$$F_y = Y + mg \cos(\theta) \sin(\phi) = \Delta Y + mg \cos(\theta) \sin(\phi)$$

$$F_z = Z + mg \cos(\theta) \cos(\phi) = \Delta Z - mg \cos(\theta_0) \cos(\phi_0) + mg \cos(\theta) \cos(\phi)$$

In these equations:

- X, Y, Z are the aerodynamic forces acting in the body frame.
- F_x, F_y, F_z are the total forces acting on the airplane, which include gravitational forces.
- mg represents the airplane's weight, where m is the mass and g is the gravitational acceleration.
- θ and ϕ are the pitch and roll angles of the airplane, respectively.
- $\Delta X, \Delta Y, \Delta Z$ represent the perturbations in the aerodynamic forces from the trim condition.

5.2.2 Equations of Motion for Translation

The translational equations of motion are derived from Newton's second law and account for both the external forces and the airplane's mass. The Aerodynamic Forces F_x, F_y, F_z are used to calculate the change in velocity components u, v, and w (longitudinal, lateral, and vertical velocities in the body frame)

5.2.3 Equations of Motion for Rotation

The rotational dynamics of the airplane are determined by the moments acting on the airplane and are described by the rotational form of Newton's second law. The moments L, M, N (roll, pitch, and yaw moments) are used to calculate the angular accelerations.

5.2.4 Integration Using Runge-Kutta 4th Order (RK4) Method

The translational and rotational equations of motion, derived from the forces and moments, are integrated over time using the Runge-Kutta 4th order (RK4) method. The RK4 method is a numerical integration technique that provides a good balance between computational efficiency and accuracy, particularly for nonlinear differential equations such as the RBD equations.

At each time step, the RK4 method computes the next state (positions, velocities, angular velocities) of the airplane by solving the following system of equations iteratively:

1. Compute the forces and moments based on the current state of the airplane and the pilot's inputs.
2. Use these forces and moments to solve the equations of motion for translational and rotational accelerations.
3. Update the state of the airplane (position, velocity, orientation) by integrating these accelerations using the RK4 method.
4. Repeat this process for each time step until the desired simulation time is reached.

The RK4 method's iterative process ensures that the nonlinear dynamics of the airplane are captured accurately over time, allowing for realistic predictions of how the airplane responds to pilot inputs.

5.2.5 Converting Between Body-Fixed and Inertial Frames

The integration process involves updating the airplane's position and orientation in the inertial (earth-fixed) frame. However, since the forces and moments are computed in the body-fixed frame, a transformation is necessary to convert these values between frames. The transformation matrix $[T]_{EB}$ relates the body-fixed velocities to the inertial frame:

$$\begin{bmatrix} \dot{x}_E \\ \dot{y}_E \\ \dot{z}_E \end{bmatrix} = [T]_{EB} \begin{bmatrix} u \\ v \\ w \end{bmatrix}$$

Where:

- $\dot{x}_E, \dot{y}_E, \dot{z}_E$ are the velocity components in the inertial frame.
- u, v, w are the velocity components in the body frame.
- $[T]_{EB}$ is the transformation matrix that accounts for the airplane's orientation in space, given by the Euler angles ϕ, θ, ψ (roll, pitch, yaw).

This transformation ensures that the airplane's position and velocity in the inertial frame are updated correctly during the simulation.

5.3 Validation

The validation process is essential to ensure the accuracy of the non-linear airplane flight simulator developed.

5.3.1 Validation Using Benchmark Test Data

The first key validation method involves comparing the simulator results with benchmark test data for the same aircraft under similar conditions. Benchmark Test data for the B-747 aircraft at Flight Condition 5 is used. The benchmark test includes response plots for various inputs, such as aileron, rudder, and elevator deflections. These plots provide a standard for validating the simulator's results under similar conditions.

The simulator results are compared against these benchmark plots to evaluate how well the non-linear flight dynamics model captures the real-world behavior of the aircraft. The following variables are validated:

- Linear velocities: u , v , and w (in the body frame).
- Angular velocities: p , q , and r (roll, pitch, and yaw rates).
- Euler angles: ϕ , θ , and ψ (roll, pitch, and yaw angles).
- Trajectory: Position coordinates x_E , y_E , and z_E (in the inertial frame).

5.3.2 Validation with Matlab Code

The following key cases are used to compare the simulator's outputs against the benchmark data:

- **Response for no input:** No affects induced, all plots show excellent agreement.

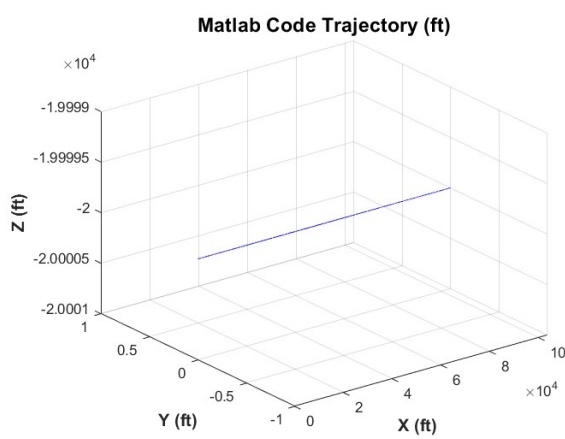


Figure 8: Matlab Simulator's plot

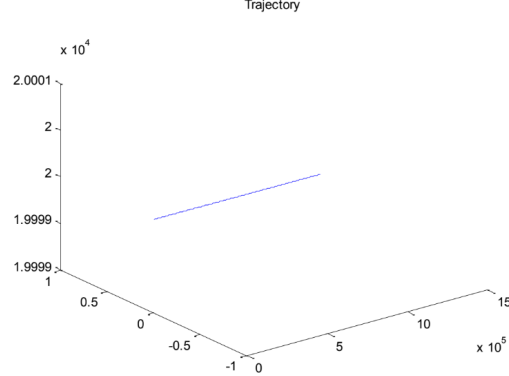


Figure 10: Reference (Benchmark) Trajectory Plot

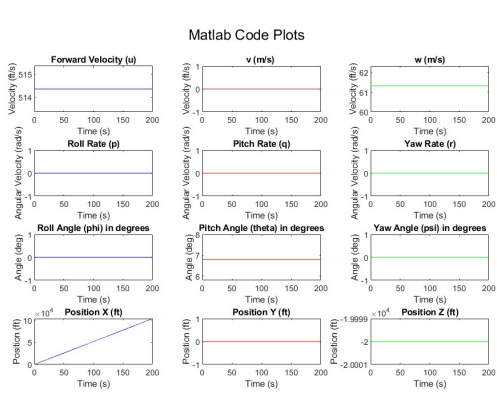


Figure 9: Matlab Simulator's Plots

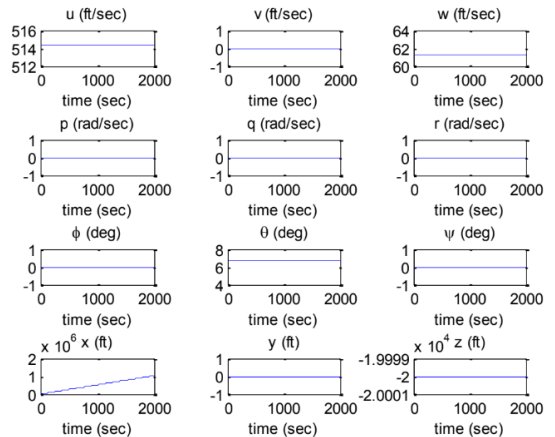


Figure 11: Reference Plots

- **+5° Aileron Deflection:** Primarily affects the roll rate (p) and yaw rate (r), inducing a rolling motion with slight yaw coupling.

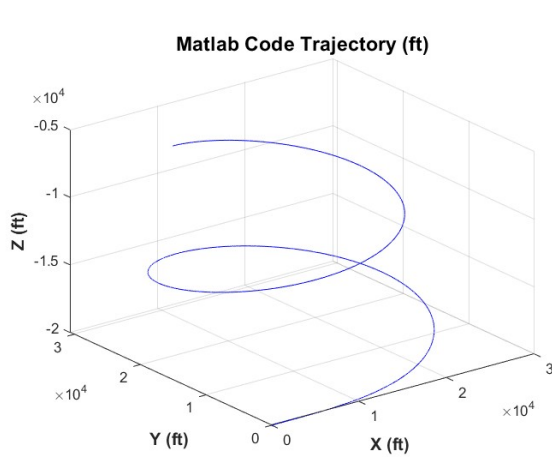


Figure 12: Simulator's Trajectory plot

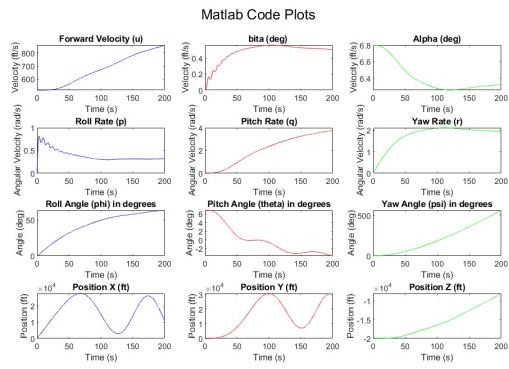


Figure 13: Simulator's Plots

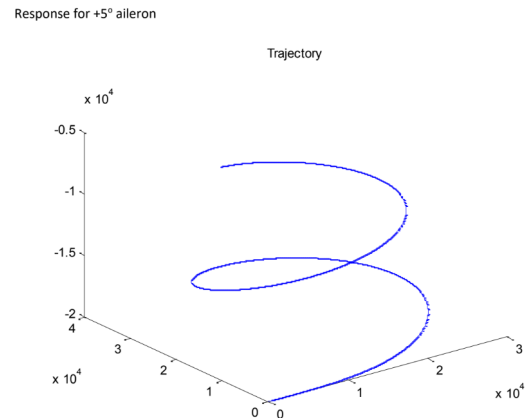


Figure 14: Reference (Benchmark) Trajectory Plot

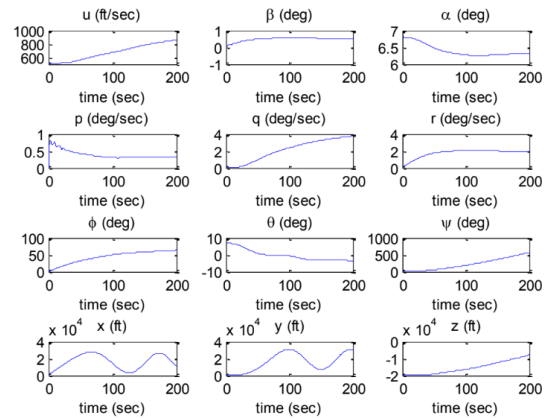


Figure 15: Reference Plots

- **-5° Aileron Deflection:** Primarily affects the roll rate (p) and yaw rate (r), inducing a rolling motion with slight yaw coupling.

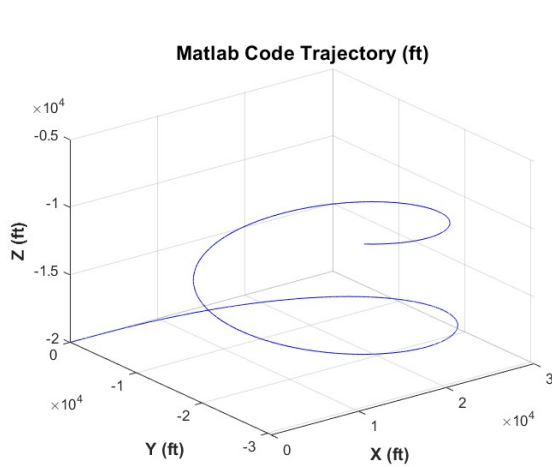


Figure 16: Simulator's Trajectory plot

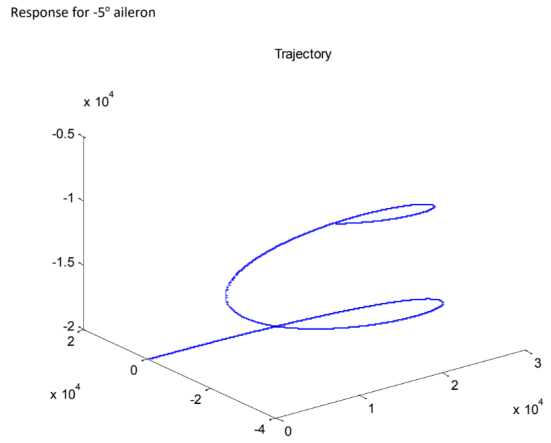


Figure 18: Reference (Benchmark) Trajectory Plot

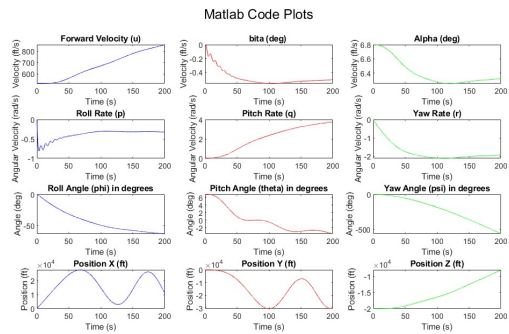


Figure 17: Simulator's Plots

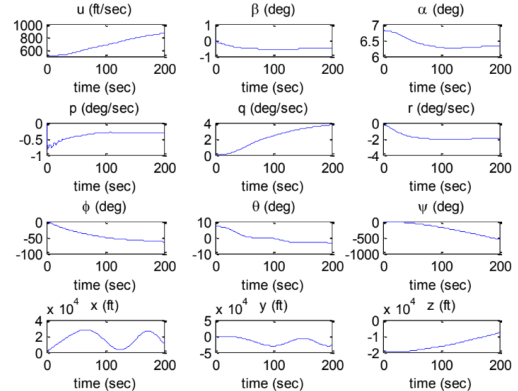


Figure 19: Reference Plots

- **+5° Rudder Deflection:** Primarily affects the yaw rate (r) and lateral velocity (v), inducing a yawing motion.

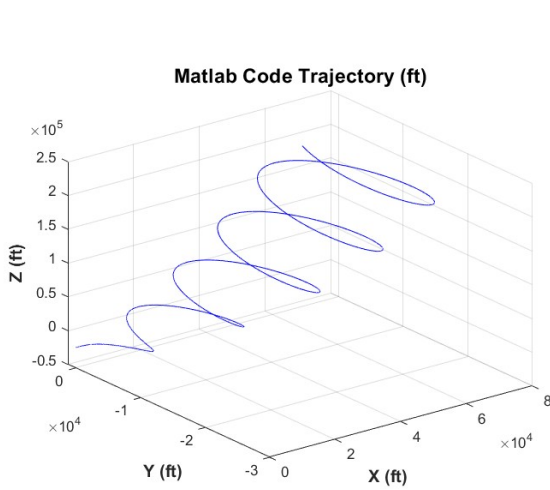


Figure 20: Simulator's Trajectory plot

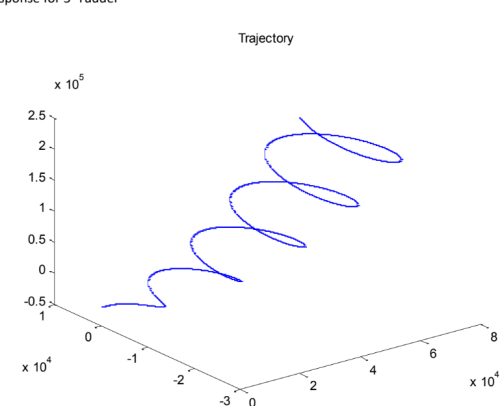


Figure 22: Reference (Benchmark) Trajectory Plot

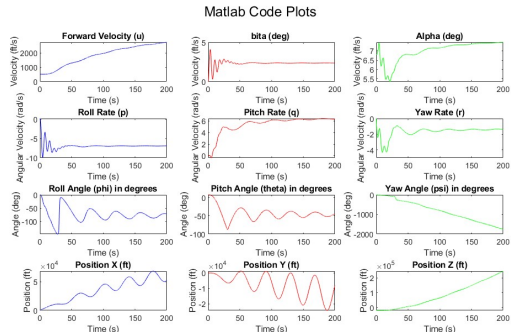


Figure 21: Simulator's Plots

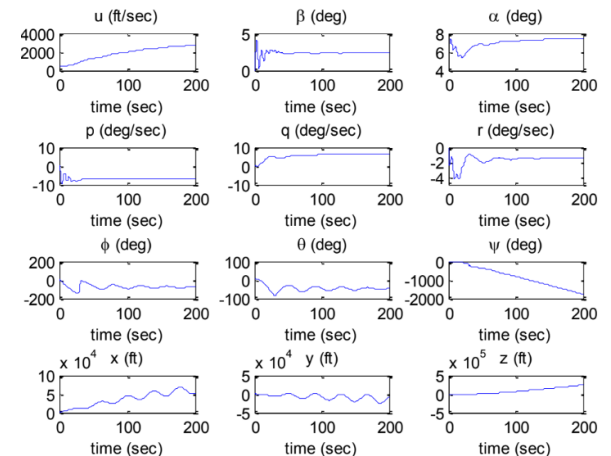


Figure 23: Reference Plots

- **-5° Rudder Deflection:** Primarily affects the yaw rate (r) and lateral velocity (v), inducing a yawing motion.

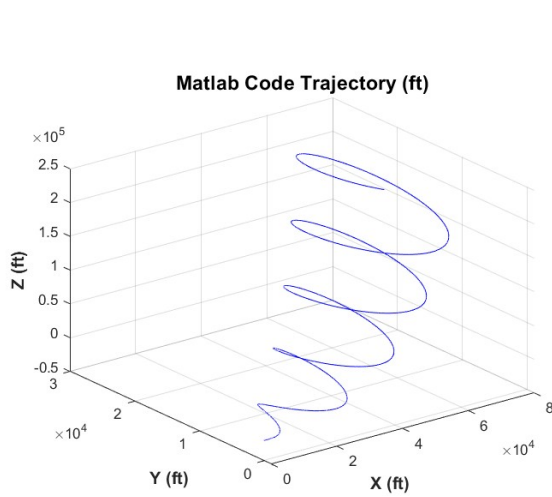


Figure 24: Simulator's Trajectory plot

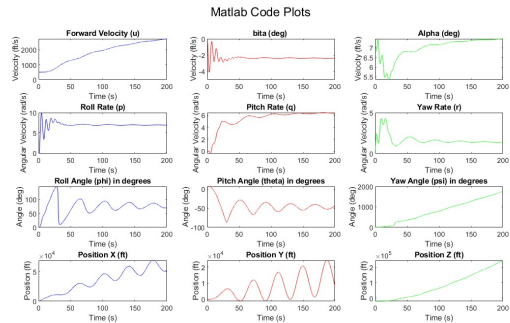


Figure 25: Simulator's Plots

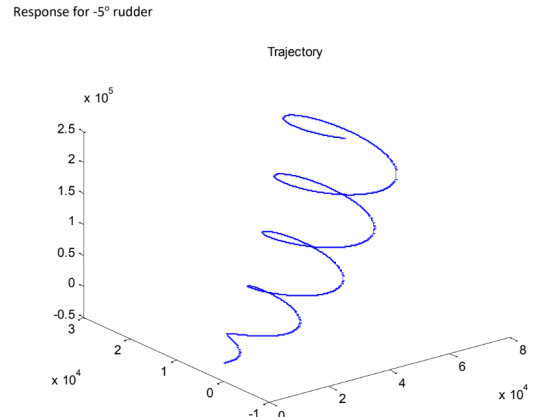


Figure 26: Reference (Benchmark) Trajectory Plot

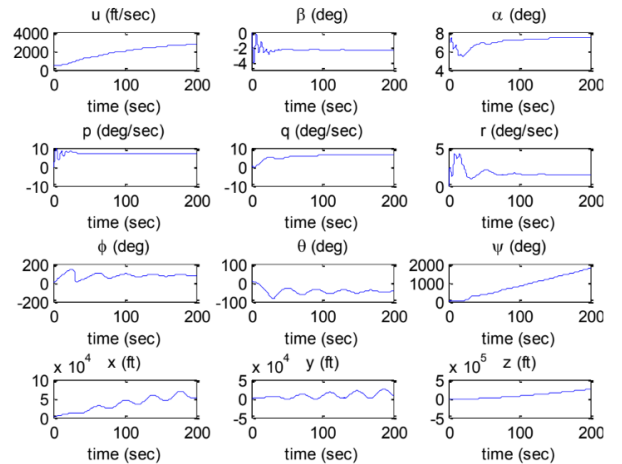


Figure 27: Reference Plots

- **+5° Elevator Deflection:** Primarily affects the pitch rate (q) and vertical velocity (w), inducing a pitching motion.

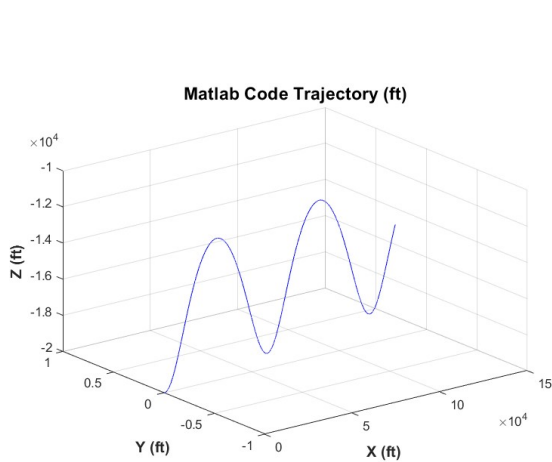


Figure 28: Simulator's Trajectory plot

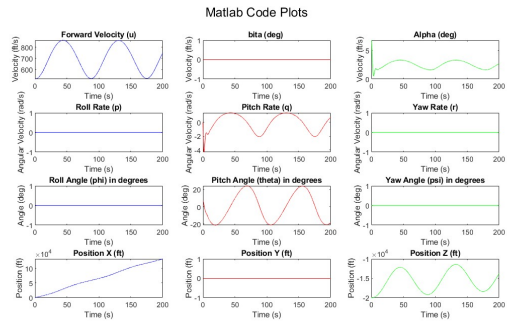


Figure 29: Simulator's Plots

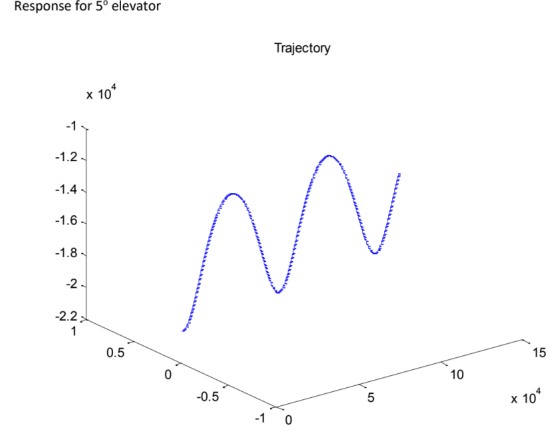


Figure 30: Reference (Benchmark) Trajectory Plot

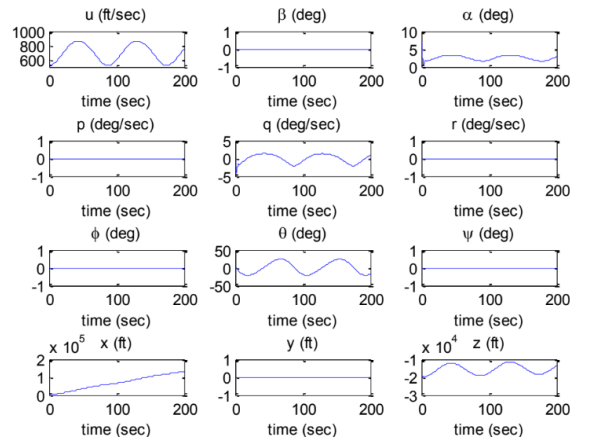


Figure 31: Reference Plots

- **-5° Elevator Deflection:** Primarily affects the pitch rate (q) and vertical velocity (w), inducing a pitching motion.

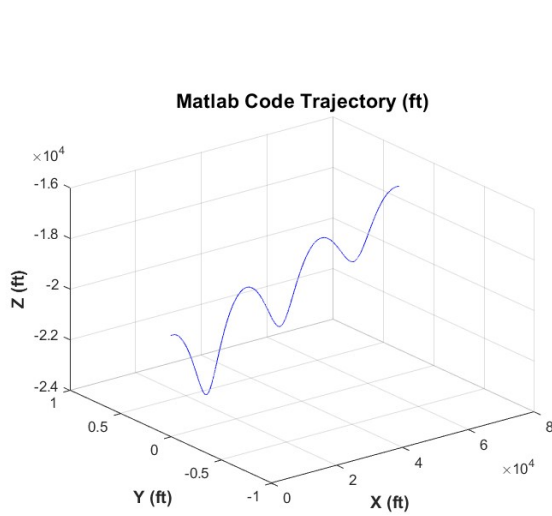


Figure 32: Simulator's Trajectory plot

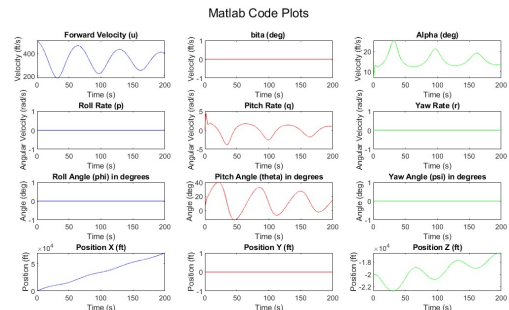


Figure 33: Simulator's Plots

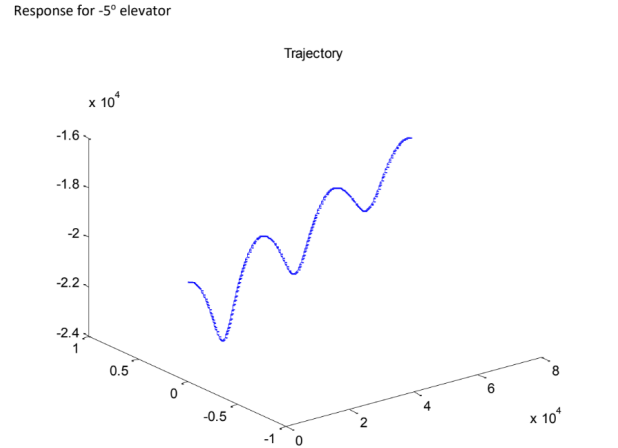


Figure 34: Reference (Benchmark) Trajectory Plot

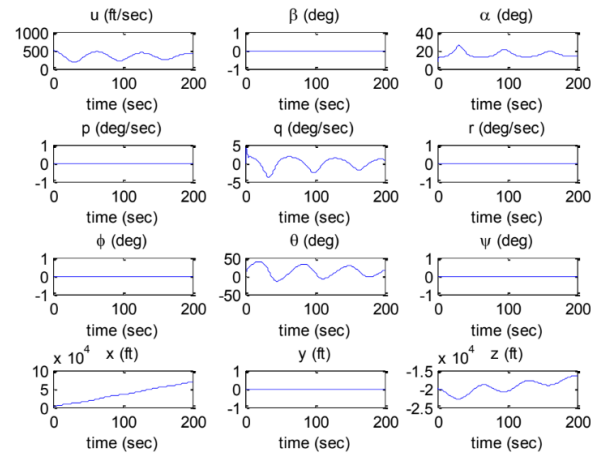


Figure 35: Reference Plots

- **Thrust Variation:** Primarily affects the forward velocity (u).

- Response for 10000 in thrust

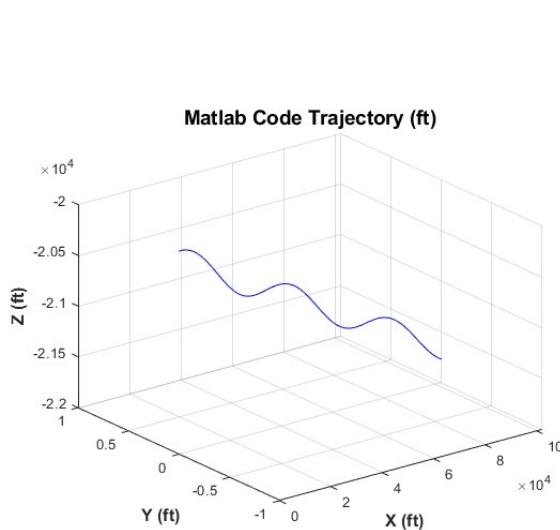


Figure 36: Simulator's Trajectory plot

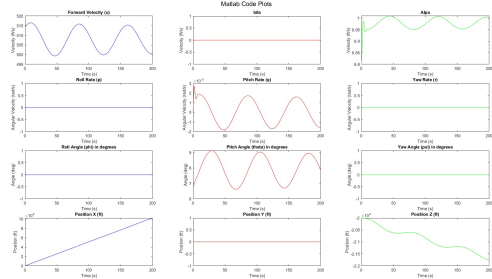


Figure 37: Simulator's Plots

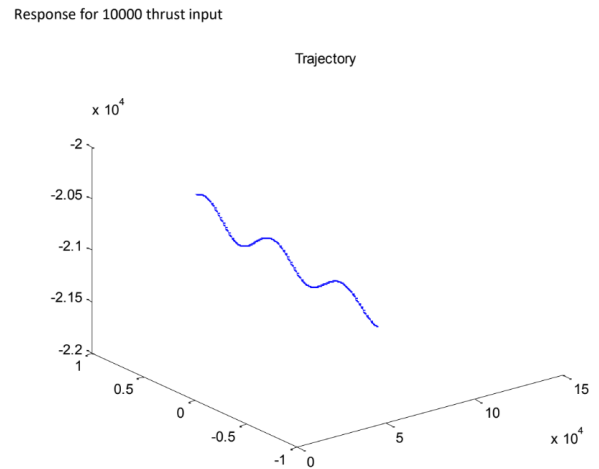


Figure 38: Reference (Benchmark) Trajectory Plot

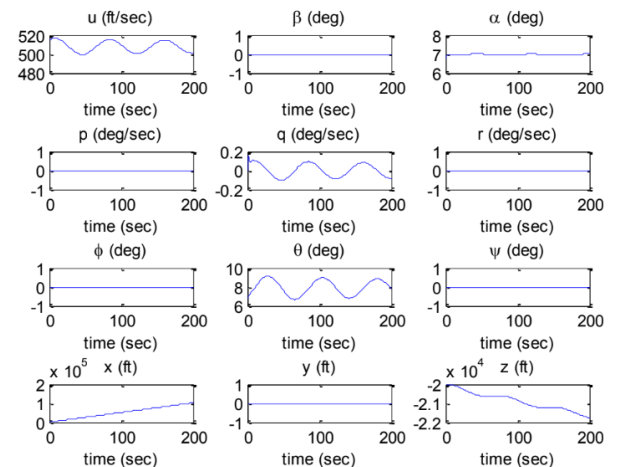


Figure 39: Reference Plots

– **Thrust Variation:** Primarily affects the forward velocity (u).

* Response for 10000 in thrust

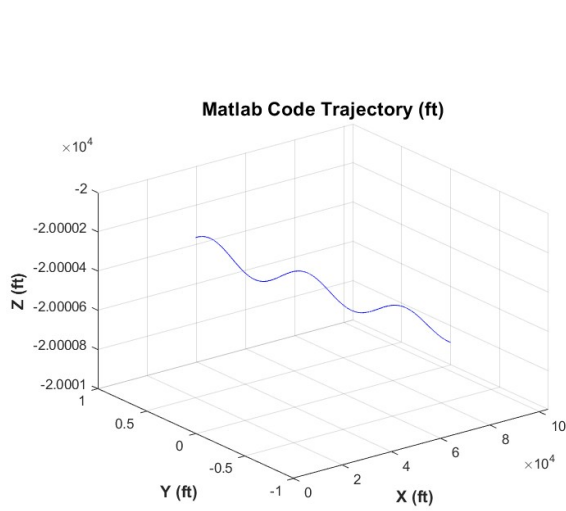


Figure 40: Simulator's Trajectory plot

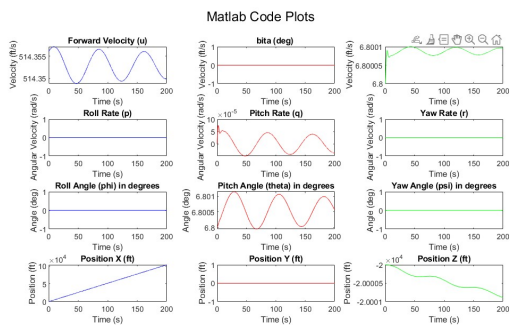


Figure 41: Simulator's Plots

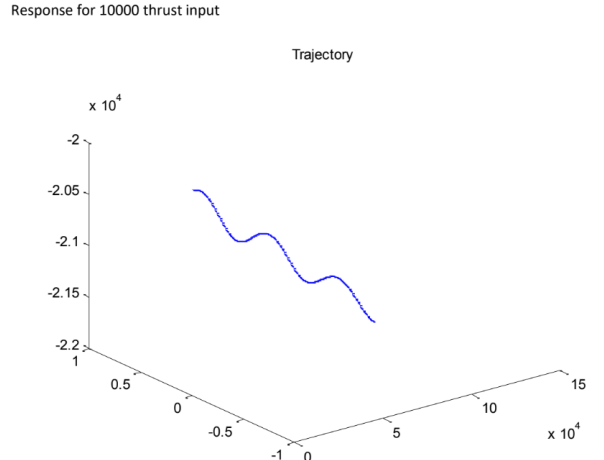


Figure 42: Reference (Benchmark) Trajectory Plot

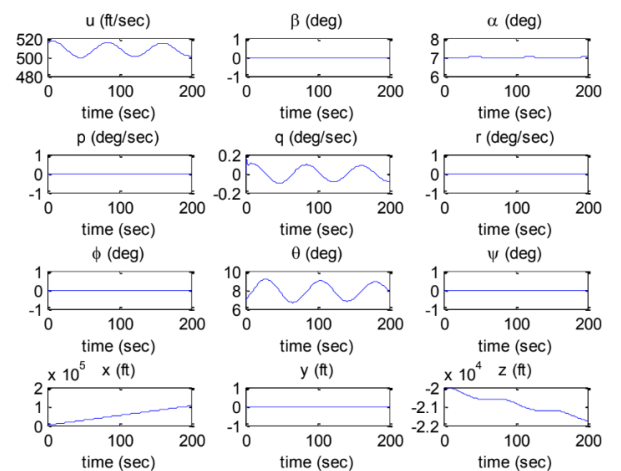


Figure 43: Reference Plots

5.3.3 Validation with Simulink

The following key cases are used to compare the simulator's outputs against the benchmark data:

- * **Response for no input:** No affects induced, all plots show excellent agreement.

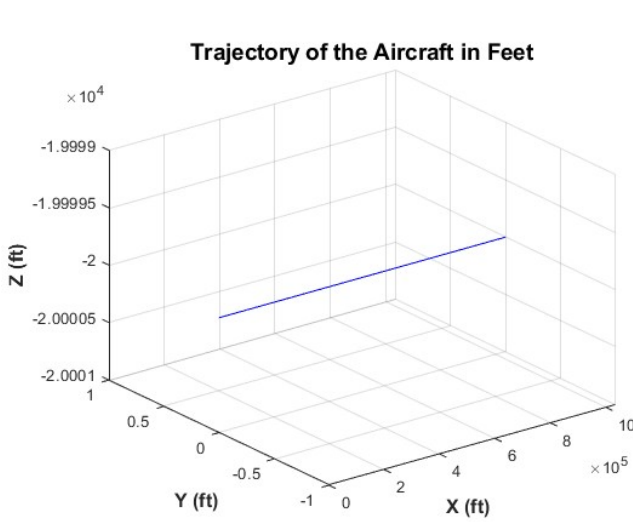


Figure 44: Simulink Simulator's plot

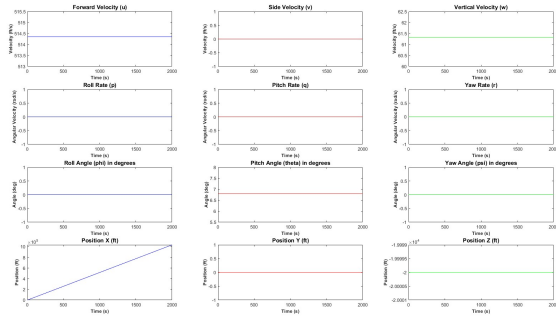


Figure 45: Simulink Simulator's Plots

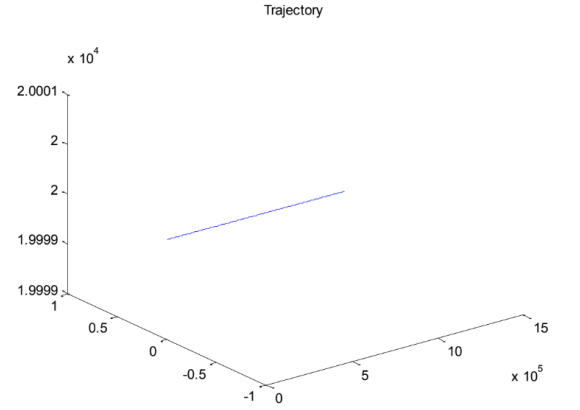


Figure 46: Reference (Benchmark) Trajectory Plot

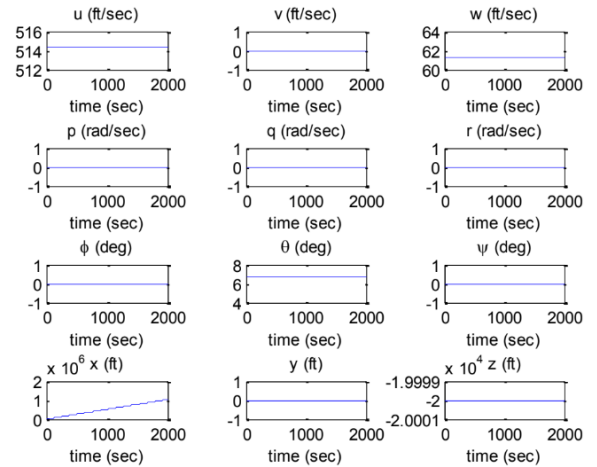


Figure 47: Reference Plots

* **+5° Aileron Deflection:** Primarily affects the roll rate (p) and yaw rate (r), inducing a rolling motion with slight yaw coupling.

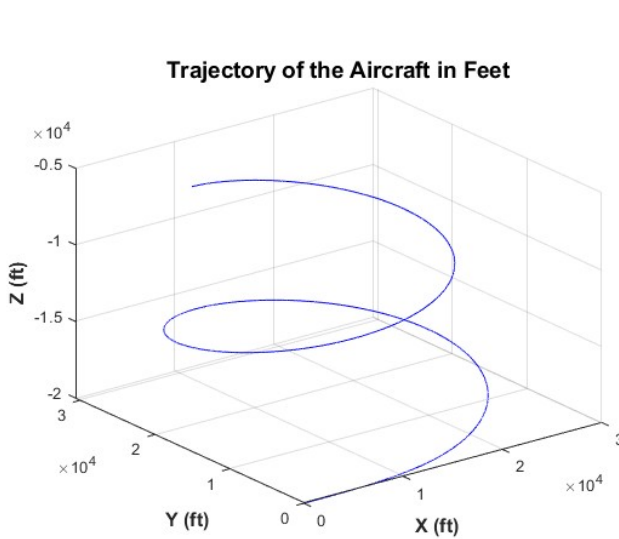


Figure 48: Simulink Simulator's Trajectory plot

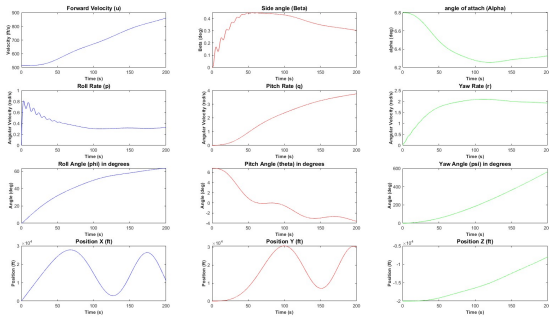


Figure 49: Simulink Simulator's Plots

Response for +5° aileron

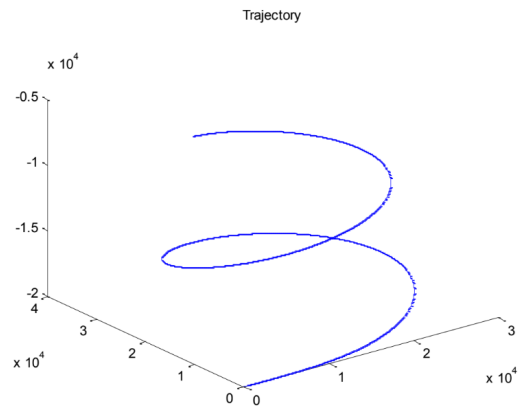


Figure 50: Reference (Benchmark) Trajectory Plot

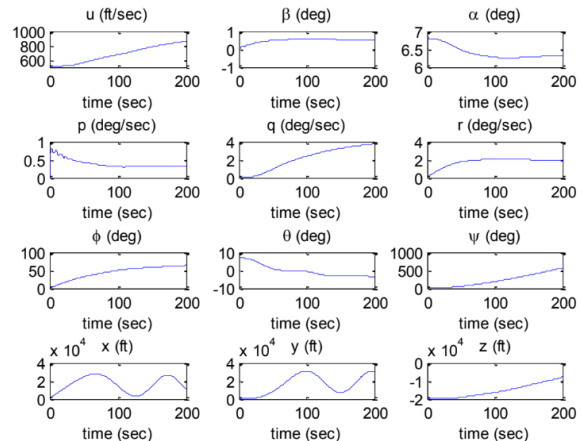


Figure 51: Reference Plots

* **-5° Aileron Deflection:** Primarily affects the roll rate (p) and yaw rate (r), inducing a rolling motion with slight yaw coupling.

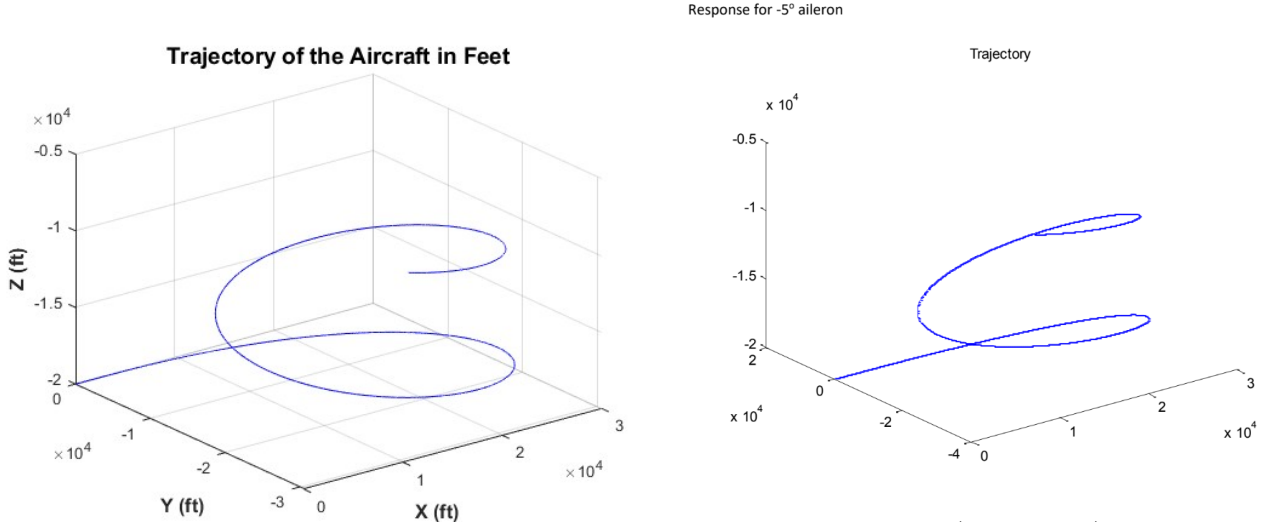


Figure 52: Simulink Simulator's Trajectory plot

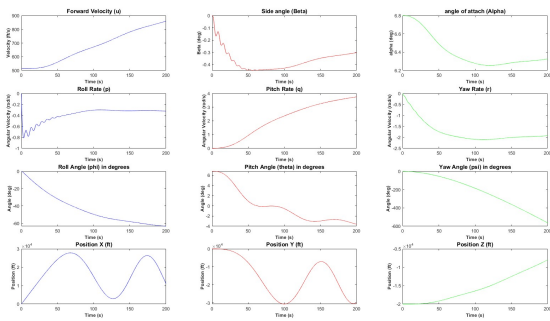


Figure 53: simulink Simulator's Plots

Response for -5° aileron

Trajectory of the Aircraft in Feet

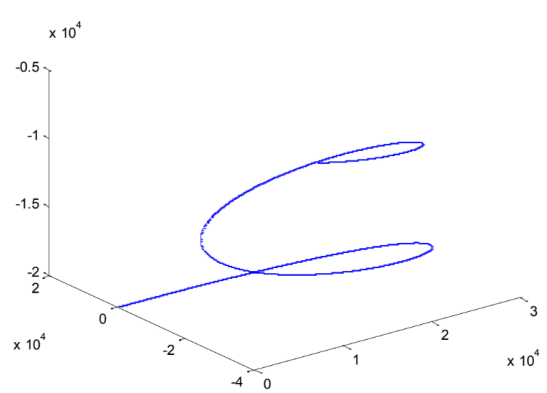


Figure 54: Reference (Benchmark) Trajectory Plot

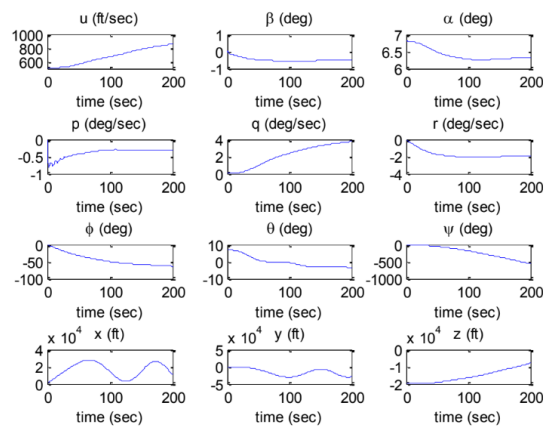


Figure 55: Reference Plots

* **+5° Rudder Deflection:** Primarily affects the yaw rate (r) and lateral velocity (v), inducing a yawing motion.

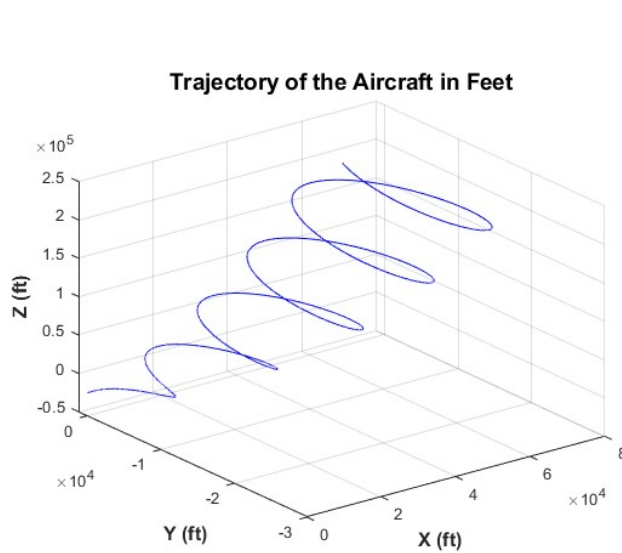


Figure 56: Simulink Simulator's Trajectory plot

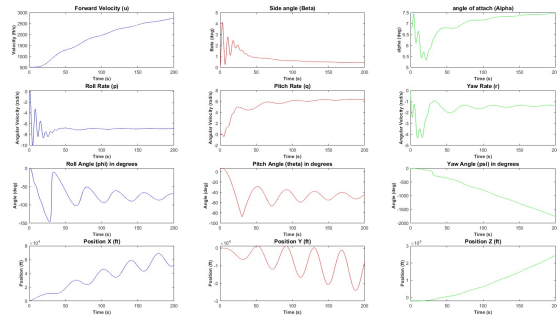


Figure 57: Simulink Simulator's Plots

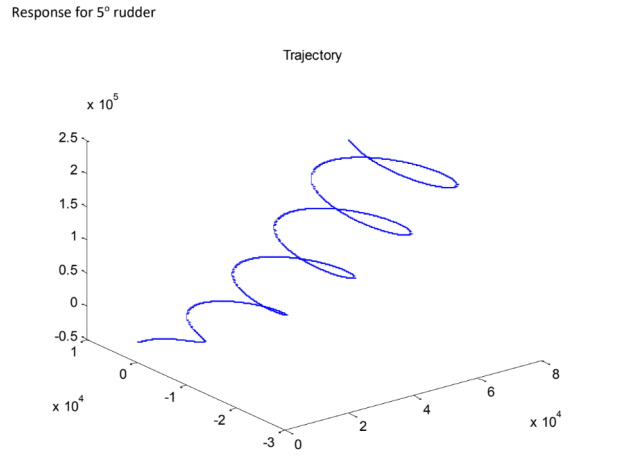


Figure 58: Reference (Benchmark) Trajectory Plot

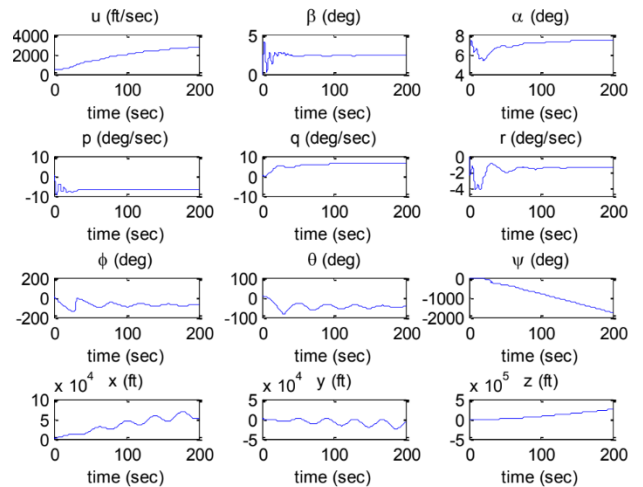


Figure 59: Reference Plots

- * **-5° Rudder Deflection:** Primarily affects the yaw rate (r) and lateral velocity (v), inducing a yawing motion.

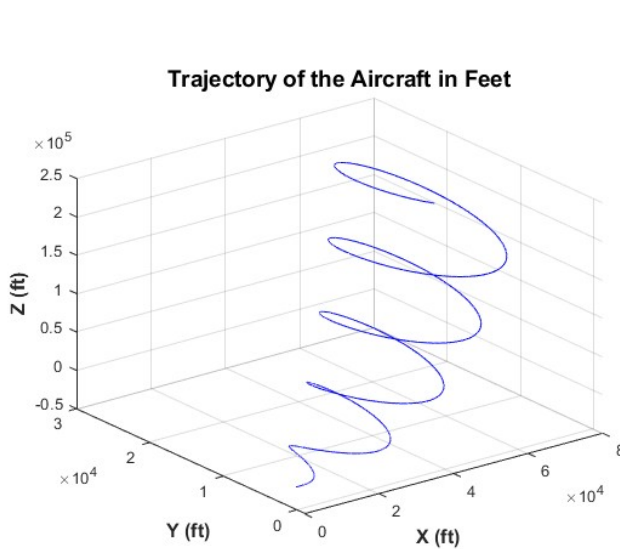


Figure 60: Simulink Simulator's Trajectory plot

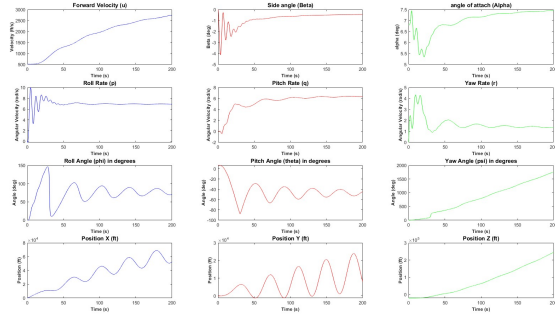


Figure 61: Simulink Simulator's Plots

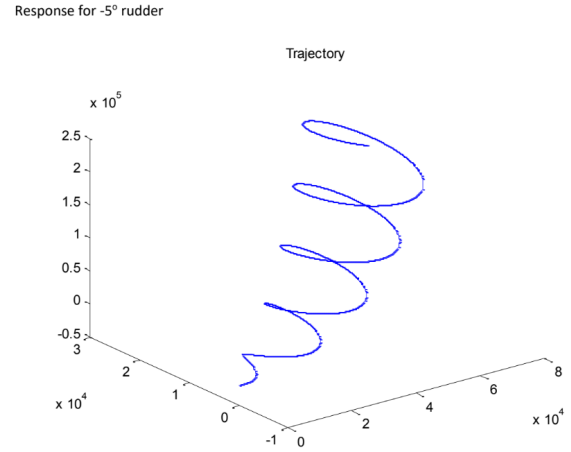


Figure 62: Reference (Benchmark) Trajectory Plot

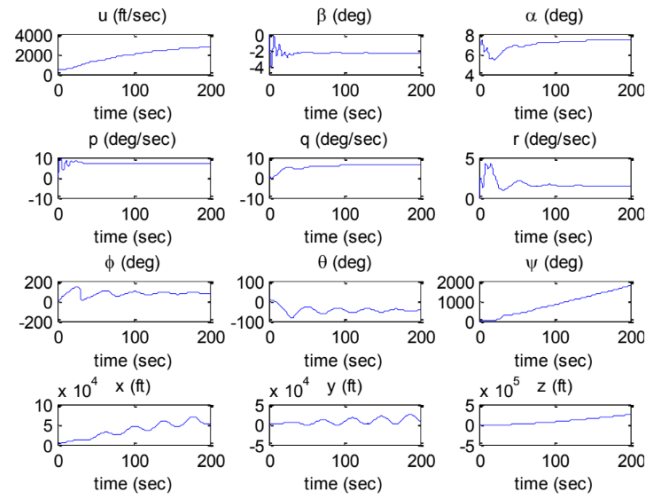


Figure 63: Reference Plots

* **+5° Elevator Deflection:** Primarily affects the pitch rate (q) and vertical velocity (w), inducing a pitching motion.

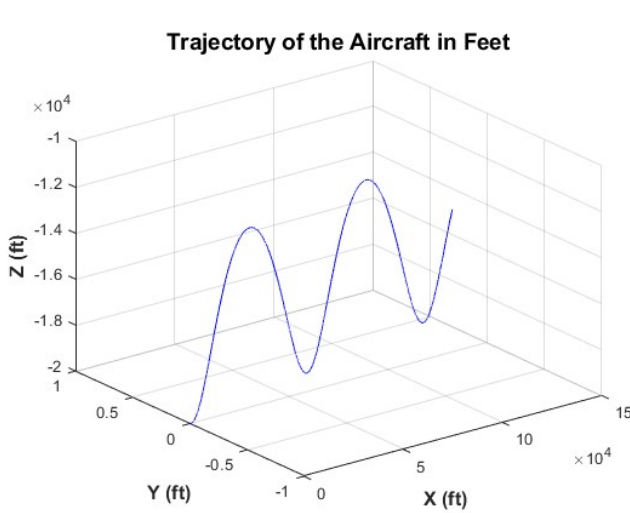


Figure 64: Simulink Simulator's Trajectory plot

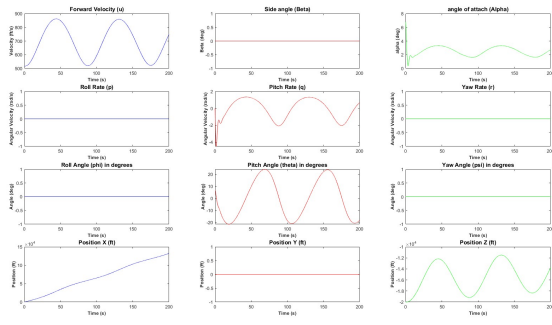


Figure 65: Simulink Simulator's Plots

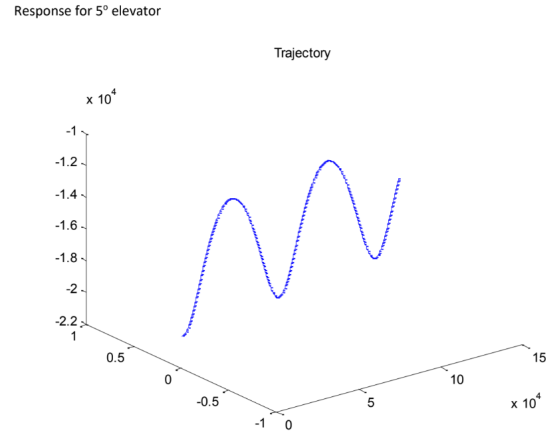


Figure 66: Reference (Benchmark) Trajectory Plot

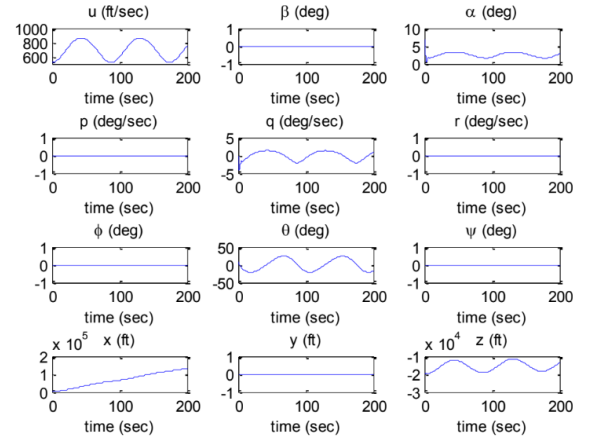


Figure 67: Reference Plots

- * **-5° Elevator Deflection:** Primarily affects the pitch rate (q) and vertical velocity (w), inducing a pitching motion.

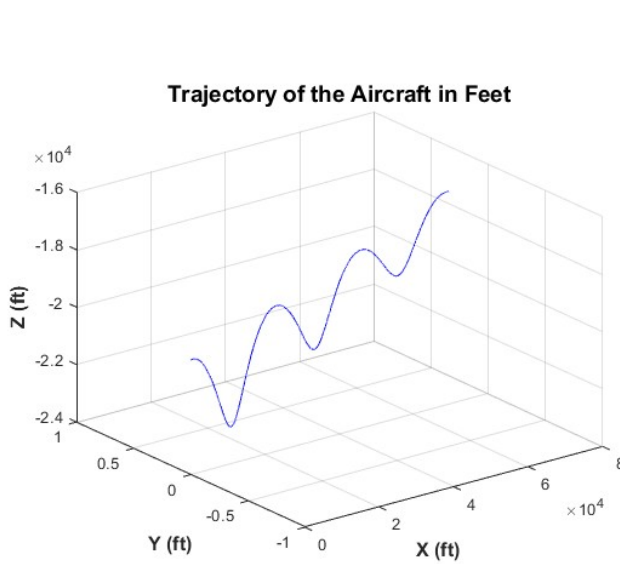


Figure 68: Simulink Simulator's Trajectory plot

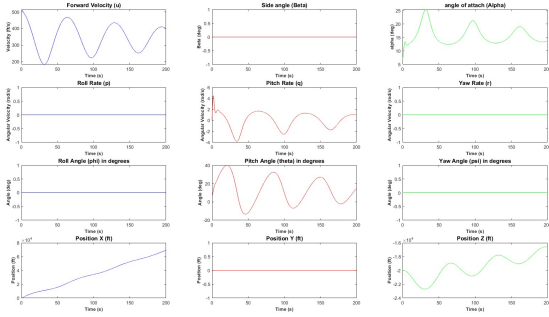


Figure 69: Simulink Simulator's Plots

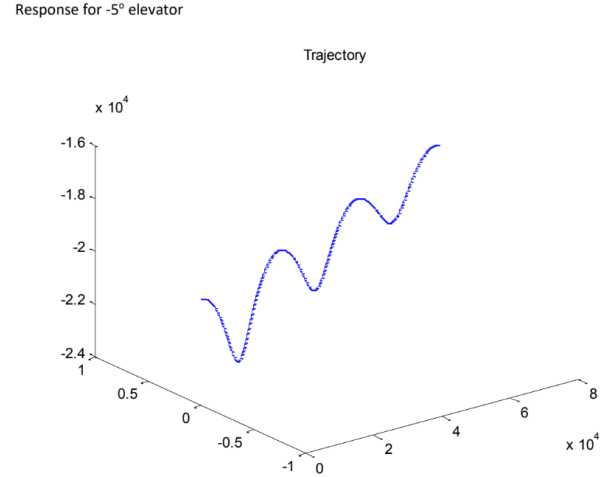


Figure 70: Reference (Benchmark) Trajectory Plot

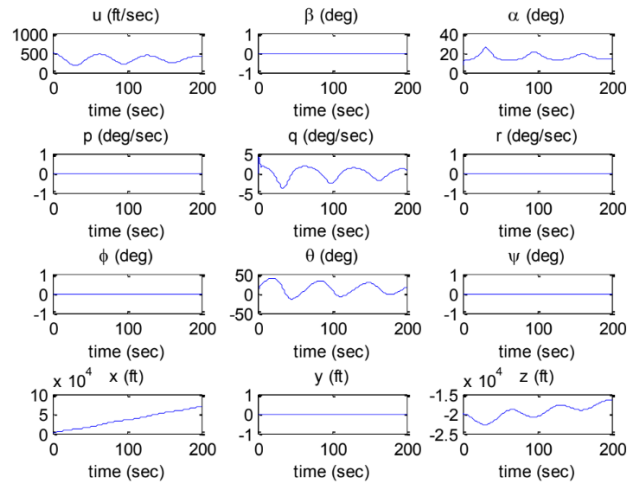


Figure 71: Reference Plots

- * **Thrust Variation:** Primarily affects the forward velocity (u).
- Response for 1000 in thrust

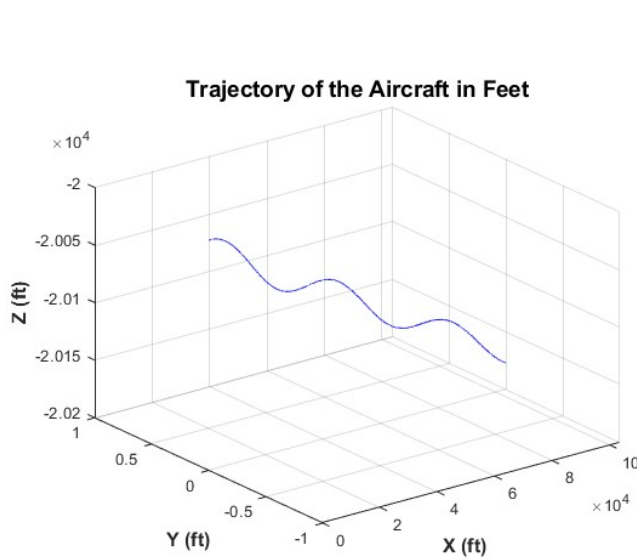


Figure 72: Simulator's Trajectory plot

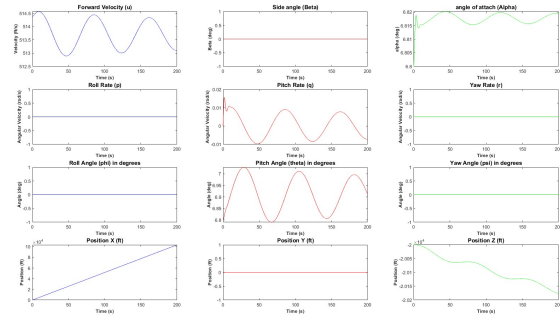


Figure 73: Simulator's Plots

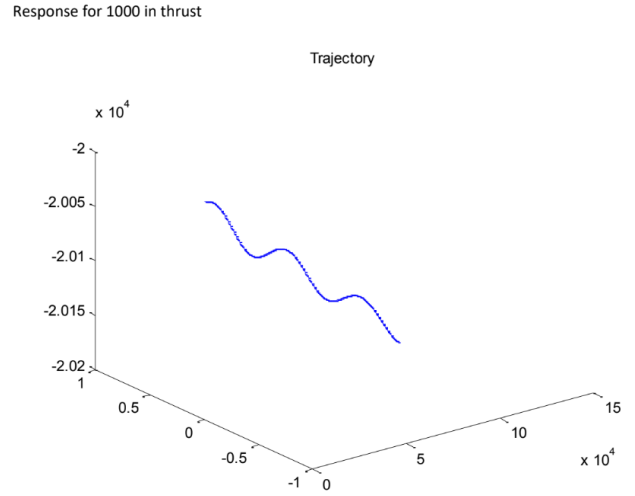


Figure 74: Reference (Benchmark) Trajectory Plot

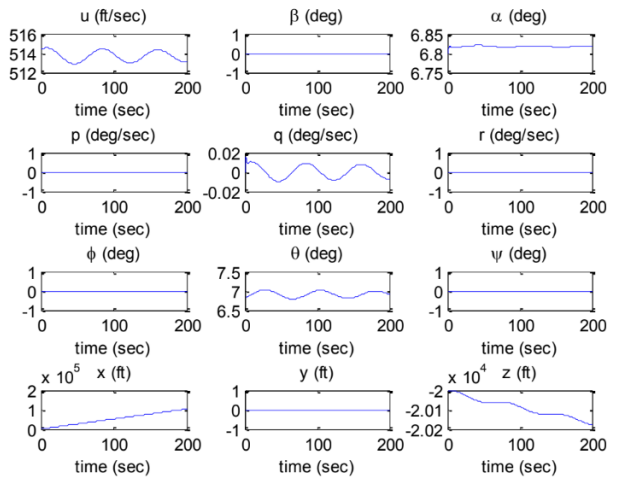


Figure 75: Reference Plots

- **Thrust Variation:** Primarily affects the forward velocity (u).
- **Response for 10000 in thrust**

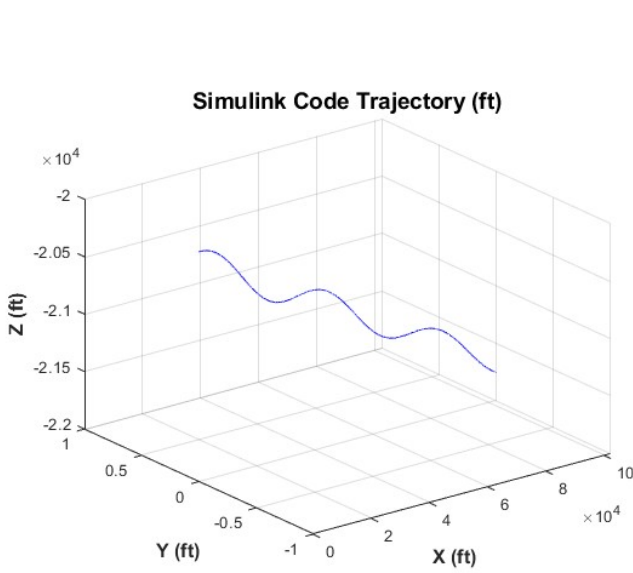


Figure 76: Simulator's Trajectory plot

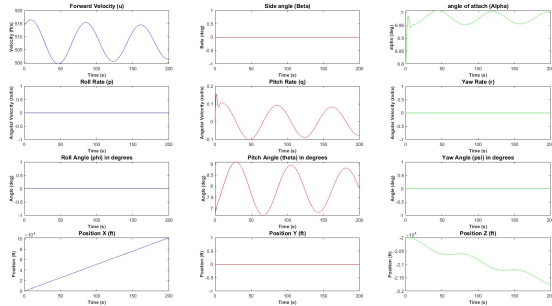


Figure 77: Simulator's Plots

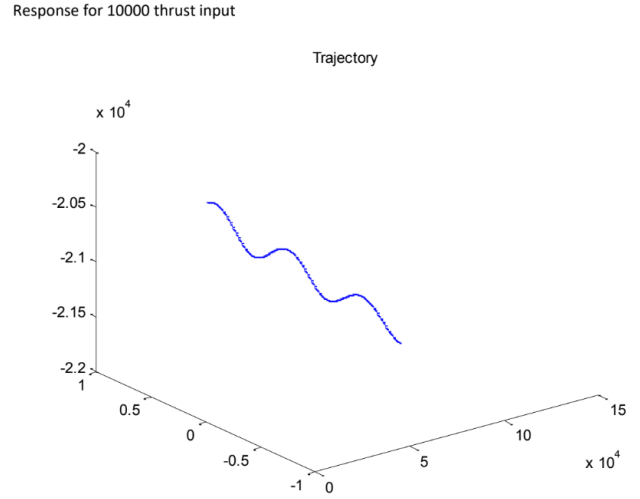


Figure 78: Reference (Benchmark) Trajectory Plot

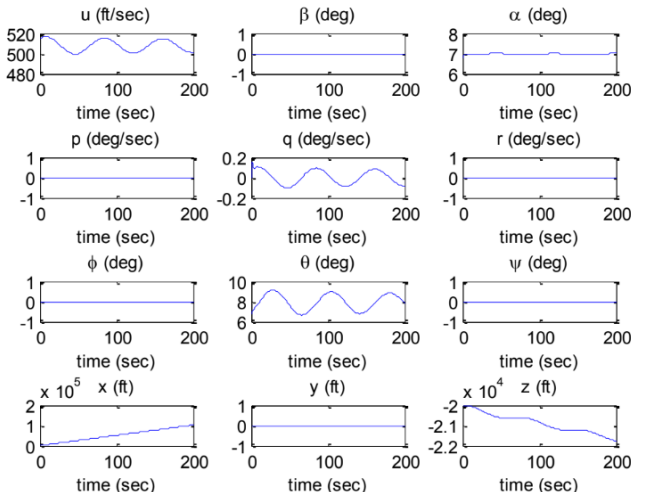


Figure 79: Reference Plots

5.4 B747-FC3 flight Condition

The below are the results for aircraft states at the flight condition number 3 at NASA Report.

- **Response for no input:** No affects induced, all plots show excellent agreement.

Simulink Code Trajectory (ft)

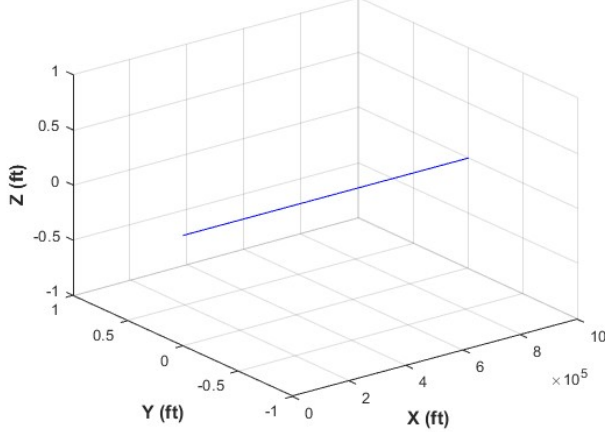


Figure 80: Simulink Trajectory Plot

Matlab Code Trajectory (ft)

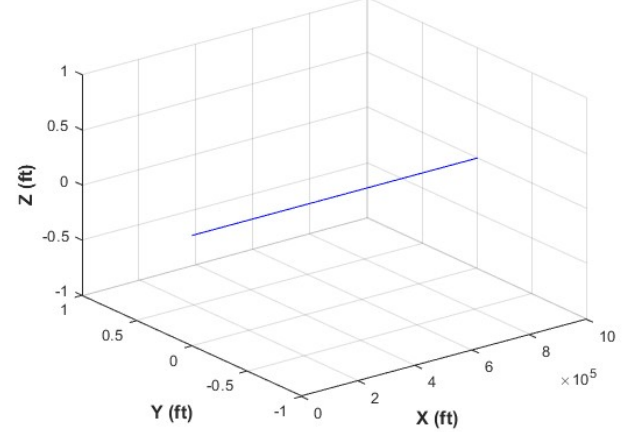


Figure 82: Matlab Trajectory Plot

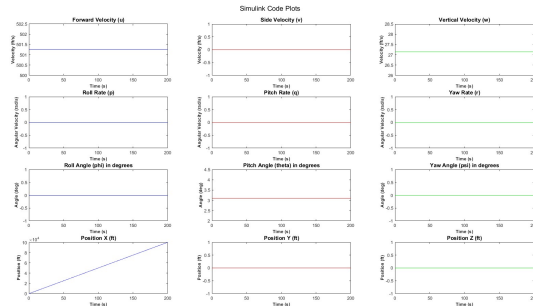


Figure 81: Simulink States Plots

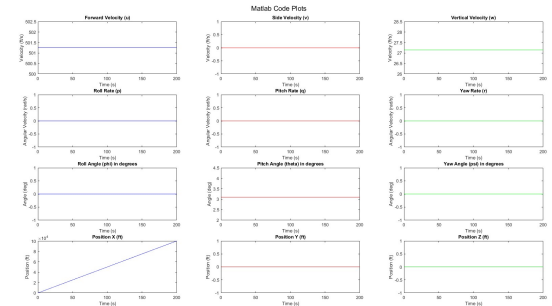


Figure 83: Matlab States Plots

- **+5° Aileron Deflection:** Primarily affects the roll rate (p) and yaw rate (r), inducing a rolling motion with slight yaw coupling.

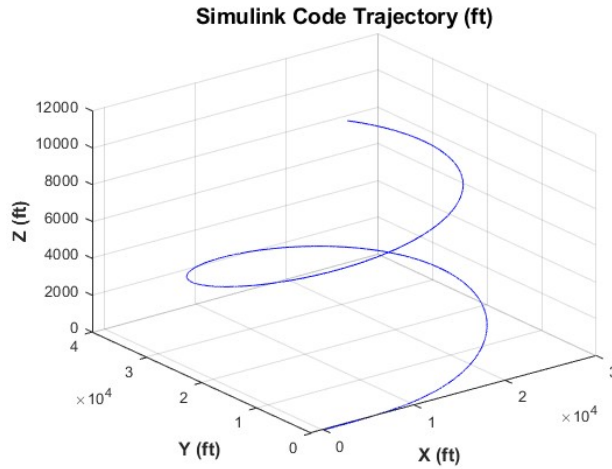


Figure 84: Simulink Trajectory Plot

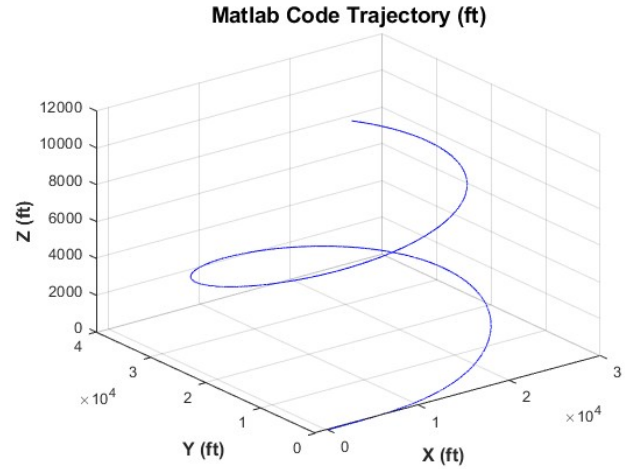


Figure 86: Matlab Trajectory Plot

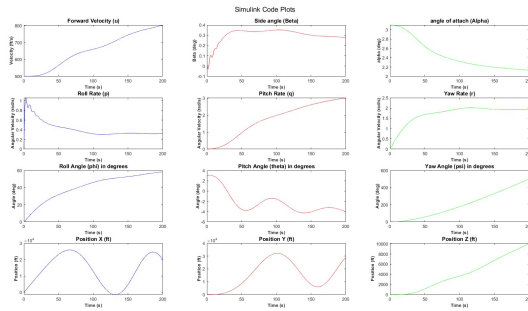


Figure 85: Simulink States Plots

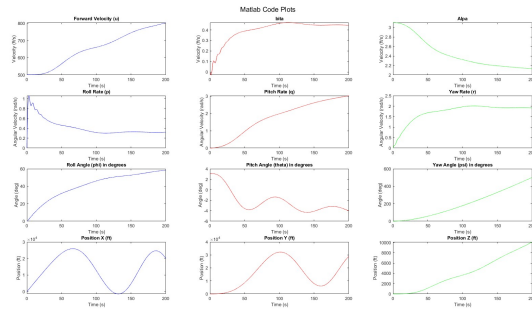


Figure 87: Matlab States Plots

- **-5° Aileron Deflection:** Primarily affects the roll rate (p) and yaw rate (r), inducing a rolling motion with slight yaw coupling.

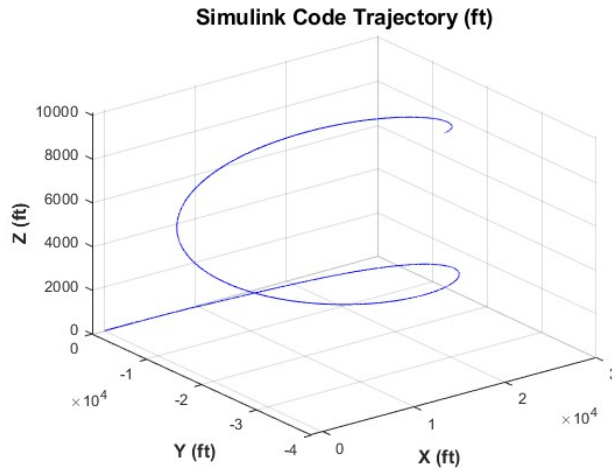


Figure 88: Simulink Trajectory Plot

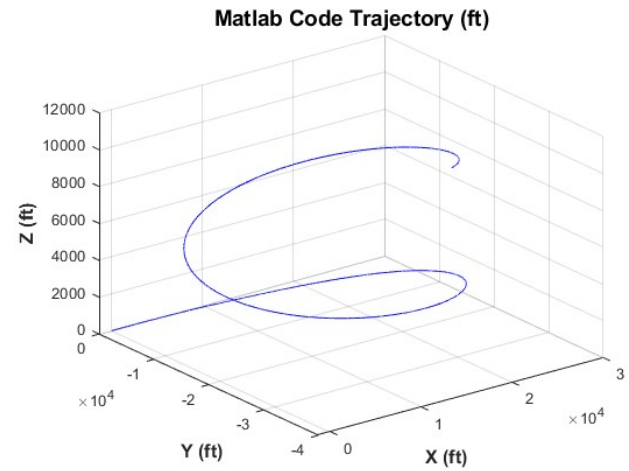


Figure 90: Matlab Trajectory Plot

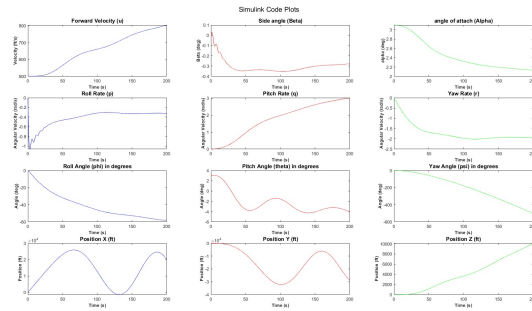


Figure 89: Simulink States Plots

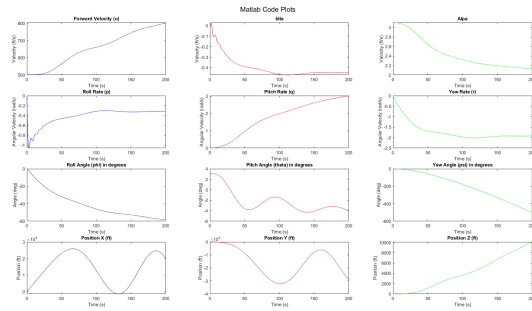


Figure 91: Matlab States Plots

- **+5° Rudder Deflection:** Primarily affects the yaw rate (r) and lateral velocity (v), inducing a yawing motion.

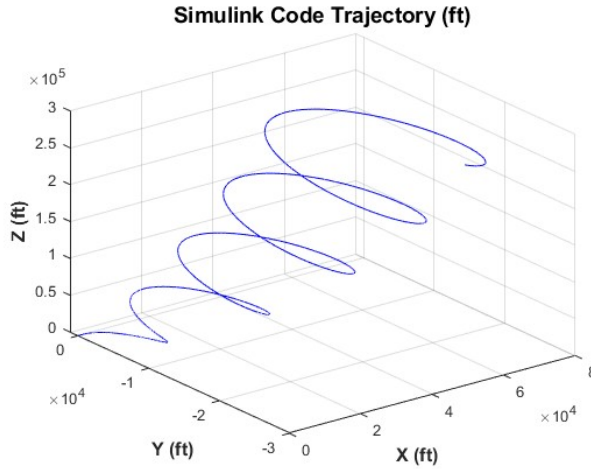


Figure 92: Simulink Trajectory Plot

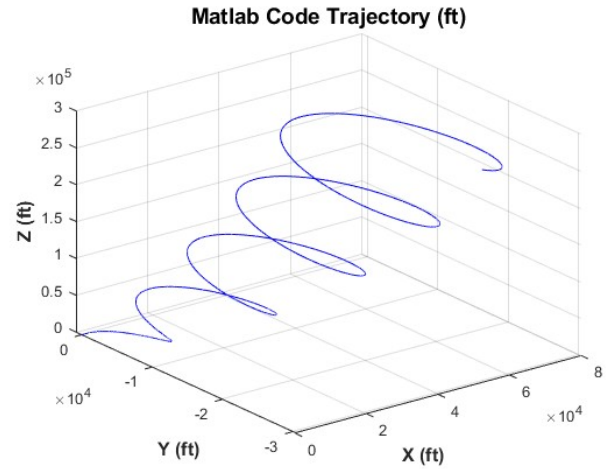


Figure 94: Matlab Trajectory Plot

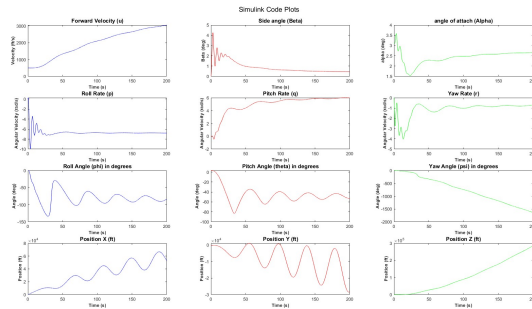


Figure 93: Simulink States Plots

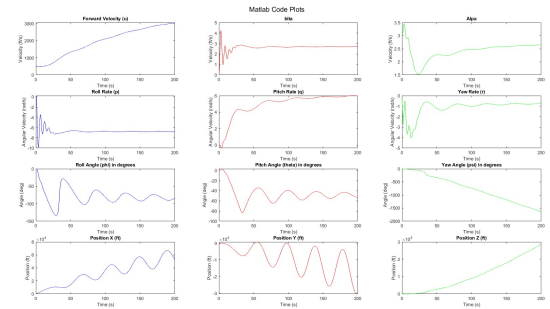


Figure 95: Matlab States Plots

- **-5° Rudder Deflection:** Primarily affects the yaw rate (r) and lateral velocity (v), inducing a yawing motion.

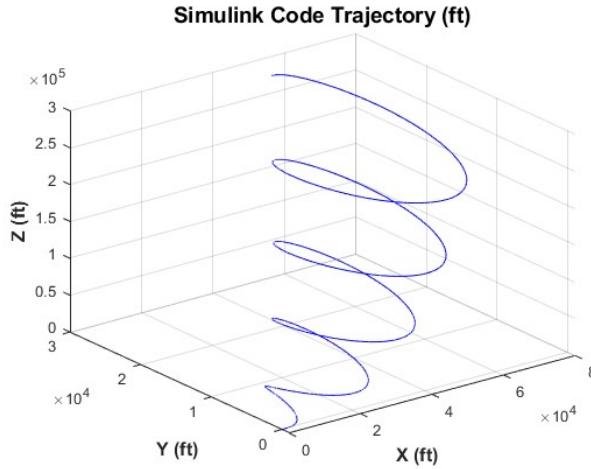


Figure 96: Simulink Trajectory Plot

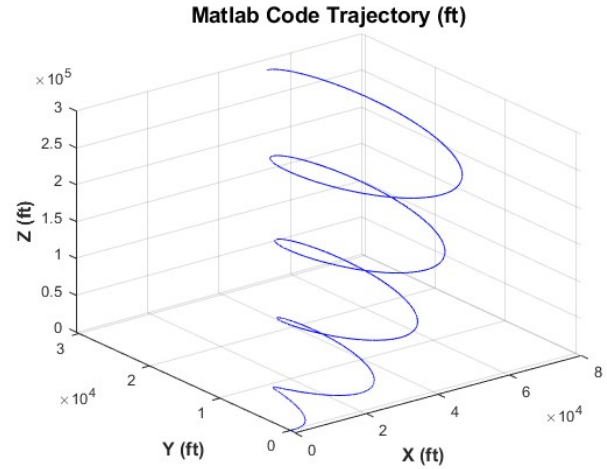


Figure 98: Matlab Trajectory Plot

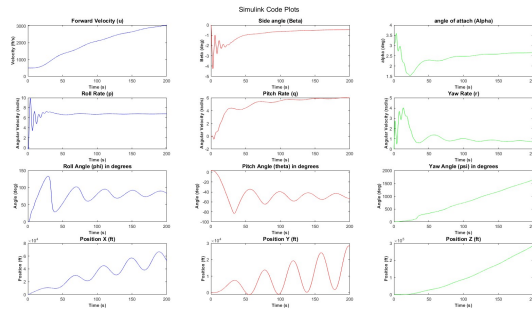


Figure 97: Simulink States Plots

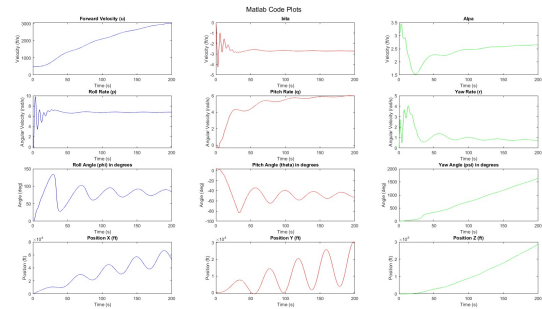


Figure 99: Matlab States Plots

- **+5° Elevator Deflection:** Primarily affects the pitch rate (q) and vertical velocity (w), inducing a pitching motion.

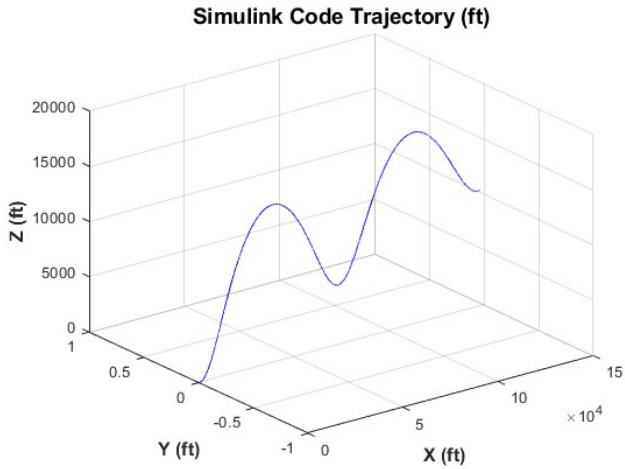


Figure 100: Simulink Trajectory Plot

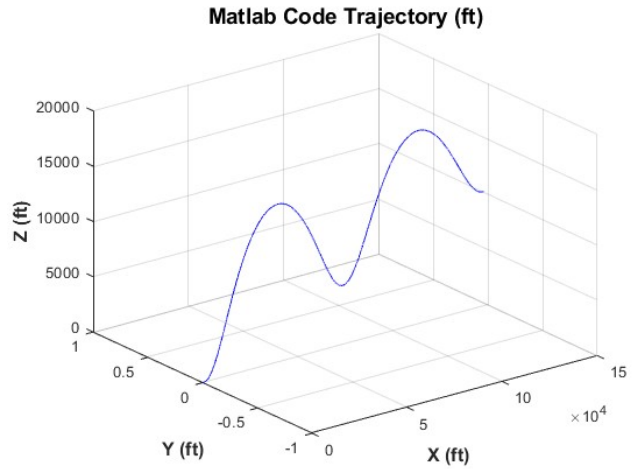


Figure 102: Matlab Trajectory Plot

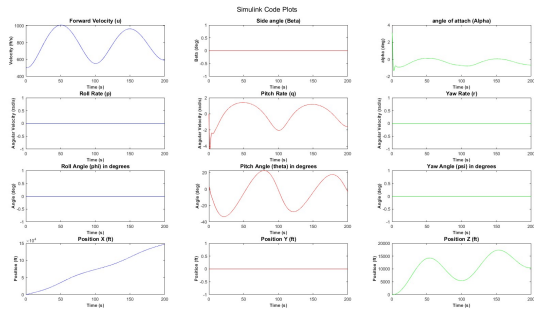


Figure 101: Simulink States Plots

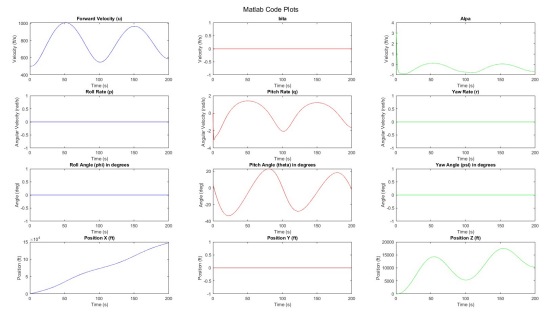


Figure 103: Matlab States Plots

- **-5° Elevator Deflection:** Primarily affects the pitch rate (q) and vertical velocity (w), inducing a pitching motion.

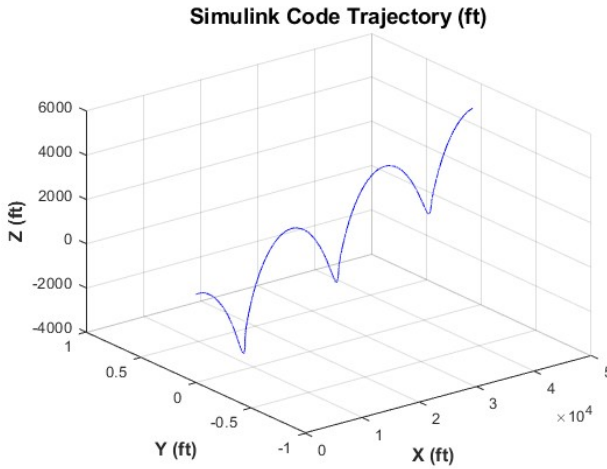


Figure 104: Simulink Trajectory Plot

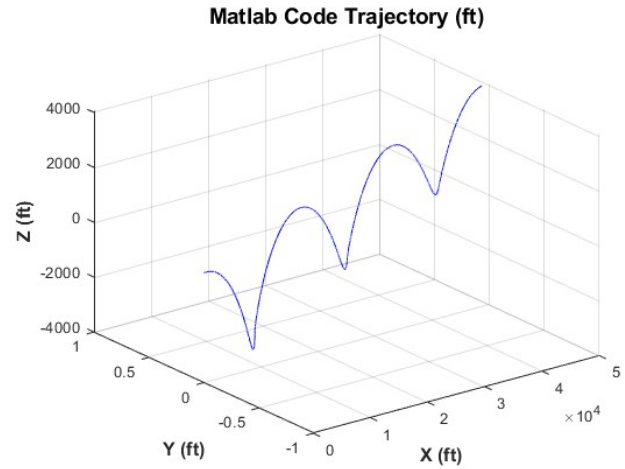


Figure 106: Matlab Trajectory Plot

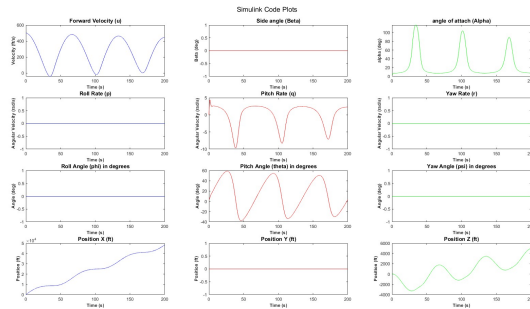


Figure 105: Simulink States Plots

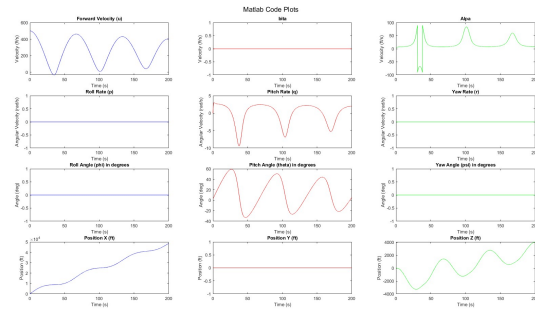


Figure 107: Matlab States Plots

- **Thrust Variation:** Primarily affects the forward velocity (u).
- **Response for 1000 in thrust**

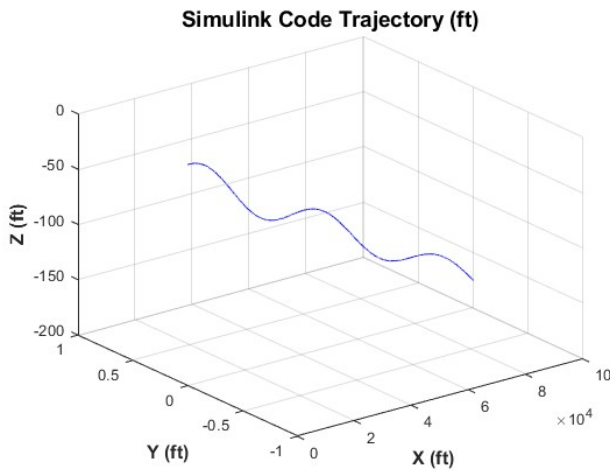


Figure 108: Simulink Trajectory Plot

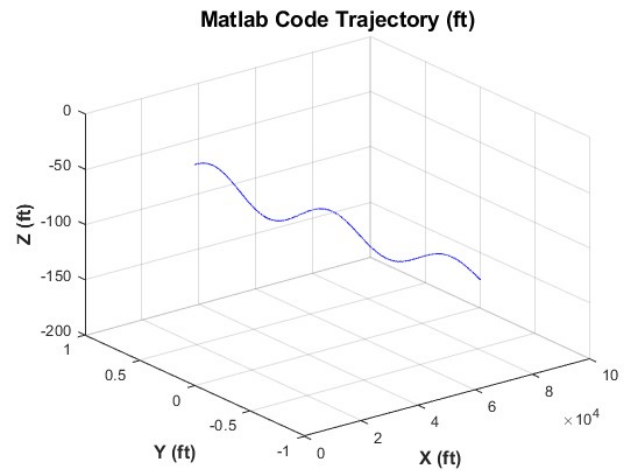


Figure 110: Matlab Trajectory Plot

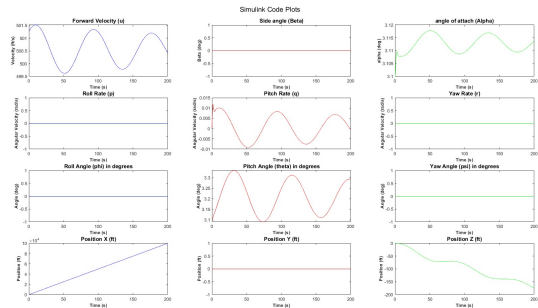


Figure 109: Simulink States Plots

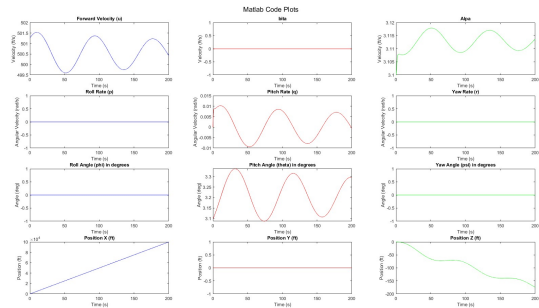


Figure 111: Matlab States Plots

- **Thrust Variation:** Primarily affects the forward velocity (u).
- **Response for 10000 in thrust**

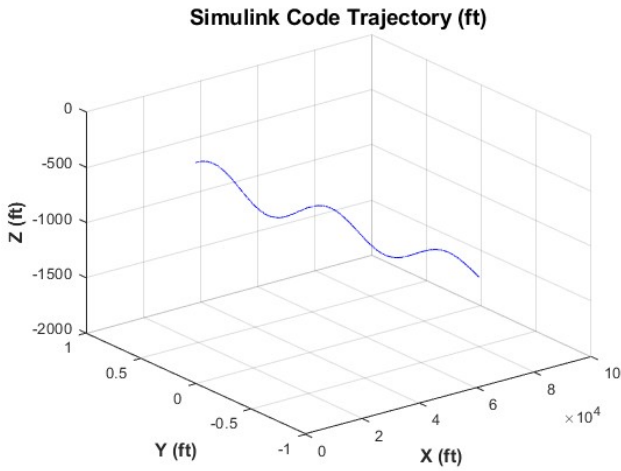


Figure 112: Simulink Trajectory Plot

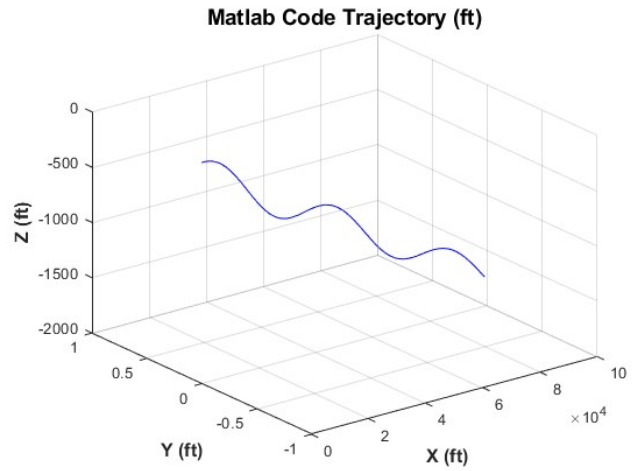


Figure 114: Matlab Trajectory Plot

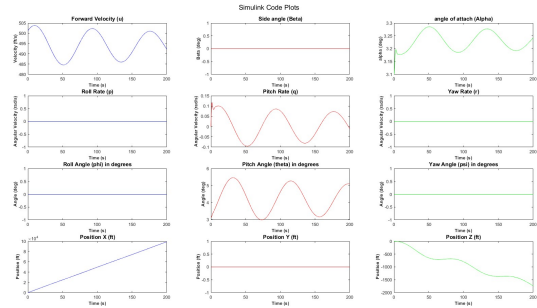


Figure 113: Simulink States Plots

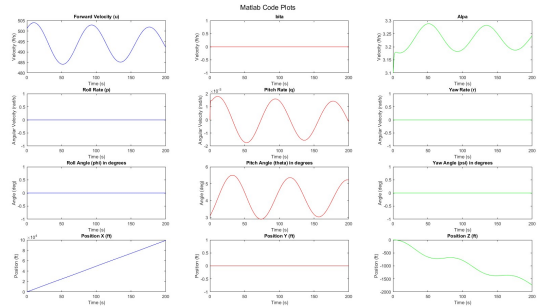


Figure 115: Matlab States Plots

6 Linearization and approximation

6.1 Steps

1-Equilibrium balance

analyse the equation in the equilibrium state and determine which state will be zero.

2-Small disturbance theory

assume each state is equivalent to the initial state + the change that happened in that state.

3-Make approximations

$$\cos(\Delta x) = 1$$

$$\sin(\Delta x) = \Delta x$$

$$\Delta x \Delta y = 0$$

where Δx and Δy are small

4-Taylor series

use Taylor series to represent the change in the state due to each of the other states

6.2 Lateral linearization

6.2.1

$$Y = mg \cos(\theta) \sin(\phi) = m(\dot{\nu} + ru - pw)$$

1. equilibrium balance

$$Y_0 = mg \cos(\theta_0) \sin(\phi_0) = m(\dot{\nu}_0 + r_0 u_0 - p_0 w_0)$$

where $Y_0 = 0$, $\phi_0 = 0$, $\dot{\nu}_0 = 0$, $r_0 = 0$, and $p_0 = 0$. we get:

$$0 = mg \cos(\theta_0) \sin(0) = m(0 + 0 \cdot u_0 - 0 \cdot w_0)$$

which simplifies to:

$$0 = 0$$

Thus, the equation reduces to a trivial identity under these conditions.

2. Small disturbance and approximations

Starting with the equation:

$$Y_0 + \Delta Y + mg \cos(\theta_0 + \Delta\theta) \sin(\phi_0 + \Delta\phi) = m(\dot{\nu}_0 + \Delta\dot{\nu} + (r_0 + \Delta r)(u_0 + \Delta u) - (p_0 + \Delta p)(w_0 + \Delta w))$$

with the conditions $Y_0 = 0$, $\phi_0 = 0$, $\dot{\nu}_0 = 0$, $r_0 = 0$, and $p_0 = 0$.

This becomes:

$$\Delta Y + mg \Delta\phi [\cos(\theta_0) \cos(\Delta\theta) - \sin(\theta_0) \sin(\Delta\theta)] = m(\Delta\dot{\nu} + \Delta r u_0 + \Delta p \omega_0)$$

Now, assuming $\cos(\Delta\theta) = 1$ and $\sin(\Delta\theta) = \Delta\theta$, we get:

$$\Delta Y + mg \Delta\phi \cos(\theta_0) - mg \Delta\phi \sin(\theta_0) \Delta\theta = m(\Delta\dot{\nu} + \Delta r u_0 - \Delta p \omega_0)$$

Then, if $\Delta\theta \Delta\phi = 0$, it further simplifies to:

$$\Delta Y + mg \Delta\phi \cos(\theta_0) = m(\Delta\dot{\nu} + \Delta r u_0 - \Delta p \omega_0)$$

3. Taylor series

Starting with the equation:

$$\frac{\Delta Y}{m} = Y_\nu \Delta\nu + Y_p \Delta p + Y_r \Delta r + Y_{\delta a} \Delta\delta a + Y_{\delta r} \Delta\delta r$$

By substituting the obtained equation from part b, we have:

$$\Delta\dot{\nu} = Y_\nu \Delta\nu + Y_p \Delta p + Y_r \Delta r + Y_{\delta a} \Delta\delta a + Y_{\delta r} \Delta\delta r + g \cos(\theta_0) \Delta\phi - \Delta r u_0 + \Delta p \omega_0$$

6.2.2

$$r = \dot{\psi} \cos(\theta) \cos(\phi) - \dot{\theta} \sin(\phi)$$

1. Equilibrium balance:

$$\begin{aligned} r &= \dot{\psi}_0 \cos(\theta_0) \cos(\phi_0) - \dot{\theta}_0 \sin(\phi_0) \\ r &= \dot{\psi}_0 \cos(\theta_0) \cos(\phi_0) - \dot{\theta}_0 \sin(\phi_0) \end{aligned}$$

Substituting the values $r_0 = 0$, $\dot{\psi}_0 = 0$, $\phi_0 = 0$, and $\dot{\theta}_0 = 0$, we have:

$$0 = 0 \cdot \cos(0) \cos(0) - 0 \cdot \sin(0)$$

This simplifies to:

$$0 = 0$$

2. small disturbance and approximation

$$r_0 + \Delta r = (\dot{\psi}_0 + \Delta\dot{\psi}) \cos(\theta_0 + \Delta\theta) \cos(\phi_0 + \Delta\phi) - (\dot{\theta}_0 + \Delta\dot{\theta}) \sin(\phi_0 + \Delta\phi)$$

Given the conditions $r_0 = 0$, $\dot{\psi}_0 = 0$, $\phi_0 = 0$, and $\dot{\theta}_0 = 0$, we have:

$$\Delta r = \Delta\dot{\psi} [\cos(\theta_0) \cos(\Delta\theta) - \sin(\theta_0) \sin(\Delta\theta)] \cos(\Delta\phi) - \Delta\dot{\theta} \sin(\Delta\phi)$$

Using the approximations $\cos(\Delta\theta) \approx 1$ and $\sin(\Delta\theta) \approx \Delta\theta$, this becomes:

$$\Delta r = \Delta\dot{\psi} \cos(\theta_0) - \sin(\theta_0) \Delta\theta \Delta\dot{\psi} \cos(\Delta\phi) - \Delta\dot{\theta} \Delta\phi$$

By further approximating $\Delta\theta \Delta\dot{\psi} = 0$ and $\Delta\dot{\theta} \Delta\phi = 0$, we arrive at:

$$\Delta r = \Delta\dot{\psi} \cos(\theta_0)$$

3. Taylor series

$$\Delta\dot{\psi} = \Delta r \sec(\theta_0)$$

$$p = \dot{\phi} - \dot{\psi} \sin(\theta)$$

1. Equilibrium balance

Starting with the equation:

$$p_0 = \dot{\phi}_0 - \dot{\psi}_0 \sin(\theta_0)$$

Given the conditions $p_0 = 0$, $\dot{\phi}_0 = 0$, and $\dot{\psi}_0 = 0$, we get

$$0 = 0 - 0 \cdot \sin(\theta_0)$$

which is trivial

$$0 = 0$$

2. Small disturbance and approximation

$$p_0 + \Delta p = \dot{\phi}_0 + \Delta\dot{\phi} - (\dot{\psi}_0 + \Delta\dot{\psi}) \sin(\theta_0 + \Delta\theta)$$

Substituting the values $p_0 = 0$, $\dot{\phi}_0 = 0$, and $\dot{\psi}_0 = 0$, we have:

$$\Delta p = \Delta\dot{\phi} - \Delta\dot{\psi} [\sin(\theta_0) \cos(\Delta\theta) + \cos(\theta_0) \sin(\Delta\theta)]$$

By approximating $\cos(\Delta\theta) \approx 1$ and $\sin(\Delta\theta) \approx \Delta\theta$, we get:

$$\Delta p = \Delta\dot{\phi} - \Delta\dot{\psi} (\sin(\theta_0) + \cos(\theta_0) \Delta\theta) \Delta\dot{\psi}$$

By further approximating $\Delta\theta \Delta\dot{\psi} = 0$, this simplifies to:

$$\Delta p = \Delta\dot{\phi} - \Delta\dot{\psi} \sin(\theta_0)$$

3. Taylor series

by referring to equation 2 where

$$\Delta r = \Delta\dot{\psi} \cos(\theta_0)$$

then we get:

$$\Delta\dot{\phi} = \Delta p + \Delta r \tan(\theta_0)$$

$$N = -I_{xz}\dot{p} + I_z\dot{r} + pq(I_y - I_x) + I_{xz}qr$$

] The coupled equations

$$L = I_x\dot{p} - I_{xz}\dot{r} + qr(I_z - I_y) - I_{xz}pq$$

$$N = -I_{xz}\dot{p} + I_z\dot{r} + pq(I_y - I_x) + I_{xz}qr$$

1. Equilibrium balance

$$L_0 = I_x\dot{p}_0 - I_{xz}\dot{r}_0 + qr(I_z - I_y) - I_{xz}pq_0$$

$$N_0 = -I_{xz}\dot{p}_0 + I_z\dot{r}_0 + pq(I_y - I_x) + I_{xz}qr_0$$

with $L_0 = 0$, $N_0 = 0$, $\dot{p}_0 = 0$, $\dot{r}_0 = 0$, $r_0 = 0$, $q_0 = 0$, and $p_0 = 0$ bot equations give trivial solution

2. Small disturbance and approximation

$$L_0 + \Delta L = I_x(\dot{p}_0 + \Delta\dot{p}) - I_{xz}(\dot{r}_0 + \Delta\dot{r}) + (q_0 + \Delta q)(r_0 + \Delta r)(I_z - I_y) - I_{xz}(p_0 + \Delta p)(q_0 + \Delta q)$$

$$N_0 + \Delta N = -I_{xz}(\dot{p}_0 + \Delta\dot{p}) + I_z(\dot{r}_0 + \Delta\dot{r}) + (p_0 + \Delta p)(q_0 + \Delta q)(I_y - I_x) + I_{xz}(q_0 + \Delta q)(r_0 + \Delta r)$$

With $L_0 = 0$, $N_0 = 0$, $\dot{p}_0 = 0$, $\dot{r}_0 = 0$, $r_0 = 0$, $q_0 = 0$, $p_0 = 0$, the equations reduce to:

$$\Delta L = \Delta\dot{p}I_x - I_{xz}\Delta r\Delta\dot{r}$$

$$\Delta N = -\Delta\dot{p}I_{xz} + I_z\Delta\dot{r}$$

In matrix form, we can write:

$$\begin{bmatrix} \Delta L \\ \Delta N \end{bmatrix} = \begin{bmatrix} I_x & -I_{xz} \\ -I_{xz} & I_z \end{bmatrix} \begin{bmatrix} \Delta\dot{p} \\ \Delta\dot{r} \end{bmatrix}$$

Thus, we get:

$$\begin{bmatrix} \Delta\dot{p} \\ \Delta\dot{r} \end{bmatrix} = \frac{1}{I_z I_x - I_{xz}^2} \begin{bmatrix} I_z + I_{xz} \\ I_{xz} + I_x \end{bmatrix} \begin{bmatrix} \Delta L \\ \Delta N \end{bmatrix}$$

$$G = \frac{1}{I_z I_x - I_{xz}^2}$$

Then:

$$\Delta\dot{p} = G(I_z\Delta L + I_{xz}\Delta N)$$

$$\Delta\dot{r} = G(I_{xz}\Delta L + I_x\Delta N)$$

3. Taylor series

$$\frac{\Delta L}{I_x} = L_\nu\Delta\nu + L_p\Delta p + L_r\Delta r + L_{\delta a}\Delta\delta a + L_{\delta r}\Delta\delta r$$

$$\frac{\Delta N}{I_x} = N_\nu\Delta\nu + N_p\Delta p + N_r\Delta r + N_{\delta a}\Delta\delta a + N_{\delta r}\Delta\delta r$$

Letting

$$L'_a = \frac{1}{G}L_a + \frac{I_{xz}}{I_x}N_a, \quad N'_a = \frac{I_{xz}}{I_z}L_a + \frac{1}{G}N_a$$

Then we have the equations for \dot{p} and \dot{r} :

$$\Delta\dot{p} = L'_\nu\Delta\nu + L'_p\Delta p + L'_r\Delta r + L'_{\delta a}\Delta\delta a + L'_{\delta r}\Delta\delta r$$

$$\Delta\dot{r} = N'_\nu\Delta\nu + N'_p\Delta p + N'_r\Delta r + N'_{\delta a}\Delta\delta a + N'_{\delta r}\Delta\delta r$$

Lateral State Space representation:

$$\begin{bmatrix} \Delta\dot{\nu} \\ \Delta\dot{p} \\ \Delta\dot{r} \\ \Delta\dot{\phi} \\ \Delta\dot{\psi} \end{bmatrix} = \begin{bmatrix} Y_\nu & Y_p + \omega_0 & Y_r - u_0 & g \cos(\theta_0) & 0 \\ L'_\nu & L'_p & L'_r & 0 & 0 \\ N'_\nu & N'_p & N'_r & 0 & 0 \\ 0 & 1 & \tan(\theta_0) & 0 & 0 \\ 0 & 0 & \sec(\theta_0) & 0 & 0 \end{bmatrix} \begin{bmatrix} \Delta\nu \\ \Delta p \\ \Delta r \\ \Delta\phi \\ \Delta\psi \end{bmatrix} + \begin{bmatrix} Y_{\delta a} & Y_{\delta r} \\ L'_{\delta a} & L'_{\delta r} \\ N'_{\delta a} & N'_{\delta r} \\ 0 & 0 \\ 0 & 0 \end{bmatrix} \begin{bmatrix} \Delta\delta a \\ \Delta\delta r \end{bmatrix}$$

6.3 Longitudinal linearization

6.3.1

$$X - mg \sin(\theta_0) = m(\dot{u}_0 + q_0 w_0 - r_0 \nu_0)$$

1. Equilibrium balance:

$$X_0 - mg \sin(\theta_0) = m(\dot{u}_0 + q_0 w_0 - r_0 \nu_0)$$

where $\dot{u}_0 = 0$, $q_0 = 0$, $r_0 = 0$, $\nu_0 = 0$. The equation reduces to:

$$X_0 = mg \sin(\theta_0)$$

2. Small disturbance

$$X_0 + \Delta X - mg \sin(\theta_0 + \Delta\theta) = m(\dot{u}_0 + \Delta\dot{u} + (q_0 + \Delta q)(w_0 + \Delta w))$$

where $\dot{u}_0 = 0$, $q_0 = 0$, $r_0 = 0$, $\nu_0 = 0$.

We get:

$$X_0 + \Delta X - mg(\sin(\theta_0) \cos(\Delta\theta) + \cos(\theta_0) \sin(\Delta\theta)) = m(\Delta\dot{u} + \Delta q \Delta w + \Delta q w_0 - \Delta r \Delta\nu)$$

Approximating $\cos(\Delta\theta) = 1$, $\sin(\Delta\theta) = \Delta\theta$, $\Delta r \Delta\nu = 0$, and $\Delta q \Delta w = 0$, we get:

$$X_0 + \Delta X - mg(\sin(\theta_0) + \cos(\theta_0)\Delta\theta) = m(\Delta\dot{u} + \Delta q w_0)$$

We know from step a that

$$X_0 - mg \sin(\theta_0) = 0$$

by substituting,

$$\Delta X = m(g \cos(\theta_0)\Delta\theta + (\Delta\dot{u} + \Delta q w_0))$$

3. Taylor series

$$\frac{\Delta X}{m} = X_u \Delta u + X_w \Delta w + X_{\delta e} \Delta \delta_e + X_{\delta t} \Delta \delta_t$$

$$\Delta\dot{u} = X_u \Delta u + X_w \Delta w + X_{\delta e} \Delta \delta_e + X_{\delta t} \Delta \delta_t - g \Delta\theta \cos(\theta_0) - \Delta q w_0$$

6.3.2

$$Z + mg \cos(\theta) \cos(\phi) = m(\dot{w} + p\nu - qu)$$

1. Equilibrium balance

$$Z_0 + mg \cos(\theta_0) \cos(\phi_0) = m(\dot{w}_0 + p_0 \nu_0 - q_0 u_0)$$

With $\phi_0 = 0$, $\dot{w}_0 = 0$, $p_0 = 0$, $\nu_0 = 0$, $q_0 = 0$, the equation reduces to:

$$Z_0 = -mg \cos(\theta_0)$$

2. Small disturbance

$$Z_0 + \Delta Z + mg \cos(\theta_0 + \Delta\theta) \cos(\phi_0 + \Delta\phi) = m(\dot{w}_0 + \Delta\dot{w}_0 + (p_0 + \Delta p)(\nu_0 + \Delta\nu) - (q_0 + \Delta q)(u_0 + \Delta u))$$

With $\phi_0 = 0$, $\dot{w}_0 = 0$, $p_0 = 0$, $\nu_0 = 0$, and $q_0 = 0$, the equation reduces to:

$$Z_0 + \Delta Z + mg [\cos(\theta_0) \cos(\Delta\theta) - \sin(\theta_0) \sin(\Delta\theta)] = m(\Delta\dot{w} + \Delta p \Delta\nu - \Delta q u_0 - \Delta q \Delta u)$$

After approximating $\cos(\Delta\theta) = 1$, $\sin(\Delta\theta) = \Delta\theta$, $\cos(\Delta\phi) = 1$, $\Delta p \Delta\nu = 0$, and $\Delta q \Delta u = 0$, we get:

$$Z_0 + \Delta Z + mg \cos(\theta_0) - mg \Delta\theta \sin(\theta_0) = m(\Delta\dot{w} - u_0 \Delta q)$$

from part a we know that:

$$Z_0 + mg \cos(\theta_0) = 0$$

Then we have:

$$\Delta Z = mg \Delta\theta \sin(\theta_0) + m(\Delta\dot{w} - u_0 \Delta q)$$

3. Taylor series

$$\frac{\Delta Z}{m} = Z_u \Delta u + Z_w \Delta w + Z_{\dot{w}} \Delta \dot{w} + Z_q \Delta q + Z_{\delta e} \Delta \delta e + Z_{\delta t} \Delta \delta t$$

Then we get:

$$\Delta\dot{w} = \frac{Z_u \Delta u}{1 - Z_{\dot{w}}} + \frac{Z_w \Delta w}{1 - Z_{\dot{w}}} + \frac{Z_q \Delta q}{1 - Z_{\dot{w}}} + \frac{Z_{\delta e} \Delta \delta e}{1 - Z_{\dot{w}}} + \frac{Z_{\delta t} \Delta \delta t}{1 - Z_{\dot{w}}} - \frac{g \Delta\theta \sin(\theta_0)}{1 - Z_{\dot{w}}} + \frac{u_0 \Delta q}{1 - Z_{\dot{w}}}$$

6.3.3

$$M = I_y \dot{q} + r q (I_x - I_z) + I_{xz} (p^2 - r^2)$$

1. Equilibrium balance

$$M_0 = I_y \dot{q}_0 + r_0 q_0 (I_x - I_z) + I_{xz} (p_0^2 - r_0^2)$$

where $M_0 = 0$, $\dot{q}_0 = 0$, $r_0 = 0$, $q_0 = 0$, $p_0 = 0$

This leads to trivial solution:

$$0 = 0 \quad (\text{trivial solution})$$

2. Small disturbance

$$M_0 + \Delta M = I_y (\dot{q}_0 + \Delta \dot{q}) + (r_0 + \Delta r)(q_0 + \Delta q)(I_x - I_z) + I_{xz} ((p_0 + \Delta p)^2 - (r_0 + \Delta r)^2)$$

Where:

$$M_0 = 0, \quad \dot{q}_0 = 0, \quad r_0 = 0, \quad q_0 = 0, \quad p_0 = 0$$

This reduces to:

$$\Delta M = I_y \Delta \dot{q} + \Delta r \Delta q (I_x - I_z) + I_{xz} ((\Delta p)^2 - (\Delta r)^2)$$

With approximations:

$$\Delta r \Delta q = 0, \quad (\Delta p)^2 = 0, \quad \text{and} \quad (\Delta r)^2 = 0$$

Which gives:

$$\Delta M = I_y \Delta \dot{q}$$

3. Taylor series

$$\frac{\Delta M}{I_y} = M_u \Delta u + M_w \Delta w + M_{\dot{w}} \Delta \dot{w} + M_q \Delta q + M_{\delta e} \Delta \delta e + M_{\delta t} \Delta \delta t$$

from part 6.32, we can substitute with \dot{w}

$$\begin{aligned} \Delta \dot{q} &= (M_u + M_{\dot{w}} \frac{Z_u}{1 - Z_{\dot{w}}}) \Delta u + (M_w + M_{\dot{w}} \frac{Z_w}{1 - Z_{\dot{w}}}) \Delta w - M_{\dot{w}} \frac{g \sin(\theta_0)}{1 - Z_{\dot{w}}} \Delta \theta \\ &+ (M_q + M_{\dot{w}} \frac{Z_q + u_0}{1 - Z_{\dot{w}}}) \Delta q + (M_{\delta e} + M_{\dot{w}} \frac{Z_{\delta e}}{1 - Z_{\dot{w}}}) \Delta \delta e + (M_{\delta t} + M_{\dot{w}} \frac{Z_{\delta t}}{1 - Z_{\dot{w}}}) \Delta \delta t \end{aligned}$$

6.3.4

$$q = \dot{\theta} \cos \phi + \dot{\psi} \cos \theta \sin \phi$$

1. Equilibrium balance

$$q_0 + \Delta q = \dot{\theta}_0 \cos \phi_0 + \dot{\psi}_0 \cos \theta_0 \sin \phi_0$$

Since $q_0 = 0, \dot{\theta}_0 = 0, \phi_0 = 0, \dot{\psi}_0 = 0$, the equation reduces to the trivial solution: $0 = 0$.

2. Small disturbance:

$$q_0 + \Delta q = (\dot{\theta}_0 + \Delta \dot{\theta}) \cos(\phi_0 + \Delta \phi) + (\dot{\psi}_0 + \Delta \dot{\psi}) \cos(\theta_0 + \Delta \theta) \sin(\phi_0 + \Delta \phi)$$

With $q_0 = 0, \dot{\theta}_0 = 0, \phi_0 = 0, \dot{\psi}_0 = 0$, the equation reduces to

$$\Delta q = \Delta \dot{\theta} \cos(\Delta \phi) + \Delta \psi (\cos(\theta_0) \cos(\Delta \theta) - \sin(\theta_0) \sin(\Delta \theta)) \sin(\Delta \phi)$$

With the approximations $\cos(\Delta \phi) = 1, \sin(\Delta \theta) = \Delta \theta, \cos(\Delta \theta) = 1$, and $\sin(\Delta \phi) = \Delta \phi$, we get

$$\Delta q = \Delta \dot{\theta} + \Delta \psi (\Delta \phi \cos(\theta_0) - \sin(\theta_0) \Delta \theta \Delta \phi)$$

With the approximations $\Delta \psi \Delta \phi = 0$ and $\Delta \theta \Delta \phi \Delta \psi = 0$, we obtain

$$\Delta q = \Delta \dot{\theta}$$

3. Taylor series

$$\Delta \dot{\theta} = \Delta q$$

Longitudinal State Space representation

$$\begin{bmatrix} \Delta \dot{u} \\ \Delta \dot{w} \\ \Delta \dot{q} \\ \Delta \dot{\theta} \end{bmatrix} = \begin{bmatrix} X_u & X_w & -w_0 & -g \cos(\theta_0) \\ \frac{Z_u}{1-Z_{\dot{w}}} & \frac{Z_w}{1-Z_{\dot{w}}} & \frac{Z_q+u_0}{1-Z_{\dot{w}}} & -\frac{g \sin(\theta_0)}{1-Z_{\dot{w}}} \\ M_u + M_{\dot{w}} \frac{Z_u}{1-Z_{\dot{w}}} & M_w + M_{\dot{w}} \frac{Z_w}{1-Z_{\dot{w}}} & M_q + M_{\dot{w}} \frac{Z_q+u_0}{1-Z_{\dot{w}}} & -M_{\dot{w}} \frac{g \sin(\theta_0)}{1-Z_{\dot{w}}} \\ 0 & 0 & 1 & 0 \end{bmatrix} \begin{bmatrix} \Delta u \\ \Delta w \\ \Delta q \\ \Delta \theta \end{bmatrix} + \begin{bmatrix} X_{\delta e} & X_{\delta t} \\ \frac{Z_{\delta e}}{1-Z_{\dot{w}}} & \frac{Z_{\delta t}}{1-Z_{\dot{w}}} \\ M_{\delta e} + M_{\dot{w}} \frac{Z_{\delta e}}{1-Z_{\dot{w}}} & M_{\delta t} + M_{\dot{w}} \frac{Z_{\delta t}}{1-Z_{\dot{w}}} \\ 0 & 0 \end{bmatrix} \begin{bmatrix} \Delta \delta e \\ \Delta \delta t \end{bmatrix}$$

6.4 Longitudinal approximations

6.4.1 Short-period appoximation

An approximation to the short-period mode of motion can be obtained by assuming $u = 0$ and dropping the X-force equation.

$$\begin{bmatrix} \Delta \dot{w} \\ \Delta \dot{q} \end{bmatrix} = \begin{bmatrix} \frac{Z_w}{1-Z_{\dot{w}}} & \frac{Z_q+u_0}{1-Z_{\dot{w}}} \\ M_w + M_{\dot{w}} \frac{Z_w}{1-Z_{\dot{w}}} & M_q + M_{\dot{w}} \frac{Z_q+u_0}{1-Z_{\dot{w}}} \end{bmatrix} \begin{bmatrix} \Delta w \\ \Delta q \end{bmatrix} + \begin{bmatrix} \frac{Z_{\delta e}}{1-Z_{\dot{w}}} & \frac{Z_{\delta t}}{1-Z_{\dot{w}}} \\ M_{\delta e} + M_{\dot{w}} \frac{Z_{\delta e}}{1+Z_{\dot{w}}} & M_{\delta t} + M_{\dot{w}} \frac{Z_{\delta t}}{1+Z_{\dot{w}}} \end{bmatrix} \begin{bmatrix} \Delta \delta e \\ \Delta \delta t \end{bmatrix}$$

To calculate the frequency ω and damping ratio ζ we need to get the charactaristique equation

$$|\lambda I - A| = 0$$

This would give

$$\lambda^2 - \left(\frac{Z_w + M_{\dot{w}}(Z_q + u_0)}{1 - Z_{\dot{w}}} + M_q \right) \lambda + \frac{Z_w M_q - M_w(Z_q + u_0)}{1 - Z_{\dot{w}}} = 0$$

and since $\lambda^2 - 2\zeta\omega_n\lambda + \omega_n^2 = 0$ Then:

$$\omega_n^2 = \sqrt{\frac{Z_w M_q - M_w(Z_q + u_0)}{1 - Z_{\dot{w}}}}$$

$$\zeta = \frac{\frac{Z_w + M_{\dot{w}}(Z_q + u_0)}{1 - Z_{\dot{w}}} + M_q}{2\sqrt{\frac{Z_w M_q - M_w(Z_q + u_0)}{1 - Z_{\dot{w}}}}}$$

6.4.2 Long-period approximation

An approximation to the long-period mode can be obtained by neglecting the pitching moment equation and assuming that the change in angle of attack is 0; that is
We set \dot{W} equation equal to 0:

$$0 = Z_u u + Z_w W + (Z_q + u_0)q - g \sin \theta_0 \theta + Z_{\delta e} \delta e + Z_{\delta t} \delta t$$

We know that $\dot{\theta} = q$ and we neglect the change in w which corresponds to the change in angle of attack then by some simplification:

$$\dot{\theta} = -\frac{Z_u}{Z_q + u_0} u + \frac{g \sin \theta_0}{Z_q + u_0} \theta - \frac{Z_{\delta e}}{Z_q + u_0} \delta e - \frac{Z_{\delta t}}{Z_q + u_0} \delta t$$

Then we get

$$\begin{bmatrix} \Delta \dot{u} \\ \Delta \dot{\theta} \end{bmatrix} = \begin{bmatrix} X_u & -g \cos \theta_0 \\ -\frac{Z_u}{Z_q + u_0} & \frac{g \sin \theta_0}{Z_q + u_0} \end{bmatrix} \begin{bmatrix} \Delta u \\ \Delta \theta \end{bmatrix} + \begin{bmatrix} X_{\delta e} & X_{\delta t} \\ -\frac{Z_{\delta e}}{Z_q + u_0} & -\frac{Z_{\delta t}}{Z_q + u_0} \end{bmatrix} \begin{bmatrix} \Delta \delta e \\ \Delta \delta t \end{bmatrix}$$

To calculate the frequency ω and damping ratio ζ we need to get the characteristic equation

$$|\lambda I - A| = 0$$

This would give

$$\lambda^2 - \left(\frac{g \sin(\theta_0)}{Z_q + u_0} + X_u \right) \lambda + \frac{g(X_u \sin(\theta_0) - Z_u \cos(\theta_0))}{Z_q + u_0}$$

and since $\lambda^2 - 2\zeta\omega_n\lambda + \omega_n^2 = 0$ Then:

$$\omega_n = \sqrt{\frac{g(X_u \sin(\theta_0) - Z_u \cos(\theta_0))}{Z_q + u_0}}$$

$$\zeta = \frac{\frac{g \sin(\theta_0)}{Z_q + u_0} + X_u}{2\sqrt{\frac{g(X_u \sin(\theta_0) - Z_u \cos(\theta_0))}{Z_q + u_0}}}$$

6.5 Lateral-approximations

6.5.1 3-DOF spiral approximation

To make this approximation we need to make 3 major assumptions:

- Neglecting Y -force equation.
- Neglecting $\Delta\psi$ equation.
- Assuming $\Delta v = 0$.

$$\begin{bmatrix} \Delta\dot{p} \\ \Delta\dot{r} \\ \Delta\dot{\phi} \end{bmatrix} = \begin{bmatrix} L'_p & L'_r & 0 \\ N'_p & N'_r & 0 \\ 1 & \tan(\theta_0) & 0 \end{bmatrix} \begin{bmatrix} \Delta p \\ \Delta r \\ \Delta\phi \end{bmatrix} + \begin{bmatrix} L'_{\delta_r} \\ N'_{\delta_r} \\ 0 \end{bmatrix} [\Delta\delta_r]$$

6.5.2 3-DOF Dutch-roll approximations

This approximation is made by neglecting rolling and yawing $L'_r = N'_p = 0$

$$\begin{bmatrix} \Delta\dot{v} \\ \Delta\dot{p} \\ \Delta\dot{r} \end{bmatrix} = \begin{bmatrix} Y_v & Y_p + w_0 & Y_r - u_0 \\ L'_v & L'_p & 0 \\ N'_v & 0 & N'_r \end{bmatrix} \begin{bmatrix} \Delta v \\ \Delta p \\ \Delta r \end{bmatrix} + \begin{bmatrix} Y_{\delta_a} & Y_{\delta_r} \\ L'_{\delta_a} & L'_{\delta_r} \\ N'_{\delta_a} & N'_{\delta_r} \end{bmatrix} \begin{bmatrix} \Delta\delta_a \\ \Delta\delta_r \end{bmatrix}$$

6.5.3 2-DOF Dutch-roll approximations

In this mode, the airplane is modeled with the following assumption:
Neglecting the L-moment equation $\Delta\theta = 0$

$$\begin{bmatrix} \Delta\dot{v} \\ \Delta\dot{r} \end{bmatrix} = \begin{bmatrix} Y_v & Y_r - u_0 \\ N'_v & N'_r \end{bmatrix} \begin{bmatrix} \Delta v \\ \Delta r \end{bmatrix} + \begin{bmatrix} Y_{\delta_a} & Y_{\delta_r} \\ N'_{\delta_a} & N'_{\delta_r} \end{bmatrix} \begin{bmatrix} \Delta\delta_a \\ \Delta\delta_r \end{bmatrix}$$

6.5.4 1-DOF Dutch-roll

In this approximation, the airplane is modeled with the following assumption:

$$\dot{P} = L'_p \Delta P + L'_{\delta_a} \Delta\delta_a$$

6.6 applying on B747-FC3 Flight Condition

Longitudinal Mode State-Space Manual Linearization

$$A = \begin{bmatrix} -0.0050 & 0.0743 & 0 & -32.1270 \\ -0.0832 & -0.7585 & 505.8904 & -1.7932 \\ 0.0003 & -0.0026 & -1.8170 & 0.0040 \\ 0 & 0 & 1.0000 & 0 \end{bmatrix}$$

$$B = \begin{bmatrix} 1.1800 & 0.0001 \\ -22.4673 & -0.0000 \\ -1.3503 & 0.0000 \\ 0 & 0 \end{bmatrix}$$

$$C = \begin{bmatrix} 1 & 0 & 0 & 0 \\ 0 & 1 & 0 & 0 \\ 0 & 0 & 1 & 0 \\ 0 & 0 & 0 & 1 \end{bmatrix}$$

$$D = \begin{bmatrix} 0 & 0 \\ 0 & 0 \\ 0 & 0 \\ 0 & 0 \end{bmatrix}$$

Longitudinal Mode Transfer Function Manual Linearization

- Transfer Function for δ_e with output u :

$$\frac{1.18s^3 + 1.37s^2 - 7.221s + 31.19}{s^4 + 2.581s^3 + 2.719s^2 + 0.01519s + 0.01502}$$

- Transfer Function for δ_e with output w :

$$\frac{-22.47s^3 - 724.2s^2 - 1.083s - 3.834}{s^4 + 2.581s^3 + 2.719s^2 + 0.01519s + 0.01502}$$

- Transfer Function for δ_e with output q :

$$\frac{-1.35s^3 - 0.9718s^2 - 0.01316s + 6.389 \times 10^{-19}}{s^4 + 2.581s^3 + 2.719s^2 + 0.01519s + 0.01502}$$

- Transfer Function for δ_e with output θ :

$$\frac{-1.35s^2 - 0.9718s - 0.01316}{s^4 + 2.581s^3 + 2.719s^2 + 0.01519s + 0.01502}$$

- Transfer Function for δ_t with output u :

$$\frac{5.05 \times 10^{-5}s^3 + 0.0001299s^2 + 0.0001377s - 8.102 \times 10^{-6}}{s^4 + 2.581s^3 + 2.719s^2 + 0.01519s + 0.01502}$$

- Transfer Function for δ_t with output w :

$$\frac{-2.267 \times 10^{-6}s^3 + 0.0000147s^2 + 1.007 \times 10^{-6}s + 7.804 \times 10^{-7}}{s^4 + 2.581s^3 + 2.719s^2 + 0.01519s + 0.01502}$$

- Transfer Function for δ_t with output q :

$$\frac{3.07 \times 10^{-7}s^3 + 2.57 \times 10^{-7}s^2 + 2.667 \times 10^{-8}s + 2.153 \times 10^{-26}}{s^4 + 2.581s^3 + 2.719s^2 + 0.01519s + 0.01502}$$

- Transfer Function for δ_t with output θ :

$$\frac{3.07 \times 10^{-7}s^2 + 2.57 \times 10^{-7}s + 2.667 \times 10^{-8}}{s^4 + 2.581s^3 + 2.719s^2 + 0.01519s + 0.01502}$$

Lateral Mode State-Space Manual Linearization

$$A = \begin{bmatrix} -0.1430 & 0.0541 & -0.9985 & 0.0640 & 0 \\ -0.0064 & -1.1162 & 0.3921 & 0 & 0 \\ 0.0017 & -0.0487 & -0.2534 & 0 & 0 \\ 0 & 1.0000 & 0.0542 & 0 & 0 \\ 0 & 0 & 1.0015 & 0 & 0 \end{bmatrix}$$

$$B = \begin{bmatrix} 0 & 11.3452 \\ 0.2275 & 0.2867 \\ 0.0240 & -0.6190 \\ 0 & 0 \\ 0 & 0 \end{bmatrix}$$

$$C = \begin{bmatrix} 1 & 0 & 0 & 0 & 0 \\ 0 & 1 & 0 & 0 & 0 \\ 0 & 0 & 1 & 0 & 0 \\ 0 & 0 & 0 & 1 & 0 \\ 0 & 0 & 0 & 0 & 1 \end{bmatrix}$$

$$D = \begin{bmatrix} 0 & 0 \\ 0 & 0 \\ 0 & 0 \\ 0 & 0 \\ 0 & 0 \end{bmatrix}$$

Lateral Mode Transfer Function Manual Linearization

- Transfer Function for δ_a with output V :

$$\frac{-0.01169s^2 + 0.002555s + 0.004347}{s^4 + 1.513s^3 + 0.4999s^2 + 0.04589s + 5.303 \times 10^{-5}}$$

- Transfer Function for δ_a with output p :

$$\frac{0.2275s^3 + 0.0996s^2 + 0.01014s - 1.906 \times 10^{-6}}{s^4 + 1.513s^3 + 0.4999s^2 + 0.04589s + 5.303 \times 10^{-5}}$$

- Transfer Function for δ_a with output r :

$$\frac{0.02403s^3 + 0.01917s^2 + 0.00228s + 3.52 \times 10^{-5}}{s^4 + 1.513s^3 + 0.4999s^2 + 0.04589s + 5.303 \times 10^{-5}}$$

- Transfer Function for δ_a with output ϕ :

$$\frac{0.2288s^2 + 0.1006s + 0.01026}{s^4 + 1.513s^3 + 0.4999s^2 + 0.04589s + 5.303 \times 10^{-5}}$$

- Transfer Function for δ_a with output ψ :

$$\frac{0.02407s^3 + 0.0192s^2 + 0.002283s + 3.525 \times 10^{-5}}{s^4 + 1.513s^3 + 0.4999s^2 + 0.04589s + 5.303 \times 10^{-5}}$$

- Transfer Function for δ_r with output V :

$$\frac{11.35s^3 + 16.17s^2 + 4.137s - 0.01333}{s^4 + 1.513s^3 + 0.4999s^2 + 0.04589s + 5.303 \times 10^{-5}}$$

- Transfer Function for δ_r with output p :

$$\frac{0.2867s^3 - 0.2021s^2 - 0.03859s + 1.209 \times 10^{-5}}{s^4 + 1.513s^3 + 0.4999s^2 + 0.04589s + 5.303 \times 10^{-5}}$$

- Transfer Function for δ_r with output r :

$$\frac{-0.619s^3 - 0.7737s^2 - 0.07542s - 0.0002232}{s^4 + 1.513s^3 + 0.4999s^2 + 0.04589s + 5.303 \times 10^{-5}}$$

- Transfer Function for δ_r with output ϕ :

$$\frac{0.2532s^2 - 0.244s - 0.04267}{s^4 + 1.513s^3 + 0.4999s^2 + 0.04589s + 5.303 \times 10^{-5}}$$

- Transfer Function for δ_r with output ψ :

$$\frac{-0.6199s^3 - 0.7748s^2 - 0.07553s - 0.0002236}{s^4 + 1.513s^3 + 0.4999s^2 + 0.04589s + 5.303 \times 10^{-5}}$$

6.6.1 Longitudinal Step Response

Elevator Input Step Responses

Each graph below shows the step response for Non-linear simulation, Linear full model, Short period, and Long period approximations for different elevator deflections δ_e .

Step Response with Elevator Deflection $\delta_e = 1^\circ$

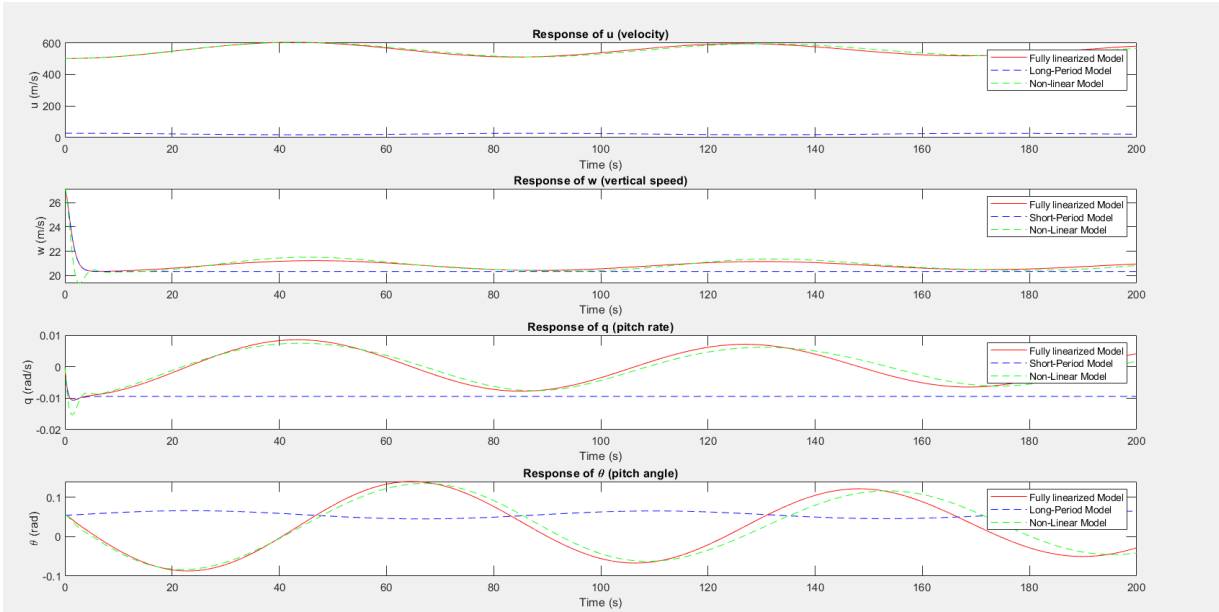


Figure 116: Step response with $\delta_e = 1^\circ$

Comment: At this low deflection angle, the responses across Non-linear, Linear full model, Short period, and Long period approximations remain closely aligned. The Short period approximation captures the quick oscillations and returns to equilibrium without significant deviation, indicating stability in short-term pitch dynamics. The Linear and Non-linear models follow each other closely, suggesting the linearized model is accurate for small deflections.

Step Response with Elevator Deflection $\delta_e = 5^\circ$

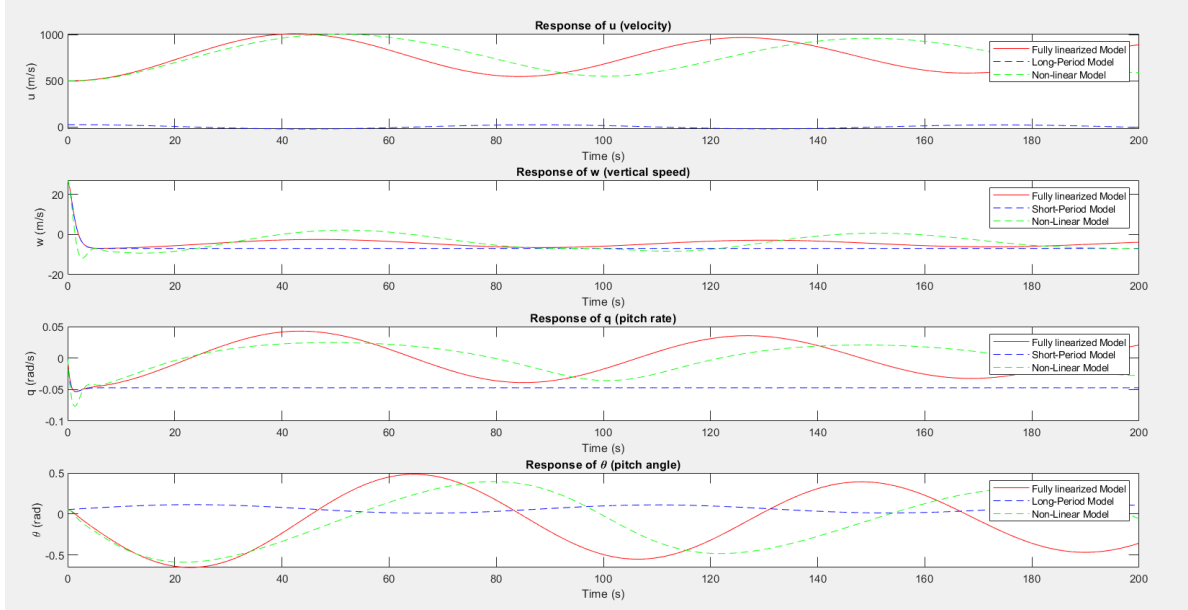


Figure 117: Step response with $\delta_e = 5^\circ$

Comment: With a moderate increase in elevator deflection, the responses begin to differentiate slightly. The Non-linear and Linear full model responses still largely overlap, though the Long period approximation starts showing divergence in capturing the overall trend. Short period oscillations are still present and more pronounced here, highlighting the increased impact on pitch. Overall, this shows the system's sensitivity increases with elevator deflection, affecting model accuracy.

Step Response with Elevator Deflection $\delta_e = 10^\circ$

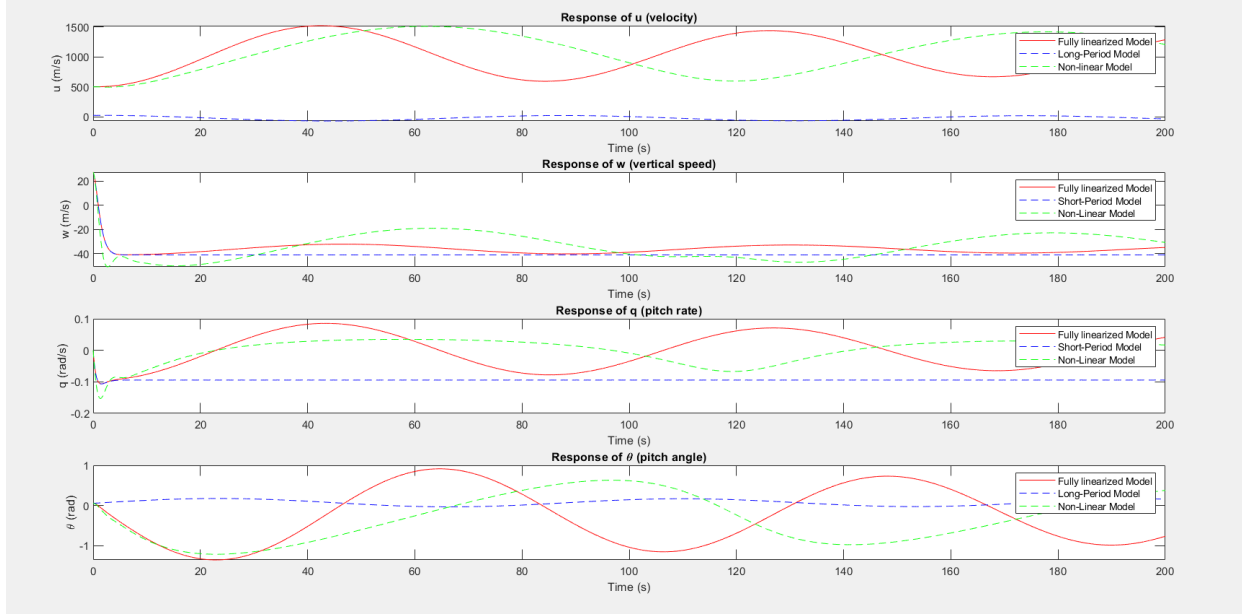


Figure 118: Step response with $\delta_e = 10^\circ$

Comment : At 10° deflection, the Non-linear model demonstrates more noticeable divergence from the Linear full model and Long period approximations. The Short period approximation remains effective in capturing immediate oscillatory behavior but falls short in long-term response accuracy. This difference suggests that larger deflections push the system into regions where linear approximations become less reliable, reflecting greater influence from non-linear aerodynamic effects.

Step Response with Elevator Deflection $\delta_e = 25^\circ$

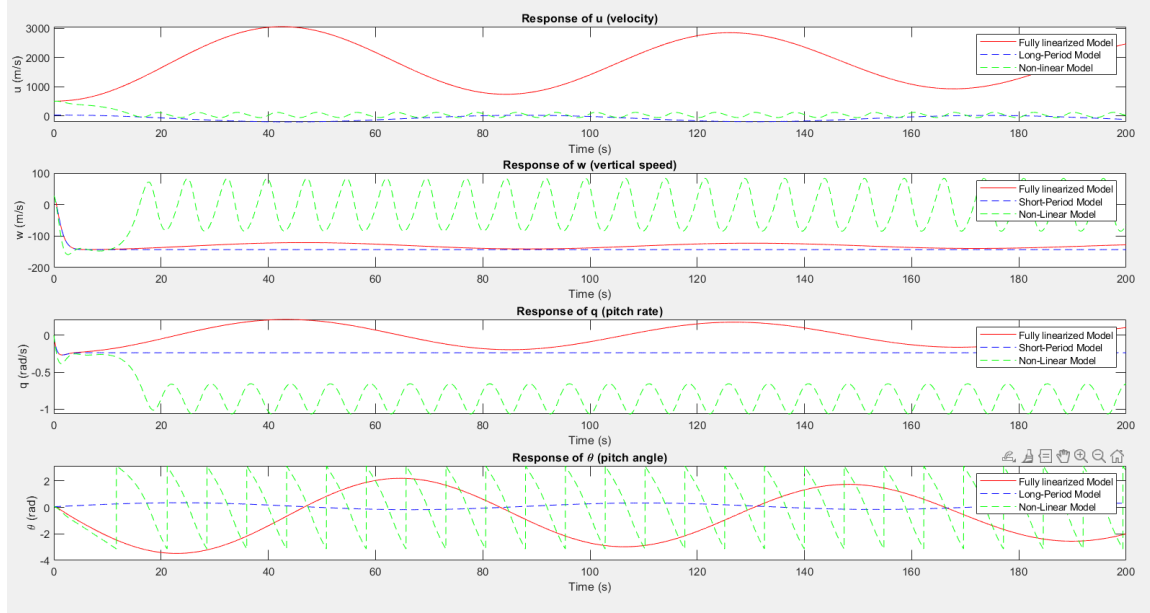


Figure 119: Step response with $\delta_e = 25^\circ$

Comment : With the highest deflection, 25° , Non-linear behavior is prominent, as the Non-linear simulation significantly diverges from all linear approximations. The Linear full model partially captures the initial response but deviates over time. The Long period approximation fails to align with Non-linear trends, and the Short period loses accuracy after initial oscillations. This demonstrates that high elevator inputs induce significant non-linear aerodynamic effects that the linear approximations cannot represent accurately.

Thrust Input Step Responses

Each graph below shows the step response for Non-linear simulation, Linear full model, Short period, and Long period approximations for different thrust inputs.

Step Response with Thrust $T = 2000$

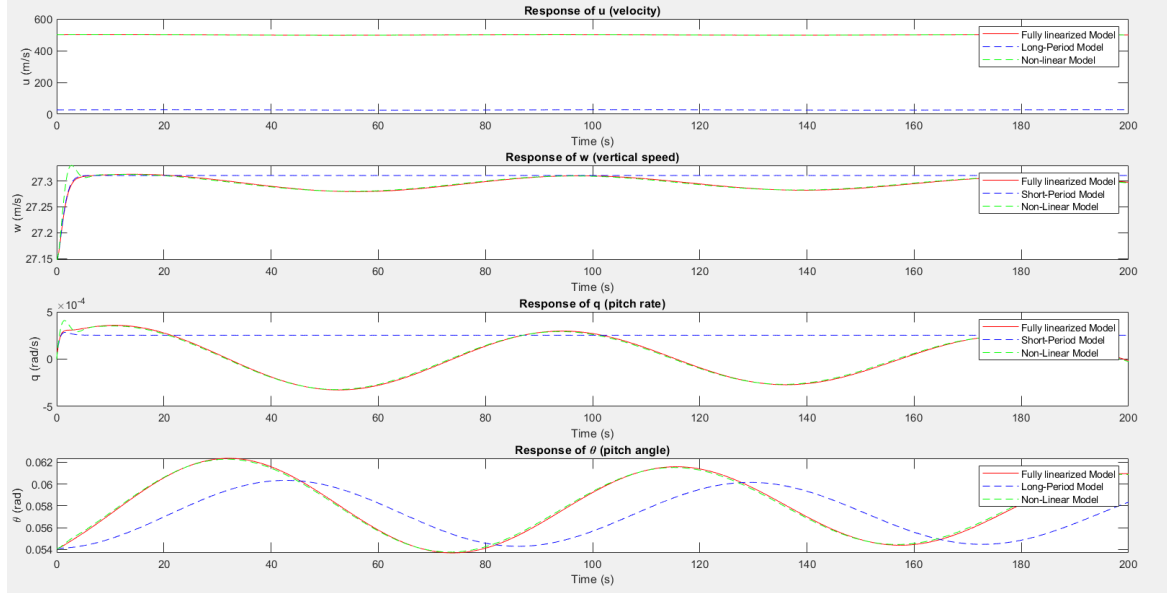


Figure 120: Step response with thrust $T = 2000$

Comment: At this low thrust level, all models, including Non-linear and Linear, show a comparable response, with minimal divergence among Short and Long period approximations. The system stabilizes quickly, reflecting that at lower thrust inputs, linear models are sufficient to represent the thrust-pitch response accurately. The oscillations are controlled, indicating minimal impact on aircraft stability.

Step Response with Thrust $T = 6000$

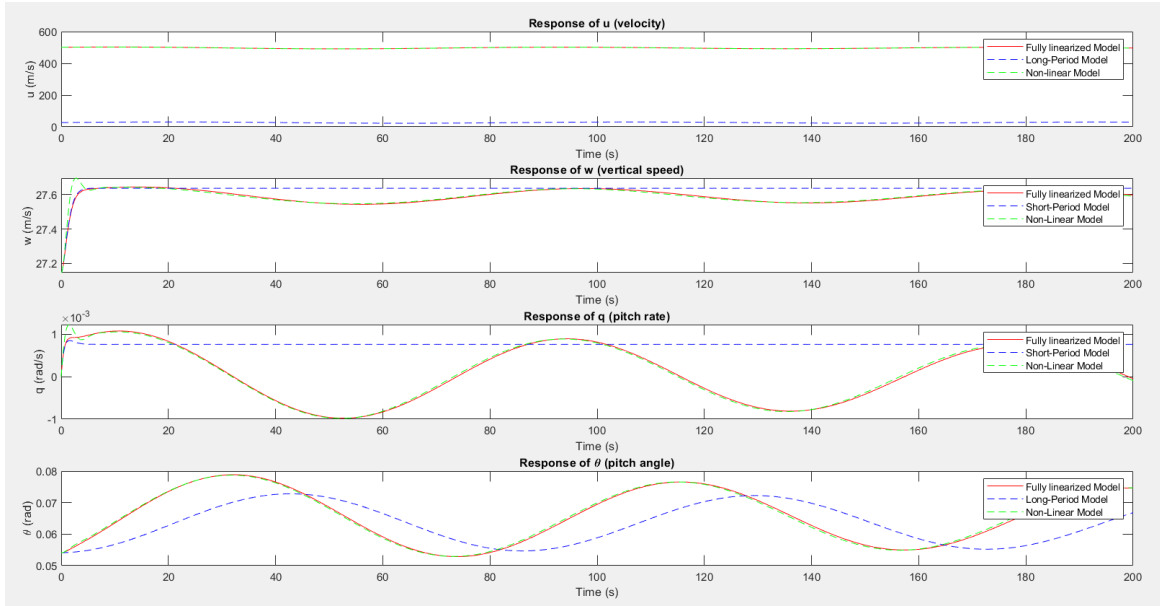


Figure 121: Step response with thrust $T = 6000$

Comment: With increased thrust, the Non-linear model begins to display slight deviation, particularly in the amplitude of oscillations. The Short period model captures initial transient dynamics, but longer-term behavior begins to differ from the Non-linear simulation. The Linear model holds closer to Non-linear than Short or Long period approximations, showing the importance of capturing both short and long-term dynamics as thrust increases.

Step Response with Thrust $T = 10000$

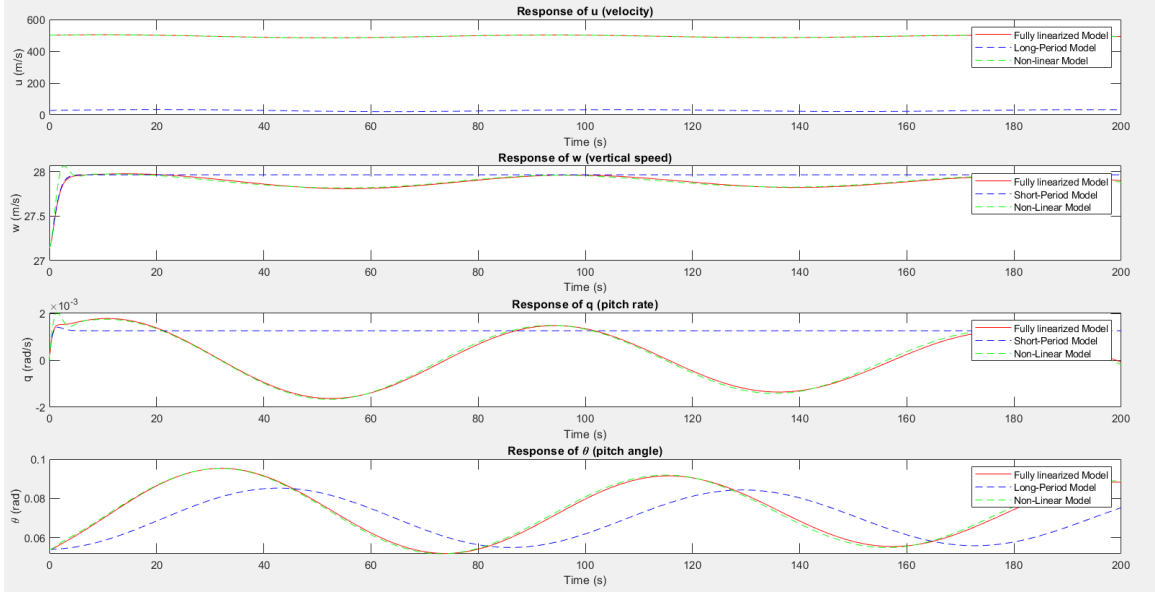


Figure 122: Step response with thrust $T = 10000$

Comment: At high thrust levels, the Non-linear simulation deviates significantly from the Linear model and both approximations. The Short period approximation captures only initial oscillations, while the Long period fails to follow the overall response. The Non-linear model reveals substantial dynamic changes, likely due to increased aerodynamic forces and stability margins affected by high thrust. This response emphasizes the non-linear complexity introduced at higher thrust inputs, where linear models lose validity.

6.6.2 Transfer Functions and Root Locus & Bode Plot for Each Input and Output State For Longitudinal Mode

The Delta Elevator (De) to Linear Velocity (u)

Full Mode Transfer Function:

$$\frac{1.18s^3 + 1.3698s^2 - 7.2213s + 31.1932}{s^4 + 2.5805s^3 + 2.7188s^2 + 0.015195s + 0.015019}$$

Long Mode Transfer Function:

$$\frac{1.18s - 1.431}{s^2 + 0.0014554s + 0.0052641}$$

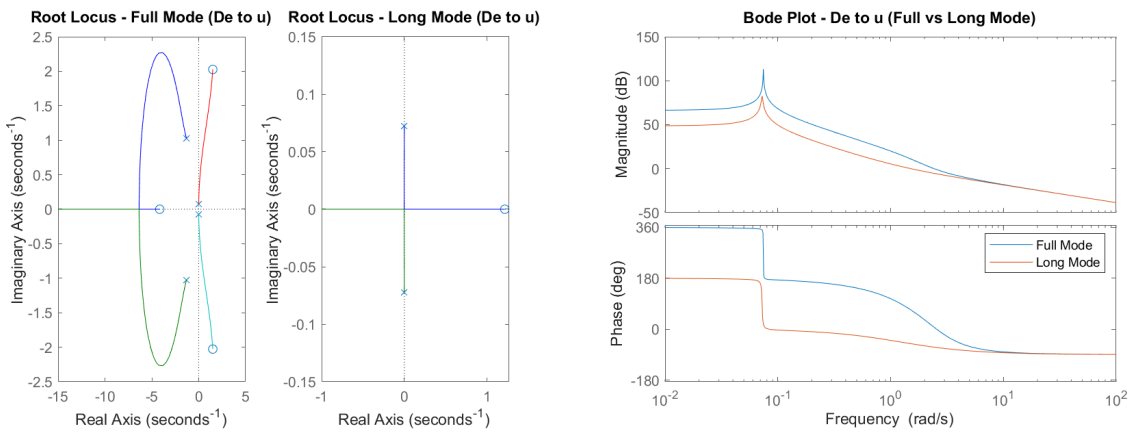


Figure 123: Root Locus and Bode plot for Δ elevator (De) to linear velocity (u)

Comment:

The Root Locus for the two modes differs because the full mode has more poles than the long mode, leading to a more complex locus shape. However, the poles near the origin are at the same values in both modes, indicating similar low-frequency behavior.

In the Bode plot, both modes follow the same trend across frequencies but exhibit a consistent 180-degree phase shift. This phase shift implies that, despite similar magnitude responses, the two modes may respond oppositely at certain frequencies.

The Delta Elevator (De) to vertical velocity (w)

Full Mode Transfer Function:

$$\frac{-22.4673s^3 - 724.1614s^2 - 1.0835s - 3.834}{s^4 + 2.5805s^3 + 2.7188s^2 + 0.015195s + 0.015019}$$

Short Mode Transfer Function:

$$\frac{-22.4673s - 723.9511}{s^2 + 2.5755s + 1.8556}$$

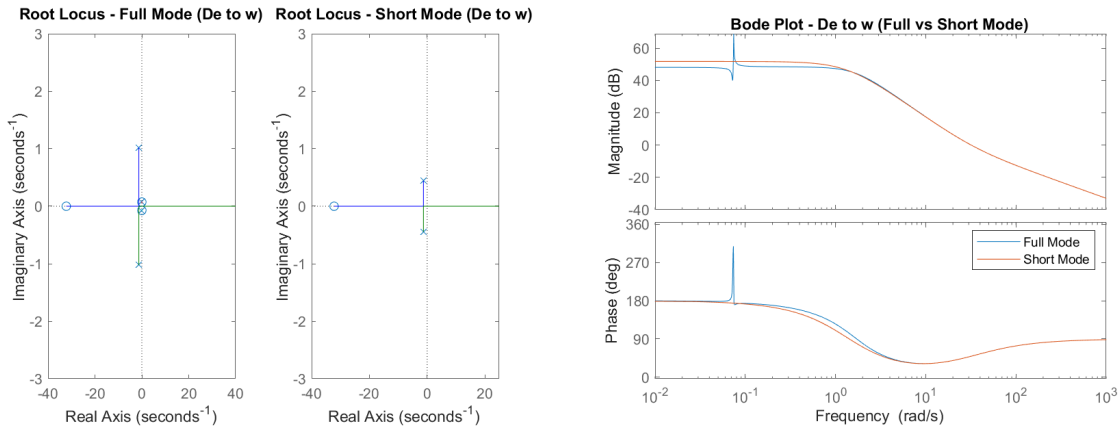


Figure 124: Root Locus and Bode plot for Δ elevator (De) to vertical velocity (w)

Comment:

The Root Locus for the two modes has the same overall shape but differs in the number of poles; the full mode contains a larger number of poles compared to the long mode. However, the poles near the origin are positioned at the same values in both modes. In the Bode plot, both models align closely with each other except at a peak occurring at 10^{-1} rad/s in the full model. This peak is larger in the full model but quickly recovers, allowing the two plots to realign closely afterward.

The Delta Elevator (De) to Pitch Rate (q)

Full Mode Transfer Function:

$$\frac{-1.3503s^3 - 0.97176s^2 - 0.01316s + 6.3887 \times 10^{-19}}{s^4 + 2.5805s^3 + 2.7188s^2 + 0.015195s + 0.015019}$$

Short Mode Transfer Function:

$$\frac{-1.3503s - 1.0031}{s^2 + 2.5755s + 1.8556}$$

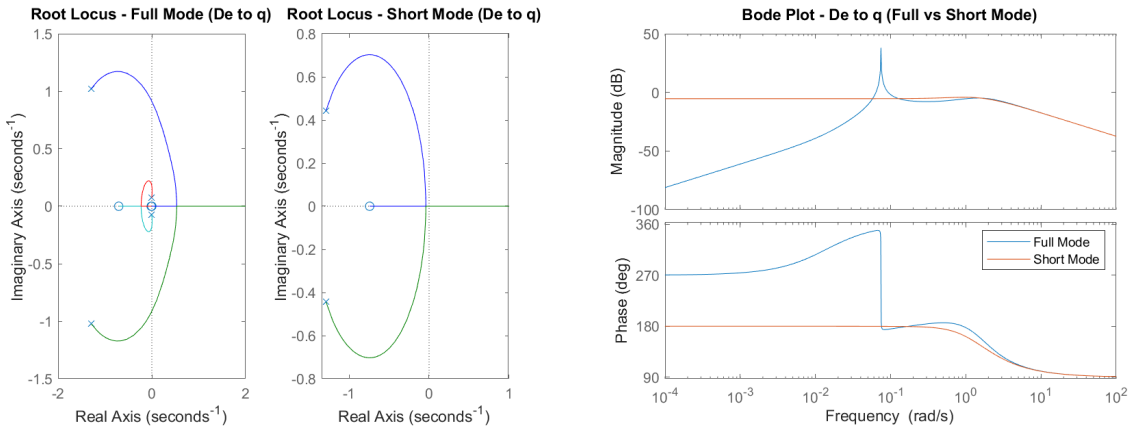


Figure 125: Root Locus and Bode plot for Δ elevator (De) to pitch rate (q)

Comment:

In the Root Locus, the two modes differ due to the full mode having a greater number of poles than the short mode, which leads to a difference in locus shape. However, both modes share some of the same pole positions. In the Bode plot, the short model behaves differently from the full model at frequencies below 10^{-1} rad/s, but beyond this point, both plots follow a similar trend, aligning closely with each other.

The Delta Elevator (De) to Pitch Angle (θ)

Full Mode Transfer Function:

$$\frac{-1.3503s^2 - 0.97176s - 0.01316}{s^4 + 2.5805s^3 + 2.7188s^2 + 0.015195s + 0.015019}$$

Long Mode Transfer Function:

$$\frac{0.04411s + 0.00041561}{s^2 + 0.0014454s + 0.0052641}$$

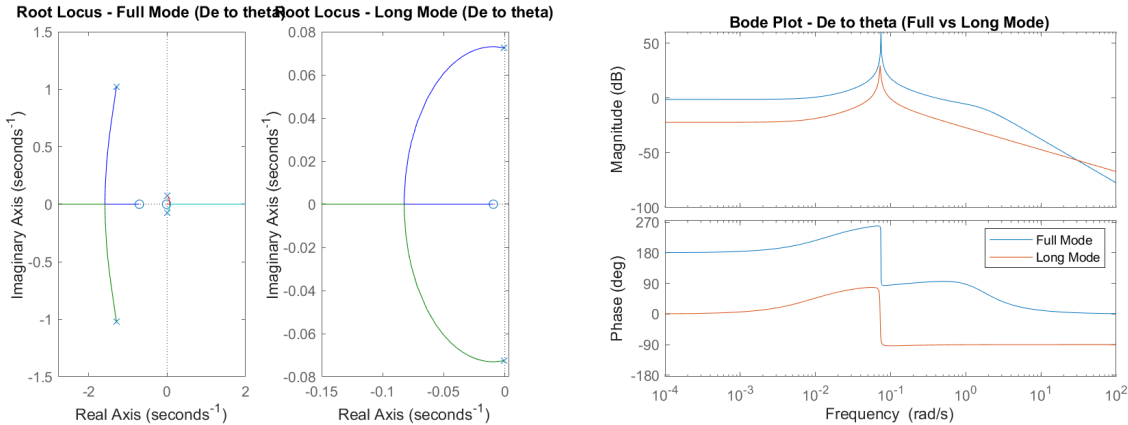


Figure 126: Root Locus and Bode plot for Δ elevator (De) to pitch angle (θ)

Comment:

The Root Locus for the two modes differs because the full mode has a larger number of poles compared to the long mode. However, the poles near the origin are positioned at the same value in both modes. In the Bode plot, both modes follow the same trend but exhibit a 180-degree phase shift across all frequencies.

The Thrust (Th) to Linear Velocity (u)

Full Mode Transfer Function:

$$\frac{5.05 \times 10^{-5}s^3 + 0.0001299s^2 + 0.00013771s - 8.1018 \times 10^{-6}}{s^4 + 2.5805s^3 + 2.7188s^2 + 0.015195s + 0.015019}$$

Long Mode Transfer Function:

$$\frac{5.05 \times 10^{-5}s - 3.2299 \times 10^{-7}}{s^2 + 0.0014454s + 0.0052641}$$

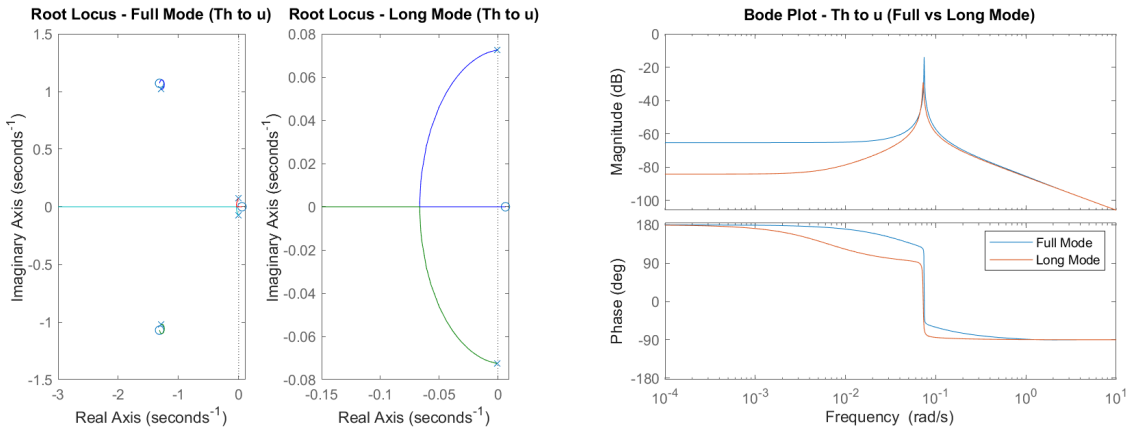


Figure 127: Root Locus and Bode plot for Thrust (Th) to linear velocity (u)

Comment:

The Root Locus for the two modes differs due to the full mode having a larger number of poles than the long mode. However, the poles near the origin are positioned at the same value in both modes. In the Bode plot, both modes follow a similar trend across all frequencies, except in the range from 10^{-3} to 10^{-1} rad/s, where there is a slight difference in phase and magnitude (dB), though it remains minor.

The Thrust (Th) to vertical velocity (w)

Full Mode Transfer Function:

$$\frac{-2.2673 \times 10^{-6}s^3 + 0.00014698s^2 + 1.007 \times 10^{-6}s - 7.8039 \times 10^{-7}}{s^4 + 2.5805s^3 + 2.7188s^2 + 0.015195s + 0.015019}$$

Short Mode Transfer Function:

$$\frac{-22.4673s - 723.9511}{s^2 + 2.5755s + 1.8556}$$

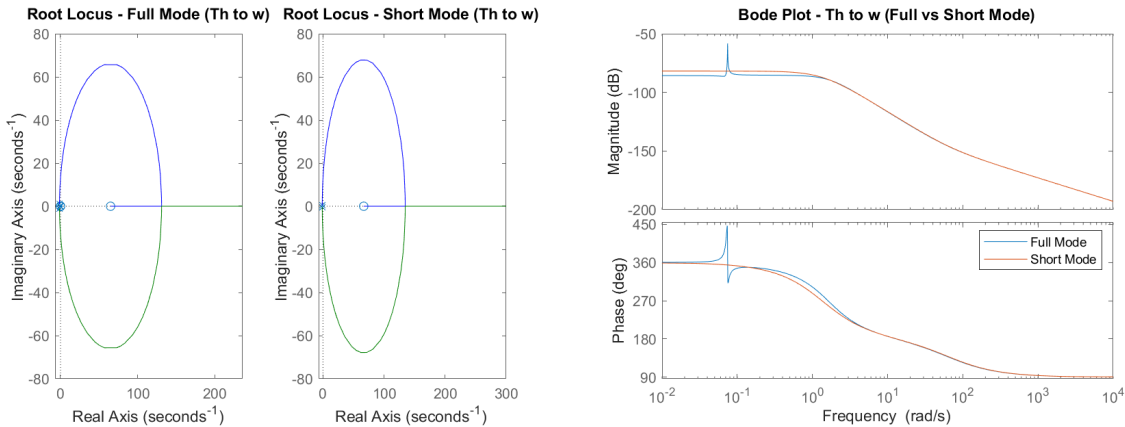


Figure 128: Root Locus and Bode plot for Thrust (Th) to vertical velocity (w)

Comment:

In the Root Locus, the short approximation positions poles nearly identically to the full model, resulting in similar system behavior. This similarity is also evident in the Bode plot, where both plots align closely with each other except at a peak occurring at 10^{-1} rad/s in the full model. In the full model, this peak is larger but quickly recovers, allowing the two plots to realign closely afterward.

The Thrust (Th) to Pitch Rate (q)

Full Mode Transfer Function:

$$\frac{3.0701 \times 10^{-7}s^3 + 2.57 \times 10^{-7}s^2 + 2.6671 \times 10^{-8}s + 2.1531 \times 10^{-26}}{s^4 + 2.5805s^3 + 2.7188s^2 + 0.015195s + 0.015019}$$

Short Mode Transfer Function:

$$\frac{-1.3503s - 1.0031}{s^2 + 2.5755s + 1.8556}$$

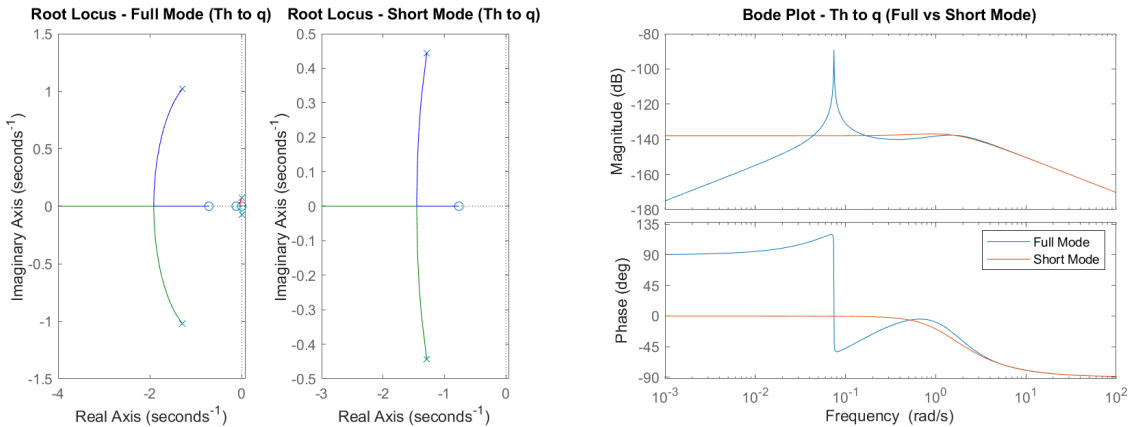


Figure 129: Root Locus and Bode plot for Thrust (Th) to pitch rate (q)

Comment:

In the Root Locus, both models exhibit nearly the same shape, but the poles are positioned at different values. Specifically, the pole in the short mode is approximately half the imaginary axis value of the full mode's pole. In the Bode plot, the short model behaves differently than the full model before a frequency of 10^{-1} rad/s, but beyond this point, both plots follow a similar trend, aligning closely with each other.

The Thrust (Th) to Pitch Angle (θ)

Full Mode Transfer Function:

$$\frac{3.0701 \times 10^{-7}s^2 + 2.57 \times 10^{-7}s + 2.6671 \times 10^{-8}}{s^4 + 2.5805s^3 + 2.7188s^2 + 0.015195s + 0.015019}$$

Long Mode Transfer Function:

$$\frac{4.4819 \times 10^{-9}s + 8.3247 \times 10^{-9}}{s^2 + 0.0014454s + 0.0052641}$$

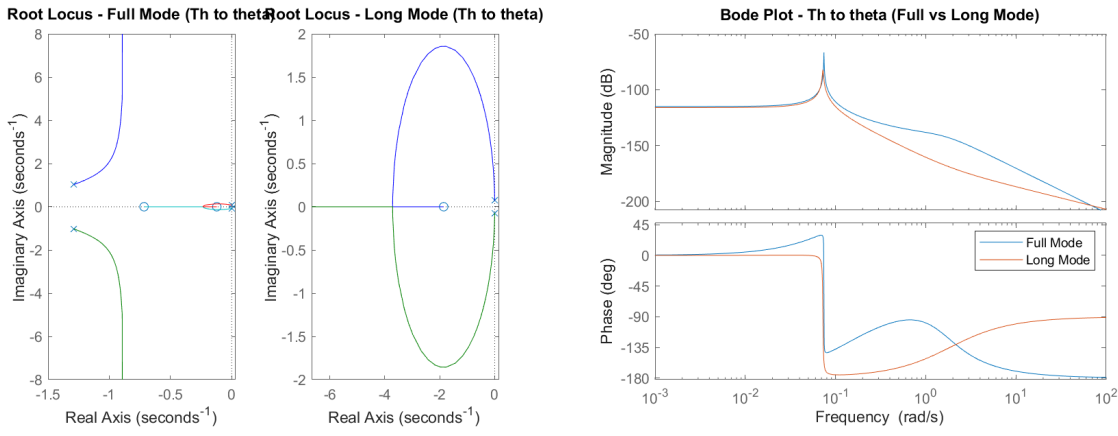


Figure 130: Root Locus and Bode plot for Thrust (Th) to pitch angle (θ)

Comment:

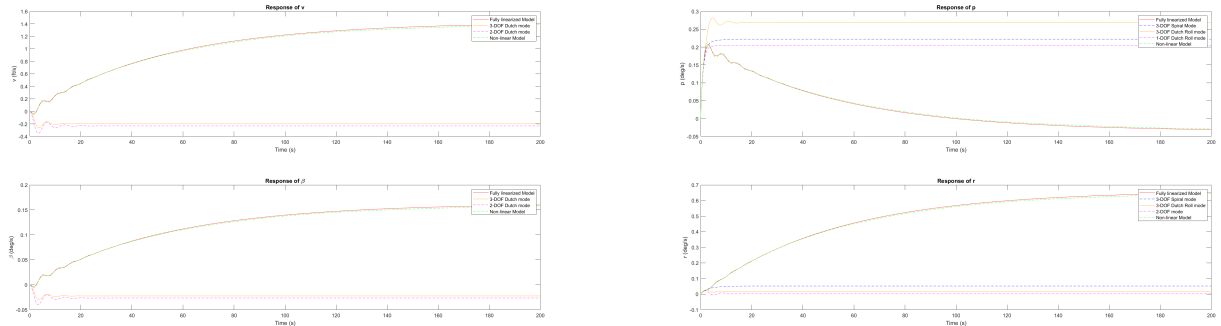
The Root Locus for the long approximation places poles closer to the origin, providing a slower, more stable response for pitch angle control. The full model's poles are further left, indicating higher responsiveness. In the Bode plot, both models behave similarly up to a frequency of 10^{-1} rad/s, after which noticeable differences in both phase and gain (dB) begin to appear.

6.6.3 Lateral Step Response

Aileron Input Step Responses

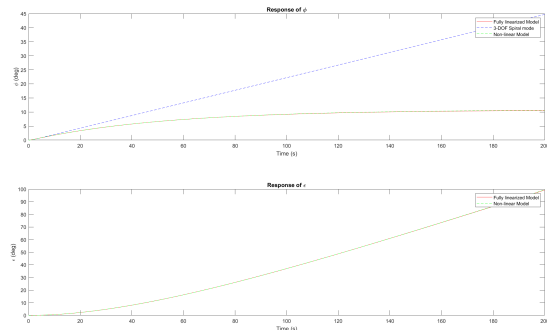
Each graph below shows the step response for Non-linear simulation, Linear full model, 3-DOF, 2-DOF, and 1-DOF approximations for different aileron deflections δ_a .

Step Response with Aileron Deflection $\delta_a = 1^\circ$



(a) Step Response for $\delta_a = 1^\circ$ ($V-\beta$)

(b) Step Response for $\delta_a = 1^\circ$ ($p-r$)



(c) Step Response for $\delta_a = 1^\circ$ ($\phi-\epsilon$)

Figure 131: Step responses for $\delta_a = 1^\circ$

Comment:

- The aileron deflection predominantly excites roll dynamics with coupled yaw and sideslip motions.
- The fully linearized model and the non-linear model show excellent agreement.
- The 3-DOF Spiral mode predicts roll instability over time, while the Dutch Roll mode underestimates lateral and yaw dynamics.
- The responses highlight the coupling between roll, yaw, and sideslip motion in lateral-directional dynamics.

Step Response with Aileron Deflection $\delta_a = 5^\circ$

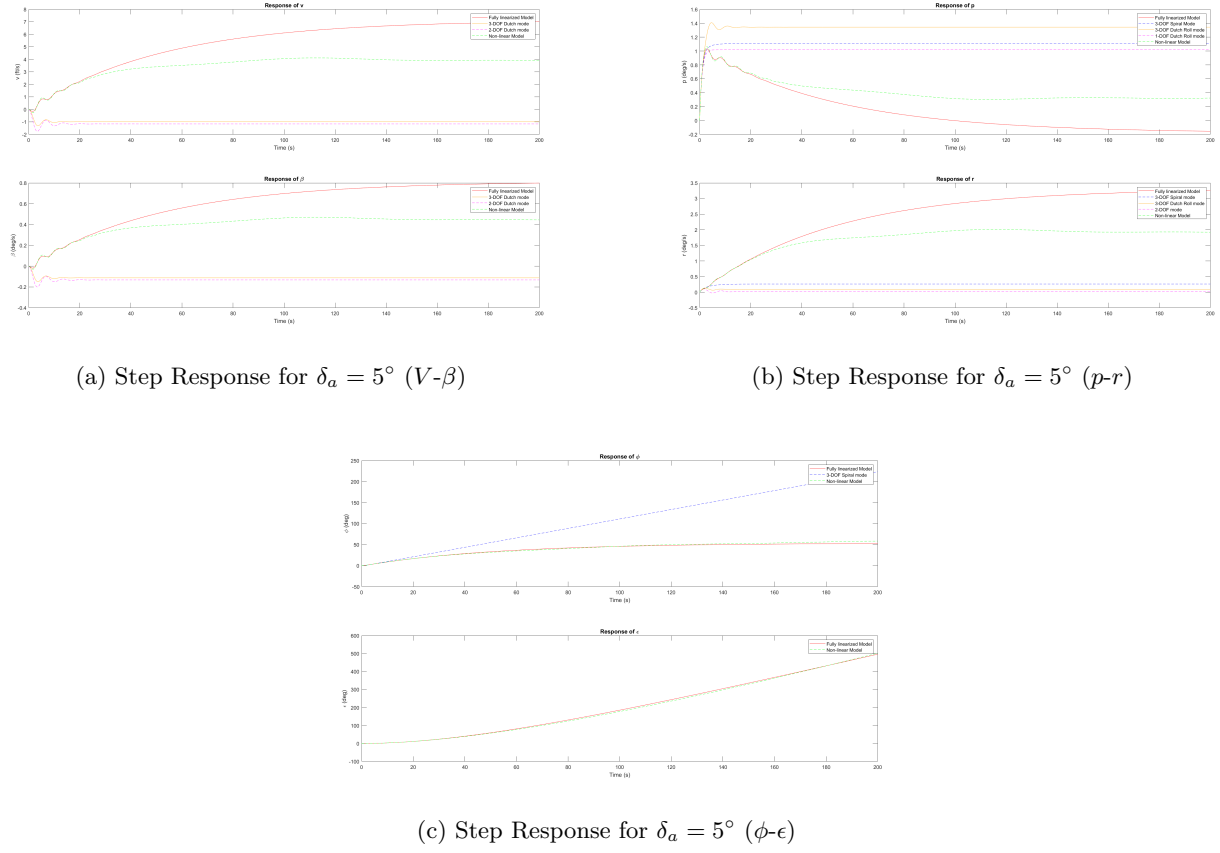
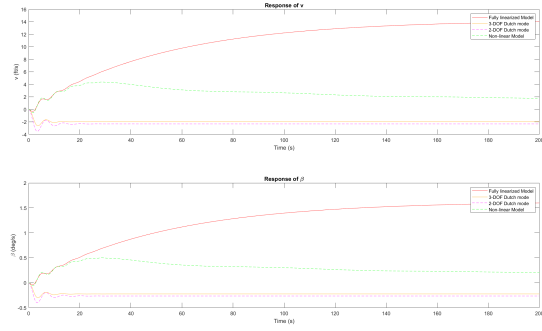


Figure 132: Step responses for $\delta_a = 5^\circ$

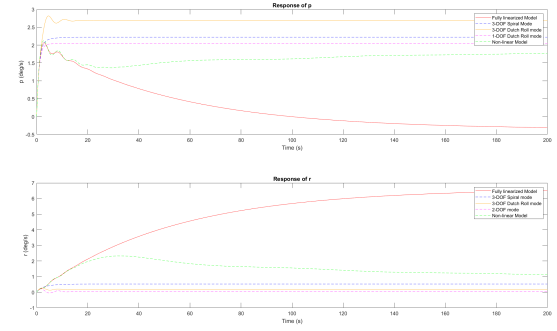
Comment:

- The aileron deflection predominantly excites roll dynamics with coupled yaw and sideslip motions.
- The fully linearized model and the non-linear model show excellent agreement.
- The 3-DOF Spiral mode predicts roll instability over time, while the Dutch Roll mode underestimates lateral and yaw dynamics.
- The responses highlight the coupling between roll, yaw, and sideslip motion in lateral-directional dynamics.

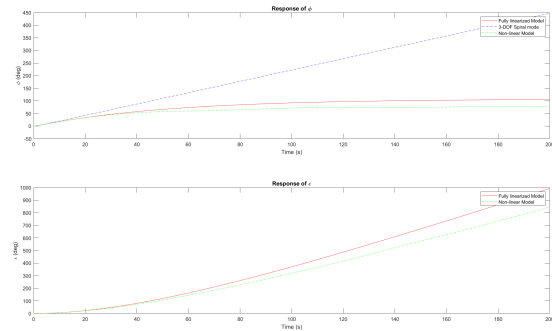
Step Response with Aileron Deflection $\delta_a = 10^\circ$



(a) Step Response for $\delta_a = 10^\circ$ ($V-\beta$)



(b) Step Response for $\delta_a = 10^\circ$ ($p-r$)



(c) Step Response for $\delta_a = 10^\circ$ ($\phi-\epsilon$)

Figure 133: Step responses for $\delta_a = 10^\circ$

Comment:

- The aileron deflection predominantly excites roll dynamics with coupled yaw and sideslip motions.
- The fully linearized model and the non-linear model show excellent agreement.
- The 3-DOF Spiral mode predicts roll instability over time, while the Dutch Roll mode underestimates lateral and yaw dynamics.
- The responses highlight the coupling between roll, yaw, and sideslip motion in lateral-directional dynamics.

Step Response with Aileron Deflection $\delta_a = 25^\circ$

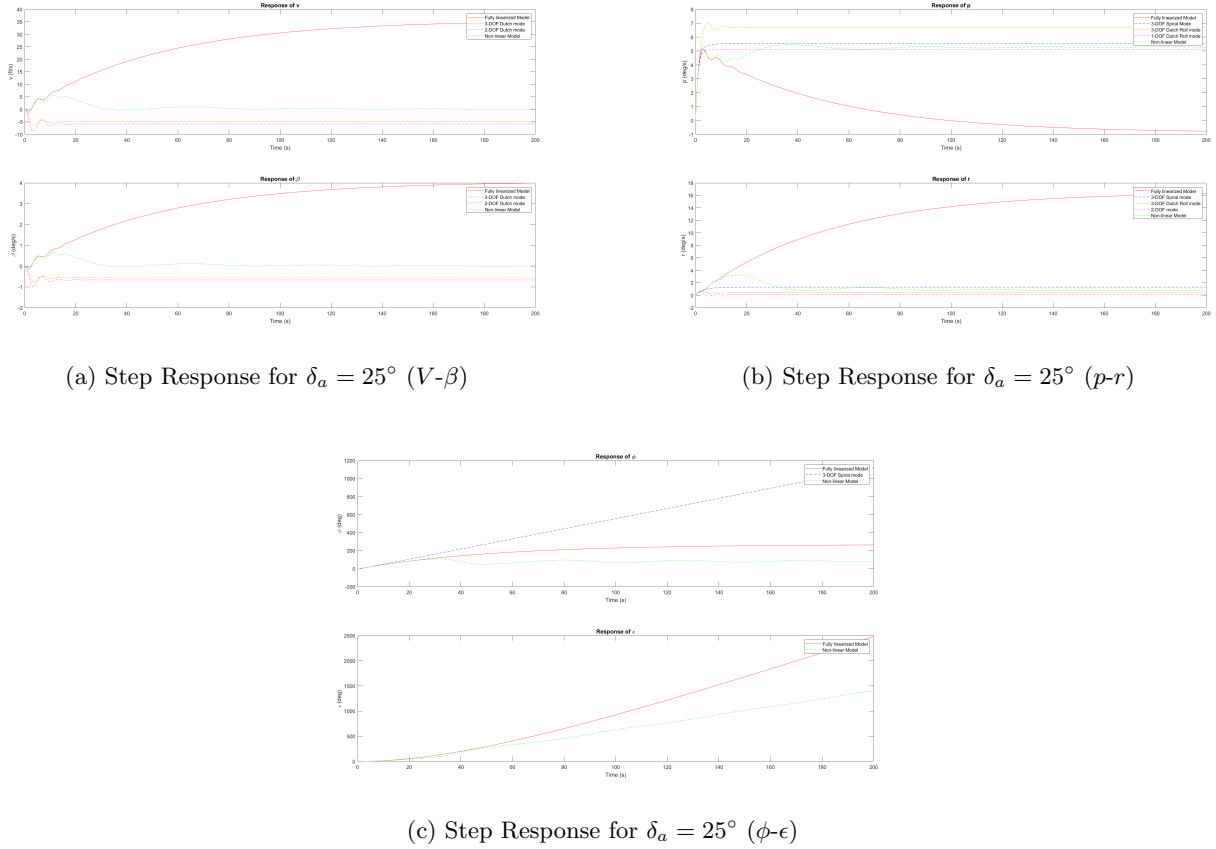


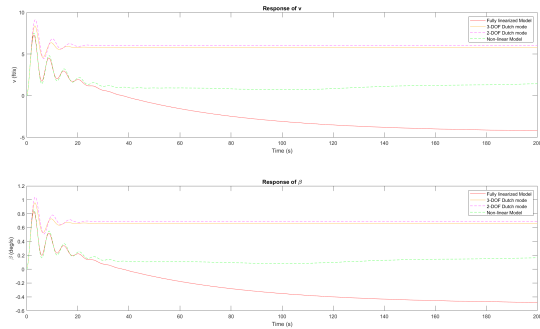
Figure 134: Step responses for $\delta_a = 25^\circ$

Comment:

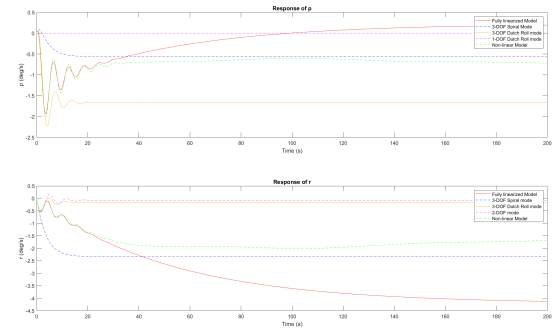
- The aileron deflection predominantly excites roll dynamics with coupled yaw and sideslip motions.
- The fully linearized model and the non-linear model show excellent agreement.
- The 3-DOF Spiral mode predicts roll instability over time, while the Dutch Roll mode underestimates lateral and yaw dynamics.
- The responses highlight the coupling between roll, yaw, and sideslip motion in lateral-directional dynamics.

Rudder Input Step Responses

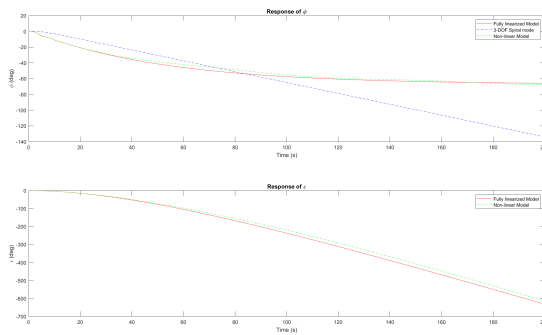
Each graph below shows the step response for Non-linear simulation, Linear full model, 3-DOF, 2-DOF, and 1-DOF approximations for different rudder inputs.



(a) Step Response for $\delta_r = 1^\circ$ ($V-\beta$)



(b) Step Response for $\delta_r = 1^\circ$ ($p-r$)



(c) Step Response for $\delta_r = 1^\circ$ ($\phi-\epsilon$)

Figure 135: Step responses for $\delta_r = 1^\circ$

Comment:

- The aileron deflection predominantly excites roll dynamics with coupled yaw and sideslip motions.
- The fully linearized model and the non-linear model show excellent agreement.
- The 3-DOF Spiral mode predicts roll instability over time, while the Dutch Roll mode underestimates lateral and yaw dynamics.
- The responses highlight the coupling between roll, yaw, and sideslip motion in lateral-directional dynamics.

Step response with Rudder Deflection $\delta_r = 5^\circ$

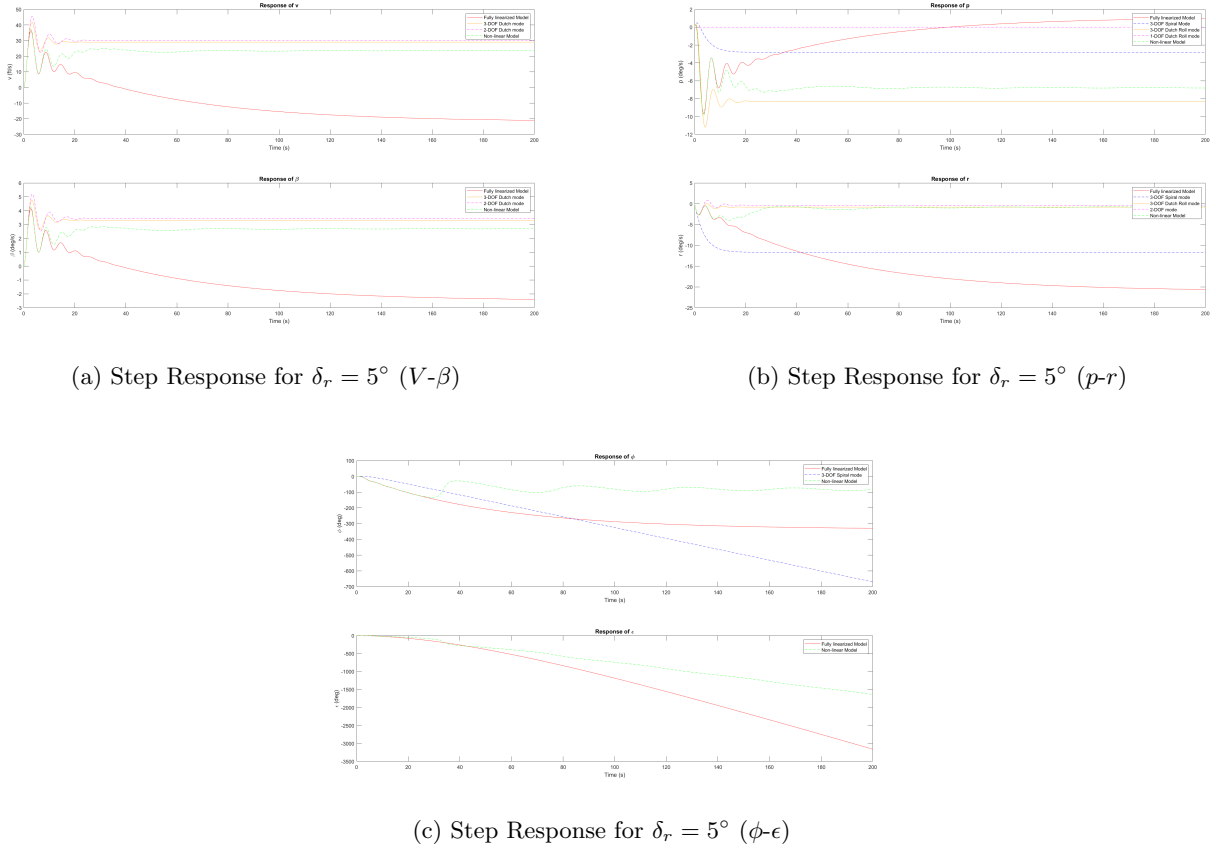


Figure 136: Step responses for $\delta_r = 5^\circ$

Comment:

- The aileron deflection predominantly excites roll dynamics with coupled yaw and sideslip motions.
- The fully linearized model and the non-linear model show excellent agreement.
- The 3-DOF Spiral mode predicts roll instability over time, while the Dutch Roll mode underestimates lateral and yaw dynamics.
- The responses highlight the coupling between roll, yaw, and sideslip motion in lateral-directional dynamics.

Step response with Rudder Deflection $\delta_r = 10^\circ$

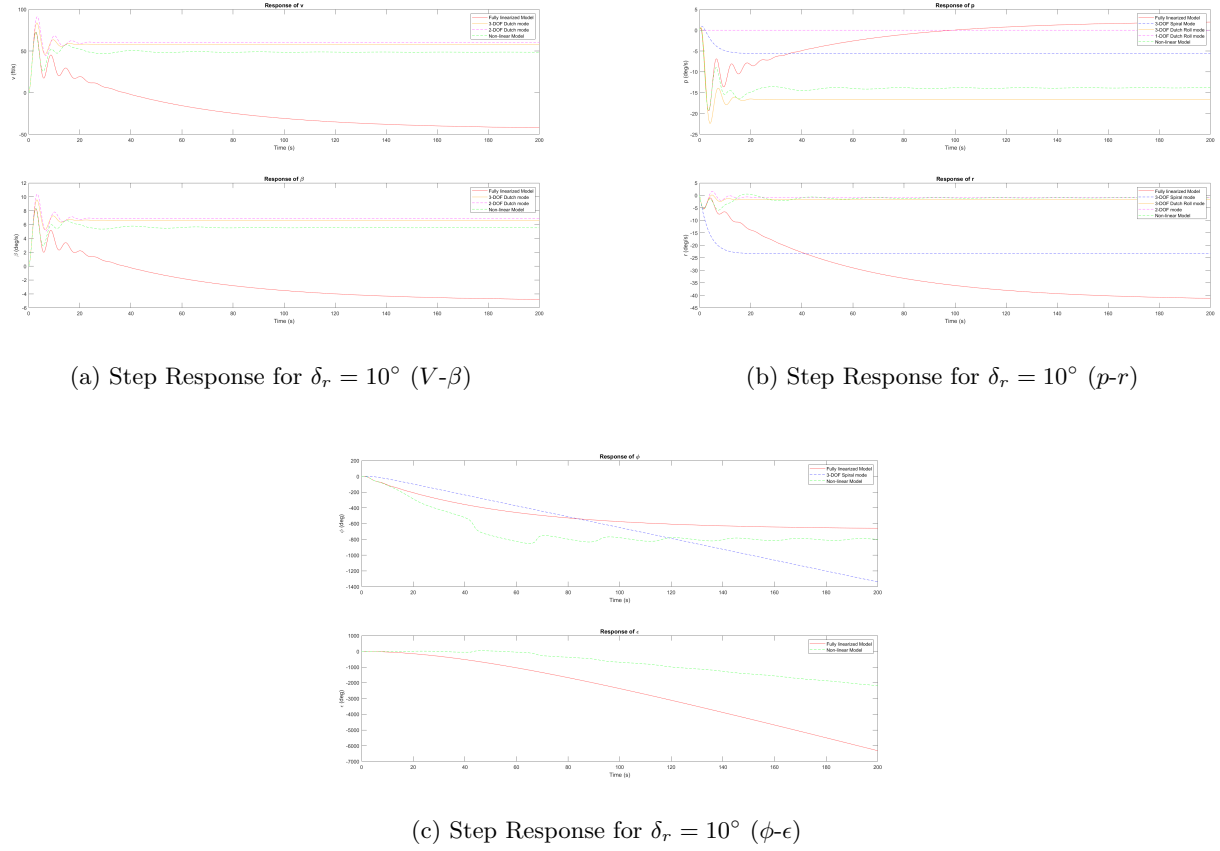


Figure 137: Step responses for $\delta_r = 10^\circ$

Comment:

- The aileron deflection predominantly excites roll dynamics with coupled yaw and sideslip motions.
- The fully linearized model and the non-linear model show excellent agreement.
- The 3-DOF Spiral mode predicts roll instability over time, while the Dutch Roll mode underestimates lateral and yaw dynamics.
- The responses highlight the coupling between roll, yaw, and sideslip motion in lateral-directional dynamics.

Step response with Rudder Deflection $\delta_r = 25^\circ$

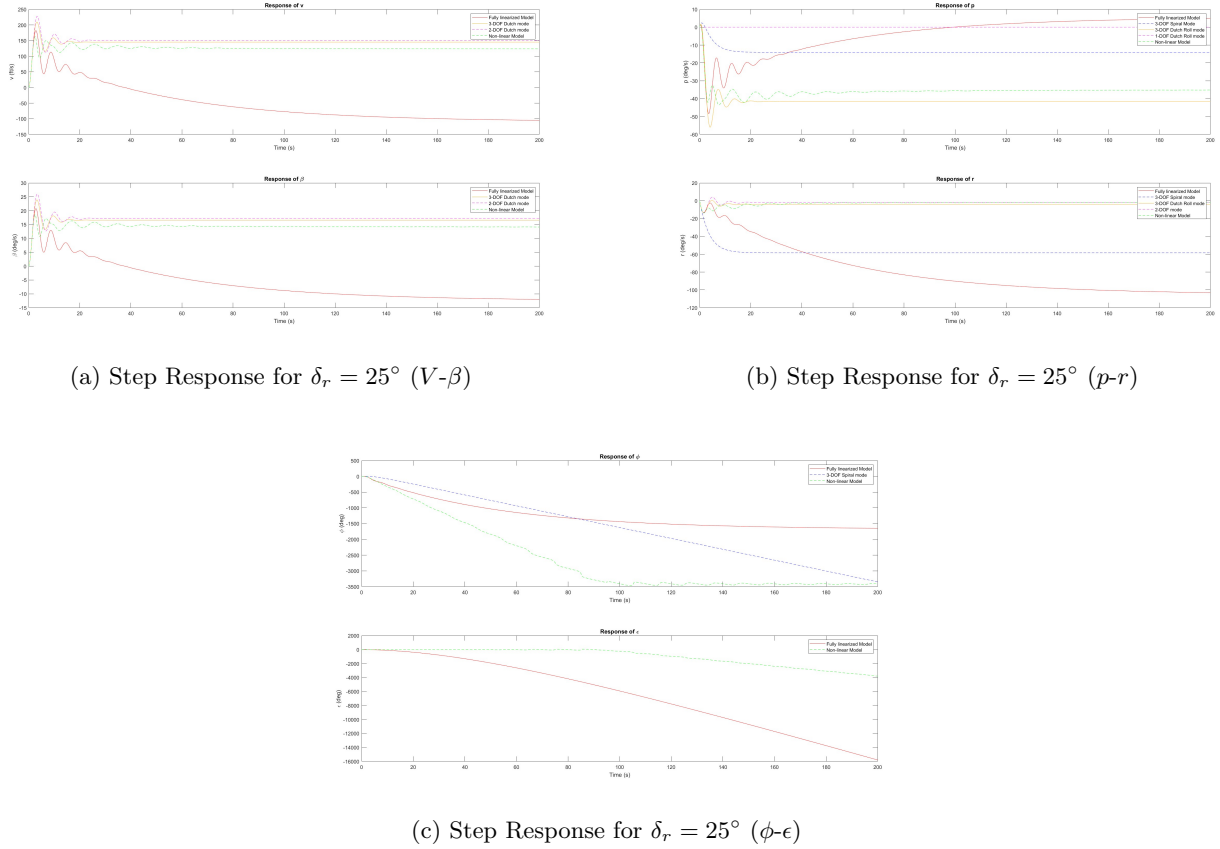


Figure 138: Step responses for $\delta_r = 25^\circ$

Comment:

- The aileron deflection predominantly excites roll dynamics with coupled yaw and sideslip motions.
- The fully linearized model and the non-linear model show excellent agreement.
- The 3-DOF Spiral mode predicts roll instability over time, while the Dutch Roll mode underestimates lateral and yaw dynamics.
- The responses highlight the coupling between roll, yaw, and sideslip motion in lateral-directional dynamics.

6.6.4 Transfer Functions and Root Locus & Bode Plot for Each Input and Output State For Lateral Mode

The Aileron Deflection (Da) to Side Velocity (v)

Full Mode Transfer Function:

$$\frac{-5.87s^2 + 1.2827s + 2.182}{s^4 + 1.5126s^3 + 1.5437s^2 + 1.4025s + 0.026622}$$

3-DOF Dutch Roll Mode Transfer Function:

$$\frac{-5.87s - 11.8808}{s^3 + 1.5126s^2 + 1.5245s + 1.057}$$

2-DOF Dutch Roll Mode Transfer Function:

$$\frac{-12.0456}{s^2 + 0.3964s + 0.90722}$$

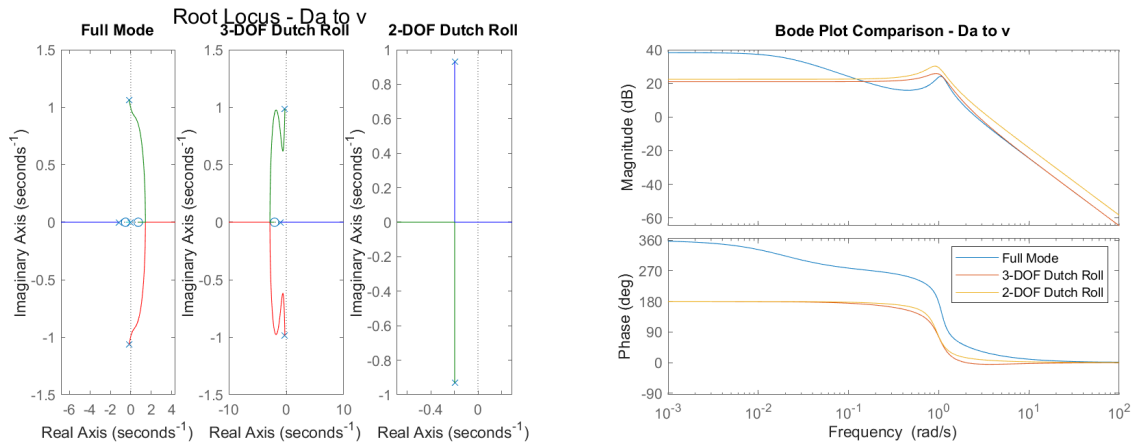


Figure 139: Root Locus and Bode plot for Δ aileron (Da) to side velocity (v)

Comment:

The Root Locus for the full mode differs from that of the 3-DOF Dutch roll due to the presence of two zeros in the full mode, whereas the 3-DOF model has only one zero, and the 2-DOF model has none. This difference in zeros leads to distinct Root Locus patterns across the modes.

In the Bode plots, the full mode shows approximately double the magnitude and a 180-degree phase shift compared to the 3-DOF and 2-DOF modes over the lower frequency range (up to 10^0 rad/s). Beyond this point, all modes converge, aligning closely in both phase and magnitude.

The Aileron Deflection (Da) to Roll Rate (p)

Full Mode Transfer Function:

$$\frac{0.22748s^3 + 0.099595s^2 + 0.2853s - 0.00095702}{s^4 + 1.5126s^3 + 1.5437s^2 + 1.4025s + 0.026622}$$

3-DOF Dutch Roll Mode Transfer Function:

$$\frac{0.22748s^2 + 0.090173s + 0.28396}{s^3 + 1.5126s^2 + 1.5245s + 1.057}$$

1-DOF Roll Mode Transfer Function:

$$\frac{0.22748}{s + 1.1162}$$

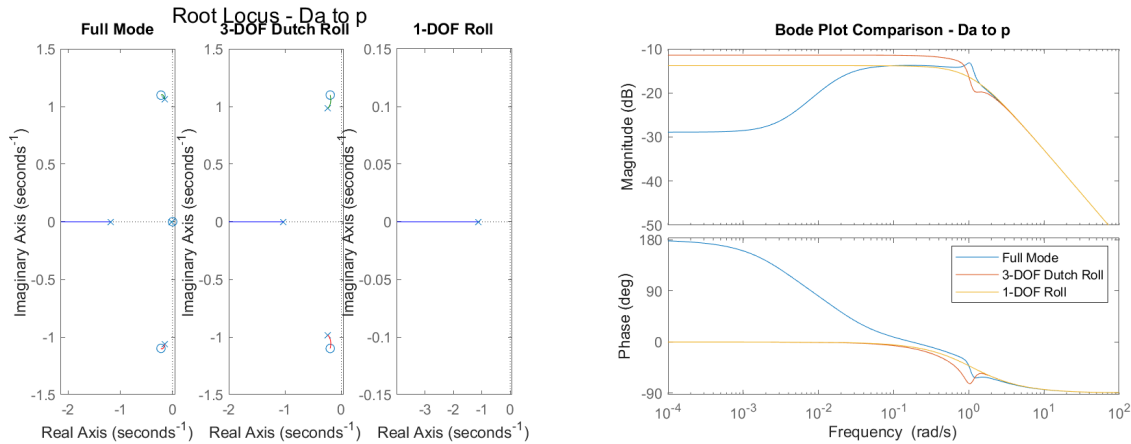


Figure 140: Root Locus and Bode plot for Δ aileron (Da) to roll rate (p)

Comment:

The Root Locus for the full mode has 3 zeros and 4 poles, while the 3-DOF model has 2 zeros and 3 poles, excluding the zero and pole at the origin present in the full mode. The 1-DOF model, by contrast, has only one pole and no zeros, resulting in a simpler locus shape.

In the Bode plots, the full mode exhibits approximately three times the magnitude and a 180-degree phase shift compared to the 3-DOF and 1-DOF modes over the lower frequency range (up to 10^0 rad/s). Beyond this frequency, all modes closely align in both phase and magnitude.

The Aileron Deflection (Da) to Yaw Rate (r)

Full Mode Transfer Function:

$$\frac{0.02403s^3 + 0.019173s^2 + 0.017182s + 0.017671}{s^4 + 1.5126s^3 + 1.5437s^2 + 1.4025s + 0.026622}$$

3-DOF Dutch Roll Mode Transfer Function:

$$\frac{0.02403s^2 + 0.03026s + 0.018768}{s^3 + 1.5126s^2 + 1.5245s + 1.057}$$

2-DOF Dutch Roll Mode Transfer Function:

$$\frac{0.02403s + 0.0034363}{s^2 + 0.3964s + 0.90722}$$

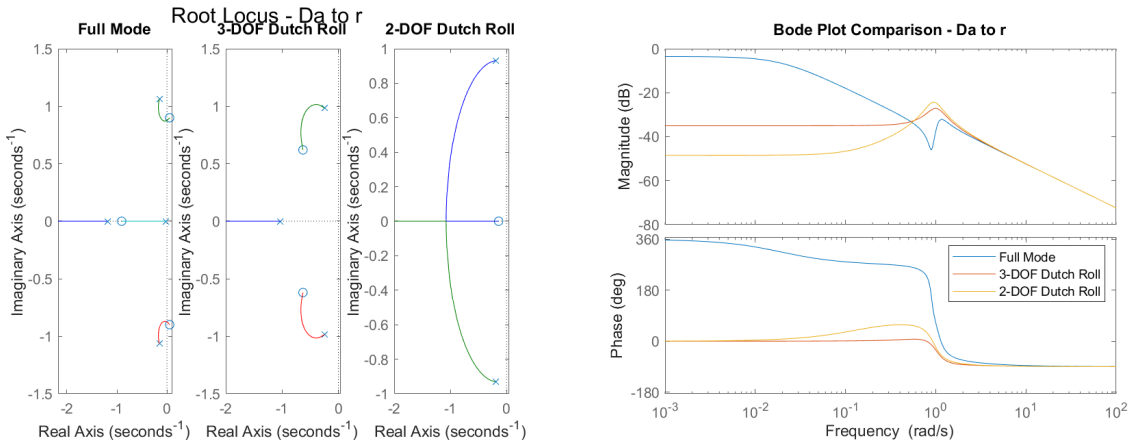


Figure 141: Root Locus and Bode plot for Δ aileron (Da) to yaw rate (r)

Comment:

The Root Locus for the full mode has 3 zeros and 4 poles, while the 3-DOF model has 2 zeros and 3 poles, excluding the zero and pole located on the real axis. The 2-DOF model has only one zero and two poles, resulting in a simpler locus shape for each reduced mode.

In the Bode plots, the magnitude for the full mode starts at 0 dB, while the 3-DOF model begins at -38 dB and the 2-DOF model at -50 dB. Additionally, there is a 360-degree phase shift between the full mode and both the 3-DOF and 2-DOF modes over the lower frequency range (up to 10^0 rad/s). Beyond this frequency, all modes align closely in both phase and magnitude.

The Aileron Deflection (Da) to Roll Angle (phi)

Full Mode Transfer Function:

$$\frac{0.22878s^2 + 0.10063s + 0.28623}{s^4 + 1.5126s^3 + 1.5437s^2 + 1.4025s + 0.026622}$$

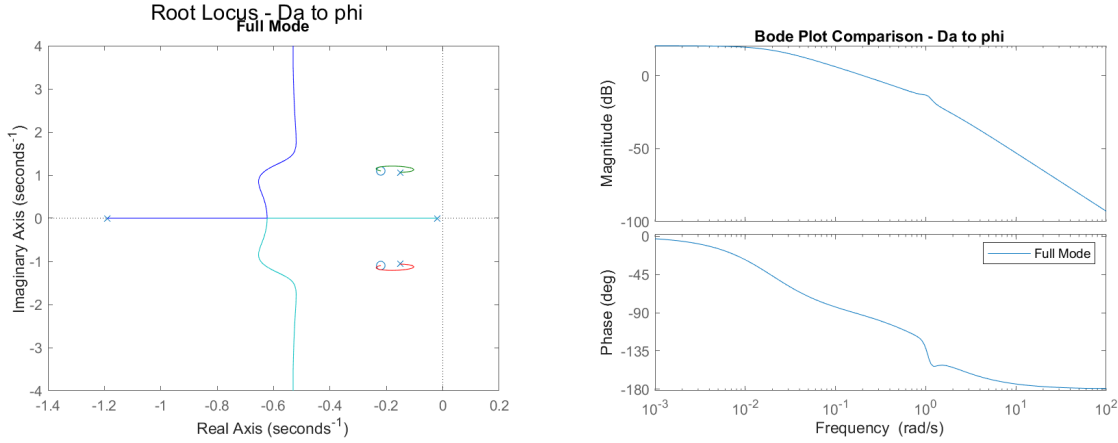


Figure 142: Root Locus and Bode plot for Δ aileron (Da) to roll angle (phi)

Comment:

This transfer function appears only in the full mode, as shown in the Root Locus, where it has two zeros and four poles. In the Bode plot, both the phase and magnitude decrease over the entire frequency range, with the phase starting at 0° and dropping to -180°, and the magnitude starting at 20 dB and decreasing to -100 dB.

The Aileron Deflection (Da) to Yaw Angle (epsi)

Full Mode Transfer Function:

$$\frac{0.024066s^3 + 0.019201s^2 + 0.017208s + 0.017697}{s^5 + 1.5126s^4 + 1.5437s^3 + 1.4025s^2 + 0.026622s}$$

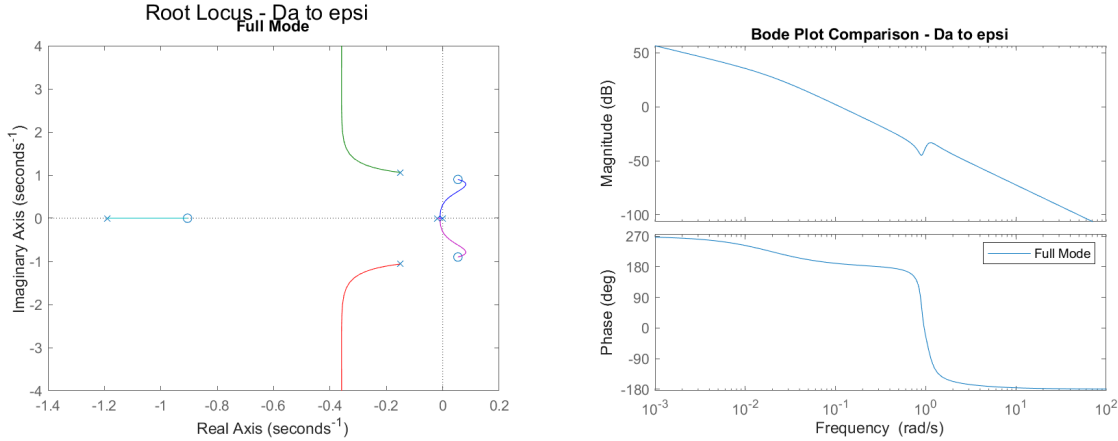


Figure 143: Root Locus and Bode plot for Δ aileron (Da) to yaw angle (epsi)

Comment:

This transfer function appears only in the full mode, as shown in the Root Locus, where it has three zeros and five poles. Two of the zeros are located on the positive real axis, and there is a pole at the origin, making the system critically stable.

In the Bode plot, both the phase and magnitude decrease over the entire frequency range, with the phase starting at 270° and dropping to -180°, and the magnitude starting at 50 dB and decreasing to -100 dB.

The Rudder Deflection (Dr) to Side Velocity (v)

Full Mode Transfer Function:

$$\frac{11.3452s^3 + 333.5847s^2 + 360.2753s - 6.6895}{s^4 + 1.5126s^3 + 1.5437s^2 + 1.4025s + 0.026622}$$

3-DOF Dutch Roll Mode Transfer Function:

$$\frac{11.3452s^2 + 333.5847s + 351.5074}{s^3 + 1.5126s^2 + 1.5245s + 1.057}$$

2-DOF Dutch Roll Mode Transfer Function:

$$\frac{11.3452s + 313.1369}{s^2 + 0.3964s + 0.90722}$$

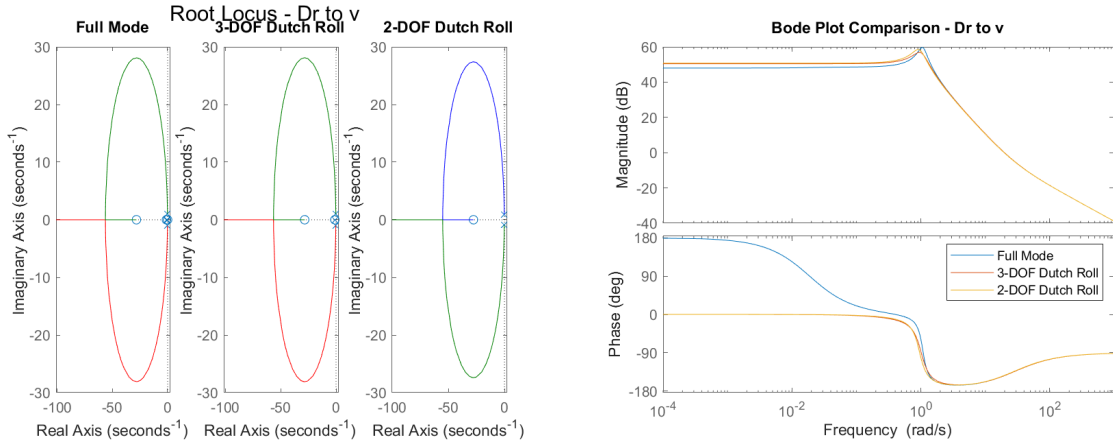


Figure 144: Root Locus and Bode plot for Δ rudder (Dr) to side velocity (v)

Comment:

In the Root Locus, the full mode, 3-DOF, and 2-DOF models have different numbers of zeros and poles, but their Root Locus shapes are nearly identical. This similarity may be due to the fact that in each plot, the number of zeros is only one less than the number of poles.

In the Bode plot, all three models show identical magnitude responses throughout the frequency range, starting at 50 dB. However, there is an initial phase shift between the full mode and the 3-DOF and 2-DOF models up to a frequency of 10^0 rad/s, after which all three models align closely in phase.

The Rudder Deflection (Dr) to Roll Rate (p)

Full Mode Transfer Function:

$$\frac{0.28673s^3 - 0.20211s^2 - 1.7836s + 0.0060693}{s^4 + 1.5126s^3 + 1.5437s^2 + 1.4025s + 0.026622}$$

3-DOF Spiral Mode Transfer Function:

$$\frac{0.28673s - 0.17004}{s^2 + 1.3696s + 0.30196}$$

3-DOF Dutch Roll Mode Transfer Function:

$$\frac{0.28673s^2 + 0.040588s - 1.7567}{s^3 + 1.5126s^2 + 1.5245s + 1.057}$$

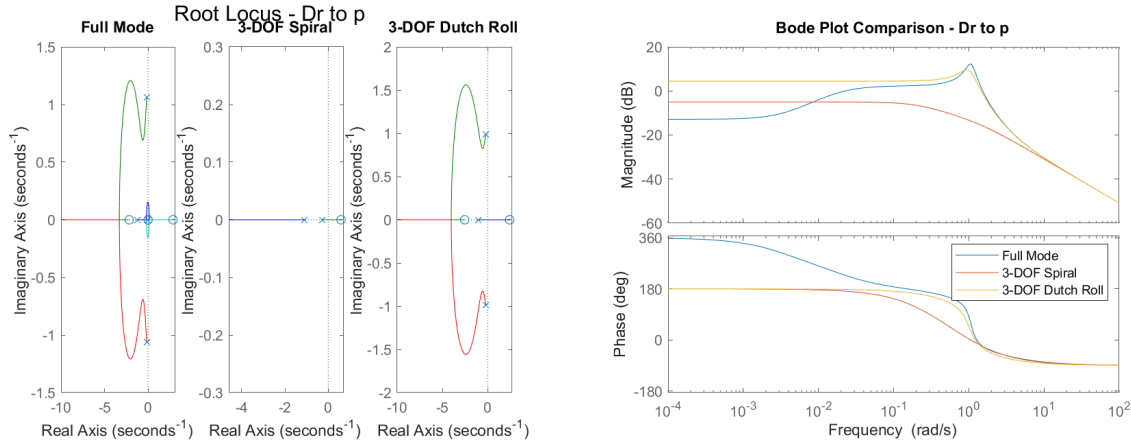


Figure 145: Root Locus and Bode plot for Δ rudder (Dr) to roll rate (p)

Comment:

The Root Locus for the full mode has 3 zeros and 4 poles, while the 3-DOF spiral model has 2 poles and 1 zero, and the 3-DOF Dutch roll model has 3 poles and 2 zeros.

Notably, the Root Locus shape for the 3-DOF Dutch roll model closely resembles that of the full mode.

In the Bode plots, the magnitude for the full mode starts at -10 dB, while the 3-DOF spiral model begins at -5 dB, and the 3-DOF Dutch roll model starts at 5 dB.

Additionally, there is a 180-degree phase shift between the full mode and both the 3-DOF spiral and Dutch roll modes over the lower frequency range (up to 10^0 rad/s). Beyond this frequency, all modes closely align in both phase and magnitude. In the frequency range from 10^{-1} to 10^0 rad/s, there is a slight phase variation between the 3-DOF spiral and Dutch roll models, but they quickly realign for the remainder of the frequency range.

The Rudder Deflection (Dr) to Yaw Rate (r)

Full Mode Transfer Function:

$$\frac{-0.61896s^3 - 0.77368s^2 - 0.16993s - 0.11207}{s^4 + 1.5126s^3 + 1.5437s^2 + 1.4025s + 0.026622}$$

3-DOF Spiral Mode Transfer Function:

$$\frac{-0.61896s - 0.70488}{s^2 + 1.3696s + 0.30196}$$

3-DOF Dutch Mode Transfer Function:

$$\frac{-0.61896s^2 - 0.7597s - 0.17149}{s^3 + 1.5126s^2 + 1.5245s + 1.057}$$

2-DOF Roll Mode Transfer Function:

$$\frac{-0.61896s - 0.068798}{s^2 + 0.3964s + 0.90722}$$

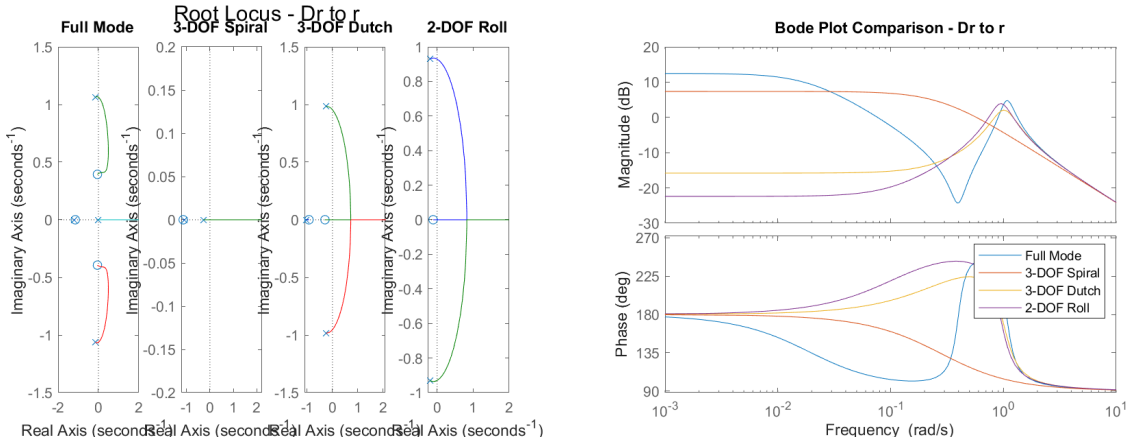


Figure 146: Root Locus and Bode plot for Δ rudder (Dr) to yaw rate (r)

Comment:

In the Root Locus, the full mode has 3 zeros and 4 poles, while the 3-DOF spiral mode has 2 poles and 1 zero, with this zero positioned on the real axis in the full mode. The 3-DOF Dutch roll and 2-DOF roll modes share the same Root Locus shape. Although the 3-DOF model includes an additional pole and zero at the origin compared to the 2-DOF model, these do not affect the final Root Locus shape.

In the Bode plots, both the full mode and 3-DOF spiral mode start with similar magnitude trends, beginning at 12 dB and 9 dB, respectively, and following the same trend for the first half of the frequency range. The 3-DOF Dutch roll and 2-DOF roll modes start at -18 dB and -21 dB, respectively, and also share a similar magnitude trend in the first half. In terms of phase, all modes start at 180° , but each mode behaves differently throughout the frequency range, gradually converging to the same phase at the final frequency, 10^1 rad/s.

The Rudder Deflection (Dr) to Roll Angle (phi)

Full Mode Transfer Function:

$$\frac{0.2532s^2 - 0.24401s - 1.7928}{s^4 + 1.5126s^3 + 1.5437s^2 + 1.4025s + 0.026622}$$

3-DOF Spiral Mode Transfer Function:

$$\frac{0.2532s - 0.20822}{s^3 + 1.3696s^2 + 0.30196s}$$

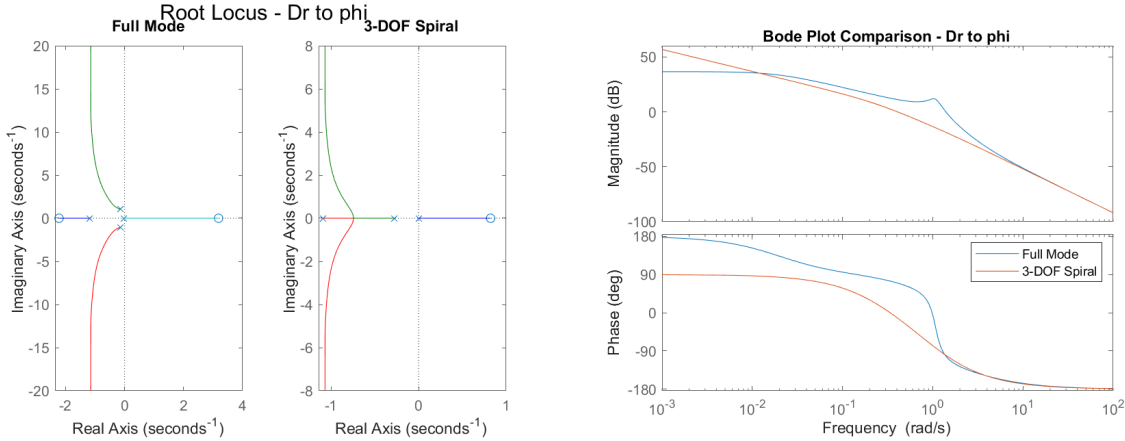


Figure 147: Root Locus and Bode plot for Δ aileron (Dr) to roll angle (ϕ)

Comment:

In the Root Locus, the full mode has 4 poles and 2 zeros, while the 3-DOF spiral mode has only 1 zero and 3 poles. This difference in the number of zeros and poles results in distinct Root Locus shapes for the two modes.

In the Bode plot, both modes follow the same trend in both magnitude and phase over the entire frequency range. However, at the beginning of the range, up to 10^0 rad/s, there is a 90-degree phase shift. This phase difference gradually decreases with increasing frequency until it aligns at 10^0 rad/s.

The Rudder Deflection (Dr) to Yaw Angle (epsi)

Full Mode Transfer Function:

$$\frac{-0.61986s^3 - 0.77481s^2 - 0.17018s - 0.11223}{s^5 + 1.5126s^4 + 1.5437s^3 + 1.4025s^2 + 0.026622s}$$

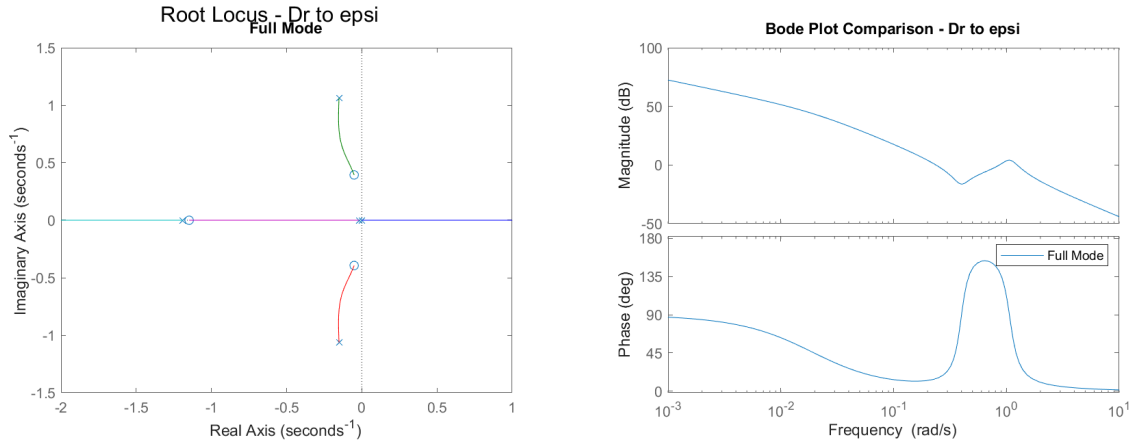


Figure 148: Root Locus and Bode plot for Δ aileron (Dr) to yaw angle (epsi)

Comment:

This transfer function appears only in the full mode, as shown in the Root Locus, where it has three zeros and five poles. A pole is located at the origin, making the system critically stable.

In the Bode plot, both the phase and magnitude decrease over the entire frequency range. The phase starts at 90° and drops to -180°, with a significant peak occurring at 10^0 rad/s. The magnitude begins at 70 dB and decreases to -50 dB.

6.7 Longitudinal autopilot

6.7.1 Pitch control

The purpose of this section is to design the control loop to control the altitude using pitch, where the pitch is controlled using a elevator:

elevator deflection (δ_e) \rightarrow pitch angle (θ) \rightarrow altitude (H)

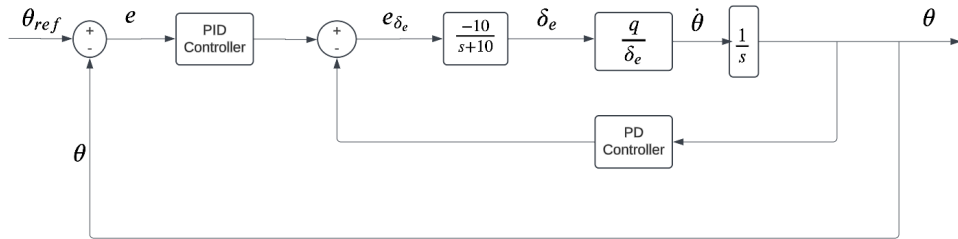


Figure 149: Control loop block diagram

Where:

$$\frac{q}{\delta_e} = \frac{-1.35s^3 - 0.9718s^2 - 0.01316s + 6.389 \times 10^{-19}}{s^4 + 2.581s^3 + 2.719s^2 + 0.01519s + 0.01502}$$

and $\frac{-10}{s+10}$ is the transfer function representing the servo actuator dynamics, The negative sign is introduced to counteract the negative sign in $\frac{q}{\delta_e}$, or alternatively, it can be achieved physically by installing the servo in reverse.

1-Design requirements

According to Cooper Harper flying qualities, we chose a $\zeta_{min} = 0.3$ and $\zeta_{max} = 2$ for the short period mode, and for the long-period we set $\zeta_{min} = 0.04$.

| Phugoid mode | |
|--------------|----------------|
| Level 1 | $\zeta > 0.04$ |
| Level 2 | $\zeta > 0$ |
| Level 3 | $T > 55s$ |

| Short period mode | Category A and C | | Category B | |
|-------------------|------------------|---------------|---------------|---------------|
| | ζ_{min} | ζ_{max} | ζ_{min} | ζ_{max} |
| Level 1 | 0.35 | 1.30 | 0.3 | 2.0 |
| Level 2 | 0.25 | 2.00 | 0.2 | 2.0 |
| Level 3 | 0.15 | - | 0.15 | - |

2- Open Loop analysis:

As seen from the root locus after applying the boundaries of $\zeta_{min} = 0.04$ for long period and $\zeta_{min} = 0.3$ for short period, we can clearly see in the figures below that the short period's poles are achieving the design requirements, while the long-period's poles aren't.

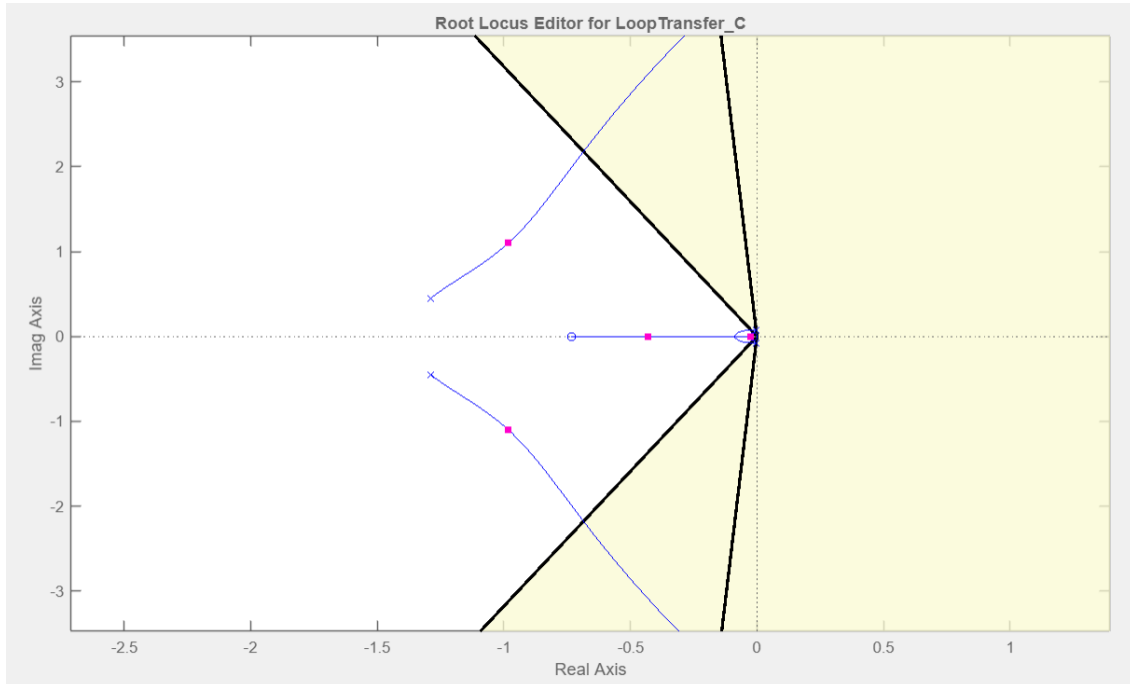


Figure 150: Open loop short period

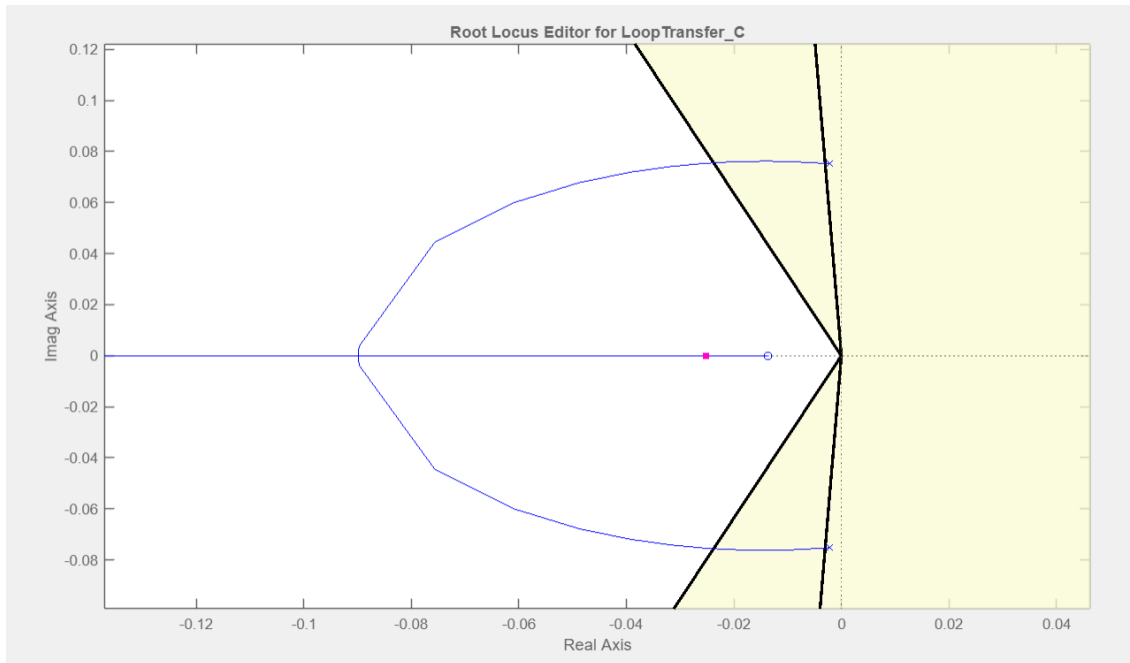


Figure 151: Open loop Long period

Also, we can notice in the step response shown below that the settling time is 151 seconds with an overshoot percentage of 69.4%. Therefore, pitch control is required.

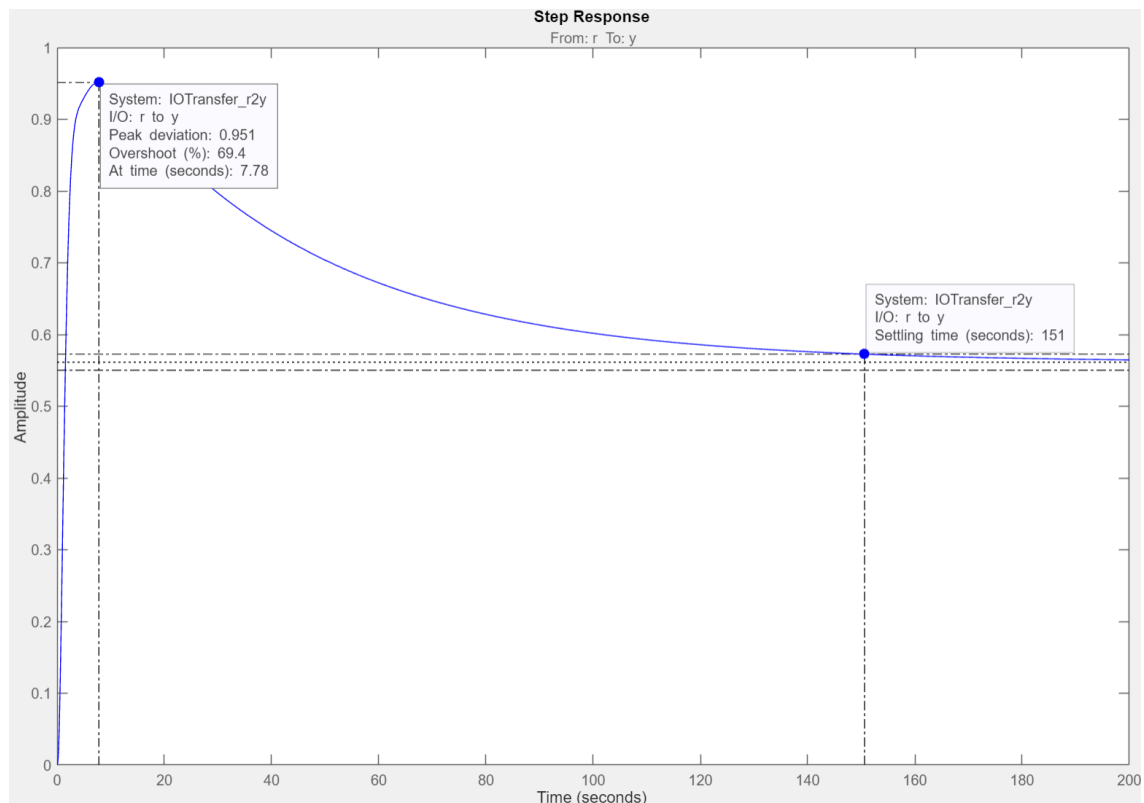


Figure 152: Open Loop Step Response

3- Closed Loop analysis:

To tune the model in Matlab we used the Control System Designer application. After trial and error, we reached this final pole position.

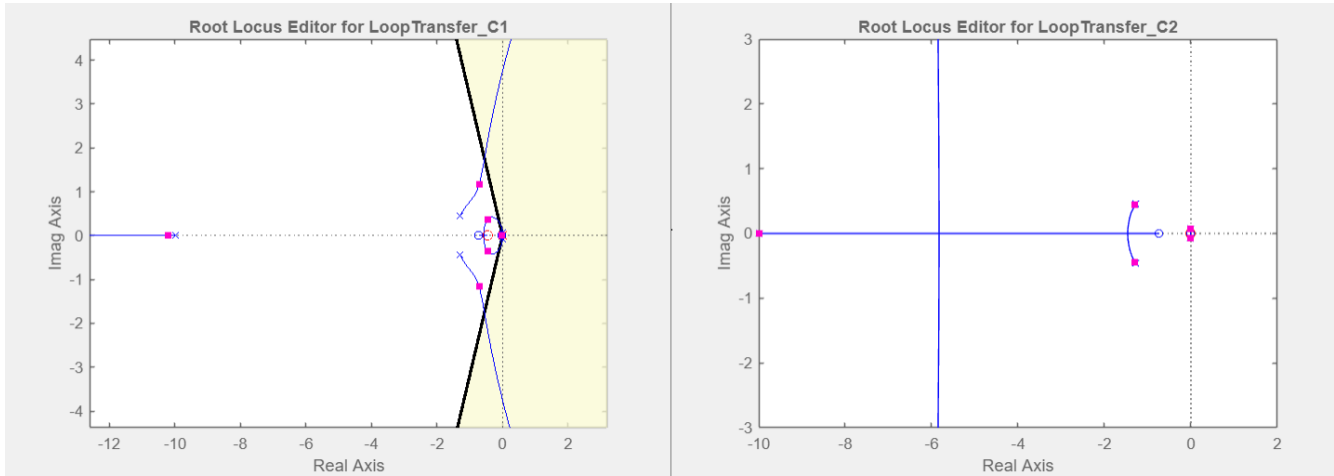


Figure 153: Closed loop root locus with control

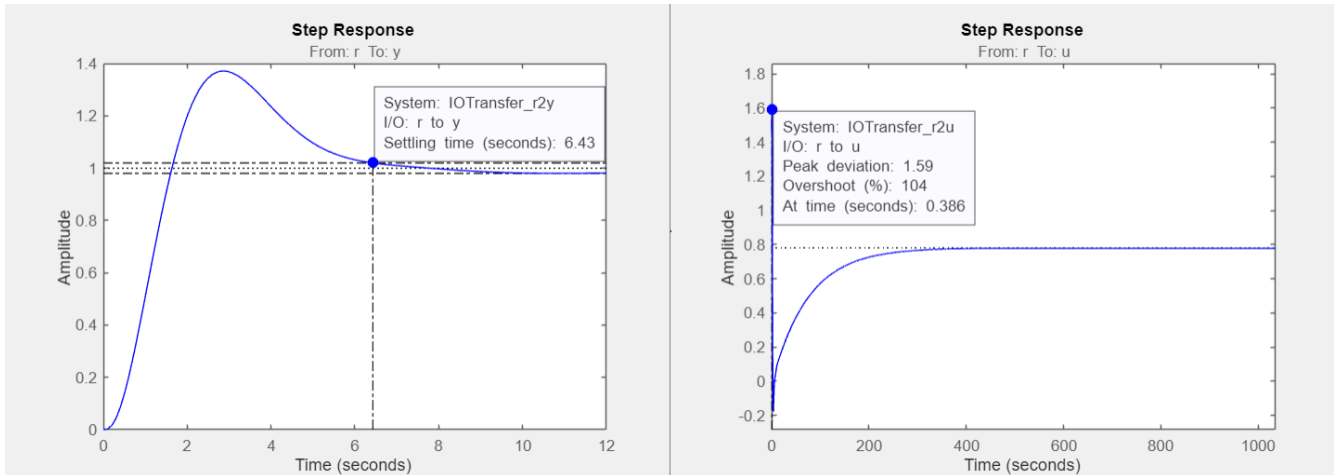


Figure 154: Closed loop step response

After tuning, the output values of the transfer functions of the controller turned out to be:

PI:

$$\frac{1.4618(s + 0.4445)}{s}$$

PD:

$$0.005915s$$

The final settling time was 6.43 seconds, with a percentage overshoot of 37.1, and a peak deviation of 1.59.

The peak deviation indicates that for each $1^\circ \delta_e$, the pitch angle will change with 1.59° . Thus with the maximum deviation of 15° for elevator, the pitch angle will be $\theta = 15 \cdot 1.59 = 23.85^\circ$.

4- Simulink Model:

After implementing the Milti Input Multi Output (MIMO) system in Simulink, these results were obtained when giving a command $\theta = 15 \text{ deg}$

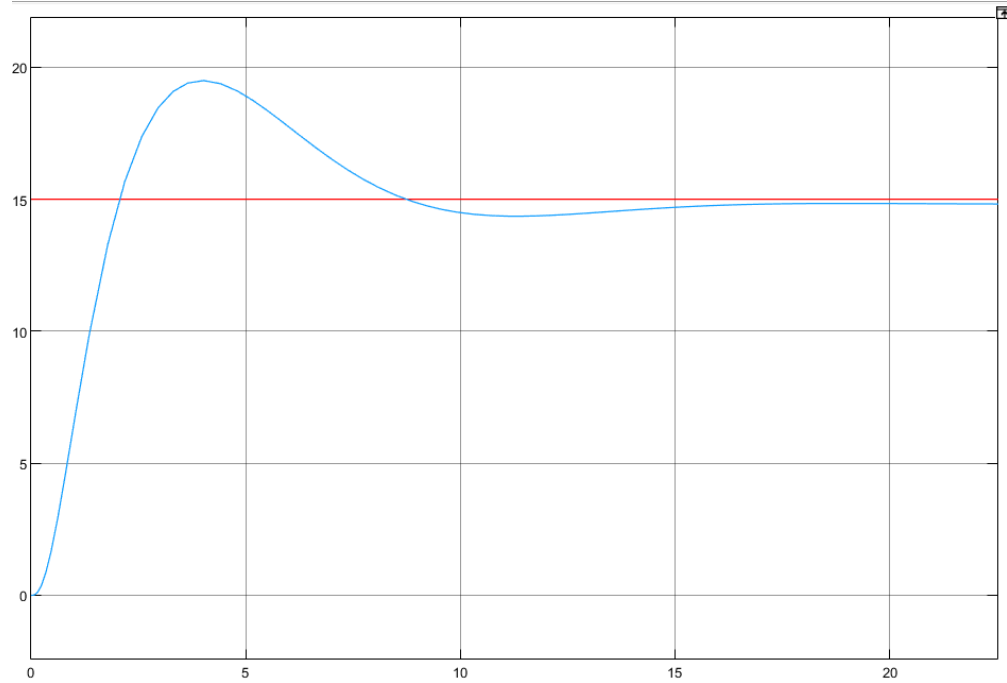


Figure 155: Step Response when $\theta = 15^\circ$

To calculate the altitude, we used the following equations:

$$\dot{h} = V_{T0} \sin(\gamma)$$

Where

$$\gamma = \theta - \alpha$$

$$\theta = \theta_0 + \Delta\theta$$

$$\alpha = \tan^{-1} \left(\frac{w}{u} \right)$$

$$u = u_0 + \Delta u$$

$$w = w_0 + \Delta w$$

$$V_{T0} = \sqrt{u^2 + v^2 + w^2} = \sqrt{u^2 + w^2}$$

By differentiating \dot{h} , we can get $H = h + h_0$ where $h_0 = -z_0$

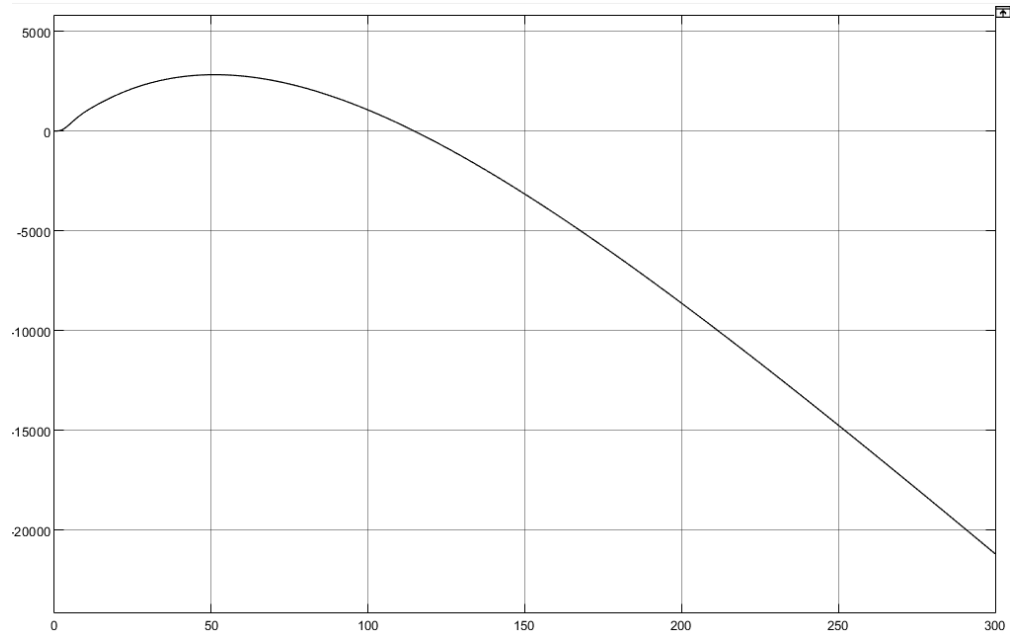


Figure 156: Altitude vs. time when $\theta = 15^\circ$

We observe that the airplane initially ascends but then begins to descend. This behavior can be explained by the decrease in velocity; as the velocity decreases, the airplane lacks sufficient energy to sustain both a pitch angle of 15° and a continued increase in altitude. Consequently, it starts to descend while maintaining the pitch angle of 15° . A graph of the velocity is provided below to illustrate this behavior.

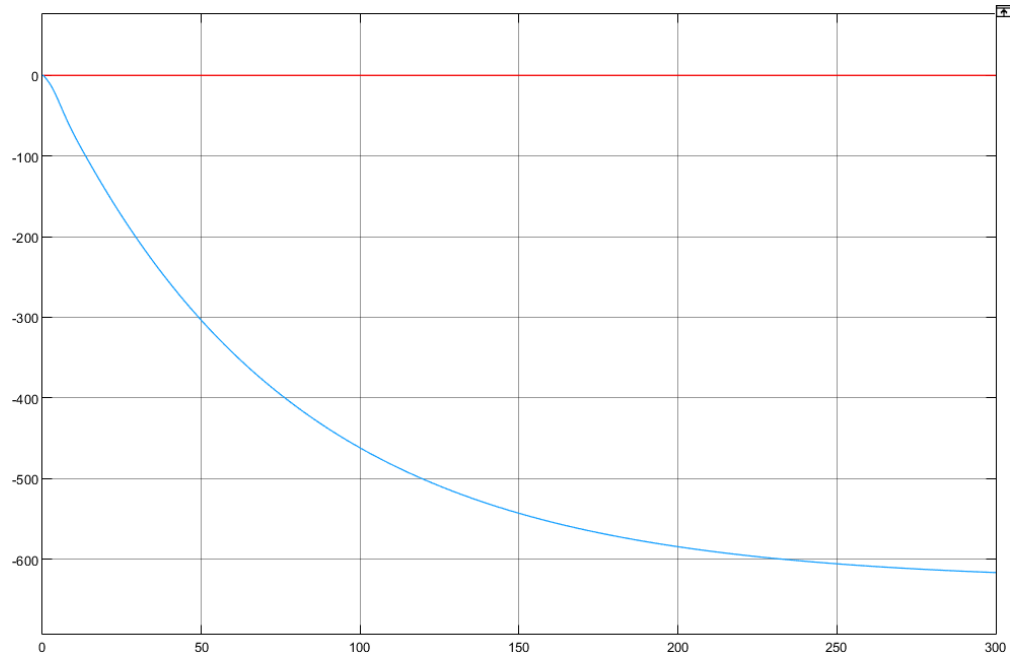


Figure 157: Velocity vs. time when $\theta = 15^\circ$

6.7.2 Altitude Controller

The purpose of this section is to design the altitude control loop using pitch as the intermediate variable. The control process follows this sequence:

- **Input Command:** Commanded altitude (h_{com}) is compared to the actual altitude (h).
- **Error Correction:** A proportional or proportional-integral (P or PI) controller processes the altitude error to generate the commanded pitch angle (θ_{com}).
- **Pitch Loop Dynamics:** The commanded pitch angle (θ_{com}) is passed through the pitch control loop, resulting in the actual pitch angle (θ).
- **Altitude Dynamics:** The actual pitch angle (θ) affects the climb angle (γ) and subsequently the altitude (h).

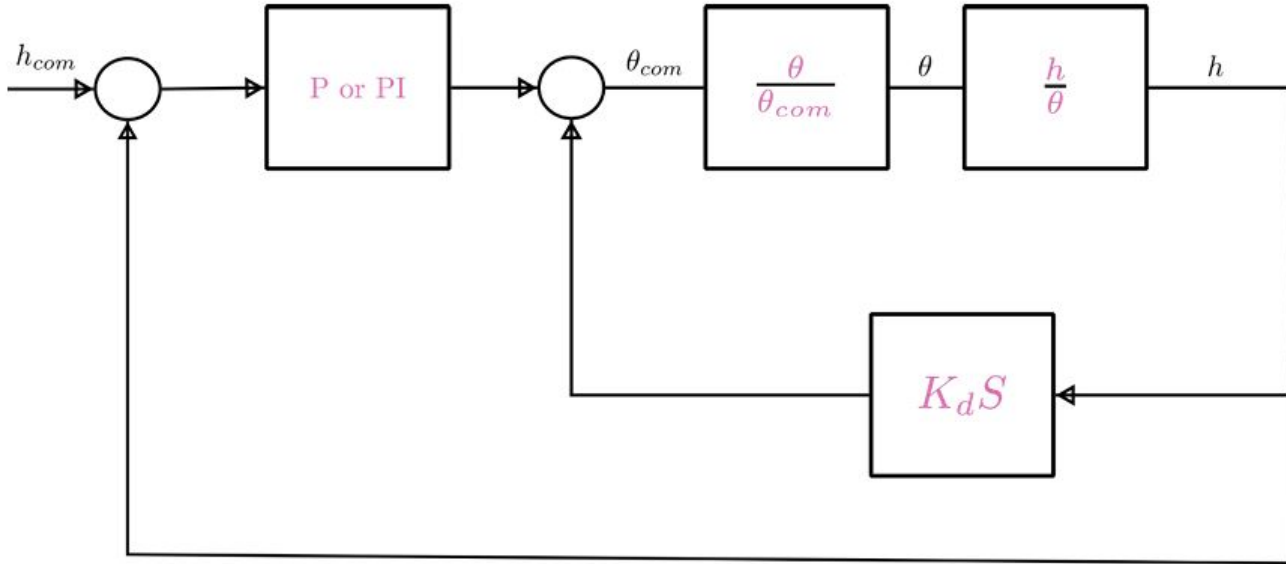


Figure 158: Control loop block diagram for the altitude controller.

The block diagram of the altitude control system is shown above. The pitch control loop is embedded as the inner loop, with its closed-loop transfer function $\frac{\theta}{\theta_{com}}$. The system also incorporates altitude dynamics represented by $\frac{h}{\theta}$.

1- Mathematical Formulation:

We derive the relationship between altitude (h) and pitch angle (θ) as follows:

1. Vertical Acceleration:

The vertical acceleration a_z is defined as:

$$a_z = \dot{w} + pv - qu$$

After linearization, assuming small perturbations about the equilibrium state:

$$a_z = \dot{w} - U_0 q$$

Where:

2. U_0 : Forward velocity at equilibrium.
3. q : Pitch rate.
4. \dot{w} : Derivative of vertical velocity.

5. Altitude Dynamics:

Using the relation $\ddot{h} = -a_z$, the Laplace transform yields:

$$h(s) = -\frac{a_z}{s^2}$$

Substituting $a_z = \dot{w} - U_0 q$:

$$h(s) = -\frac{1}{s^2} (\dot{w} - U_0 q)$$

6. Transfer Function:

Relating h to θ , we obtain:

$$\frac{h}{\theta} = -\frac{1}{s^2} \left(\frac{w}{\delta_e} - U_0 \frac{q}{\theta} \right)$$

Simplifying further using approximations for $\frac{q}{\delta_e}$ and $\frac{\theta}{\delta_e}$:

$$\frac{h}{\theta} = -\frac{U_0}{s} \left(\frac{\alpha/\delta_e}{\theta/\delta_e} - 1 \right)$$

2- Open-Loop Analysis:

The open-loop transfer function from the commanded altitude (h_{com}) to the actual altitude (h) is given by:

$$\frac{h}{h_{com}} = \frac{-328.4s^4 - 837.1s^3 + 7026s^2 + 3302s + 19.1}{s^7 + 12.58s^6 + 27.76s^5 + 38.62s^4 + 23.77s^3 + 6.862s^2 + 0.0878s}$$

This transfer function represents the dynamics of the altitude control system and includes the inner pitch control loop.

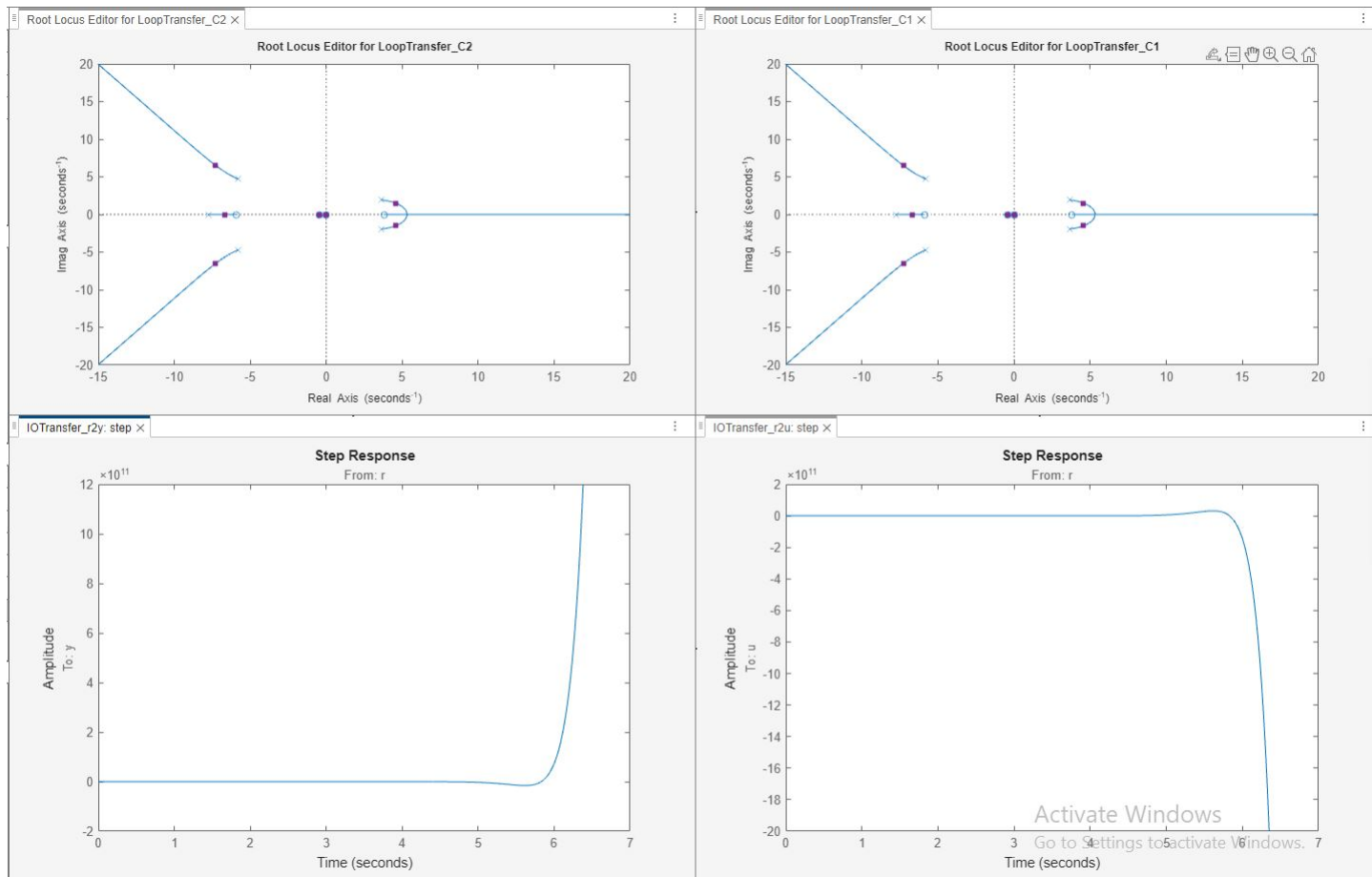


Figure 159: Open-loop step response and root locus analysis.

The figure above shows the open-loop response, including the step response and root locus. It indicates that the system's response does not meet the desired specifications, requiring closed-loop control for improvement.

3- Closed-Loop Analysis:

The closed-loop altitude control system incorporates a PI controller to process the altitude error. The transfer function of the PI controller is:

$$C(s) = \frac{0.00048163(s + 0.004667)}{s}$$

When the PI controller is applied, the resulting closed-loop transfer function becomes:

$$\frac{h}{h_{com}} = \frac{-0.1582s^5 - 0.4039s^4 + 3.382s^3 + 1.606s^2 + 0.01662s + 4.293 \times 10^{-5}}{s^8 + 12.58s^7 + 27.76s^6 + 38.46s^5 + 23.37s^4 + 10.24s^3 + 1.694s^2 + 0.01662s + 4.293 \times 10^{-5}}$$

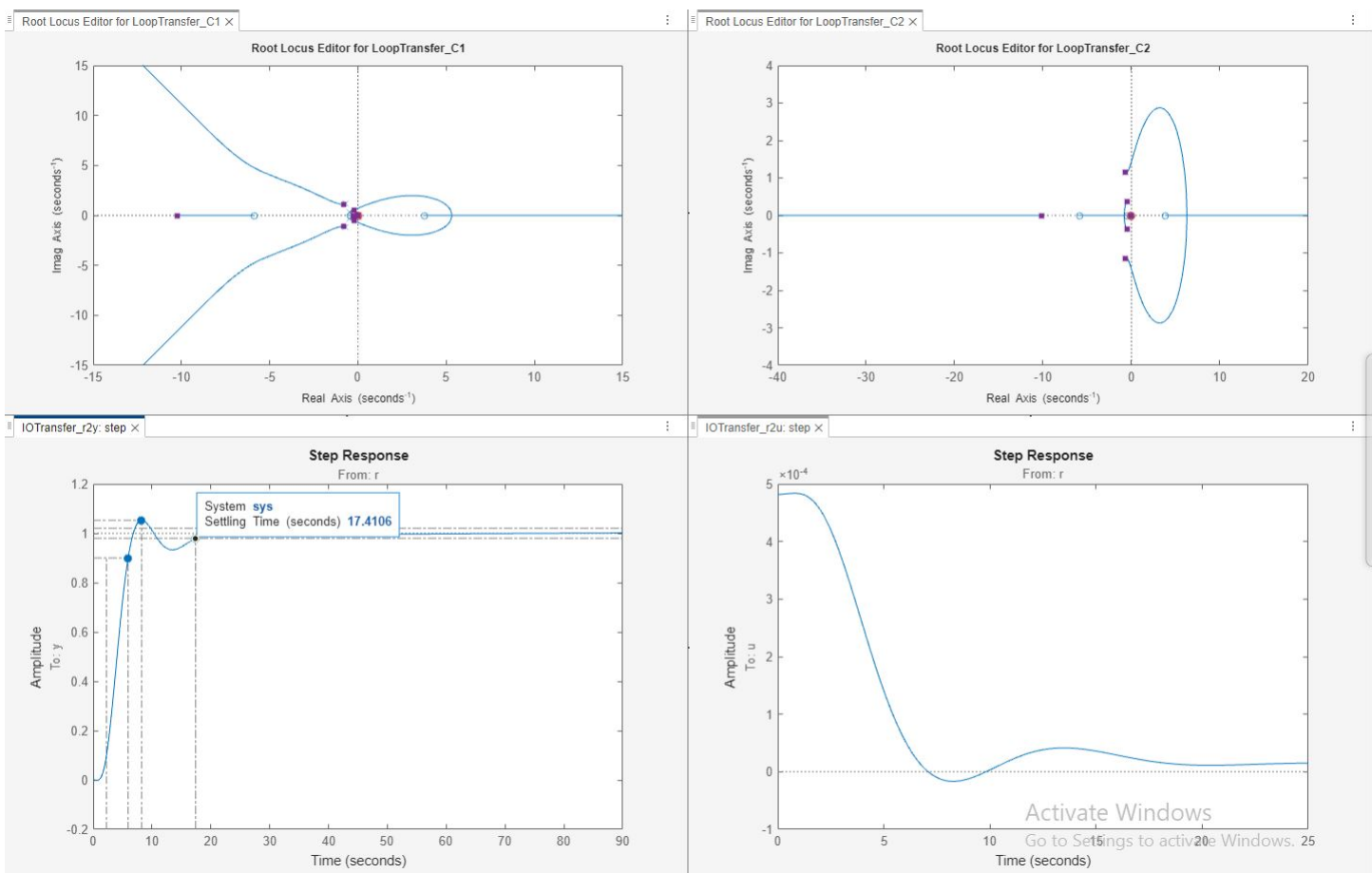


Figure 160: Closed-loop step response and root locus analysis.

The figure above shows the closed-loop step response and root locus. With the PI controller, the system achieves improved settling time and reduced overshoot, meeting the design requirements for altitude control.

The final settling time was 17.4106 seconds for each 1 step input for altitude (in feet), which corresponds approximately to 0.028 degrees of elevator deflection.

4- Simulink Model:

To validate the altitude control system, a Simulink model was created. The model includes the PI controller, pitch control dynamics, and altitude transfer function.

The system was tested with a 200-foot step input. The altitude reached the target with a settling time of approximately 17.41 seconds, matching MATLAB results. This corresponds to an elevator deflection of about 0.028 degrees.

The figures below show the simulation results: simulation:

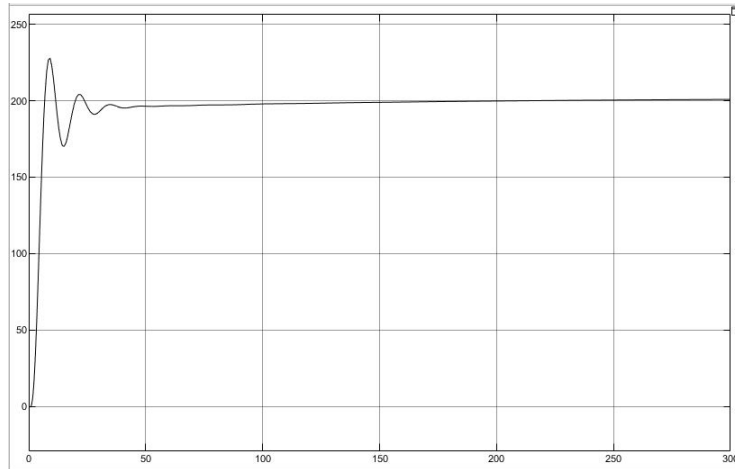


Figure 161: Simulink model output showing the altitude response to a step input of 200 feet.

The first figure above validates that the altitude successfully reaches the commanded value of 200 feet within the expected settling time.

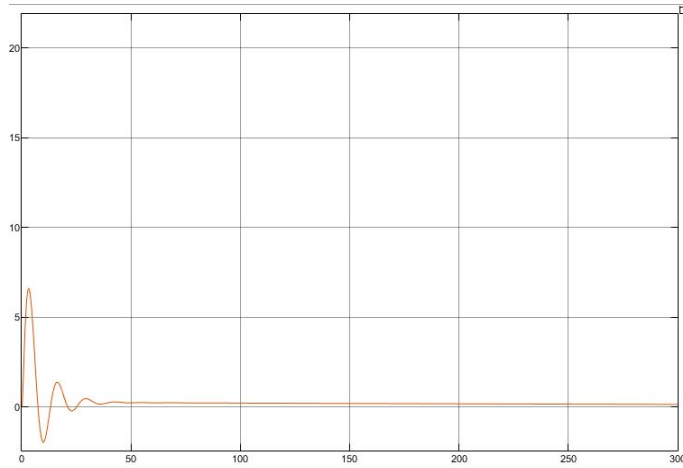


Figure 162: Simulink model output showing the pitch angle response (θ) to a step input of 200 feet.

The second figure shows that the pitch angle (θ) changes to nearly 5.6 degrees for the step input of 200 feet. This result is consistent with the altitude input and confirms the control system's stability and responsiveness.

These results validate the design objectives of the altitude control system, demonstrating that it performs as expected under simulation conditions.

6.8 Velocity Control

In this section, we discuss the velocity control mechanism for an aircraft achieved through throttle adjustments. The throttle serves as the primary actuator to regulate engine power,

which directly influences the velocity of the aircraft. The command velocity is computed using the following equation:

$$OL_{u_{ucom}} = -\text{servo} \cdot \text{engine_timelag} \cdot u_{dT} \quad (1)$$

Now we analyze the performance of the untuned velocity control system using the open-loop transfer function in the MATLAB `sisotool` environment. The plots in Figure 163 illustrate the root locus and step response of the system before tuning, providing insights into its behavior. The root locus plots (LoopTransfer_C1 and LoopTransfer_C2) in the upper portion of Figure 163 reveal several important characteristics. The poles of the system move along asymptotes towards infinity, indicating potential instability. In LoopTransfer_C1, some poles cross into the right-hand side of the complex plane, signifying an unstable open-loop system. The insufficient damping of poles in the left-hand plane suggests that the system would exhibit oscillatory behavior if closed-loop control were applied. Additionally, the lack of pole-zero proximity in the stable region indicates poor transient response characteristics. The step response plots (IOTransfer_r2u and IOTransfer_r2y) in the lower portion of Figure 163 also highlight significant issues in the system's dynamics. The step response of IOTransfer_r2u shows a very large transient amplitude, indicating excessive overshoot and instability. Similarly, the step response of IOTransfer_r2y exhibits unbounded behavior with oscillations and significant deviation from the desired steady-state value. These responses demonstrate the system's inability to control its dynamics effectively in the untuned state. From these observations, it is evident that the untuned system is unstable and exhibits poor transient response. To achieve stability and proper dynamic behavior, it is essential to tune the controller to place the poles of the closed-loop system in the left-hand plane with adequate damping.

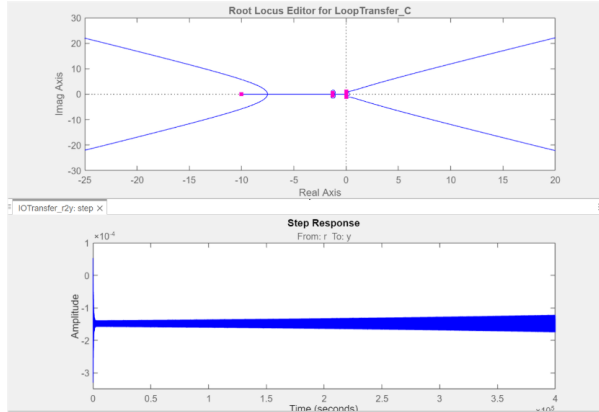


Figure 163: Root locus and step response plots for the untuned velocity control system.

The performance of the velocity control system was improved by tuning the open-loop transfer function using MATLAB `sisotool`. The tuning involved modifications to the compensators C_1 (PI Controller) and C_2 (Lead Compensator) as follows:

- For C_1 (PI Controller), the transfer function is given by:

$$C_1(s) = \frac{-1606.2(s + 0.2334)}{s} \quad (2)$$

This includes a real zero at -0.2334 with a damping ratio of 1, a frequency of 0.2334, and an integrator at $s = 0$.

- For C_2 (Lead Compensator), the transfer function is given by:

$$C_2(s) = \frac{-1.6408 \times 10^5(s - 0.0007846)}{(s + 1.307)} \quad (3)$$

This includes a real pole at -1.307 with a damping ratio of 1 and a frequency of 1.307, and a real zero at 0.0007846 with a damping ratio of -1 and a frequency of 0.0007846.

Figure 164 shows the root locus and step response plots of the tuned system.

The root locus plots (LoopTransfer_C1 and LoopTransfer_C2) in the upper portion of Figure 164 indicate significant improvements in the system's stability and dynamics. In LoopTransfer_C1, the addition of the real zero and integrator has ensured that the poles remain in the left-hand plane, resulting in a stable system. Similarly, the adjustments in LoopTransfer_C2 have ensured that the poles and zeros are appropriately distributed, contributing to a stable response with adequate damping. The overall root locus behavior shows a well-tuned system with reduced potential for oscillatory or unstable behavior.

The step response plots (IOTransfer_r2y and IOTransfer_r2u) in the lower portion of Figure 164 further confirm the improved performance. The step response of IOTransfer_r2y shows a smooth transient response with minimal overshoot and a settling time of approximately 52.1 seconds, indicating improved transient stability and reduced oscillations. On the other hand, the step response of IOTransfer_r2u demonstrates the system's ability to handle control input dynamics effectively, with a stable response achieved over time despite initial transient variations.

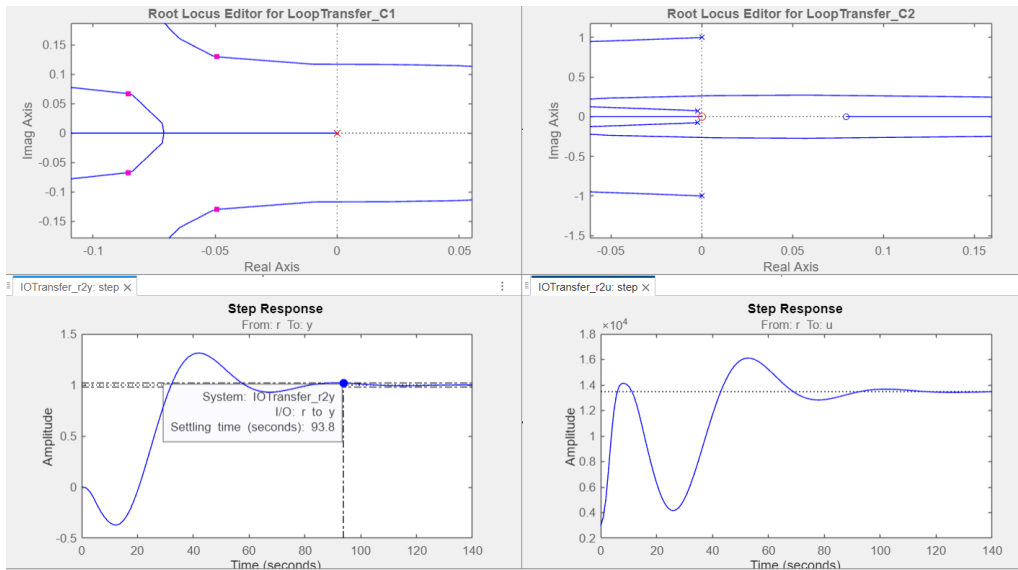


Figure 164: Root locus and step response plots for the tuned velocity control system.

To evaluate the performance of the control system, the tuned transfer functions were implemented in a Simulink model to design the control loop. The input command for the velocity (u) was set to 10, and the results are illustrated in the plots below.

The first plot (Figure 165) shows the red curve, which represents the desired velocity (u), and the brown curve, which represents the system's actual performance in reaching the desired velocity. The control system effectively tracks the desired velocity, demonstrating a smooth transient response. There is an initial overshoot, which peaks at approximately 15 before gradually settling around the desired velocity of 10. This indicates that the system achieves satisfactory stability and demonstrates an acceptable transient performance, with minimal oscillations in the settling phase. Such behavior is indicative of a well-tuned controller, capable of handling velocity commands effectively.

The second plot (Figure 166) illustrates the altitude gained by the aircraft during the simulation. The altitude increases steadily over time, following a near-linear trajectory. This response suggests that the system maintains consistent climb performance while executing the control input for velocity. The absence of fluctuations in altitude highlights the robustness of the control system in managing vertical dynamics in conjunction with velocity control.

In conclusion, the Simulink simulation confirms that the tuned control system performs effectively, achieving the desired velocity while ensuring smooth altitude transitions. These results validate the design of the control loop using the tuned transfer functions.

Figure 167 shows the throttle input used by the controller to achieve the desired velocity

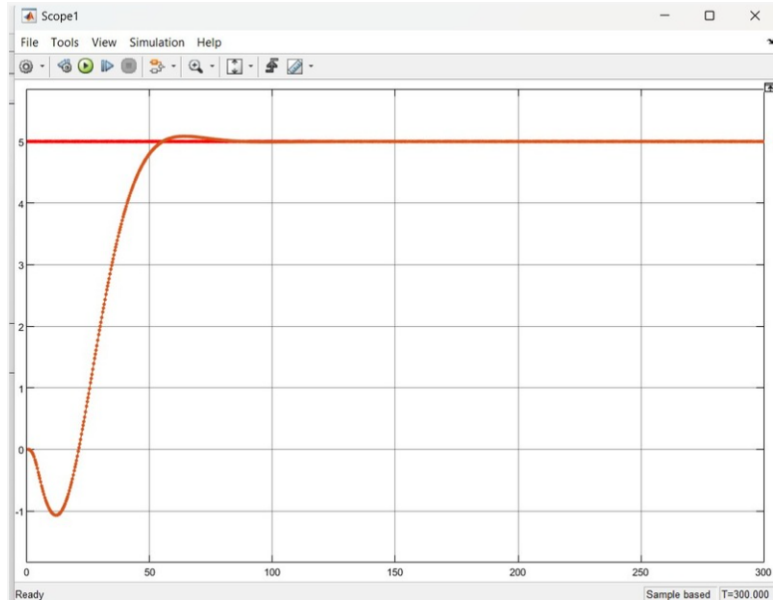


Figure 165: Velocity response: The red curve represents the desired velocity ($u = 5$), and the brown curve shows the system's performance in tracking the desired velocity.

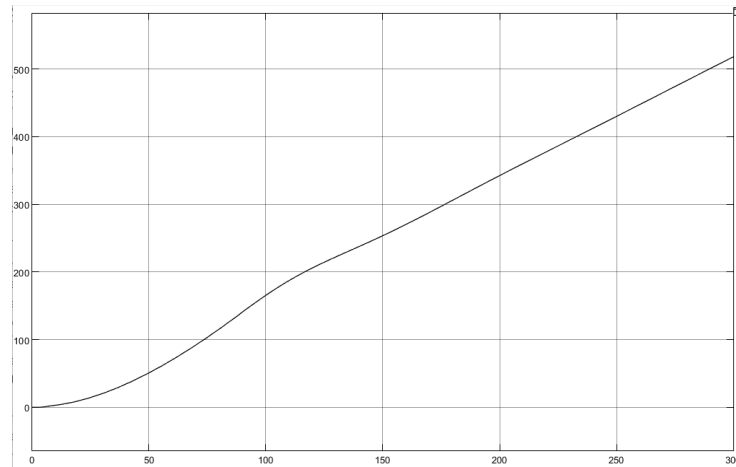


Figure 166: Altitude response: The altitude gained by the aircraft over time, showing steady and consistent climb performance.

($u = 10$). Initially, the throttle exhibits high-frequency oscillations, reflecting the controller's efforts to correct large velocity discrepancies during the transient phase. As the system stabilizes, the throttle reduces sharply to counteract overshoot and then gradually adjusts to maintain the desired velocity. By around 200 seconds, the throttle settles into a steady-state value, demonstrating effective control.

While the initial oscillations indicate room for further tuning to smooth the transient response, the system successfully achieves stability and consistent throttle control in the steady state.

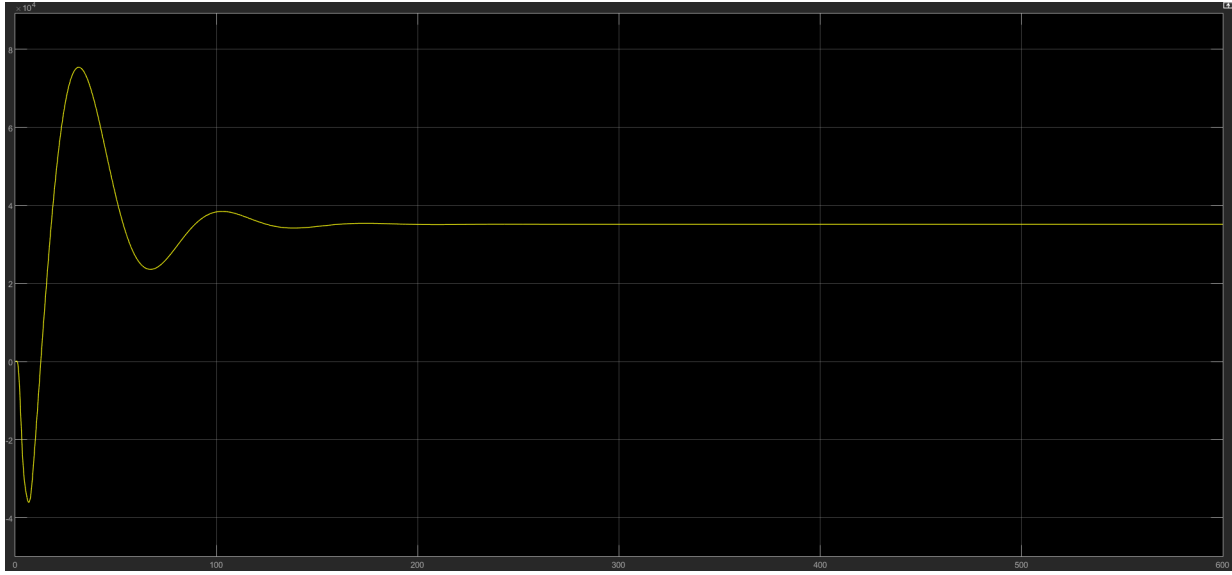


Figure 167: Throttle response: The throttle input used by the controller to achieve the desired velocity ($u = 5$).

6.9 Lateral Autopilot

The lateral autopilot plays a vital role in stabilizing and controlling an aircraft's motion in the lateral-directional plane. It ensures smooth, coordinated turns by managing the rudder and aileron. When combined with the longitudinal autopilot, the system achieves a coordinated level turn, maintaining both heading and altitude effectively.

Coordinated turns are necessary to ensure passenger comfort and minimize energy losses.

Without coordination, lateral forces or sideslip may occur, resulting in discomfort and increased drag. In manually controlled flights, pilots adjust the rudder, aileron, and elevator to achieve coordination. In contrast, the lateral autopilot automates these tasks, improving efficiency and precision.

This section outlines the design of a lateral autopilot system, incorporating yaw damper and roll controllers, as well as an outer-loop heading control.

6.9.1 Yaw Damper Control

The role of the yaw damper is to enhance damping in the Dutch roll mode, a lightly damped oscillatory motion, to stabilize yaw dynamics.

To perform a coordinated turn, both the aileron and rudder are used to produce the required bank angle ϕ and yawing acceleration r to achieve no slip or zero lateral acceleration while turning, compensating for adverse yaw. The yaw damper autopilot design is shown in the block diagram below.

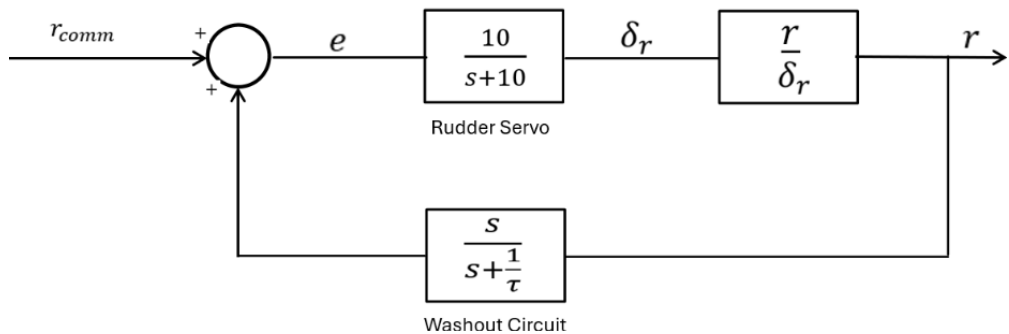


Figure 168: Yaw Damper controller

This block diagram includes the transfer function of yaw rate with respect to rudder deflection, $\frac{r}{\delta_r}$, in addition to the rudder servo dynamics transfer function. To achieve a turn with a yaw acceleration of non-zero steady-state value, a washout circuit (high-pass filter) is required, as illustrated in the block diagram.

The yaw rate transfer function is given as:

$$\frac{r}{\delta_r} = \frac{-0.6149s^3 - 0.7762s^2 - 0.1704s - 0.1123}{s^5 + 1.509s^4 + 1.479s^3 + 1.401s^2 + 0.02655s}$$

The rudder servo actuator dynamics transfer function is represented by:

$$\frac{10}{s + 10}$$

1 - Design Requirements:

According to Cooper-Harper flying qualities, for Category B, Level 1, we chose a minimum damping ratio $\zeta_{min} = 0.08$.

2 - Closed-Loop Analysis:

Using the SISO tool in MATLAB for the high-pass filter (washout circuit) design, we first inserted the minimum design requirements on the open-loop root locus with a damping ratio of $\zeta_d = 0.08$. After trial and error, we determined the final pole position, as shown below:

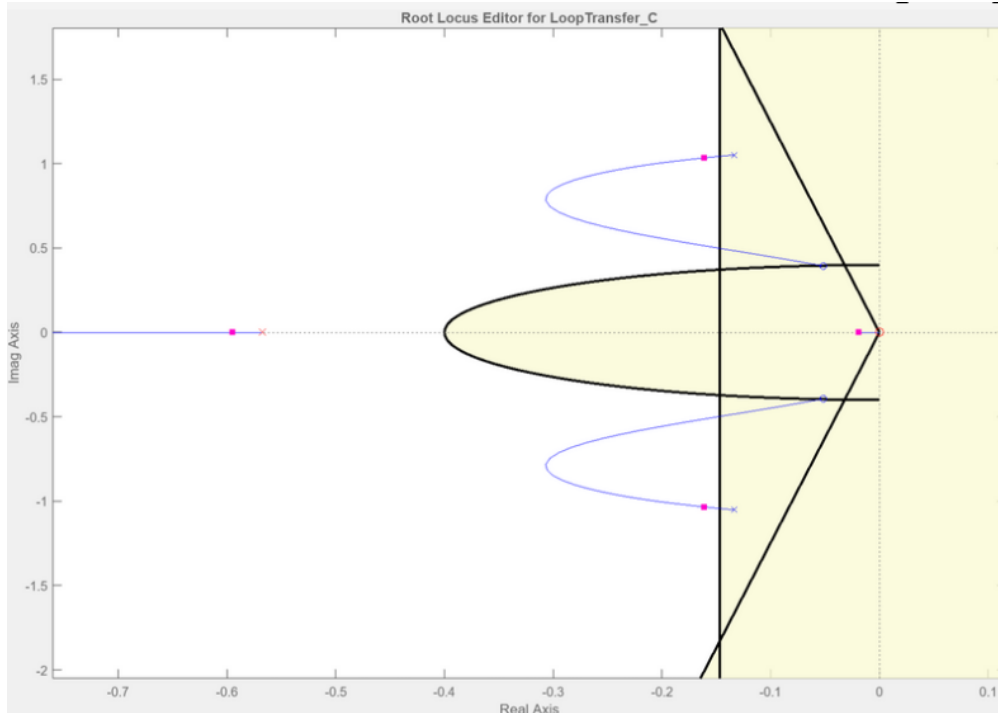


Figure 169: Root locus of closed-loop transfer function

After tuning and designing the high-pass filter, the impulse response for the output and δ_r control action are as follows:

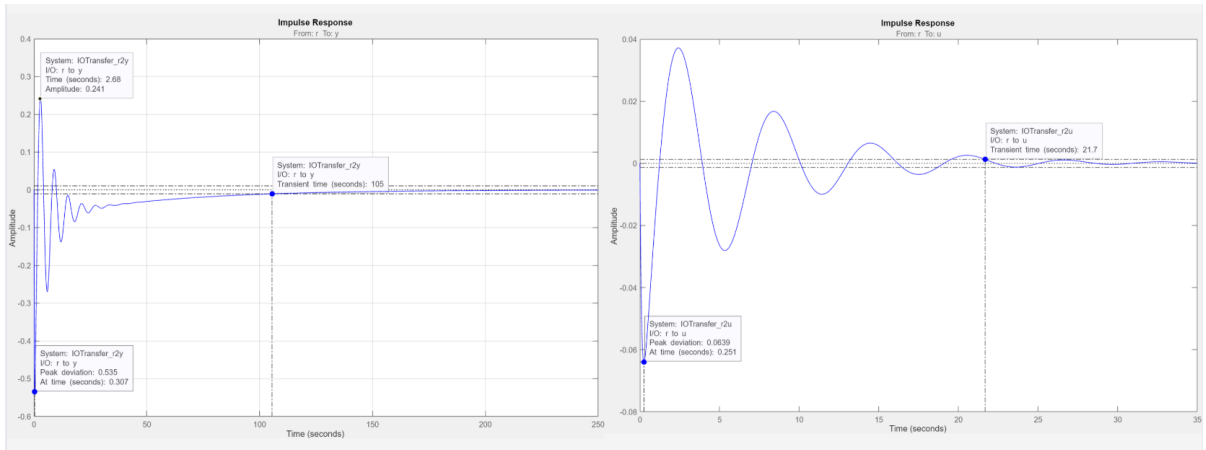


Figure 170: Yaw Damper Closed-Loop Impulse Response

The washout circuit results in a settling time of $T_s = 0.307$ seconds and a control action peak response of 0.0639 radians.

The transfer function of the washout circuit is:

$$\frac{0.13388 s}{s + 0.5674}$$

3 - Simulink Model:

After implementing the Multi-Input Multi-Output (MIMO) system in Simulink, the following results were obtained when giving a command $r_{\text{comm}} = 0$. The control behavior, angles, and rate responses are shown in the figures below:

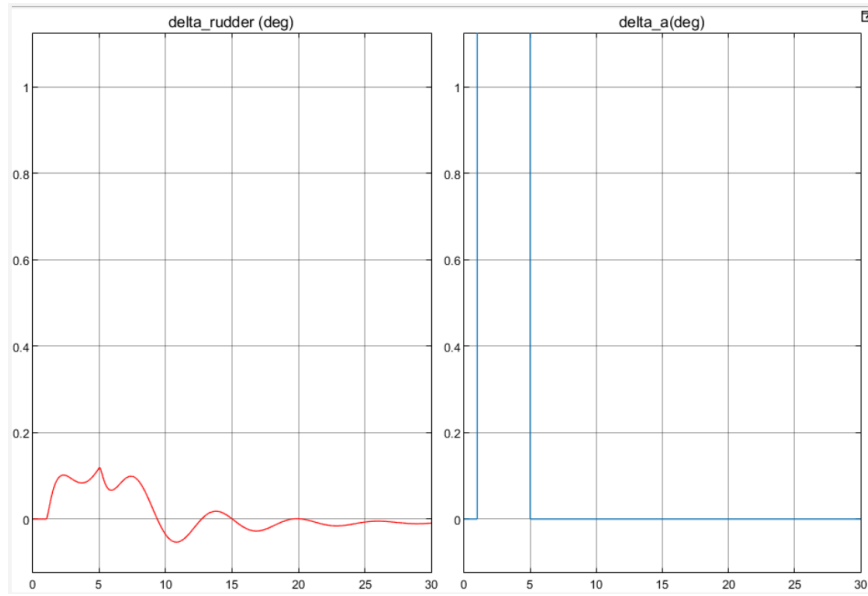


Figure 171: Control Surfaces Behavior

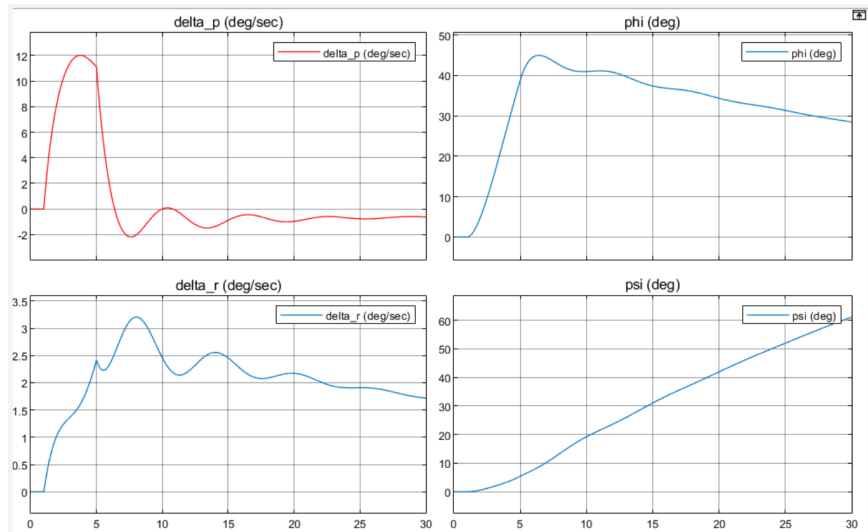


Figure 172: Control Surfaces Responses

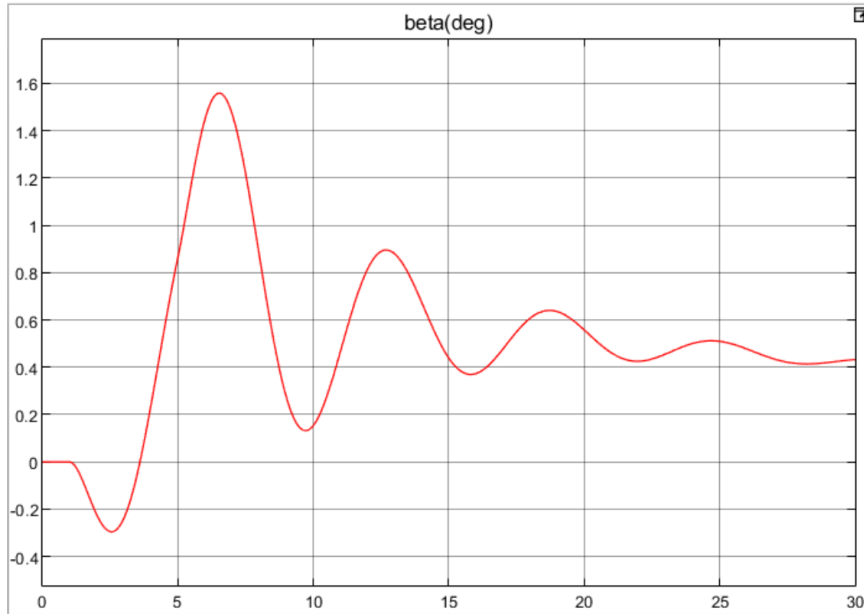


Figure 173: Angles and Rates Response

Comments over response plots

The response plots demonstrate that the lateral autopilot system, including the yaw damper, roll controller, and heading controller, functions effectively:

- The control surfaces exhibit stable behavior with well-damped oscillations.
 - Bank angle and heading changes are achieved smoothly with minimal overshoot or instability.
 - The sideslip angle (β) is well-controlled, ensuring coordinated turns.
- These results validate the controllers' design and confirm their ability to meet performance requirements.

6.9.2 Roll control

To control the other state, we need to design a roll controller, but since the open loop tf was already stable, there was no control needed, as shown in the following block diagram.

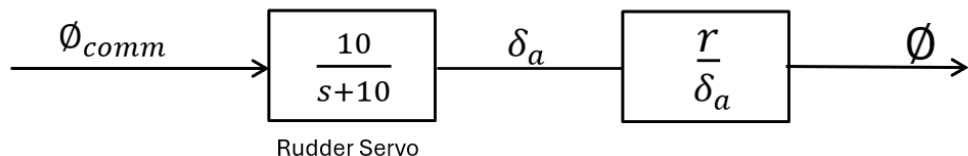


Figure 174: Roll Damper controller

As shown in the figure. It includes the transfer function of the roll angle w.r.t. aileron a/ (δ_a) but for the coordinated plane. We add the servo dynamics transfer function to express ailerons servos.

1- Open Loop analysis:

As seen from the root locus after applying the boundaries of $\zeta_{min} = 0.08$. we can clearly see in the figures below that the poles are achieving the design requirements.

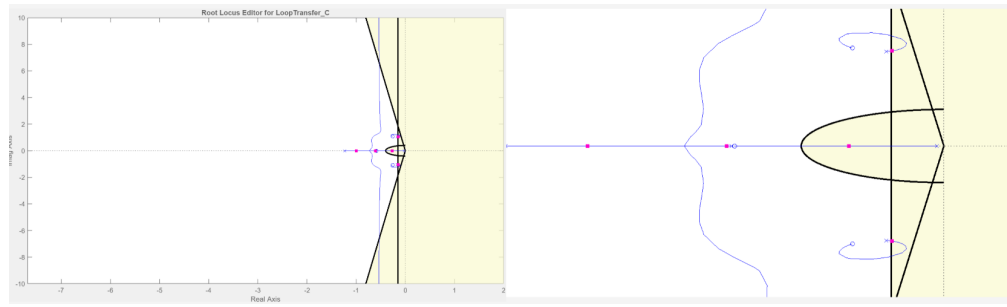


Figure 175: Root locus of open loop TF

Also, we can notice in the step response shown below that the Transient time is 16.3 seconds , and control action peak response of 0.173 rad.

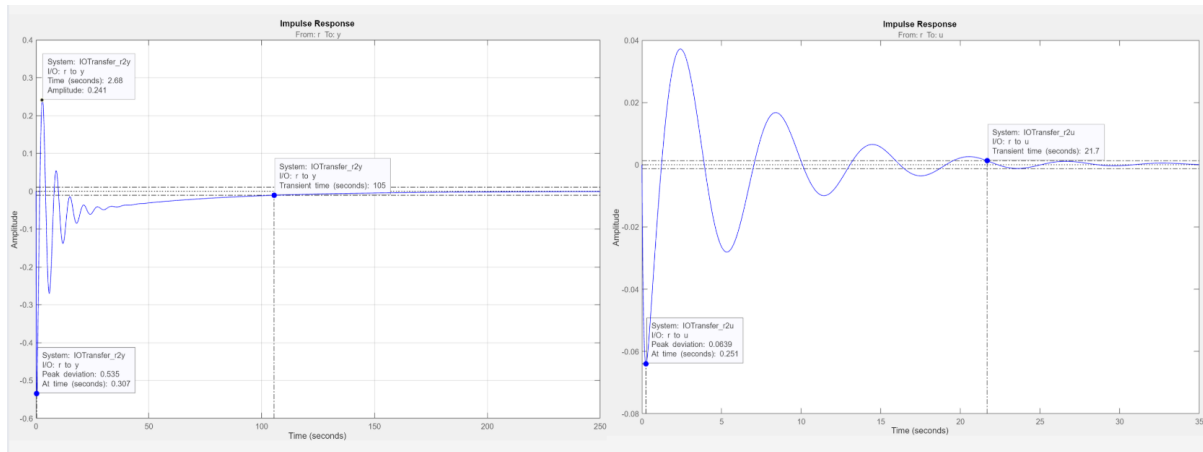


Figure 176: Impulse response of open loop TF $\phi/(\delta_a)$.

6.9.3 Heading controller design

To achieve coordination where the total acceleration is equal to zero, we will have to obtain a certain bank angle ϕ which corresponds for a certain speed U_0 and a certain turning rate $\dot{\psi}_0$, and this bank angle can be obtained from the free body diagram of the airplane during turn. As we have already obtained the yaw damper, we want to control the heading ψ now.

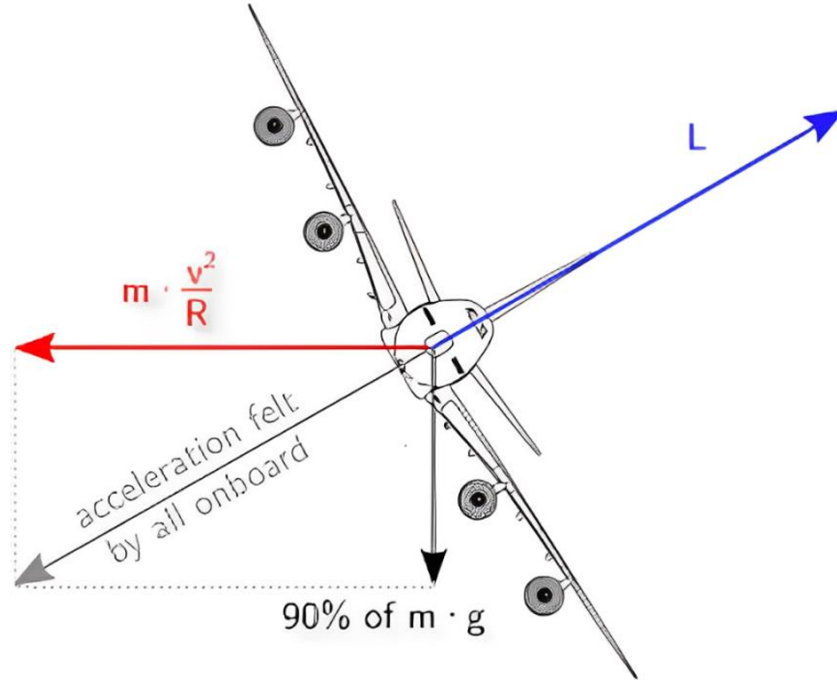


Figure 177: free body diagram of the airplane during turn.

Knowing that the tangential velocity is U_0 and that R is the radius of the turn:

$$U_0 = R \cdot \dot{\psi}$$

To control the heading (ψ), the aircraft must bank to achieve the desired directional change. This process results in a coordinated turn with an angular rate of $\dot{\psi}$.

When the aircraft is banked at an angle ϕ , the forces along the body y-axis are balanced. The relationship is expressed as:

$$mg \sin \phi = mu_0 \dot{\psi} \cos \phi$$

Since the bank angle ϕ is typically small ($\phi \ll 1$), the approximation $\tan \phi \approx \phi$ can be used. Therefore, the bank angle is calculated as:

$$\phi = \frac{u_0 \dot{\psi}}{g}$$

For a given desired heading ψ_d , the heading ψ must follow ψ_d gradually. The dynamics are expressed as:

$$\tau_\psi \dot{\psi} + \psi = \psi_{\text{com}}$$

Rearranging gives:

$$\frac{\dot{\psi}}{\psi_{\text{com}}} = \frac{1}{\tau_\psi s + 1}, \quad \frac{\dot{\psi}}{\psi_{\text{com}}} = \frac{\frac{1}{\tau_\psi}}{s + \frac{1}{\tau_\psi}}$$

This acts as a low-pass filter that suppresses higher frequency noise. The desired bank angle is then calculated as:

$$\dot{\phi}_{\text{com}} = \frac{u_0 \dot{\psi}}{g} = \frac{u_0}{\tau_\psi g} (\psi_{\text{com}} - \psi)$$

For this system, τ_ψ is chosen between 15 s and 20 s, depending on the specific aircraft and its objectives.

Now integrating the controllers to operate simultaneously on the aircraft using the Simulink model. the following limits were applied during simulation:

- The command bank angle (ϕ_{com}) was limited to $\pm 30^\circ$.
- The rudder deflection (δ_r) was limited to $\pm 15^\circ$.
- The aileron deflection (δ_a), which is the sum of both left and right aileron deflections, was limited to $\pm 50^\circ$.

A step input of 360° in heading was tested, and the settling time and coordination were verified by observing the slip angle (β).

The resulting simulation outputs are as follows:

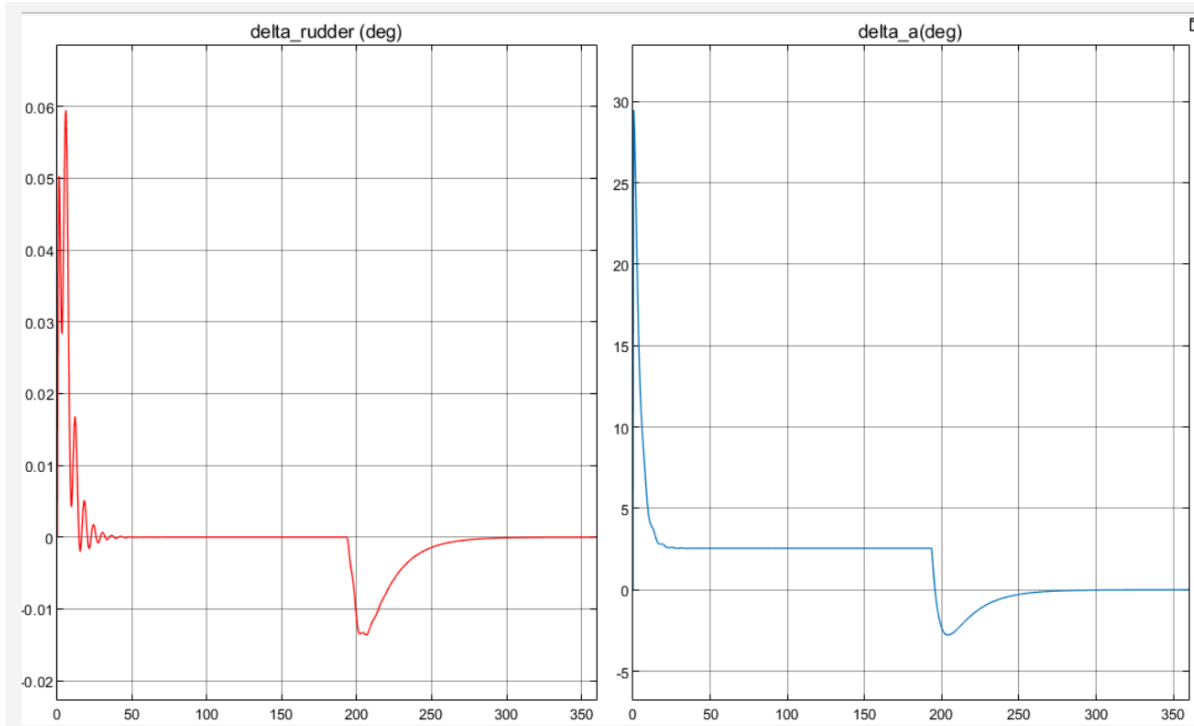


Figure 178: Control Surfaces Behavior from Lateral Autopilot

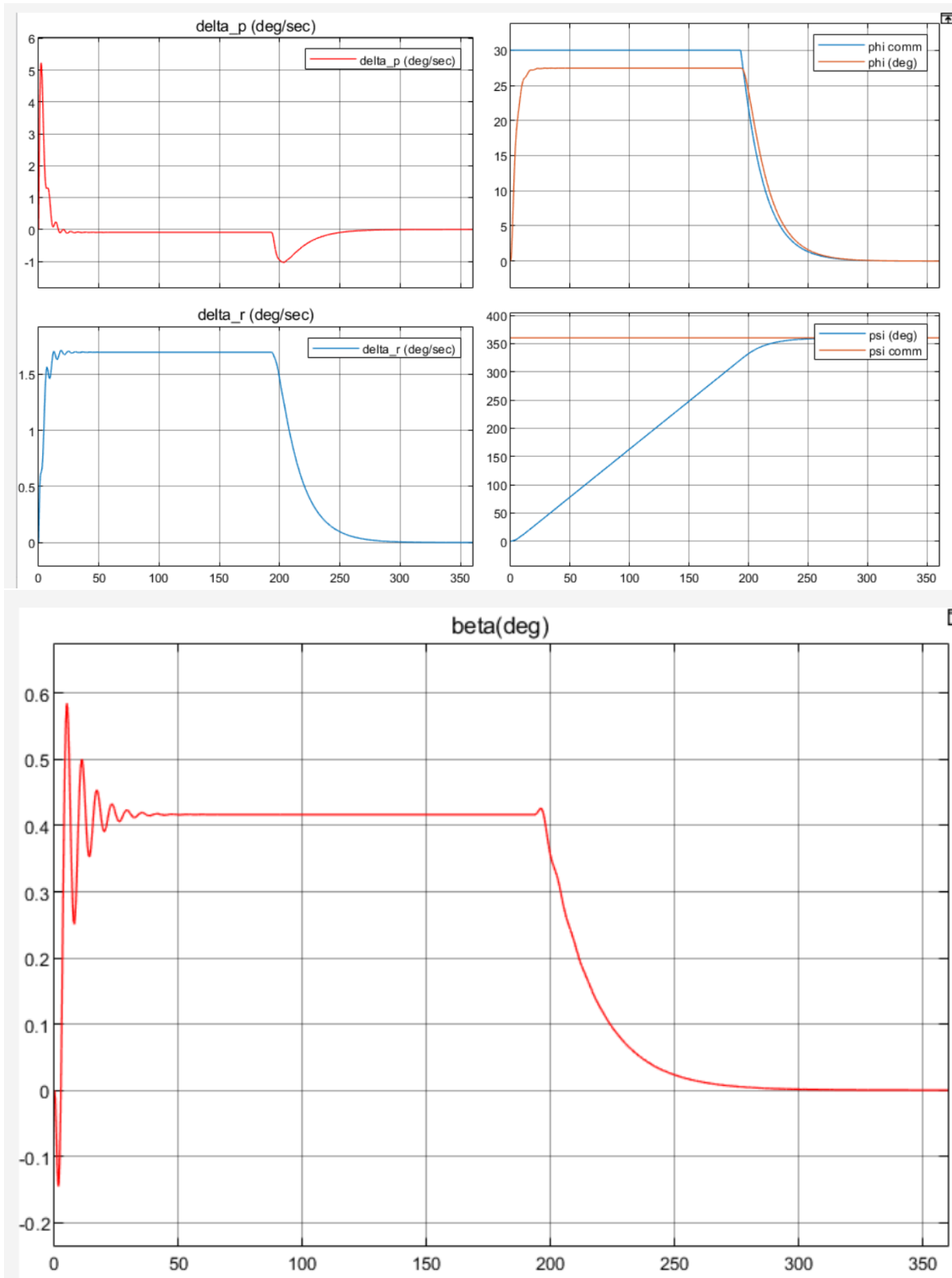


Figure 179: Lateral Autopilot's states responses.

Overall Performance

The plots validate the lateral autopilot's performance across multiple states:

- The rudder and aileron deflections effectively counteract disturbances and maintain stability.

- The roll and yaw dynamics are well-controlled, achieving rapid stabilization and smooth transitions.
- The heading and bank angles accurately follow commands, with minimal deviation.
- The sideslip angle response confirms the system's capability to maintain coordinated turns without lateral acceleration.
- The system demonstrates robust and efficient lateral control, meeting design expectations.

7 Nonlinear Simulation and Mission

In this section, we will evaluate the lateral and longitudinal autopilot controllers for the B747 airplane flight condition 3 using a realistic 6DOF nonlinear airplane dynamics model. Unlike the linearized state-space model, this nonlinear model incorporates coupling between longitudinal and lateral dynamics, offering a more accurate representation of the airplane's behavior and enabling simultaneous testing of all controllers.

The focus will be on testing the autopilot's ability to manage four critical control actions—aileron, rudder, elevator, and thrust—to maintain the required attitude and altitude during complex maneuvers, such as coordinated-level turns, climbs, and descents. The evaluation aims to validate both individual controller components and their combined performance in executing a complete autonomous mission.

This section will include:

- Development of a testing loop to integrate the controllers with the simulator, providing real-time feedback for continuous adjustment of control actions.
- Independent testing of pitch control, velocity control, altitude hold, and lateral control to verify their specific functionalities.
- Combined testing of lateral and longitudinal controllers to assess their coordinated operation during turns and altitude maintenance.
- Execution of a full autonomous mission to demonstrate the integration and reliability of the autopilot system in realistic flight scenarios.

The autonomous mission will simulate sequential phases of climbing, cruising, turning, and descending, ensuring the autopilot system's ability to handle dynamic flight conditions and transitions seamlessly.

7.1 Developing the Test Loop

A closed-loop system was developed to integrate the autopilot with the non-linear simulator:

- The autopilot generated control actions (aileron, rudder, elevator, thrust).
- These actions were fed into the non-linear simulator, which calculated the updated airplane states.
- The updated states were fed back as sensor signals to the autopilot for further action.

This feedback mechanism ensured a dynamic and realistic testing process as shown in the below flow diagram.

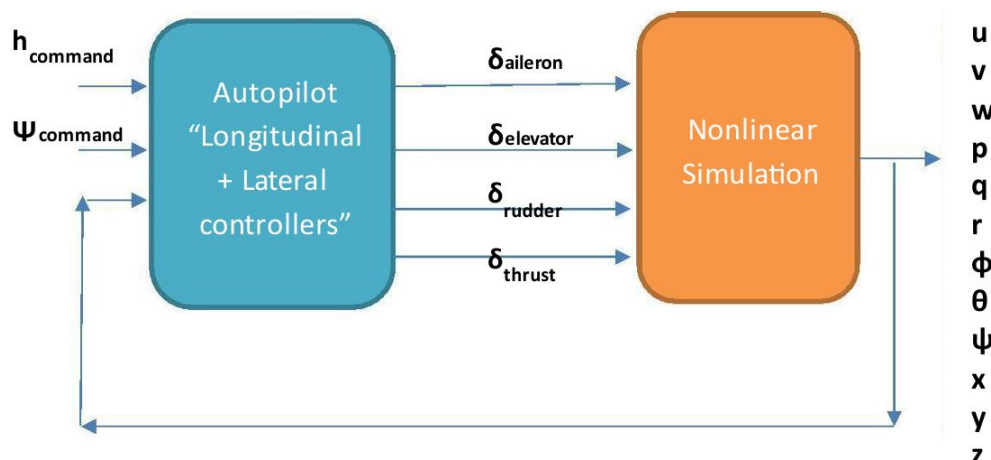


Figure 180: Flowchart of flight Controller closed loop

7.2 Simulation of Linear and Non-Linear Models

7.2.1 Pitch Controller Test

- **Commanded input:** delta pitch angle of 5° .
- **Observed States:** Pitch angle (θ), velocity (u), flight path angle (γ), altitude (H), and elevator deflection (δ_e) for linear and non-linear Model.

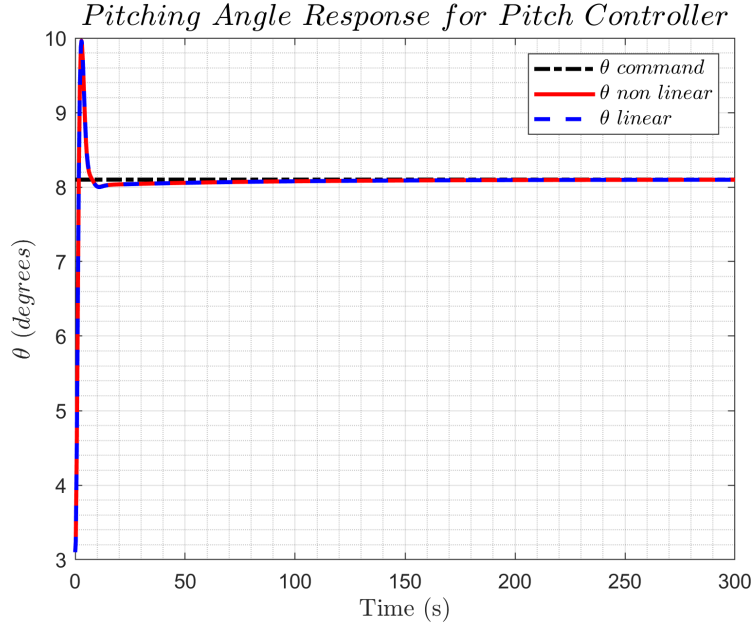


Figure 181: θ Response for Pitch Controller for linear and nonlinear models

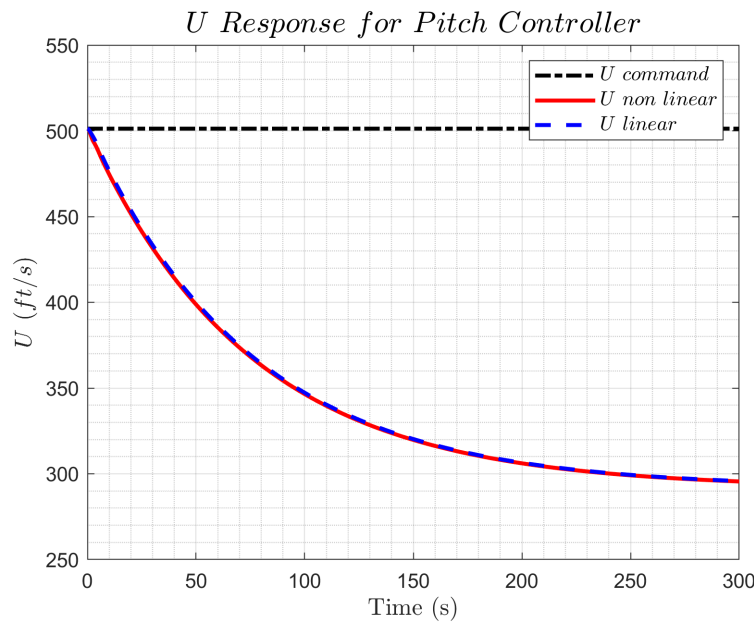


Figure 182: U Response for Pitch Controller for linear and nonlinear models

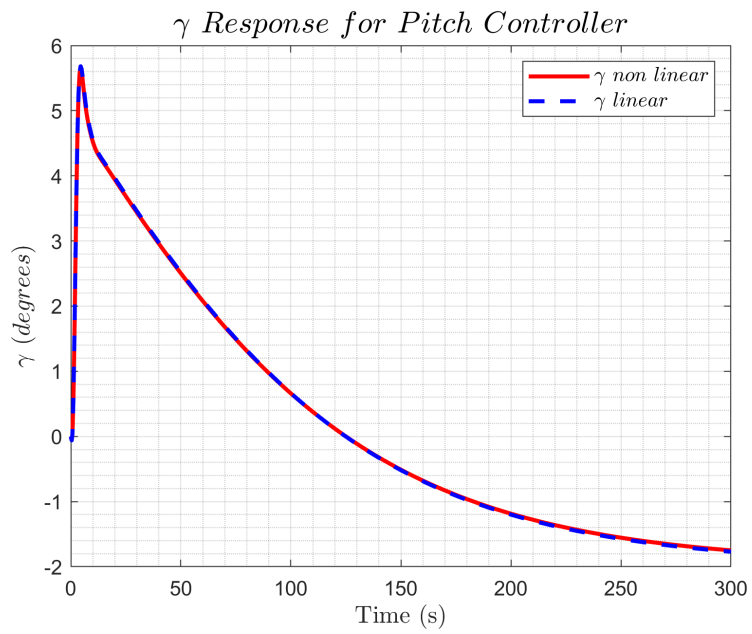


Figure 183: γ Response for Pitch Controller for linear and nonlinear models

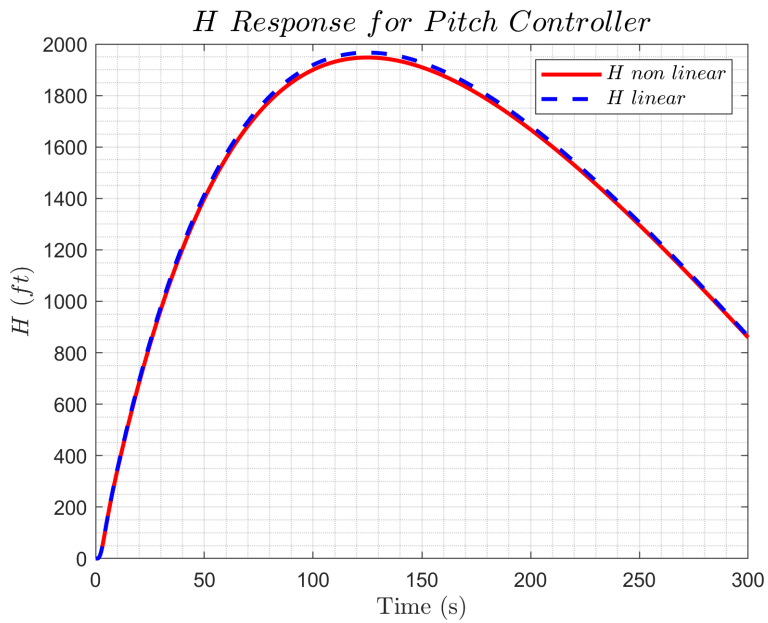


Figure 184: H Response for Pitch Controller for linear and nonlinear models

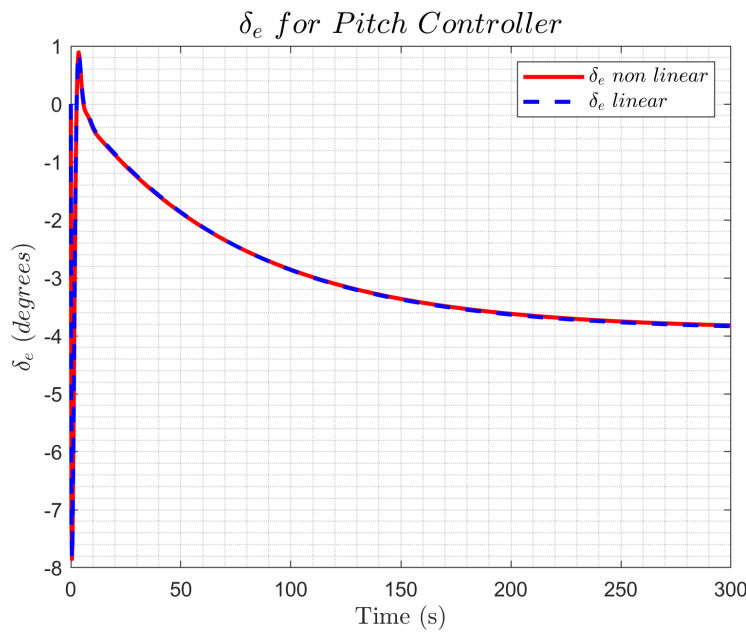


Figure 185: δ_e Response for Pitch Controller for linear and nonlinear models

- **Result Comments :** The responses of the linear and nonlinear models exhibit an almost identical match, aligning closely with the pitch controller output from the longitudinal autopilot section.

7.2.2 Pitch Controller and Velocity Controller Test

- **Commanded input:** delta velocity of 20 ft/s.
- **Observed States:** Pitch angle (θ), velocity (u), flight path angle (γ), altitude (H), elevator deflection (δ_e), and throttle input (δ_{th}) for linear and nonlinear models.

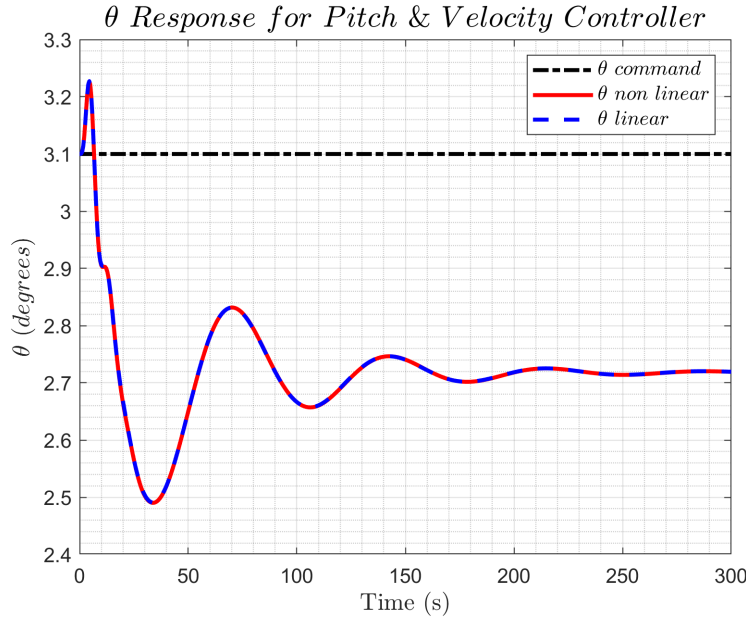


Figure 186: θ Response for Pitch and Velocity Controller for linear and nonlinear models

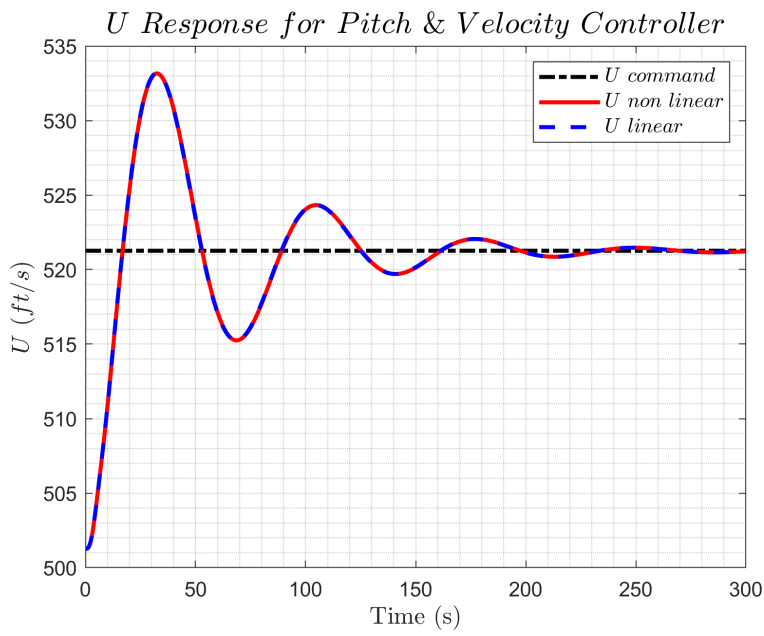


Figure 187: u Response for Pitch and Velocity Controller for linear and nonlinear models

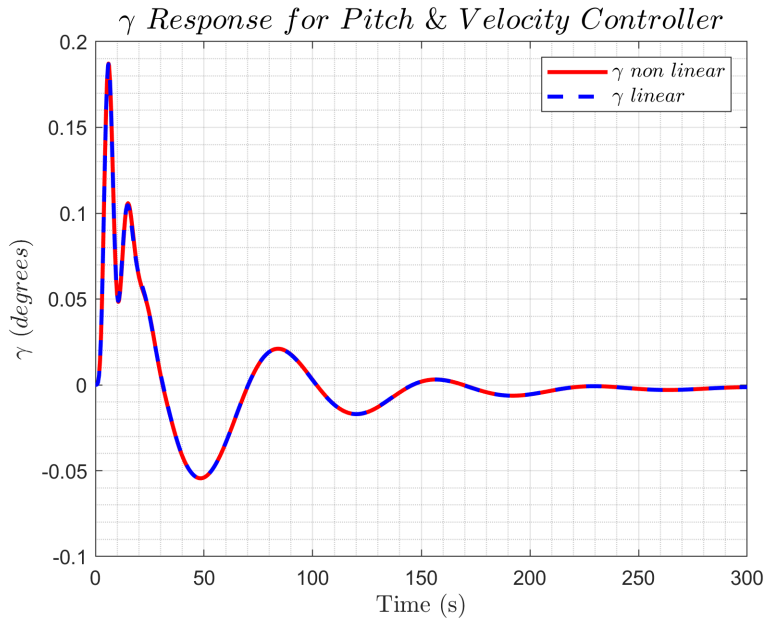


Figure 188: γ Response for Pitch and Velocity Controller for linear and nonlinear models

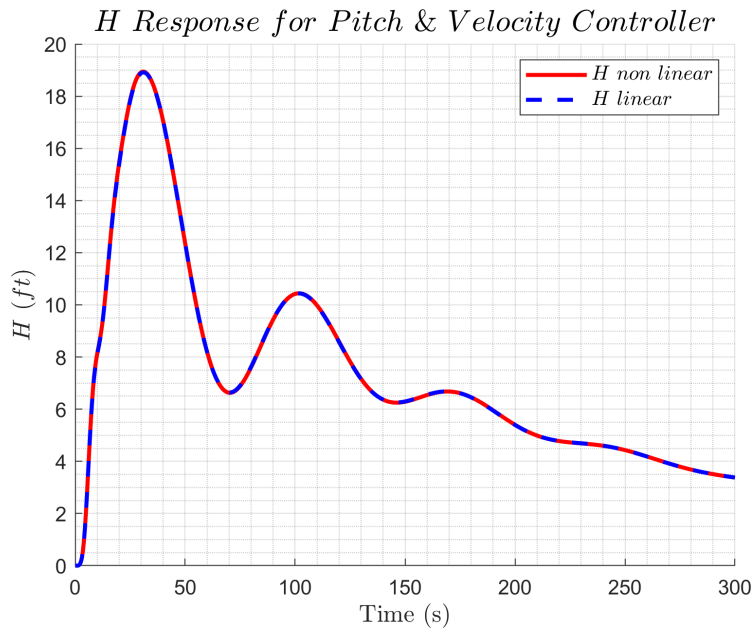


Figure 189: H Response for Pitch and Velocity Controller for linear and nonlinear models

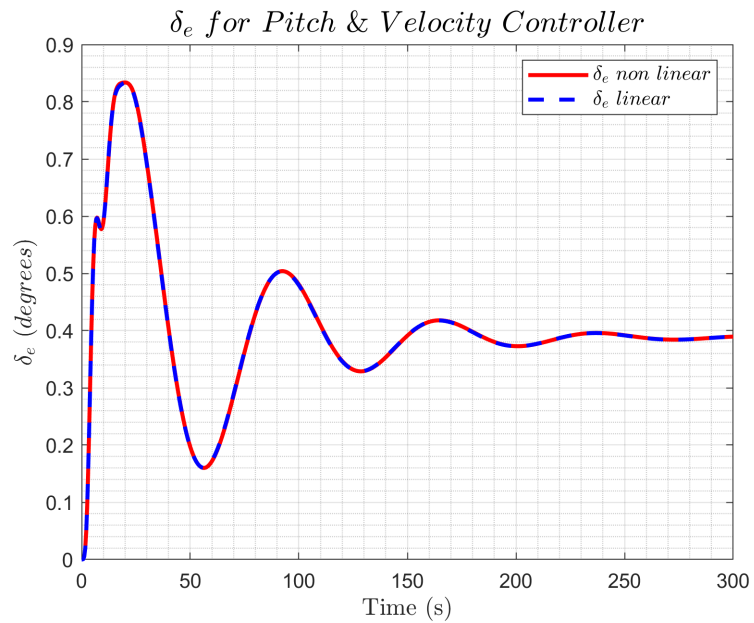


Figure 190: (δ_e) Response for Pitch and Velocity Controller for linear and nonlinear models

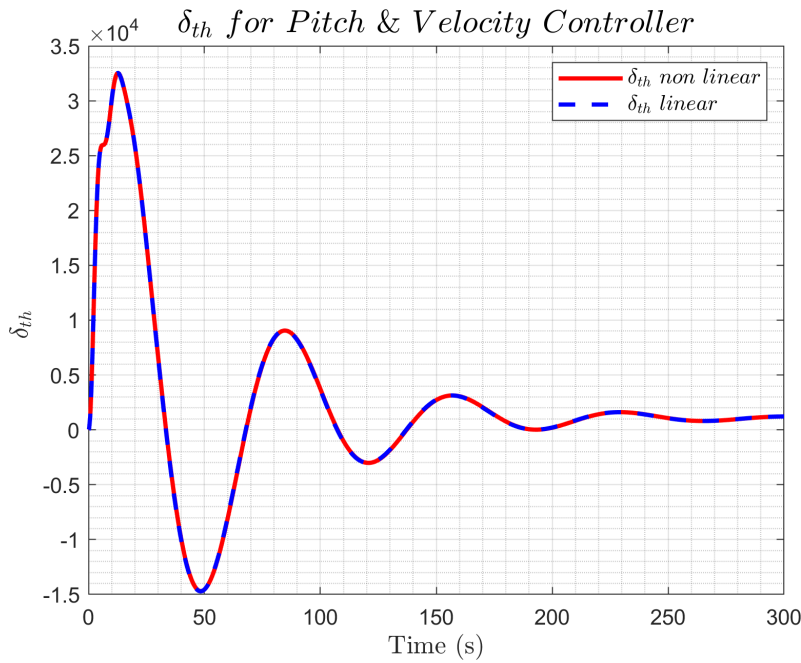


Figure 191: (δ_{th}) Response for Pitch and Velocity Controller for linear and nonlinear models

- **Result Comments:** The responses of the linear and nonlinear models exhibit a high degree of similarity. Both controllers effectively coordinated to achieve the desired velocity and maintain stable flight, validating their combined functionality.

7.2.3 Altitude Hold Controller Test

- **Commanded input:** delta Altitude 200 ft with velocity of 20 ft/s.
- **Observed States:** Pitch angle (θ), velocity (u), flight path angle (γ), altitude (H), elevator deflection (δ_e), and throttle input (δ_{th}) for linear and nonlinear models.

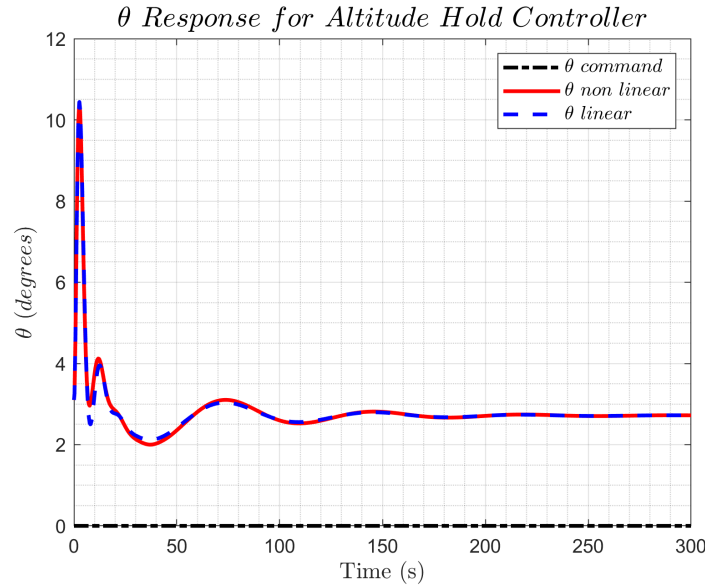


Figure 192: θ Response for Altitude Hold Controller for linear and nonlinear models

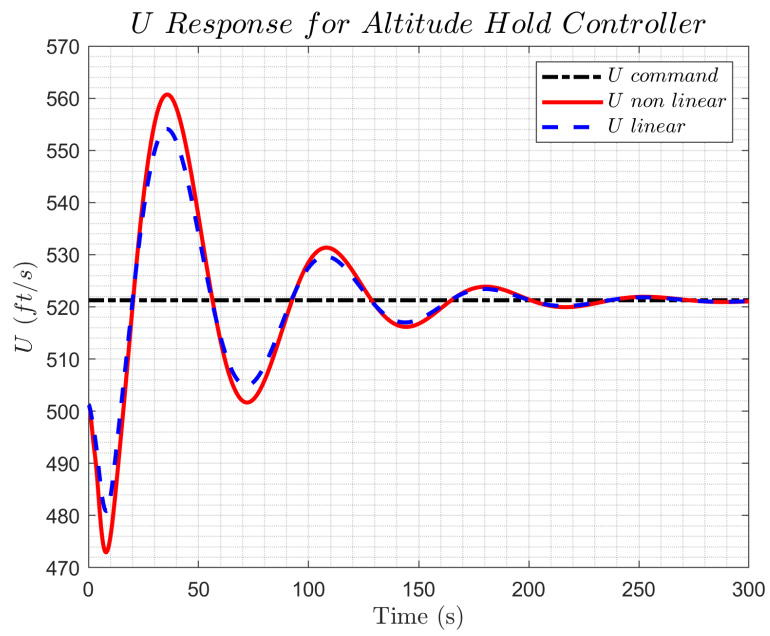


Figure 193: u Response for Altitude Hold Controller for linear and nonlinear models

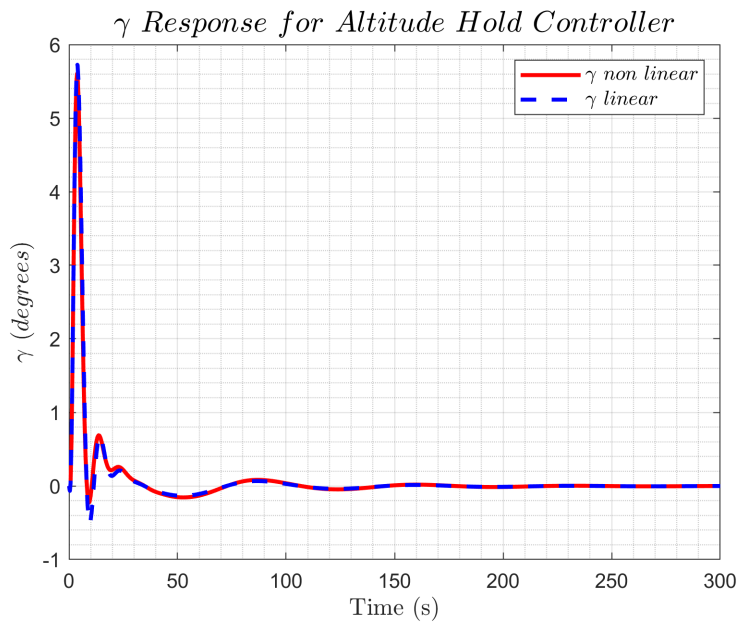


Figure 194: γ Response for Altitude Hold Controller for linear and nonlinear models

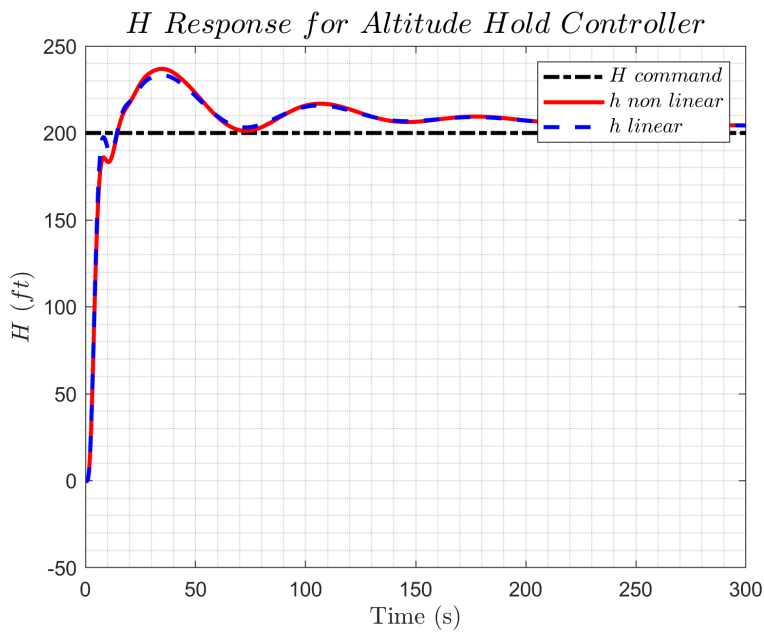


Figure 195: H Response for Altitude Hold Controller for linear and nonlinear models

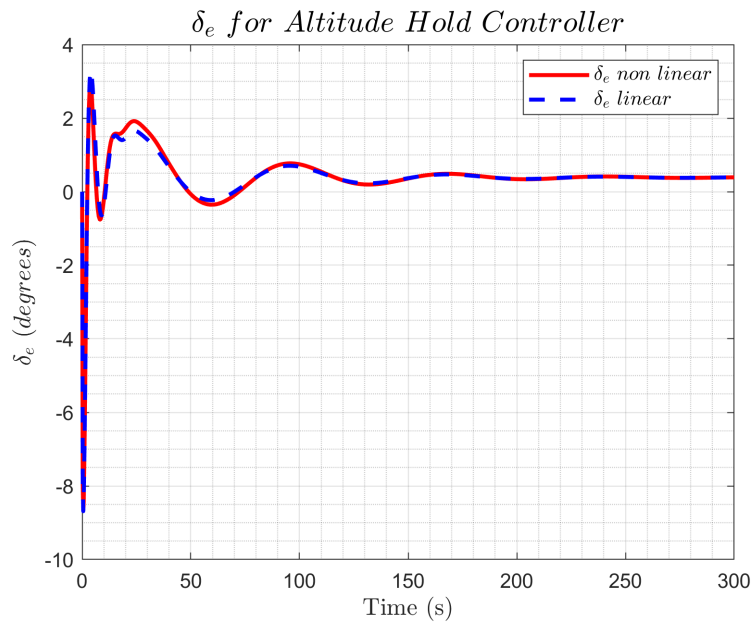


Figure 196: (δ_e) Response for Altitude Hold Controller for linear and nonlinear models

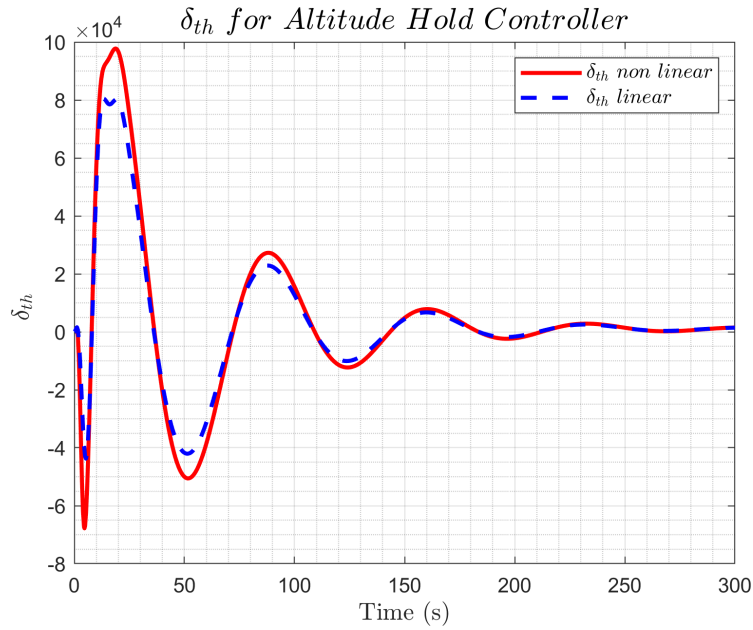


Figure 197: (δ_{th}) Response for Altitude Hold Controller for linear and nonlinear models

- **Result Comments:** The responses of the linear and non-linear models closely align, validating the functionality of the altitude hold controller. Minor differences in throttle input (δ_{th}) and Velocity U were observed, reflecting the increased complexity of the non-linear model.

7.2.4 Lateral Controller Test

- **Commanded input:** Heading change of 360° .
- **Observed States:** Sideslip angle (β), roll angle (ϕ), heading angle (ψ), altitude (H), rudder deflection (δ_r), and aileron deflection (δ_a) for linear and nonlinear models.

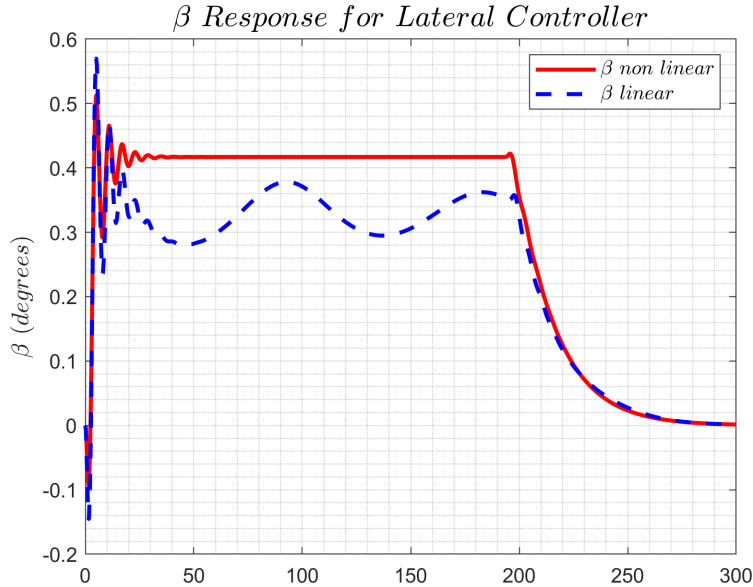


Figure 198: β Response for Lateral Controller for linear and nonlinear models

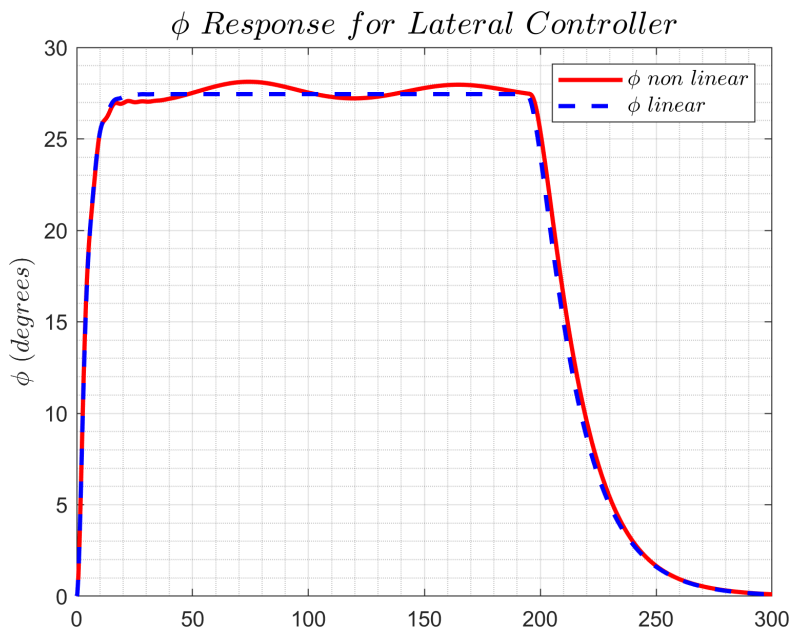


Figure 199: ϕ Response for Lateral Controller for linear and nonlinear models

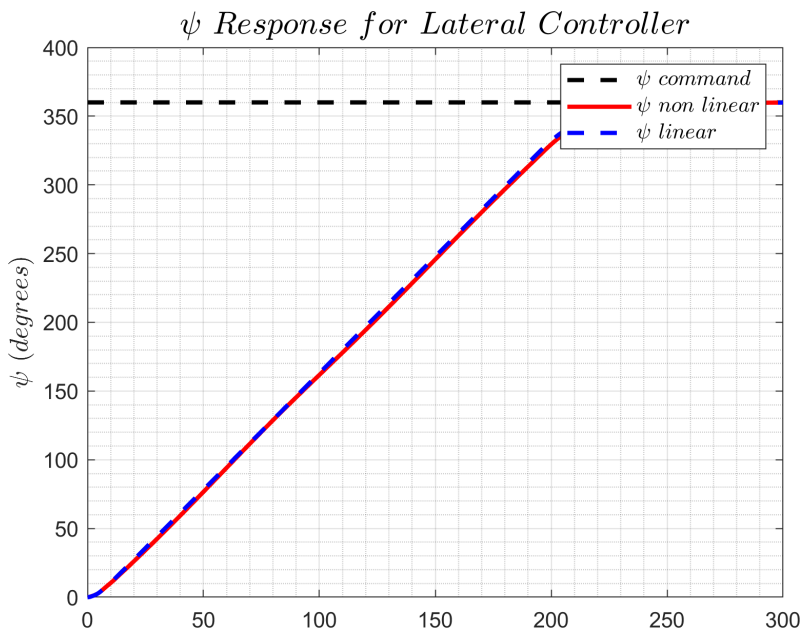


Figure 200: ψ Response for Lateral Controller for linear and nonlinear models

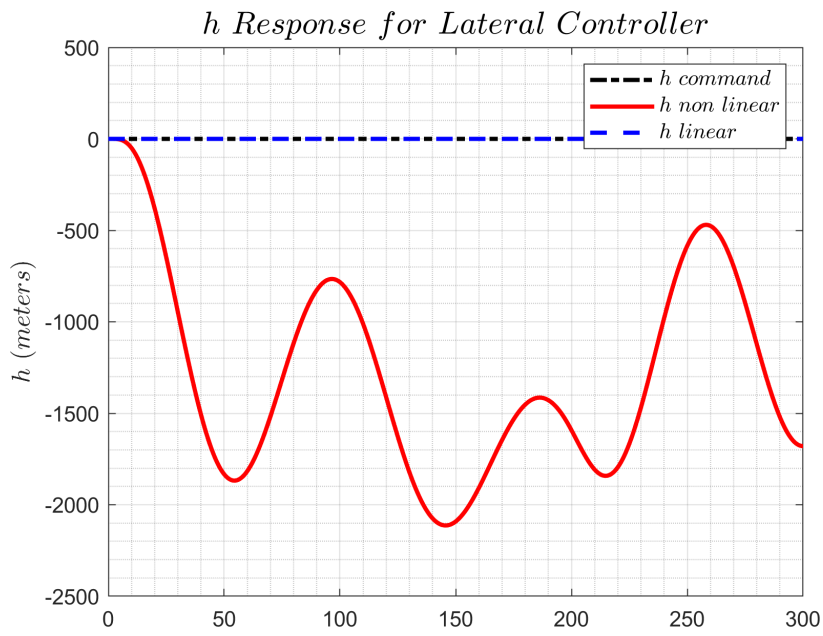


Figure 201: h Response for Lateral Controller for linear and nonlinear models

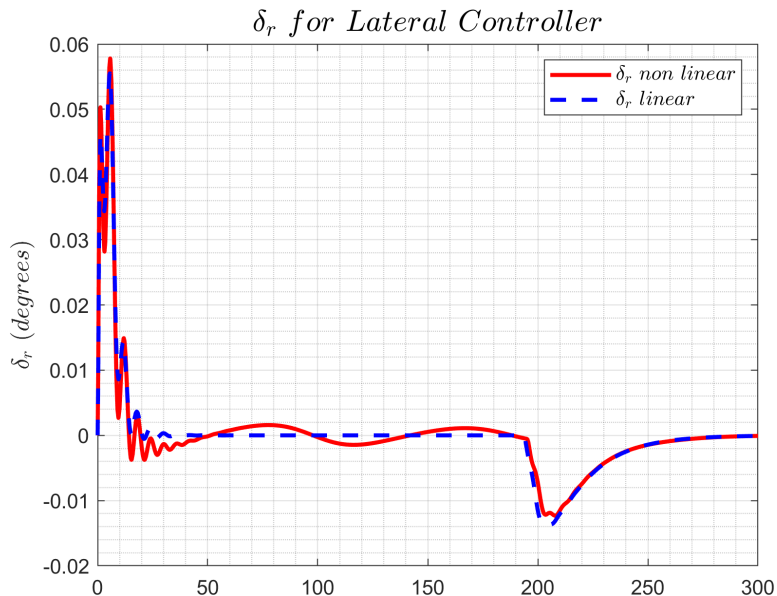


Figure 202: (δ_r) Response for Lateral Controller for linear and nonlinear models

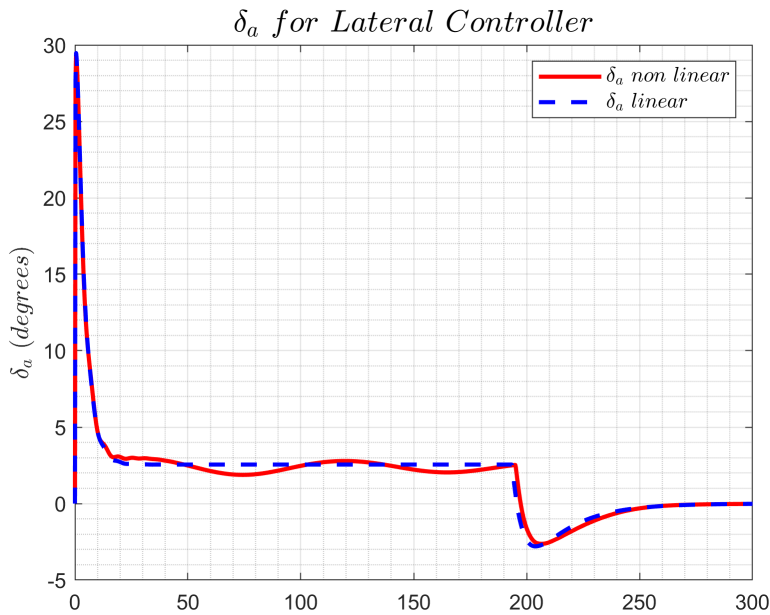


Figure 203: (δ_a) Response for Lateral Controller for linear and nonlinear models

- Result Comments:** The responses from the linear and nonlinear models show consistency across most states. Minor differences in roll angle (ϕ) and sideslip angle (β) were observed in the nonlinear model due to its increased complexity. The altitude response in the nonlinear model exhibited significant nonlinearity, affecting the lateral controller's performance, while the linear model showed no change in altitude.

7.2.5 Lateral Controller and Altitude Hold Controller Test

- Commanded input:** Heading change of 360° with altitude hold with 0 ft.
- Observed States:** Sideslip angle (β), roll angle (ϕ), heading angle (ψ), altitude (H), rudder deflection (δ_r), aileron deflection (δ_a), elevator deflection (δ_e), and throttle input (δ_{th}) for linear and nonlinear models.

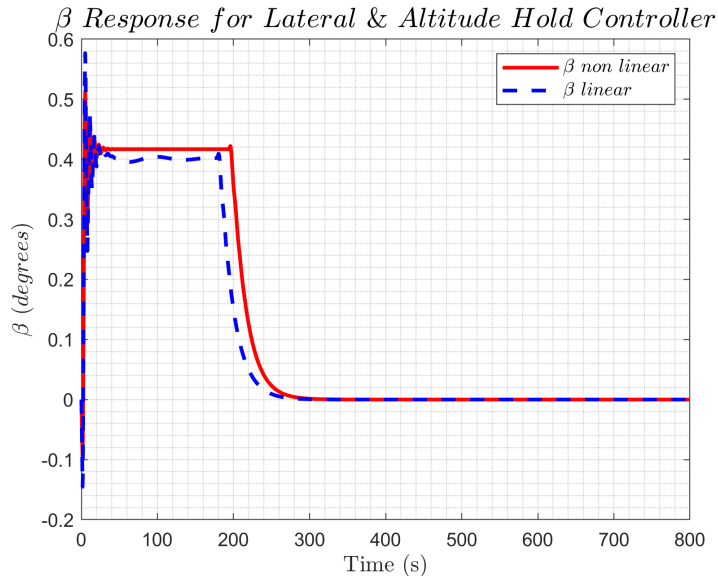


Figure 204: β Response for Lateral and Altitude Hold Controller for linear and nonlinear models

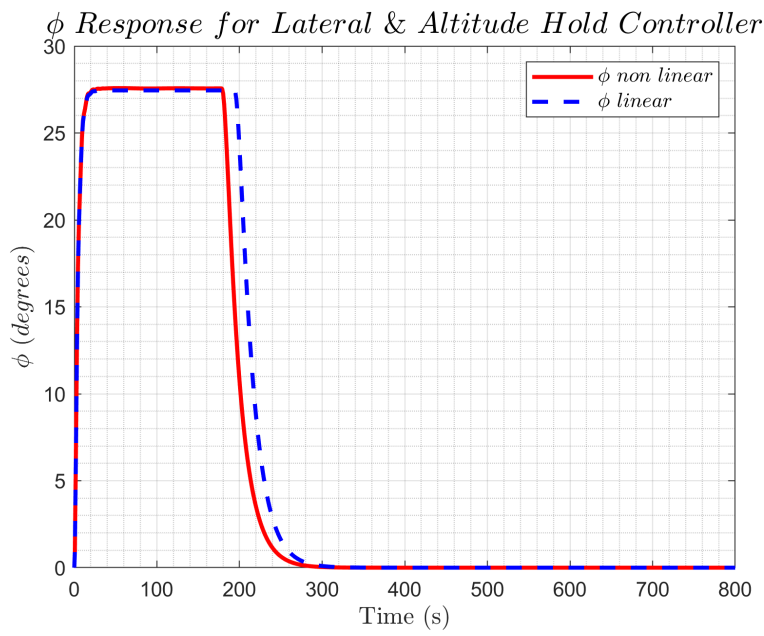


Figure 205: ϕ Response for Lateral and Altitude Hold Controller for linear and nonlinear models

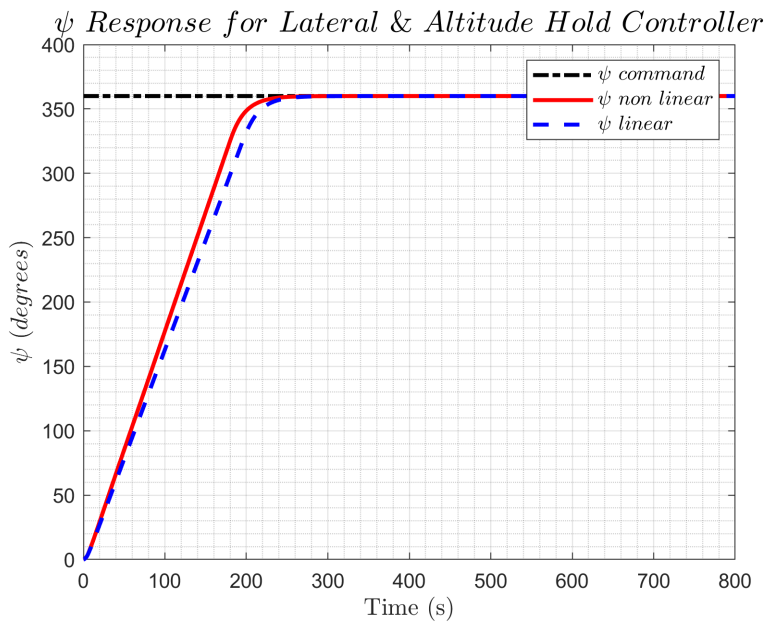


Figure 206: ψ Response for Lateral and Altitude Hold Controller for linear and nonlinear models

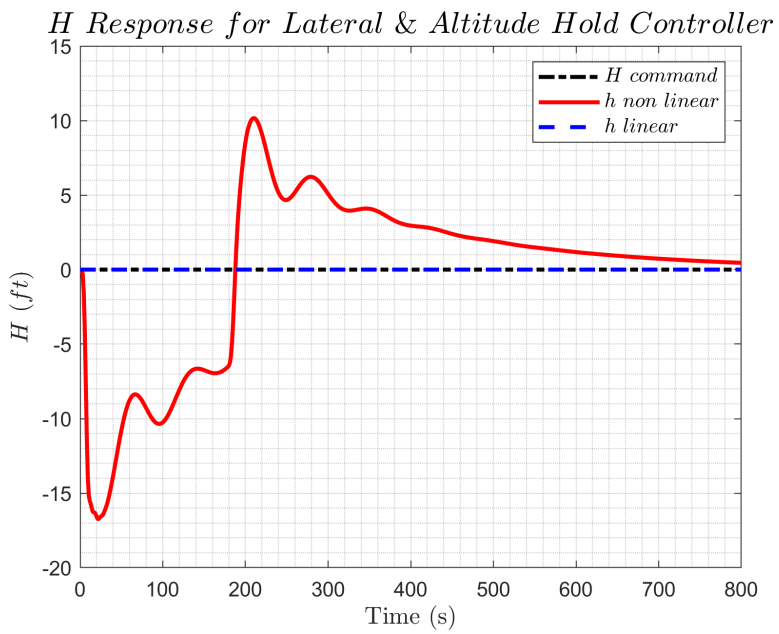


Figure 207: H Response for Lateral and Altitude Hold Controller for linear and nonlinear models

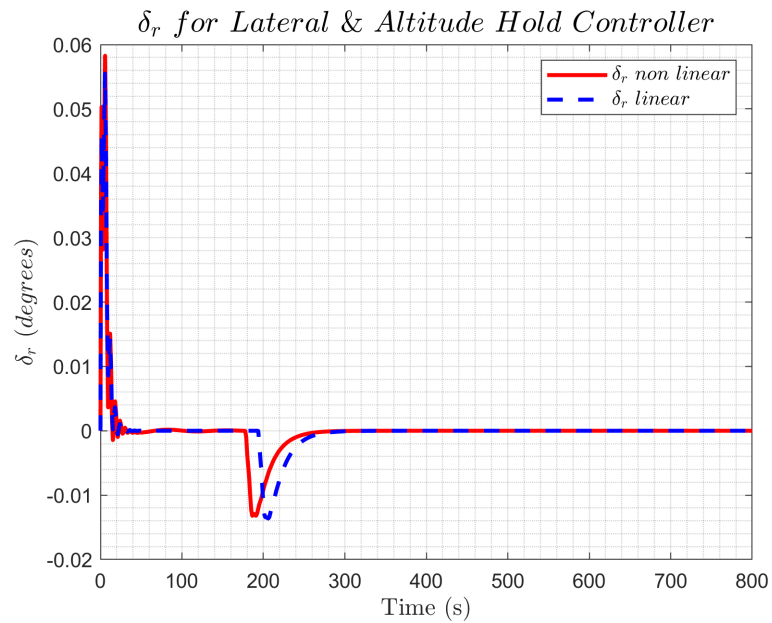


Figure 208: (δ_r) Response for Lateral and Altitude Hold Controller for linear and nonlinear models

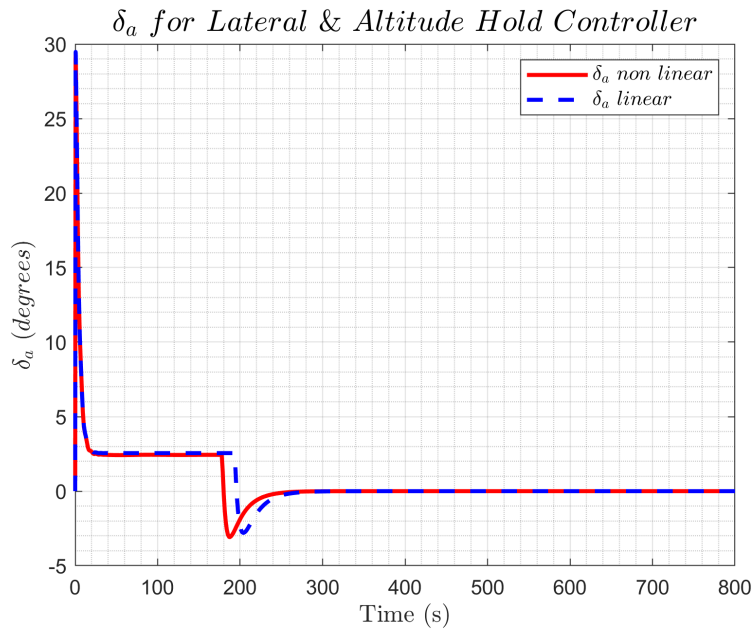


Figure 209: (δ_a) Response for Lateral and Altitude Hold Controller for linear and nonlinear models

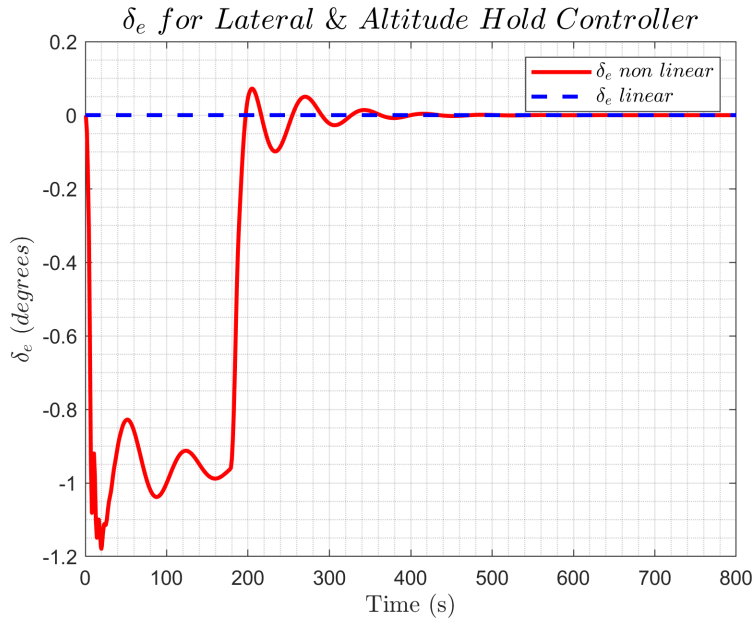


Figure 210: (δ_e) Response for Lateral and Altitude Hold Controller for linear and nonlinear models

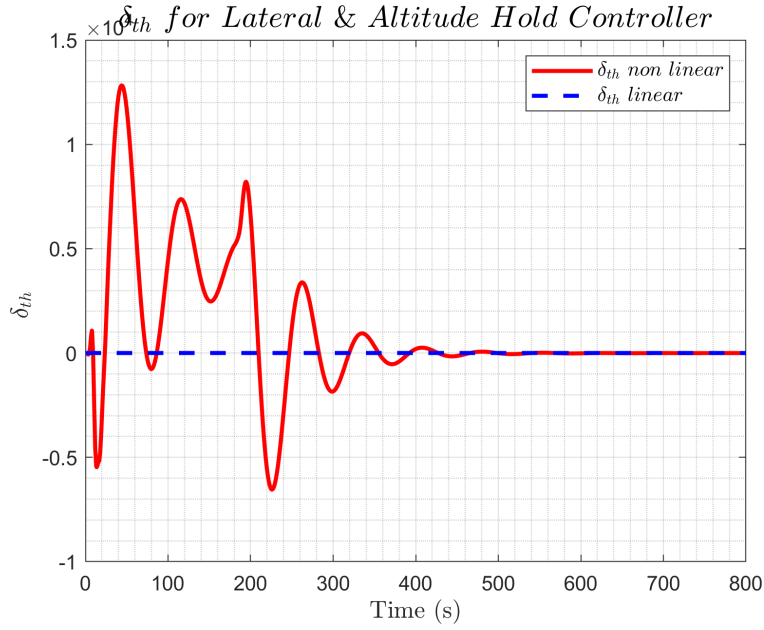


Figure 211: (δ_{th}) Response for Lateral and Altitude Hold Controller for linear and nonlinear models

- **Result Comments:** The responses of the linear and nonlinear models were consistent across observed states. The lateral controller effectively managed heading changes, and the altitude hold controller maintained the desired altitude, demonstrating successful coordination between lateral and longitudinal controls, resulting in a successfully achieved coordinated level turn.

7.2.6 Complete Autonomous Mission

After validating the functionality of the longitudinal and lateral controllers, a complete mission was performed to evaluate the integrated autopilot system. The mission included a sequence of maneuvers: climb, cruise, turn, and descent. The detailed mission phases are as follows:

- **Mission Phases:**
 1. **Climb:** Ascend to an altitude of 10,000 ft at a climb rate of 1500 ft/min.
 2. **Cruise:** Maintain constant velocity and heading for 2 minutes.
 3. **Turn:** Execute a coordinated 360-degree turn.
 4. **Cruise:** Continue at constant velocity and heading for another 2 minutes.
 5. **Climbing Turn:** Execute a 30-degree heading change with a step altitude increase of 100 ft.
 6. **Descent:** Descend to the starting altitude at a descent rate of 1500 ft/min.

To execute this mission, the autopilot was provided with input commands for altitude (H) and heading angle (ψ). These inputs, representing the mission phases, are detailed in Table 4.

Table 4: Mission segments points.

| Altitude (H) input signal | | Heading angle (ψ) input signal | |
|---------------------------|---------------|---------------------------------------|------------------------|
| Time (s) | Altitude (ft) | Time (s) | Heading ($^{\circ}$) |
| 0 | 0 | 0 | 0 |
| 400 | 10000 | 400 | 0 |
| 520 | 10000 | 520 | 0 |
| 760 | 10000 | 760 | 360 |
| 880 | 10000 | 880 | 360 |
| 880 | 10100 | 1000 | 360 |
| 1000 | 10100 | 1000 | 390 |
| 1400 | 0 | 1400 | 390 |
| 1800 | 0 | 1800 | 0 |

After providing the input signals to the autopilot, the following figures display the corresponding responses for the altitude (H) and the heading angle (ψ):

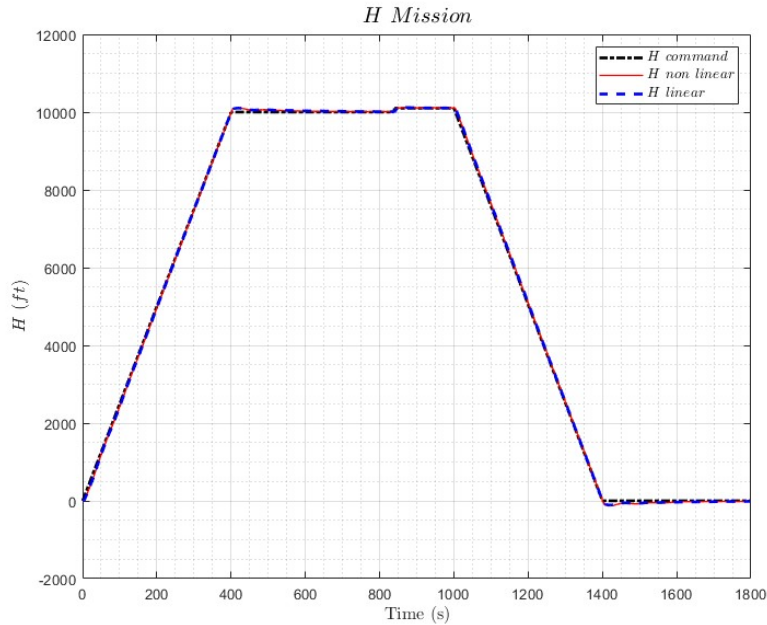


Figure 212: Altitude (H) Response for Mission

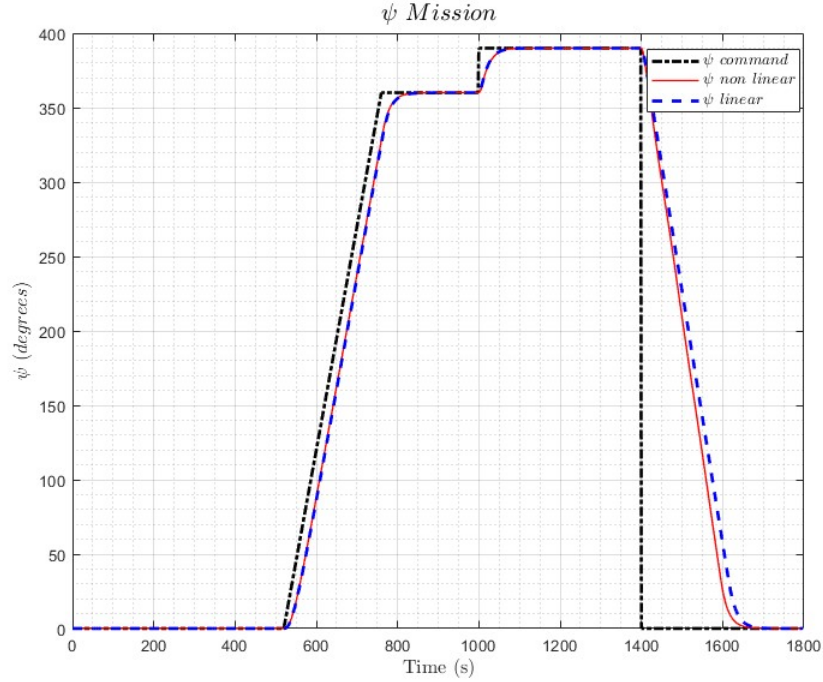


Figure 213: Heading Angle (ψ) Response for Mission

- **Result Comments:** The altitude (H) and heading angle (ψ) responses confirmed the seamless integration and flawless operation of all controllers. The autopilot demonstrated exceptional performance, achieving precise control and successfully accomplishing all mission objectives.

7.3 Flight Gear Simulation

The mission was conducted using the Flight Gear simulator, linked to Simulink. The Boeing 747-400 model was installed, and the autopilot was successfully operated to execute the required mission. A video animation of the simulation can be accessed here:[Flight Gear Mission](#)

8 References

- [1]R. C. Nelson, Flight stability and automatic control. Boston, Mass.: McGraw Hill, 1998.
- [2]D. Barry, "How long do pilots really spend on autopilot?," Cranfield.ac.uk, 2018.
<https://insights.cranfield.ac.uk/blog/how-long-do-pilots-really-spend-on-autopilot>
- [3]Wikipedia Contributors, "Autopilot," Wikipedia, Dec. 23, 2018.
<https://en.wikipedia.org/wiki/Autopilot>
- [4]"SAS, Autopilots and Flight Directors - What's in a Name? — helicoptermaintenancemagazine.com," helicoptermaintenancemagazine.com.
<https://helicoptermaintenancemagazine.com/article/sas-autopilots-and-flight-directors-what>
- [5]V. Sazdovski, T. Kolemishevska-Gugulovska, and M. Stankovski, "KALMAN FILTER IMPLEMENTATION FOR UNMANNED AERIAL VEHICLES NAVIGATION DEVELOPED WITHIN A GRADUATE COURSE," IFAC Proceedings Volumes, vol. 38, no. 1, pp. 12–17, 2005, doi: <https://doi.org/10.3182/20050703-6-cz-1902.02265>.
- [6]Airbus, "Safety innovation 1: Fly-by-wire (FBW)," Airbus.com, 2023.
<https://www.airbus.com/en/newsroom/stories/2022-06-safety-innovation-1-fly-by-wire-fbw>
- [7]Bae Systems, "What are fly-by-wire systems?," BAE Systems — United States, 2023.
<https://www.baesystems.com/en-us/definition/what-are-fly-by-wire-systems>
- [8]"PX4 Open Source Autopilot," PX4 Open Source Autopilot, 2019. <https://px4.io/>
- [9]"Open Source Drone Software. Versatile, Trusted, Open. ArduPilot.," ardupilot.org.
<https://ardupilot.org/>
- [10]"CubePilot — Autopilot-on-Module — Blue Manufactured in USA — Blue Assembled in USA — Pixhawk Original Team," Cubepilot.org, 2024.
https://cubepilot.org//cube/features?utm_source=unmannedsystemstechnology.comutm_medium=referral

9 Appendix

9.1 Appendix A Matlab Codes

9.1.1 MATLAB Code for Solving the System of ODEs Using the RK4 Method

```
1 function [t, y] = RK4_solver(ode_func, y0, t0, tf, n)
2 % RK4_SOLVER Solves a system of ODEs using the 4th-order Runge-Kutta method.
3 %
4 % Inputs:
5 %   ode_func - function handle of the system of ODEs (dy/dt = f(t, y))
6 %   y0       - vector of initial conditions (column vector)
7 %   t0       - initial time
8 %   tf       - final time
9 %   n        - number of steps
10 %
11 % Outputs:
12 %   t        - time vector
13 %   y        - solution matrix (each row corresponds to time steps)
14
15 h = (tf - t0) / n;           % Step size
16 t = linspace(t0, tf, n); % Time vector
17 y = zeros(length(y0), n);% Solution matrix
18 y(:,1) = y0;                % Set initial condition
19
20 % RK4 Loop
21 for i = 1:n
22     k1 = h * ode_func(t(i), y(:,i));
23     k2 = h * ode_func(t(i) + 0.5*h, y(:,i) + 0.5*k1);
24     k3 = h * ode_func(t(i) + 0.5*h, y(:,i) + 0.5*k2);
25     k4 = h * ode_func(t(i) + h, y(:,i) + k3);
26     y(:,i+1) = y(:,i) + (1/6)*(k1 + 2*k2 + 2*k3 + k4);
27 end
28 y=y(:,1:n); % to remove the last row
29 end
30
31 % Define the system of ODEs as a function handle
32 ode_system = @(t, y) [sin(t) + cos(y(1)) + sin(y(2));
33                      cos(t) + sin(y(2))];
34
35 % Initial conditions
36 y0 = [-1; 1];
37 t0 = 0;
38 tf = 20;
39 n = 100; % Number of steps
40
41 % Call the RK4 solver function
42 [t, y] = RK4_solver(ode_system, y0, t0, tf, n);
43
44 % Plot the results
45 plot(t, y(1,:), t, y(2,:));
46 legend('y_1', 'y_2');
47 xlabel('Time t');
48 ylabel('Solutions y_1 and y_2');
49 title('Solutions of the ODE system using RK4');
50
51 % Validate against ode45
52 [t_ode45, y_ode45] = ode45(ode_system, [t0 tf], y0);
53 hold on;
54 plot(t_ode45, y_ode45(:,1), '--', t_ode45, y_ode45(:,2), '--');
55 legend('y_1 RK4', 'y_2 RK4', 'y_1 ode45', 'y_2 ode45');
```

9.1.2 MATLAB Code for Solving Airplane EOM

```
1 function diff=getstates(t, y)
2 global F
3 global m
4 global I
5 global M
6 %% Allocating the States Vector
7 velocities=y(1:3); % Allocating velocity positions
```

```

8 angular_velocities=y(4:6); % Allocating angular velocity positions
9 angles=y(7:9); % Allocating angles positions
10 position=y(10:12); % Allocating xyz positions
11 %% Differential Equations Setup
12 velocities_dot=(1/m)*F - cross(angular_velocities ,velocities); % Velocity
13 derivative equations
14 angular_velocities_dot=I\(\M-cross(angular_velocities,I*angular_velocities));
15 % Angular Velocity derivative equations
16 angles_dot=[1, sin(angles(1)) * tan(angles(2)), cos(angles(1)) * tan(angles
17 (2));
18 0, cos(angles(1)), -sin(angles(1));
19 0, sin(angles(1)) / cos(angles(2)), cos(angles(1)) / cos(angles(2))] *
20 angular_velocities; % Angles derivative equations
21 positions_dot=eu12rotm([angles(3) angles(2) angles(1)])*velocities; %
22 Position derivatives equations
23 diff=[velocities_dot; angular_velocities_dot; angles_dot; positions_dot]; %
24 Creating the differential equation matrix
25 end

1 %% Setup Parameters
2 t0 = 0; % Initial time
3 tf = 25; % Final Time
4 n = 10000; % Number of Steps
5 %% Identifying Variables
6 global F
7 global m
8 global I
9 global M
10 F=[10;5;3]; % Forces Input
11 M=[10;15;20]; % Moments Input
12 m=30; % Mass Input
13 I=[1,-2,-1;-2,5,-4;-1,-4,0.2]; % Inertia Input
14
15 initial=[10;2;0;2*pi/180;pi/180;0;20*pi/180;15*pi/180;30*pi/180;2;4;7]; % Initial
16 Parameters
17 [t2, y2] = RK4_solver(@getstates, initial, t0, tf, n); % Solving the airplane EOM
18 equations
19 % Modified plotting with 4 figures, each having 3 plots (Simulink vs. MATLAB
20 comparison)
21 %
22 simOut = sim('simulinktask2', 'ReturnWorkspaceOutputs', 'on');
23
24 % Extracting the outputs from the Simulink model
25 t = simOut.tout; % Time vector
26 out = simOut; % Store Simulink outputs (make sure 'out' is a structured output
27 in the model)
28
29 % Figure 1: Velocities (u, v, w)
30 figure;
31 vel_names = {'u', 'v', 'w'};
32 for i = 1:3
33 subplot(3,1,i)
34 plot(t,out.velocities.Data(:,i), 'r', t2, y2(i,:), 'b--')
35 title(['Velocity: ', vel_names{i}])
36 xlabel("Time (Sec)")
37 ylabel([vel_names{i}, ' (m/sec)'])
38 legend('Simulink', 'MATLAB')
39 end
40 sgttitle("Velocities Comparison")
41
42 % Figure 2: Angular Velocities (p, q, r)
43 figure;
44 ang_vel_names = {'p', 'q', 'r'};
45 for i = 1:3
46 subplot(3,1,i)
47 plot(t,out.angular_velocities.Data(:,i), 'r', t2, y2(i+3,:), 'b--')
48 title(['Angular Velocity: ', ang_vel_names{i}])
49 xlabel("Time (Sec)")
50 ylabel([ang_vel_names{i}, ' (rad/sec)'])
51 legend('Simulink', 'MATLAB')
52 end

```

```

49 sgttitle("Angular Velocities Comparison")
50
51 % Figure 3: Angles (phi, theta, psi)
52 figure;
53 angle_names = {'\phi (\phi)', '\theta (\theta)', '\psi (\psi)'};
54 for i = 1:3
55 subplot(3,1,i)
56 plot(t,wrapToPi(out.angles.Data(:,i)), 'r', t2, wrapToPi(y2(i+6,:)), 'b--')
57 title(['Angle: ', angle_names{i}])
58 xlabel("Time (Sec)")
59 ylabel([angle_names{i}, '(rad)'])
60 legend('Simulink', 'MATLAB')
61 end
62 sgttitle("Angles Comparison")
63
64 % Figure 4: Positions (x, y, z)
65 figure;
66 pos_names = {'x', 'y', 'z'};
67 for i = 1:3
68 subplot(3,1,i)
69 plot(t,out.position.Data(:,i), 'r', t2, y2(i+9,:), 'b--')
70 title(['Position: ', pos_names{i}])
71 xlabel("Time (Sec)")
72 ylabel([pos_names{i}, '(m)'])
73 legend('Simulink', 'MATLAB')
74 end
75 sgttitle("Positions Comparison")

```

9.1.3 MATLAB Code for calculating forces and moments

```

1 function diff=F_M_Cal(SD,Delta,Initial_F_M, phi,theta,psi)
2 global m g I
3 % Force and moment matrix, based on stability derivatives
4 F_M_Matrix = [SD(1) 0 SD(4) 0 0 0 0 0 SD(11) SD(14);
5 0 SD(17) 0 0 0 0 0 SD(26) 0 0;
6 SD(2) 0 SD(5) SD(7) 0 SD(8) 0 0 0 SD(12) SD(15);
7 0 0 0 SD(21) 0 SD(23) SD(27) SD(29) 0 0;
8 SD(3) 0 SD(6) SD(9) 0 SD(10) 0 0 0 SD(13) SD(16);
9 0 0 0 SD(22) 0 SD(24) SD(28) SD(30) 0 0];
10
11 % Calculate the linear change in forces and moments
12 Delta_F_M = F_M_Matrix * Delta; % Perturbations in forces and moments
13
14
15 F_M = Delta_F_M + Initial_F_M + [-m * g * sin(theta); m * g * cos(theta) *
16 sin(phi); m * g * cos(theta) * cos(phi); 0; 0; 0];
17
18 diff=F_M;
end

```

9.1.4 MATLAB Code for transforming lateral derivatives

```

1 function SD_Lat=LateralFunc(SD_Lat_dash,Ixz,Izz,Ixx,V)
2
3 G=1/(1-Ixz^2/(Ixx*Izz));
4 A=Ixz/Ixx;
5 B=Ixz/Izz;
6 dashed=[SD_Lat_dash(3);SD_Lat_dash(5);SD_Lat_dash(7);SD_Lat_dash(13);
7 SD_Lat_dash(11)
8 SD_Lat_dash(4);SD_Lat_dash(6);SD_Lat_dash(8);SD_Lat_dash(14);
9 SD_Lat_dash(12)];
10 Matrix=[G 0 0 0 0 G*A 0 0 0 0;
11 0 G 0 0 0 0 G*A 0 0 0;
12 0 0 G 0 0 0 0 G*A 0 0;
13 0 0 0 G 0 0 0 0 G*A;
14 G*B 0 0 0 0 G 0 0 0 0;
15 0 G*B 0 0 0 0 G 0 0 0;
16 0 0 G*B 0 0 0 0 G 0 0;
17 0 0 0 G*B 0 0 0 0 G 0;
18 0 0 0 G*B 0 0 0 0 G];

```

```

18
19
20 star=[SD_Lat_dash(9);SD_Lat_dash(10)];
21 non_dashed=inv(Matrix)*dashed;
22 non_stared=star*V;
23 SD_Lat=[SD_Lat_dash(1);SD_Lat_dash(2);non_dashed(1);non_dashed(6);
24 non_dashed(2);non_dashed(7);non_dashed(3);non_dashed(8);
25 non_stared(1);non_stared(2);non_dashed(5);non_dashed(10);
26 non_dashed(4);non_dashed(9)];
27 end

```

9.1.5 MATLAB Code for RK4 modified

```

1 function [t, y] = RK4_solver(ode, y0, t0, tf, n, SD, Initial_F_M, dc, dt)
2 global M m
3 global F I g
4 h = (tf - t0) / n; % Step size
5 t = linspace(t0, tf, n+1); % Time vector
6 y = zeros(length(y0), n+1); % Solution matrix
7 y(:,1) = y0; % Set initial condition
8 wdot_0 = 0;
9 % RK4 Loop
10 for i = 1:n
11     k1 = h*(ode(t(i), y(:,i)));
12     k2 = h*(ode(t(i) + 0.5*h, y(:,i) + 0.5*k1));
13     k3 = h*(ode(t(i) + 0.5*h, y(:,i) + 0.5*k2));
14     k4 = h*(ode(t(i) + h, y(:,i) + k3));
15     y(:,i+1) = y(:,i) + (1/6)*(k1 + 2*k2 + 2*k3 + k4);
16
17     u = y(1, i);
18     v = y(2, i);
19     w = y(3, i);
20     p = y(4, i);
21     q = y(5, i);
22     r = y(6, i);
23     phi = y(7, i);
24     theta = y(8, i);
25     psi = y(9, i);
26     xx = y(10, i);
27     yy = y(11, i);
28     zz = y(12, i);
29
30
31
32
33
34 if i == 1
35     wdot = (w-y0(3))/dt;
36 else
37     wdot = (w-y(3, i-1))/dt;
38 end
39
40 Delta = [u-y0(1); v-y0(2); w-y0(3); wdot-wdot_0; p-y0(4); q-y0(5); r-y0(6);
41 ;dc(1);dc(2);dc(3);dc(4)];
42 F_M=F_M_Cal(SD,Delta,Initial_F_M, phi,theta,psi);
43 F=F_M(1:3);
44 M=F_M(4:6);
45
46 end
47 y=y(:,1:n); % to remove the last row
48 t=t(:,1:n);
49 end

```

9.1.6 MATLAB Code for calculating the states of airplane

```

1 % Main Script: Airplane Nonlinear Simulator with RBD Solver
2
3 % Clear workspace
4 clc;
5 clear all;
6 close all;

```

```

7 global m
8 global I
9 global F M
10 global g
11 %% Load Aircraft Data from Excel
12 filename_density_L = 'excelsheet_data_modified'; % Path to your excel sheet
13 aircraft_data = xlsread(filename_density_L, 'B2:B61'); % Read from Excel
14
15 % Time vector parameters
16 dt = aircraft_data(1);
17 tfinal = aircraft_data(2);
18 time_V = (0:dt:tfinal)';
19
20 % Initial conditions for states
21 s0 = aircraft_data(4:15);
22 sdot0 = zeros(12,1); % Initial derivative of states
23 Vto = sqrt(s0(1)^2 + s0(2)^2 + s0(3)^2); % Compute initial total velocity (Vto)
24
25 % Control actions values
26 dc = [ aircraft_data(57:59) * pi/180 ; aircraft_data(60) ]; % Control inputs in
27 radians
28
29 % Gravity, mass, and inertia values from aircraft data
30
31 m = aircraft_data(51);
32 g = aircraft_data(52);
33 Ixx = aircraft_data(53);
34 Iyy = aircraft_data(54);
35 Izz = aircraft_data(55);
36 Ixz = aircraft_data(56);
37 Ixy = 0; Iyz = 0;
38
39 % Inertia matrix and inverse inertia matrix
40 I = [Ixx, -Ixy, -Ixz; -Ixy, Iyy, -Iyz; -Ixz, -Iyz, Izz];
41 invI = inv(I);
42
43 % Stability derivatives for longitudinal motion
44 SD_Long = aircraft_data(21:36);
45 SD_Long_final = SD_Long;
46
47 % Stability derivatives for lateral motion
48 SD_Lat_dash = aircraft_data(37:50);
49 SD_Lat = LateralFunc(SD_Lat_dash, Ixz, Izz, Ixx, Vto);
50 SD_Lat_final = SD_Lat;
51
52 % Initial gravity force in body frame
53 mg0 = m * g * [sin(s0(8)); -cos(s0(8)) * sin(s0(7)); -cos(s0(8)) * cos(s0(7))];
54
55
56 %% Calculate initial forces and moments
57 phi_0=s0(7);
58 theta_0=s0(8);
59 psi_0=s0(9);
60 Initial_F_M = [m * g * sin(theta_0); -m * g * cos(theta_0) * sin(phi_0); -m * g *
61 cos(theta_0) * cos(phi_0); 0; 0; 0];
62
63 % Combine stability derivatives into a single array
64 for i = 1:16
65 SD(i) = SD_Long_final(i);
66 end
67 for j = 1:14
68 SD(j+16) = SD_Lat_final(j); % All stability derivatives in one array
69 end
70
71 % Delta represents perturbations from trim conditions
72 Delta = [0; 0; 0; 0; 0; 0; 0; dc(1); dc(2); dc(3); dc(4)]; % Initial delta u, v,
73 w, wdot, p, q, r, da, dr, de, dth
74
```

```

75 F_M=F_M_Cal(SD,Delta, Initial_F_M,phi_0,theta_0,psi_0);
76
77 F=F_M(1:3);
78 M=F_M(4:6);
79
80
81 %% Call RK4 solver with RBD Solver to simulate the airplane's motion
82 n = 1000; % Number of steps for simulation
83 velocity_dot_0=s0(1:3);
84 angular_v_dot_0=s0(4:6);
85 angles_dot_0=s0(7:9);
86 position_dot_0=s0(10:12);
87 Initial_state=[velocity_dot_0;angular_v_dot_0;angles_dot_0;position_dot_0];
88 [t2, y2] = RK4_solver(@getstates,Initial_state , 0, tfinal, n,SD, Initial_F_M,dc,
     dt);
89
90
91
92 %% Plotting
93 rad_to_deg = 180 / pi; % Conversion from radians to degrees
94
95 % Plot results (e.g., velocities, angles, positions)
96 figure;
97
98 % Plot forward, side, and vertical velocities (u, v, w)
99 subplot(4,3,1);
100 plot(t2, y2(1,:), 'b'); % u (forward velocity)
101 title('Forward Velocity (u)');
102 xlabel('Time (s)');
103 ylabel('Velocity (ft/s)');
104
105 subplot(4,3,2);
106 plot(t2, y2(2,:), 'r'); % v (side velocity)
107 title('Side Velocity (v)');
108 xlabel('Time (s)');
109 ylabel('Velocity (ft/s)');
110
111 subplot(4,3,3);
112 plot(t2, y2(3,:), 'g'); % w (vertical velocity)
113 title('Vertical Velocity (w)');
114 xlabel('Time (s)');
115 ylabel('Velocity (ft/s)');
116
117 % Angular velocities (p, q, r)
118
119 subplot(4,3,4);
120 plot(t2, y2(4,:), 'b'); % p (roll rate)
121 title('Roll Rate (p)');
122 xlabel('Time (s)');
123 ylabel('Angular Velocity (rad/s)');
124
125 subplot(4,3,5);
126 plot(t2, y2(5,:), 'r'); % q (pitch rate)
127 title('Pitch Rate (q)');
128 xlabel('Time (s)');
129 ylabel('Angular Velocity (rad/s)');
130
131 subplot(4,3,6);
132 plot(t2, y2(6,:), 'g'); % r (yaw rate)
133 title('Yaw Rate (r)');
134 xlabel('Time (s)');
135 ylabel('Angular Velocity (rad/s)');
136
137 % Euler angles (phi, theta, psi) in degrees
138
139 subplot(4,3,7);
140 plot(t2, y2(7,:) * rad_to_deg, 'b'); % phi (roll angle in degrees)
141 title('Roll Angle (phi) in degrees');
142 xlabel('Time (s)');
143 ylabel('Angle (deg)');

```

```

145 subplot(4,3,8);
146 plot(t2, y2(8,:)* rad_to_deg, 'r'); % theta (pitch angle in degrees)
147 title('Pitch Angle (theta) in degrees');
148 xlabel('Time (s)');
149 ylabel('Angle (deg)');
150
151 subplot(4,3,9);
152 plot(t2, y2(9,:)* rad_to_deg, 'g'); % psi (yaw angle in degrees)
153 title('Yaw Angle (psi) in degrees');
154 xlabel('Time (s)');
155 ylabel('Angle (deg)');
156
157 % Position (x, y, z) in feet
158
159 subplot(4,3,10);
160 plot(t2, y2(10,:), 'b');
161 title('Position X (ft)');
162 xlabel('Time (s)');
163 ylabel('Position (ft)');
164
165 subplot(4,3,11);
166 plot(t2, y2(11,:), 'r');
167 title('Position Y (ft)');
168 xlabel('Time (s)');
169 ylabel('Position (ft)');
170
171 subplot(4,3,12);
172 plot(t2, y2(12,:), 'g');
173 title('Position Z (ft)');
174 xlabel('Time (s)');
175 ylabel('Position (ft)');
176
177 % Trajectory (x vs y vs z in feet)
178 figure;
179 plot3(y2(10,:), y2(11,:), y2(12,:), 'b'); % 3D trajectory plot
180 title('Trajectory of the Aircraft in Feet');
181 xlabel('X (ft)');
182 ylabel('Y (ft)');
183 zlabel('Z (ft)');
184 grid on;
185
186 % Additional plots for angular velocities, angles, and positions can be added
187 % here
188 % RBD Solver Function with m, g, I passed as parameters

```

9.1.7 MATLAB Code Longitudinal Lateral stability analysis

```

1 % Main Script: Airplane Nonlinear Simulator with RBD Solver
2
3 % Clear workspace
4 clc;
5 clear all;
6 close all;
7 global m
8 global I
9 global F M
10 global g
11 %% Load Aircraft Data
12 %read from Excel File
13 % filename_density_L = 'ourflightcondation'; % Path to your excel sheet
14 % aircraft_data = xlsread(filename_density_L, 'B2:B61'); % Read from Excel
15
16 % read Data from CSV
17 filename_density_L = 'exelsheet_data_modified2'; % Path to your CSV file
18 aircraft_data = readmatrix(filename_density_L, 'Range', 'B2:B61'); % Read from
19 % CSV
20
21 % Time vector parameters
22 dt = aircraft_data(1);
23 tfinal = aircraft_data(2);

```

```

23 t0 = aircraft_data(3);
24
25
26 % Initial conditions for states
27 s0 = aircraft_data(4:15);
28 sdot0 = zeros(12,1); % Initial derivative of states
29 Vto = sqrt(s0(1)^2 + s0(2)^2 + s0(3)^2); % Compute initial total velocity (Vto)
30 initialstatemodified=[s0(1:3);0;s0(4:6)];
31 % Control actions values
32 dc = [ aircraft_data(57:59) * pi/180 ; aircraft_data(60) ]; % Control inputs in
            radians
33
34 % Gravity, mass, and inertia values from aircraft data
35
36 m = aircraft_data(51);
37 g = aircraft_data(52);
38 Ixx = aircraft_data(53);
39 Iyy = aircraft_data(54);
40 Izz = aircraft_data(55);
41 Ixz = aircraft_data(56);
42 Ixy = 0; Iyz = 0;
43
44 % Inertia matrix and inverse inertia matrix
45
46 I = [Ixx, -Ixy, -Ixz; -Ixy, Iyy, -Iyz; -Ixz, -Iyz, Izz];
47 invI = inv(I);
48
49 %Initial velocities and rates
50 u_0 = s0(1);
51 v_0 = s0(2);
52 w_0 = s0(3);
53 p_0 = s0(4);
54 q_0 = s0(5);
55 r_0 = s0(6);
56 phi_0 = s0(7);
57 theta_0 = s0(8);
58 psi_0 = s0(9);
59 x_0 = s0(10);
60 y_0 = s0(11);
61 z_0 = s0(12);
62 wdot_0 = 0;
63 wdot = 0;
64 mass = m;
65
66 % Stability derivatives for longitudinal motion
67 SD_Long = aircraft_data(21:36);
68 SD_Long_final = SD_Long;
69 templong = num2cell(SD_Long);
70 [Xu,Zu,Mu,Xw,Zw,Mw,Zwd,Zq,Mwd,Mq,Xde,Zde,Mde,Xth,Zdth,Mdth] = deal(templong{:});
71 clear templong;
72
73
74 % Stability derivatives for lateral motion
75 SD_Lat_dash = aircraft_data(37:50);
76 SD_Lat = LateralFunc(SD_Lat_dash, Ixz, Izz, Ixx, Vto);
77 SD_Lat_final = SD_Lat;
78 templatrel = num2cell(SD_Lat);
79 [Yv,Yb,Lb,Nb,Lp,Np,Lr,Nr,Yda,Ydr,Lda,Nda,Ldr,Ndr] = deal(templatrel{:});
80 clear templatrel;
81
82 Lv=Lb/Vto;
83 Nv=Nb/Vto;
84 Yp=0;
85 Yr=0;
86
87 % Initial gravity force in body frame
88 mg0 = m * g * [sin(s0(8)); -cos(s0(8)) * sin(s0(7)); -cos(s0(8)) * cos(s0(7))];
89 initial_F_M = m * g * [sin(s0(8)); -cos(s0(8)) * sin(s0(7)); -cos(s0(8)) * cos(s0
            (7));0;0;0]; % Simulink Input
90 M_0 = [0;0;0];
91

```

```

92 %% Matrix used in simulink
93 State_Matrix = [ Xu 0 Xw 0 0 0 0;
94 0 Yv 0 Yp 0 Yr 0;
95 Zu 0 Zw 0 Zq Lr Zwd;
96 0 Lv 0 Lp 0 Lr 0;
97 Mu 0 Mw 0 Mq 0 Mwd;
98 0 Nv 0 Np 0 Nr 0];
99
100 Control_Matrix = [0 Xde Xth 0
101 0 Yda 0 0 Ydr
102 0 Zde Zdth 0
103 Lda 0 0 Ldr
104 0 Mde Mdth 0
105 Nda 0 0 Ndr];
106
107
108 %% initial struc state
109 so_struct.x = s0(10);
110 so_struct.y = s0(11);
111 so_struct.z = s0(12);
112 so_struct.phi = s0(7);
113 so_struct.theta = s0(8);
114 so_struct.epsi = s0(9);
115 so_struct.p = s0(4);
116 so_struct.q = s0(5);
117 so_struct.r = s0(6);
118 so_struct.u = s0(1);
119 so_struct.v = s0(2);
120 so_struct.w = s0(3);
121 so_struct.alpha = s0(8);
122 so_struct.Beta = 0;
123 so_struct.V_total = Vto;
124 so_struct.W_dot = 0;
125
126 %% Combine stability derivatives into a single array
127 for i = 1:16
128 SD(i) = SD_Long_final(i);
129 end
130 for j = 1:14
131 SD(j+16) = SD_Lat_final(j); % All stability derivatives in one array
132 end
133
134 F_M_Matrix_dv = [SD(1) 0 SD(4) 0 0 0 0 0 0 SD(11) SD(14);
135 0 SD(17) 0 0 0 0 0 SD(26) 0 0;
136 SD(2) 0 SD(5) SD(7) 0 SD(8) 0 0 0 SD(12) SD(15);
137 0 SD(19)/Vto 0 0 SD(21) 0 SD(23) SD(27) SD(29) 0 0;
138 SD(3) 0 SD(6) SD(9) 0 SD(10) 0 0 0 SD(13) SD(16);
139 0 SD(20)/Vto 0 0 SD(22) 0 SD(24) SD(28) SD(30) 0 0]; %
140 Simulink Input
141 %% Calculating forces and moments
142 n = (tfinal - t0) / dt;
143 velocity_0=s0(1:3);
144 angular_v0=s0(4:6);
145 angles_0=s0(7:9);
146 position_0=s0(10:12);
147 t = (0:dt:tfinal)';
148 Initial_state=[velocity_0;angular_v0;angles_0;position_0];
149 [F,M]=F_M_Cal(SD,s0,Vto,dc,Initial_state,0);
150 [t, states] = RK4_solver(@getstates,Initial_state , 0, tfinal,n, SD,Vto, dc);
151
152 %% Initiating simulink
153 modelName = 'Final_Task3_Simulink_23b';
154 load_system(modelName);
155 set_param(modelName, 'StartTime', '0', 'StopTime', num2str(tfinal));
156 simOut = sim(modelName, 'ReturnWorkspaceOutputs', 'on');
157
158 t2 = simOut.tout; % Time vector from simout
159 y2 = simOut.simout.Data;
160 y2 = y2'; % Now y2 is [12 x 200001]
161
```

```

162 %% Task 4
163 %% Full Longitudinal System
164 % Define constants
165 theta_0 = s0(8); wo = s0(3); u_0 = s0(1); wdot=0;
166
167 % Define constants and matrices for the longitudinal state-space model
168 u = [dc(3)* ones(size(t)); 1*ones(size(t))];
169
170 A_longitudinal = [Xu, Xw,0, -g*cos(theta_0);
171                     Zu/(1-Zwd), Zw/(1-Zwd), (Zq + u_0)/(1-Zwd), -g*sin(theta_0)/(1-
172                     Zwd);
173                     Mu + Mwd*Zu/(1-Zwd), Mw + wdot*Zw/(1-Zwd), Mq + Mwd*(Zq+u_0)/(1-
174                     Zwd), -Mwd*g*sin(theta_0)/(1-Zwd);
175                     0, 0, 1, 0];
176
177 B_longitudinal = [Xde, Xth;
178                     Zde/(1-Zwd), Zdth/(1-Zwd);
179                     Mde + Mwd*Zde/(1-Zwd), Mdth + Mwd*Zdth/(1-Zwd);
180                     0, 0];
181
182 C_longitudinal = eye(4); % Observing all states
183 D_longitudinal = zeros(4, 2); % No direct feedthrough
184 % Create the state-space model
185 sys_longitudinal = ss(A_longitudinal, B_longitudinal, C_longitudinal,
186                         D_longitudinal );
187 tf_full_longitudinal = tf(sys_longitudinal);
188 x0=[u_0;w_0;q_0;theta_0];
189 [y_full, t, x] = initial(sys_longitudinal, x0, t);
190
191 % Transfer function from elevator deflection (De) to each state output
192 tf_full_longitudinal_De_with_stateu = minreal(tf_full_longitudinal(1,1)); % u
193             state
194 tf_full_longitudinal_De_with_statew = minreal(tf_full_longitudinal(2,1)); % w
195             state
196 tf_full_longitudinal_De_with_stateq = minreal(tf_full_longitudinal(3,1)); % q
197             state
198 tf_full_longitudinal_De_with_state_theta = minreal(tf_full_longitudinal(4,1)); % theta
199             state
200
201 % Transfer function from throttle (Th) to each state output
202 tf_full_longitudinal_Th_with_stateu = minreal(tf_full_longitudinal(1,2)); % u
203             state
204 tf_full_longitudinal_Th_with_statew = minreal(tf_full_longitudinal(2,2)); % w
205             state
206 tf_full_longitudinal_Th_with_stateq = minreal(tf_full_longitudinal(3,2)); % q
207             state
208 tf_full_longitudinal_Th_with_state_theta = minreal(tf_full_longitudinal(4,2)); % theta
209             state
210
211 % Long Mode For Longitudinal
212 A_longitudinal_long = [Xu, -g*cos(theta_0); -Zu/(Zq+u_0), g*sin(theta_0)/(Zq+u_0)
213 ];
214 B_longitudinal_long = [Xde, Xth; -Zde/(Zq+u_0), -Zdth/(Zq+u_0)];
215
216 % Assuming the output directly maps to the state (no C and D matrices provided,
217 % use identity matrix for direct mapping)
218 C_longitudinal_long = eye(2); % Direct mapping of state to output
219 D_longitudinal_long = zeros(2, 2); % No direct feedthrough
220
221 % Define state-space model for the long-period longitudinal system
222 sys_longitudinal_long = ss(A_longitudinal_long, B_longitudinal_long,
223                             C_longitudinal_long, D_longitudinal_long);
224 tf_long_period = tf(sys_longitudinal_long);
225
226 % Initial state vector for long-period mode (u and theta components)
227 x0_long = [u_0; theta_0];
228
229 % Run the simulation for the long-period mode with external input 'u'
230 % 'u' should be defined as the input vector for the simulation
231 [y_long, t, x_long] = lsim(sys_longitudinal_long, u, t, x0_long);
232

```

```

219 % Transfer function from elevator deflection (De) to each state output
220 tf_long_period_De_with_state_u = minreal(tf_long_period(1,1)); % u state
221 tf_long_period_De_with_state_theta = minreal(tf_long_period(2,1)); % theta state
222
223 % Transfer function from throttle (Th) to each state output
224 tf_long_period_Th_with_state_u = minreal(tf_long_period(1,2)); % u state
225 tf_long_period_Th_with_state_theta = minreal(tf_long_period(2,2)); % theta state
226
227 %% Short Mode For Longitudinal
228 A_longitudinal_short = [
229     Zw / (1 - Zwd), (Zq + u_0) / (1 - Zwd);
230     Mw + (Mwd * (Zw / (1 - Zwd))), Mq + (Mwd * ((Zq + u_0) / (1 - Zwd)))
231 ];
232 B_longitudinal_short = [
233     Zde / (1 - Zwd), Zdth / (1 - Zwd);
234     Mde + (Mwd * Zde / (1 - Zwd)), Mdth + (Mwd*Zdth / (1 - Zwd))
235 ];
236 C_longitudinal_short = eye(2); % Direct mapping of state to output
237 D_longitudinal_short = zeros(2, 2); % No direct feedthrough
238
239 % Define state-space model for the short-period longitudinal system
240 sys_longitudinal_short = ss(A_longitudinal_short, B_longitudinal_short,
241     C_longitudinal_short, D_longitudinal_short);
242 tf_short_period = tf(sys_longitudinal_short);
243
244 % Initial state vector for short-period mode ()
245 x0_short = [w_0; q_0]; % Corrected to match the 2-dimensional system
246
247 % Run the simulation for the short-period mode
248 [y_short, t, x_short] = initial(sys_longitudinal_short, x0_short, t);
249
250 % Extract and simplify transfer functions with corresponding labels
251 % Transfer function from elevator deflection (De) to each state output
252 tf_short_period_De_with_state_w = minreal(tf_short_period(1,1)); % w state
253 tf_short_period_De_with_state_q = minreal(tf_short_period(2,1)); % q state
254
255 % Transfer function from throttle (Th) to each state output
256 tf_short_period_Th_with_state_w = minreal(tf_short_period(1,2)); % w state
257 tf_short_period_Th_with_state_q = minreal(tf_short_period(2,2)); % q state
258
259 %% Full Lateral Mode System
260 A_lateral = [Yv, Yp+wo, Yr-u_0, g*cos(theta_0), 0;
261     Lv, Lp, Lr, 0, 0;
262     Nv, Np, Nr, 0, 0;
263     0, 1, tan(theta_0), 0, 0;
264     0, 0, 1/cos(theta_0), 0, 0];
265
266 B_lateral = [Yda, Ydr;
267     Lda, Ldr;
268     Nda, Ndr;
269     0, 0;
270     0, 0];
271
272 C_lateral = eye(5); % Observing all states
273 D_lateral = zeros(5, 2); % No direct feedthrough
274
275 u_lat = [dc(1)* ones(size(t)), 1*ones(size(t))]';
276
277 % Create the state-space model for the lateral dynamics
278 sys_lateral = ss(A_lateral, B_lateral, C_lateral, D_lateral);
279 tf_full_lateral = tf(sys_lateral);
280
281 % Initial state vector for the lateral dynamics
282 x0_lateral = [v_0; p_0; r_0; phi_0; psi_0]; % Define initial conditions for
283     lateral states
284
285 % Run the simulation for the lateral dynamics with the specified input
286 [y_lateral, t, x_lateral] = lsim(sys_lateral, u_lat, t, x0_lateral);

```

```

288
289 % Transfer function from aileron deflection (Da) to each state output
290 tf_full_lateral_Da_with_state_v = minreal(tf_full_lateral(1,1));
291 tf_full_lateral_Da_with_state_p = minreal(tf_full_lateral(2,1));
292 tf_full_lateral_Da_with_state_r = minreal(tf_full_lateral(3,1));
293 tf_full_lateral_Da_with_state_phi = minreal(tf_full_lateral(4,1));
294 tf_full_lateral_Da_with_state_epsi = minreal(tf_full_lateral(5,1));
295
296 % Transfer function from rudder deflection (Dr) to each state output
297 tf_full_lateral_Dr_with_state_v = minreal(tf_full_lateral(1,2));
298 tf_full_lateral_Dr_with_state_p = minreal(tf_full_lateral(2,2));
299 tf_full_lateral_Dr_with_state_r = minreal(tf_full_lateral(3,2));
300 tf_full_lateral_Dr_with_state_phi = minreal(tf_full_lateral(4,2));
301 tf_full_lateral_Dr_with_state_epsi = minreal(tf_full_lateral(5,2));
302
303 %% 3-DOF Approximations for Spiral lateral Mode
304 A_lateral_3DOF_spiral = [Lp, Lr, 0;
305                               Np, Nr, 0;
306                               1, tan(theta_0), 0];
307 % B_lateral_3DOF_spiral = [Ldr;Ndr;0];
308 B_lateral_3DOF_spiral = [Lda, Ldr;
309                               Nda, Ndr;
310                               0, 0];
311
312 % Define the output matrix to observe all states (p, r, and v)
313 C_lateral_3DOF_spiral = eye(3); % Observing all three states
314 D_lateral_3DOF_spiral = zeros(3, 2); % No direct feedthrough from input to
315           output
316
317 % Create the state-space model for the spiral mode approximation
318 sys_lateral_3DOF_spiral = ss(A_lateral_3DOF_spiral, B_lateral_3DOF_spiral,
319                               C_lateral_3DOF_spiral, D_lateral_3DOF_spiral);
320 tf_3DOF_spiral = tf(sys_lateral_3DOF_spiral);
321
322 % Initial state vector for the spiral mode with 3 DOF (initial conditions for p,
323 % r, and v)
324 x0_spiral_3DOF = [p_0; r_0; phi_0]; % Assuming zero initial conditions
325
326 % Run the simulation for the spiral mode with 3 DOF using the specified input
327 [y_spiral_3DOF, t, x_spiral_3DOF] = lsim(sys_lateral_3DOF_spiral, u_lat, t,
328                                           x0_spiral_3DOF);
329
330 % Transfer functions from rudder deflection (Dr) to each state output
331 tf_3DOF_spiral_Dr_with_state_p = minreal(tf_3DOF_spiral(1,1)); % Roll Rate (p)
332 tf_3DOF_spiral_Dr_with_state_r = minreal(tf_3DOF_spiral(2,1)); % Yaw Rate (r)
333 tf_3DOF_spiral_Dr_with_state_phi = minreal(tf_3DOF_spiral(3,1)); % Roll Angle (
334           phi)
335
336 %% 3-DOF Approximations for Dutch roll lateral Mode
337 A_lateral_3DOF_dutch = [Yv, Yp+wo, Yr-u_0;
338                           Lv, Lp, 0;
339                           Nv, 0, Nr];
340 B_lateral_3DOF_dutch = [Yda, Ydr;
341                           Lda, Ldr;
342                           Nda, Ndr];
343
344 % Output matrix to observe all states (v, p, and r)
345 C_lateral_3DOF_dutch = eye(3); % Observing all three states
346 D_lateral_3DOF_dutch = zeros(3, 2); % No direct feedthrough from input to output
347
348 % Create the state-space model for the Dutch Roll mode approximation
349 sys_lateral_3DOF_dutch = ss(A_lateral_3DOF_dutch, B_lateral_3DOF_dutch,
350                               C_lateral_3DOF_dutch, D_lateral_3DOF_dutch);
351 tf_3DOF_dutch = tf(sys_lateral_3DOF_dutch);
352
353 % Initial state vector for the Dutch Roll mode with 3 DOF (initial conditions for
354 % v, p, and r)
355 x0_dutch_3DOF = [v_0; p_0; r_0]; % Assuming zero initial conditions
356
357 % Run the simulation for the Dutch Roll mode with 3 DOF using the specified input
358 [y_dutch_3DOF, t, x_dutch_3DOF] = lsim(sys_lateral_3DOF_dutch, u_lat, t,
359                                           x0_dutch_3DOF);

```

```

351 % Transfer functions from aileron deflection (Da) to each state output
352 tf_3DOF_dutch_Da_with_state_v = minreal(tf_3DOF_dutch(1,1)); % Side velocity (v)
353 tf_3DOF_dutch_Da_with_state_p = minreal(tf_3DOF_dutch(2,1)); % Roll angle (phi)
354 tf_3DOF_dutch_Da_with_state_r = minreal(tf_3DOF_dutch(3,1)); % Yaw rate (r)
355
356 % Transfer functions from rudder deflection (Dr) to each state output
357 tf_3DOF_dutch_Dr_with_state_v = minreal(tf_3DOF_dutch(1,2));
358 tf_3DOF_dutch_Dr_with_state_p = minreal(tf_3DOF_dutch(2,2));
359 tf_3DOF_dutch_Dr_with_state_r = minreal(tf_3DOF_dutch(3,2));
360
361 %% 2-DOF Approximations for the Dutch roll lateral Mode
362 A_lateral_2DOF_dutch = [Yv, Yr-u_0;
363                         Nv, Nr];
364 B_lateral_2DOF_dutch = [Yda, Ydr;
365                         Nda, Ndr];
366
367 % Output matrix to observe both states (v and r)
368 C_lateral_2DOF_dutch = eye(2); % Observing both states
369 D_lateral_2DOF_dutch = zeros(2, 2); % No direct feedthrough from input to output
370
371 % Create the state-space model for the 2-DOF Dutch Roll mode
372 sys_lateral_2DOF_dutch = ss(A_lateral_2DOF_dutch, B_lateral_2DOF_dutch,
373                             C_lateral_2DOF_dutch, D_lateral_2DOF_dutch);
374 tf_2DOF_dutch = tf(sys_lateral_2DOF_dutch);
375
376 % Initial state vector for the 2-DOF Dutch Roll mode (initial conditions for v
377 % and r)
377 x0_dutch_2DOF = [v_0;r_0]; % Assuming zero initial conditions
378
379 % Run the simulation for the Dutch Roll mode with 2 DOF using the specified input
380 [y_dutch_2DOF, t, x_dutch_2DOF] = lsim(sys_lateral_2DOF_dutch, u_lat, t,
381                                         x0_dutch_2DOF);
382
383
384 % Transfer functions from aileron deflection (Da) to each state output
385 tf_2DOF_dutch_Da_with_state_v = minreal(tf_2DOF_dutch(1,1)); % Side velocity (v)
386 tf_2DOF_dutch_Da_with_state_r = minreal(tf_2DOF_dutch(2,1)); % Yaw rate (r)
387
388 % Transfer functions from rudder deflection (Dr) to each state output
389 tf_2DOF_dutch_Dr_with_state_v = minreal(tf_2DOF_dutch(1,2));
390 tf_2DOF_dutch_Dr_with_state_r = minreal(tf_2DOF_dutch(2,2));
391
392 %% 1-DOF Approximations for the Roll lateral Mode
393 A_lateral_1DOF = Lp; % Only the roll damping term Lp
394 B_lateral_1DOF = Lda; % Aileron control input affecting roll rate
395 C_lateral_1DOF = 1; % Observe roll rate (p) directly
396 D_lateral_1DOF = 0; % No direct feedthrough
397
398 sys_lateral_1DOF = ss(A_lateral_1DOF, B_lateral_1DOF, C_lateral_1DOF,
399                         D_lateral_1DOF);
400 % Calculate the transfer function from aileron deflection (Da) to roll rate (p)
400 tf_1DOF_roll_Da_with_state_p = minreal(tf(sys_lateral_1DOF));
401
402 % Define the input signal (u), representing aileron deflection
403 u_1dof = ones(size(t)); % Constant aileron deflection for demonstration
404
405 % Initial state vector for roll rate
406 x0_roll_1DOF = p_0; % Assuming zero initial roll rate
407
408 % Run the simulation for the roll mode with the specified input
409 [y_roll_1DOF, t, x_roll_1DOF] = lsim(sys_lateral_1DOF, u_1dof, t, x0_roll_1DOF);
410
411
412 %% Plotting
413 % MATLAB Plotting Task 3
414 rad_to_deg = 180 / pi; % Conversion from radians to degrees
415
416 % Plot results (e.g., velocities, angles, positions)
417 figure;

```

```

418 sgttitle('Matlab Code Plots');
419
420 % Plot forward, side, and vertical velocities (u, v, w)
421 subplot(4,3,1);
422 plot(t, states(1,:), 'b'); % u (forward velocity)
423 title('Forward Velocity (u)');
424 xlabel('Time (s)');
425 ylabel('Velocity (ft/s)');
426
427 % subplot(4,3,2);
428 % plot(t2, y2(2,:), 'r'); % v (side velocity)
429 % title('Side Velocity (v)');
430 % xlabel('Time (s)');
431 % ylabel('Velocity (ft/s)');
432 %
433 % subplot(4,3,3);
434 % plot(t2, y2(3,:), 'g'); % w (vertical velocity)
435 % title('Vertical Velocity (w)');
436 % xlabel('Time (s)');
437 % ylabel('Velocity (ft/s)');
438
439 subplot(4,3,2);
440 plot(t, asin(states(2,:)/Vto)*rad_to_deg, 'r'); % bita (side velocity)
441 title('bita');
442 xlabel('Time (s)');
443 ylabel('Velocity (ft/s)');
444
445 subplot(4,3,3);
446 plot(t, atan(states(3,:)./states(1,:))*rad_to_deg, 'g'); % alpha (vertical
    velocity)
447 title('Alpa');
448 xlabel('Time (s)');
449 ylabel('Velocity (ft/s)');
450
451 % Angular velocities (p, q, r)
452
453 subplot(4,3,4);
454 plot(t, states(4,:)*rad_to_deg, 'b'); % p (roll rate)
455 title('Roll Rate (p)');
456 xlabel('Time (s)');
457 ylabel('Angular Velocity (rad/s)');
458
459 subplot(4,3,5);
460 plot(t, states(5,:)*rad_to_deg, 'r'); % q (pitch rate)
461 title('Pitch Rate (q)');
462 xlabel('Time (s)');
463 ylabel('Angular Velocity (rad/s)');
464
465 subplot(4,3,6);
466 plot(t, states(6,:)*rad_to_deg, 'g'); % r (yaw rate)
467 title('Yaw Rate (r)');
468 xlabel('Time (s)');
469 ylabel('Angular Velocity (rad/s)');
470
471 % Euler angles (phi, theta, psi) in degrees
472
473 subplot(4,3,7);
474 plot(t, states(7,:) * rad_to_deg, 'b'); % phi (roll angle in degrees)
475 title('Roll Angle (phi) in degrees');
476 xlabel('Time (s)');
477 ylabel('Angle (deg)');
478
479 subplot(4,3,8);
480 plot(t, states(8,:) * rad_to_deg, 'r'); % theta (pitch angle in degrees)
481 title('Pitch Angle (theta) in degrees');
482 xlabel('Time (s)');
483 ylabel('Angle (deg)');
484
485 subplot(4,3,9);
486 plot(t, states(9,:) * rad_to_deg, 'g'); % psi (yaw angle in degrees)
487 title('Yaw Angle (psi) in degrees');

```

```

488 xlabel('Time (s)');
489 ylabel('Angle (deg)');
490
491 % Position (x, y, z) in feet
492
493 subplot(4,3,10);
494 plot(t, states(10,:), 'b');
495 title('Position X (ft)');
496 xlabel('Time (s)');
497 ylabel('Position (ft)');
498
499 subplot(4,3,11);
500 plot(t, states(11,:), 'r');
501 title('Position Y (ft)');
502 xlabel('Time (s)');
503 ylabel('Position (ft)');
504
505 subplot(4,3,12);
506 plot(t, round(states(12,:),3), 'g');
507 title('Position Z (ft)');
508 xlabel('Time (s)');
509 ylabel('Position (ft)');
510
511
512 % Trajectory (x vs y vs z in feet)
513 figure;
514 plot3(states(10,:), states(11,:), round(states(12,:),3), 'b'); % 3D trajectory
      plot
515 title('Matlab Code Trajectory (ft)', 'FontWeight', 'bold', 'FontSize', 14);
516 xlabel('X (ft)', 'FontWeight', 'bold', 'FontSize', 12);
517 ylabel('Y (ft)', 'FontWeight', 'bold', 'FontSize', 12);
518 zlabel('Z (ft)', 'FontWeight', 'bold', 'FontSize', 12);
519 grid on;
520
521 %% Simulink Plot Task 3
522 % Plot results (e.g., velocities, angles, positions)
523 figure;
524 sgttitle('Simulink Code Plots');
525 % Plot forward, side, and vertical velocities (u, v, w)
526 subplot(4,3,1);
527 plot(t2, y2(1,:), 'b'); % u (forward velocity)
528 title('Forward Velocity (u)', 'FontWeight', 'bold', 'FontSize', 12);
529 xlabel('Time (s)', 'FontWeight', 'bold', 'FontSize', 10);
530 ylabel('Velocity (ft/s)', 'FontWeight', 'bold', 'FontSize', 10);
531
532 subplot(4,3,2);
533 plot(t2, y2(2,:), 'r'); % v (side velocity)
534 title('Side Velocity (v)', 'FontWeight', 'bold', 'FontSize', 12);
535 xlabel('Time (s)', 'FontWeight', 'bold', 'FontSize', 10);
536 ylabel('Velocity (ft/s)', 'FontWeight', 'bold', 'FontSize', 10);
537
538 subplot(4,3,3);
539 plot(t2, y2(3,:), 'g'); % w (vertical velocity)
540 title('Vertical Velocity (w)', 'FontWeight', 'bold', 'FontSize', 12);
541 xlabel('Time (s)', 'FontWeight', 'bold', 'FontSize', 10);
542 ylabel('Velocity (ft/s)', 'FontWeight', 'bold', 'FontSize', 10);
543
544 %
545 % plots of alpha and beta
546 % subplot(4,3,2);
547 % plot(t2, y2(13,:)*rad_to_deg, 'r'); % v (side angle beta)
548 % title('Side angle (Beta)', 'FontWeight', 'bold', 'FontSize', 12);
549 % xlabel('Time (s)', 'FontWeight', 'bold', 'FontSize', 10);
550 % ylabel('Beta (deg)', 'FontWeight', 'bold', 'FontSize', 10);
551 %
552 % subplot(4,3,3);
553 % plot(t2, y2(14,:)*rad_to_deg, 'g'); % w (alpha )
554 % title('angle of attach (Alpha)', 'FontWeight', 'bold', 'FontSize', 12);
555 % xlabel('Time (s)', 'FontWeight', 'bold', 'FontSize', 10);
556 % ylabel('alpha (deg)', 'FontWeight', 'bold', 'FontSize', 10);
557

```

```

558
559 % Angular velocities (p, q, r)
560 subplot(4,3,4);
561 plot(t2, y2(4,:)* rad_to_deg, 'b'); % p (roll rate)
562 title('Roll Rate (p)', 'FontWeight', 'bold', 'FontSize', 12);
563 xlabel('Time (s)', 'FontWeight', 'bold', 'FontSize', 10);
564 ylabel('Angular Velocity (rad/s)', 'FontWeight', 'bold', 'FontSize', 10);
565
566 subplot(4,3,5);
567 plot(t2, y2(5,:)*rad_to_deg, 'r'); % q (pitch rate)
568 title('Pitch Rate (q)', 'FontWeight', 'bold', 'FontSize', 12);
569 xlabel('Time (s)', 'FontWeight', 'bold', 'FontSize', 10);
570 ylabel('Angular Velocity (rad/s)', 'FontWeight', 'bold', 'FontSize', 10);
571
572 subplot(4,3,6);
573 plot(t2, y2(6,:)*rad_to_deg, 'g'); % r (yaw rate)
574 title('Yaw Rate (r)', 'FontWeight', 'bold', 'FontSize', 12);
575 xlabel('Time (s)', 'FontWeight', 'bold', 'FontSize', 10);
576 ylabel('Angular Velocity (rad/s)', 'FontWeight', 'bold', 'FontSize', 10);
577
578 % Euler angles (phi, theta, psi) in degrees
579 subplot(4,3,7);
580 plot(t2, y2(7,:)* rad_to_deg, 'b'); % phi (roll angle in degrees)
581 title('Roll Angle (phi) in degrees', 'FontWeight', 'bold', 'FontSize', 12);
582 xlabel('Time (s)', 'FontWeight', 'bold', 'FontSize', 10);
583 ylabel('Angle (deg)', 'FontWeight', 'bold', 'FontSize', 10);
584
585 subplot(4,3,8);
586 plot(t2, y2(8,:)* rad_to_deg, 'r'); % theta (pitch angle in degrees)
587 title('Pitch Angle (theta) in degrees', 'FontWeight', 'bold', 'FontSize', 12);
588 xlabel('Time (s)', 'FontWeight', 'bold', 'FontSize', 10);
589 ylabel('Angle (deg)', 'FontWeight', 'bold', 'FontSize', 10);
590
591 subplot(4,3,9);
592 plot(t2, unwrap(y2(9,:)) * rad_to_deg, 'g'); % psi (yaw angle in degrees)
593 title('Yaw Angle (psi) in degrees', 'FontWeight', 'bold', 'FontSize', 12);
594 xlabel('Time (s)', 'FontWeight', 'bold', 'FontSize', 10);
595 ylabel('Angle (deg)', 'FontWeight', 'bold', 'FontSize', 10);
596
597 % Position (x, y, z) in feet
598 subplot(4,3,10);
599 plot(t2, y2(10,:), 'b');
600 title('Position X (ft)', 'FontWeight', 'bold', 'FontSize', 12);
601 xlabel('Time (s)', 'FontWeight', 'bold', 'FontSize', 10);
602 ylabel('Position (ft)', 'FontWeight', 'bold', 'FontSize', 10);
603
604 subplot(4,3,11);
605 plot(t2, y2(11,:), 'r');
606 title('Position Y (ft)', 'FontWeight', 'bold', 'FontSize', 12);
607 xlabel('Time (s)', 'FontWeight', 'bold', 'FontSize', 10);
608 ylabel('Position (ft)', 'FontWeight', 'bold', 'FontSize', 10);
609
610 subplot(4,3,12);
611 plot(t2, round(y2(12,:)), 3), 'g');
612 title('Position Z (ft)', 'FontWeight', 'bold', 'FontSize', 12);
613 xlabel('Time (s)', 'FontWeight', 'bold', 'FontSize', 10);
614 ylabel('Position (ft)', 'FontWeight', 'bold', 'FontSize', 10);
615
616 % Trajectory (x vs y vs z in feet)
617 figure;
618 plot3(y2(10,:), y2(11,:), round(y2(12,:)), 3), 'b'); % 3D trajectory plot
619 title('Simulink Code Trajectory (ft)', 'FontWeight', 'bold', 'FontSize', 14);
620 xlabel('X (ft)', 'FontWeight', 'bold', 'FontSize', 12);
621 ylabel('Y (ft)', 'FontWeight', 'bold', 'FontSize', 12);
622 zlabel('Z (ft)', 'FontWeight', 'bold', 'FontSize', 12);
623 grid on;
624
625 % Step response plots
626
627 %Longitudinal

```

```

629 %Compare 'u' (velocity) from full and long-period models
630 subplot(4,1,1);
631 plot(t, unwrap(y_full(:,1)+x0(1)), 'r', 'DisplayName', 'Fully linearized Model');
632 hold on;
633 plot(t, unwrap(y_long(:,1)+x0(1)), 'b--', 'DisplayName', 'Long-Period Model');
634 plot(t2, unwrap(y2(1,:)), 'g--', 'DisplayName', 'Non-linear Model');
635 title('Response of u (velocity)'); xlabel('Time (s)'); ylabel('u (m/s)');
636 legend;
637 hold off;
638
639 %Compare 'w' (vertical speed) from full and short-period models
640 subplot(4,1,2);
641 plot(t, unwrap(y_full(:,2)+x0(2)), 'r', 'DisplayName', 'Fully linearized Model');
642 hold on;
643 plot(t, unwrap(y_short(:,1)+x0(2)), 'b--', 'DisplayName', 'Short-Period Model');
644 plot(t, unwrap(states(3,:)), 'g--', 'DisplayName', 'Non-Linear Model');
645 title('Response of w (vertical speed)'); xlabel('Time (s)'); ylabel('w (m/s)');
646 legend;
647 hold off;
648
649 %Compare 'q' (pitch rate) from full and short-period models
650 subplot(4,1,3);
651 plot(t, unwrap(y_full(:,3)+x0(3))*(180/pi), 'r', 'DisplayName', 'Fully linearized Model'); hold on;
652 plot(t, unwrap(y_short(:,2)+x0(3))*(180/pi), 'b--', 'DisplayName', 'Short-Period Model');
653 plot(t2, unwrap(y2(5,:))*(180/pi), 'g--', 'DisplayName', 'Non-Linear Model');
654 title('Response of q (pitch rate)'); xlabel('Time (s)'); ylabel('q (deg/s)');
655 legend;
656 hold off;
657
658 %Compare '\theta' (pitch angle) from full and long-period models
659 subplot(4,1,4);
660 plot(t, (unwrap(y_full(:,4)+x0(4)))*(180/pi), 'r', 'DisplayName', 'Fully linearized Model'); hold on;
661 plot(t, (unwrap(y_long(:,2)+x0(4)))*(180/pi), 'b--', 'DisplayName', 'Long-Period Model');
662 plot(t2, (unwrap(y2(8,:)))*(180/pi), 'g--', 'DisplayName', 'Non-Linear Model');
663 title('Response of \theta (pitch angle)'); xlabel('Time (s)'); ylabel('\theta (deg)');
664 legend;
665 hold off;
666
667 % Compare 'Beta' sideslip velocity from 3DOF Dutch,2DOF dutch
668 subplot(4,1,1);
669 plot(t, (y_lateral(:,1)+x0_lateral(1))*(1/Vto), 'r', 'DisplayName', 'Fully linearized Model'); hold on;
670 plot(t, (y_dutch_3DOF(:,1)+ x0_dutch_3DOF(1))*(1/Vto), 'Color', '#FFA500', 'DisplayName', '3-DOF Dutch mode');
671 plot(t, (y_dutch_2DOF(:,1)+ x0_dutch_2DOF(1))*(1/Vto), 'm--', 'DisplayName', '2-DOF Dutch mode');
672 plot(t2, y2(2,:)*(1/Vto), 'g--', 'DisplayName', 'Non-linear Model');
673 title('Response of v'); xlabel('Time (s)'); ylabel('Beta (ft/s)');
674 legend;
675 hold off;
676
677 % Compare 'p'
678 subplot(4,1,2);
679 plot(t, y_lateral(:,2)+x0_lateral(2), 'r', 'DisplayName', 'Fully linearized Model'); hold on;
680 plot(t, y_spiral_3DOF(:,1)+x0_spiral_3DOF(1), 'b--', 'DisplayName', '3-DOF Spiral Mode');
681 plot(t, y_dutch_3DOF(:,2)+x0_dutch_3DOF(2), 'Color', '#FFA500', 'DisplayName', '3-DOF Dutch Roll mode');
682 plot(t, y_roll_1DOF(:,1)+x0_roll_1DOF, 'm--', 'DisplayName', '1-DOF Dutch Roll mode');
683 plot(t2, y2(4,:), 'g--', 'DisplayName', 'Non-linear Model');
684 title('Response of p'); xlabel('Time (s)'); ylabel('p (rad/s)');
685 legend;
686 hold off;

```

```

686
687 % Compare 'r'
688 subplot(4,1,3);
689 plot(t, y_lateral(:,3)+x0_lateral(3), 'r', 'DisplayName', 'Fully linearized Model
    '); hold on;
690 plot(t, y_spiral_3DOF(:,2)+x0_spiral_3DOF(2), 'b--', 'DisplayName', '3-DOF
    Spiralmode');
691 plot(t, y_dutch_3DOF(:,3)+x0_dutch_3DOF(3), 'Color', '#FFA500', 'DisplayName', '
    3-DOF Dutch Roll mode');
692 plot(t, y_dutch_2DOF(:,2)+ x0_dutch_2DOF(2), 'm--', 'DisplayName', '2-DOF mode');
693 plot(t2, y2(6,:), 'g--', 'DisplayName', 'Non-linear Model');
694 title('Response of r'); xlabel('Time (s)'); ylabel('r (rad/s)');
695 legend;
696 hold off;
697
698 % Compare 'phi'
699 subplot(4,1,4);
700 plot(t, y_lateral(:,4)+x0_lateral(4), 'r', 'DisplayName', 'Fully linearized Model
    '); hold on;
701 plot(t, y_spiral_3DOF(:,3)+x0_spiral_3DOF(3), 'b--', 'DisplayName', '3-DOF Spiral
    mode');
702 plot(t2, y2(7,:), 'g--', 'DisplayName', 'Non-linear Model');
703 title('Response of phi'); xlabel('Time (s)'); ylabel('\phi (rad)');
704 legend;
705 hold off;
706
707
708 % Compare 'epsi'
709 figure;
710 plot(t, y_lateral(:,5)+x0_lateral(5), 'r', 'DisplayName', 'Fully linearized
    Model'); hold on;
711 plot(t2, y2(9,:), 'g--', 'DisplayName', 'Non-linear Model');
712 title('Response of epsi'); xlabel('Time (s)'); ylabel('epsi (rad)');
713 legend;
714 hold off;
715
716
717 %% Plotting Rotlocus and Bodeplot For Longitudinal
718 % Call the function for each transfer function comparison between full and short
    modes
719
720 % Full longitudinal vs short-period
721 plotAndSaveSubplots(tf_full_longitudinal_De_with_statew,
    tf_short_period_De_with_state_w, 'Short', 'De', 'w');
722 plotAndSaveSubplots(tf_full_longitudinal_De_with_stateq,
    tf_short_period_De_with_state_q, 'Short', 'De', 'q');
723 plotAndSaveSubplots(tf_full_longitudinal_Th_with_statew,
    tf_short_period_Th_with_state_w, 'Short', 'Th', 'w');
724 plotAndSaveSubplots(tf_full_longitudinal_Th_with_stateq,
    tf_short_period_Th_with_state_q, 'Short', 'Th', 'q');
725
726 % Full longitudinal vs long-period
727 plotAndSaveSubplots(tf_full_longitudinal_De_with_stateu,
    tf_long_period_De_with_state_u, 'Long', 'De', 'u');
728 plotAndSaveSubplots(tf_full_longitudinal_De_with_state_theta,
    tf_long_period_De_with_state_theta, 'Long', 'De', 'theta');
729 plotAndSaveSubplots(tf_full_longitudinal_Th_with_stateu,
    tf_long_period_Th_with_state_u, 'Long', 'Th', 'u');
730 plotAndSaveSubplots(tf_full_longitudinal_Th_with_state_theta,
    tf_long_period_Th_with_state_theta, 'Long', 'Th', 'theta');
731
732
733
734 %% Plot and save Root Locus and Bode plots for each mode
735
736 % Define the transfer functions and labels for comparisons
737
738 % Aileron Deflection (Da) Comparisons
739 Da_v = {tf_full_lateral_Da_with_state_v, tf_3DOF_dutch_Da_with_state_v,
    tf_2DOF_dutch_Da_with_state_v};
740 Da_p = {tf_full_lateral_Da_with_state_p, tf_3DOF_dutch_Da_with_state_p,

```

```

    tf_1DOF_roll_Da_with_state_p};
741 Da_r = {tf_full_lateral_Da_with_state_r, tf_3DOF_dutch_Da_with_state_r,
    tf_2DOF_dutch_Da_with_state_r};
742 Da_phi = {tf_full_lateral_Da_with_state_phi};
743 Da_epsi = {tf_full_lateral_Da_with_state_epsi};
744
745 % Rudder Deflection (Dr) Comparisons
746 Dr_v = {tf_full_lateral_Dr_with_state_v, tf_3DOF_dutch_Dr_with_state_v,
    tf_2DOF_dutch_Dr_with_state_v};
747 Dr_p = {tf_full_lateral_Dr_with_state_p, tf_3DOF_spiral_Dr_with_state_p,
    tf_3DOF_dutch_Dr_with_state_p};
748 Dr_r = {tf_full_lateral_Dr_with_state_r, tf_3DOF_spiral_Dr_with_state_r,
    tf_3DOF_dutch_Dr_with_state_r, tf_2DOF_dutch_Dr_with_state_r};
749 Dr_phi = {tf_full_lateral_Dr_with_state_phi, tf_3DOF_spiral_Dr_with_state_phi};
750 Dr_epsi = {tf_full_lateral_Dr_with_state_epsi};
751
752
753 % Mode labels for Aileron Deflection (Da) Comparisons
754 mode_labels_Da_v = {'Full Mode', '3-DOF Dutch Roll', '2-DOF Dutch Roll'};
755 mode_labels_Da_p = {'Full Mode', '3-DOF Dutch Roll', '1-DOF Roll'};
756 mode_labels_Da_r = {'Full Mode', '3-DOF Dutch Roll', '2-DOF Dutch Roll'};
757 mode_labels_Da_phi = {'Full Mode'};
758 mode_labels_Da_epsi = {'Full Mode'};
759
760 % Mode labels for Rudder Deflection (Dr) Comparisons
761 mode_labels_Dr_v = {'Full Mode', '3-DOF Dutch Roll', '2-DOF Dutch Roll'};
762 mode_labels_Dr_p = {'Full Mode', '3-DOF Spiral', '3-DOF Dutch Roll'};
763 mode_labels_Dr_r = {'Full Mode', '3-DOF Spiral', '3-DOF Dutch Roll', '2-DOF Dutch
    Roll'};
764 mode_labels_Dr_phi = {'Full Mode', '3-DOF Spiral'};
765 mode_labels_Dr_epsi = {'Full Mode'};
766
767 %Call the function to compare each mode for specific input-output pairs
768
769 % Aileron Deflection (Da) Comparisons
770 plotAndCompareModesWithSubplots(Da_v, mode_labels_Da_v, 'Da', 'v');
771 plotAndCompareModesWithSubplots(Da_p, mode_labels_Da_p, 'Da', 'p');
772 plotAndCompareModesWithSubplots(Da_r, mode_labels_Da_r, 'Da', 'r');
773 plotAndCompareModesWithSubplots(Da_phi, mode_labels_Da_phi, 'Da', 'phi');
774 plotAndCompareModesWithSubplots(Da_epsi, mode_labels_Da_epsi, 'Da', 'epsi');
775
776 % Rudder Deflection (Dr) Comparisons
777 plotAndCompareModesWithSubplots(Dr_v, mode_labels_Dr_v, 'Dr', 'v');
778 plotAndCompareModesWithSubplots(Dr_p, mode_labels_Dr_p, 'Dr', 'p');
779 plotAndCompareModesWithSubplots(Dr_r, mode_labels_Dr_r, 'Dr', 'r');
780 plotAndCompareModesWithSubplots(Dr_phi, mode_labels_Dr_phi, 'Dr', 'phi');
781 plotAndCompareModesWithSubplots(Dr_epsi, mode_labels_Dr_epsi, 'Dr', 'epsi');
782
783 %% Display Tranfer Function For Longitudinal
784 % Call the function below for each input-output pair comparison
785
786 % Full longitudinal vs short-period
787 displayTransferFunctionAsFraction(tf_full_longitudinal_De_with_statew,
    tf_short_period_De_with_state_w, 'Short', 'De', 'w');
788 displayTransferFunctionAsFraction(tf_full_longitudinal_De_with_stateq,
    tf_short_period_De_with_state_q, 'Short', 'De', 'q');
789 displayTransferFunctionAsFraction(tf_full_longitudinal_Th_with_statew,
    tf_short_period_De_with_state_w, 'Short', 'Th', 'w');
790 displayTransferFunctionAsFraction(tf_full_longitudinal_Th_with_stateq,
    tf_short_period_De_with_state_q, 'Short', 'Th', 'q');
791
792 % Full longitudinal vs long-period
793 displayTransferFunctionAsFraction(tf_full_longitudinal_De_with_stateu,
    tf_long_period_De_with_state_u, 'Long', 'De', 'u');
794 displayTransferFunctionAsFraction(tf_full_longitudinal_De_with_state_theta,
    tf_long_period_De_with_state_theta, 'Long', 'De', 'theta');
795 displayTransferFunctionAsFraction(tf_full_longitudinal_Th_with_stateu,
    tf_long_period_Th_with_state_u, 'Long', 'Th', 'u');
796 displayTransferFunctionAsFraction(tf_full_longitudinal_Th_with_state_theta,
    tf_long_period_Th_with_state_theta, 'Long', 'Th', 'theta');
797
```

```

798 %% Display the transfer functions in fraction format
799 % Call the function below for each group of transfer functions
800
801 % Aileron Deflection (Da) Comparisons
802 displayTransferFunctionGroup(Da_v, mode_labels_Da_v, 'Da', 'v');
803 displayTransferFunctionGroup(Da_p, mode_labels_Da_p, 'Da', 'p');
804 displayTransferFunctionGroup(Da_r, mode_labels_Da_r, 'Da', 'r');
805 displayTransferFunctionGroup(Da_phi, mode_labels_Da_phi, 'Da', 'phi');
806 displayTransferFunctionGroup(Da_epsi, mode_labels_Da_epsi, 'Da', 'epsi');
807
808 % Rudder Deflection (Dr) Comparisons
809 displayTransferFunctionGroup(Dr_v, mode_labels_Dr_v, 'Dr', 'v');
810 displayTransferFunctionGroup(Dr_p, mode_labels_Dr_p, 'Dr', 'p');
811 displayTransferFunctionGroup(Dr_r, mode_labels_Dr_r, 'Dr', 'r');
812 displayTransferFunctionGroup(Dr_phi, mode_labels_Dr_phi, 'Dr', 'phi');
813 displayTransferFunctionGroup(Dr_epsi, mode_labels_Dr_epsi, 'Dr', 'epsi');
814
815 % Functions
816
817 % Define a function to display the transfer function expressions as a large
     fraction
818 function displayTransferFunctionAsFraction(tf_full, tf_mode, mode_name,
     input_name, output_name)
     % Extract numerator and denominator for the full mode transfer function
     [num_full, den_full] = tfdata(tf_full, 'v'); % Get numerator and denominator
     as vectors
     % Convert numerator and denominator to strings
     num_full_str = poly2str(num_full, 's');
     den_full_str = poly2str(den_full, 's');

     % Extract numerator and denominator for the mode transfer function (short/
     long)
     [num_mode, den_mode] = tfdata(tf_mode, 'v'); % Get numerator and denominator
     as vectors
     % Convert numerator and denominator to strings
     num_mode_str = poly2str(num_mode, 's');
     den_mode_str = poly2str(den_mode, 's');

     % Display the formatted transfer functions as a large fraction
     fprintf('Comparison for Transfer Function (%s to %s):\n', input_name,
     output_name);
     fprintf('-----\n');

     % Display the full mode transfer function in S domain format as a large
     fraction
     fprintf('Full Mode Transfer Function:\n');
     fprintf('    %s\n', num_full_str); % Numerator
     fprintf('    %s\n', repmat('-', max(length(num_full_str), length(den_full_str)),
     1)); % Divider line
     fprintf('    %s\n\n', den_full_str); % Denominator

     % Display the alternative mode (short or long) transfer function as a large
     fraction
     fprintf('%s Mode Transfer Function:\n', mode_name);
     fprintf('    %s\n', num_mode_str); % Numerator
     fprintf('    %s\n', repmat('-', max(length(num_mode_str), length(den_mode_str)),
     1)); % Divider line
     fprintf('    %s\n\n', den_mode_str); % Denominator

     % Add a line break for readability between comparisons
     fprintf('\n\n');

end
851 % Define function to display the transfer functions for a group in fraction
     format
852 function displayTransferFunctionGroup(tf_list, mode_labels, input_name,
     output_name)
     num_modes = length(tf_list);
     fprintf('Transfer Function Comparisons for %s to %s:\n', input_name,
     output_name);
     fprintf('-----\n');

```

```

856
857 for k = 1:num_modes
858     % Extract numerator and denominator
859     [num, den] = tfdata(tf_list{k}, 'v');
860     num_str = poly2str(num, 's');
861     den_str = poly2str(den, 's');
862
863     % Display transfer function for each mode
864     fprintf('%s Mode Transfer Function:\n', mode_labels{k});
865     fprintf('    %s\n', num_str); % Numerator
866     fprintf('    %s\n', repmat('-', max(length(num_str), length(den_str)), 1));
867 ); % Divider line
868     fprintf('    %s\n\n', den_str); % Denominator
869 end
870 fprintf('\n\n'); % Add extra line spacing between groups for readability
871 end
872 % Define function to plot and save Root Locus and Bode plots with subplots for
873 % each mode comparison
874 function plotAndCompareModesWithSubplots(tf_list, mode_labels, input_name,
875 output_name)
876 num_modes = length(tf_list);
877
878 % Plot Root Locus with each mode in its own subplot
879 figure;
880 set(gcf, 'WindowState', 'maximized'); % Maximize the figure window
881 for k = 1:num_modes
882     subplot(1, num_modes, k); % Create a subplot for each mode
883     rlocus(tf_list{k});
884     title(['Root Locus Comparison - ', mode_labels{k}, ', (', input_name, ' to
885 ', output_name, ')']);
886     xlabel('Real Axis');
887     ylabel('Imaginary Axis');
888 end
889 sgtitle(['Root Locus - ', input_name, ' to ', output_name]);
890 saveas(gcf, ['RootLocus_Comparison_', input_name, '_to_', output_name, '.png']);
891
892 % Plot Bode Plot with each mode in the same plot for overlay comparison
893 figure;
894 set(gcf, 'WindowState', 'maximized'); % Maximize the figure window
895 hold on;
896 for k = 1:num_modes
897     bode(tf_list{k});
898 end
899 hold off;
900 title(['Bode Plot Comparison - ', input_name, ' to ', output_name]);
901 legend(mode_labels);
902 saveas(gcf, ['BodePlot_Comparison_', input_name, '_to_', output_name, '.png']);
903 end
904
905 % Define a function to plot and save root locus and Bode plots with subplots for
906 % each transfer function
907 function plotAndSaveSubplots(tf_full, tf_short, mode_name, input_name,
908 output_name)
909 % Create figure for Root Locus with two subplots
910 figure;
911
912 % Full Mode Root Locus in the first subplot
913 subplot(1, 2, 1);
914 rlocus(tf_full);
915 title(['Root Locus - Full Mode (', input_name, ' to ', output_name, ')']);
916 xlabel('Real Axis');
917 ylabel('Imaginary Axis');
918
919 % Short Mode Root Locus in the second subplot
920 subplot(1, 2, 2);
921 rlocus(tf_short);
922 title(['Root Locus - ', mode_name, ', Mode (', input_name, ' to ', output_name
923 , ')']);

```

```

918 xlabel('Real Axis');
919 ylabel('Imaginary Axis');
920
921 % Save the combined root locus figure
922 saveas(gcf, ['RootLocus_', input_name, '_to_', output_name, '_Full_vs_',
mode_name, '.png']);
923
924 % Bode plot (Separate for Full and Short Mode)
925 figure;
926 bode(tf_full);
927 hold on;
928 bode(tf_short);
929 hold off;
930 title(['Bode Plot - ', input_name, ' to ', output_name, '(Full vs ',
mode_name, ' Mode)']);
931 legend('Full Mode', [mode_name, ' Mode']);
932 saveas(gcf, ['BodePlot_', input_name, '_to_', output_name, '_', mode_name, '.png']);
933 end

```

9.1.8 MATLAB Code for Autopilot Longitudinal Control

```

1 % Main Script: Airplane Nonlinear Simulator with RBD Solver
2
3 % Clear workspace
4 clc;
5 clear all;
6 close all;
7 global m
8 global I
9 global F M
10 global g
11 %% Load Aircraft Data
12 %read from Excel File
13 % filename_density_L = 'ourflightcondation'; % Path to your excel sheet
14 % aircraft_data = xlsread(filename_density_L, 'B2:B61'); % Read from Excel
15
16 % read Data from CSV
17 filename_density_L = 'ourflightcondation'; % Path to your CSV file
18 aircraft_data = readmatrix(filename_density_L, 'Range', 'B2:B61'); % Read from
CSV
19
20 % Time vector parameters
21 dt = aircraft_data(1);
22 tfinal = aircraft_data(2);
23 t0 = aircraft_data(3);
24
25
26 % Initial conditions for states
27 s0 = aircraft_data(4:15);
28 sdot0 = zeros(12,1); % Initial derivative of states
29 Vto = sqrt(s0(1)^2 + s0(2)^2 + s0(3)^2); % Compute initial total velocity (Vto)
30 initialstatemodified=[s0(1:3);0;s0(4:6)];
31 % Control actions values
32 dc = [ aircraft_data(57:59) * pi/180 ; aircraft_data(60) ]; % Control inputs in
radians
33
34 % Gravity, mass, and inertia values from aircraft data
35
36 m = aircraft_data(51);
37 g = aircraft_data(52);
38 Ixx = aircraft_data(53);
39 Iyy = aircraft_data(54);
40 Izz = aircraft_data(55);
41 Ixz = aircraft_data(56);
42 Ixy = 0; Iyz = 0;
43
44 % Inertia matrix and inverse inertia matrix
45
46 I = [Ixx, -Ixy, -Ixz; -Ixy, Iyy, -Iyz; -Ixz, -Iyz, Izz];
47 invI = inv(I);

```

```

48
49 D2R=pi/180;
50 R2D=180/pi;
51
52 %Initial velocities and rates
53 u_0 = s0(1);
54 v_0 = s0(2);
55 w_0 = s0(3);
56 p_0 = s0(4);
57 q_0 = s0(5);
58 r_0 = s0(6);
59 phi_0 = s0(7);
60 theta_0 = s0(8);
61 psi_0 = s0(9);
62 x_0 = s0(10);
63 y_0 = s0(11);
64 z_0 = s0(12);
65 wdot_0 = 0;
66 wdot = 0;
67 mass = m;
68
69 % Stability derivatives for longitudinal motion
70 SD_Long = aircraft_data(21:36);
71 SD_Long_final = SD_Long;
72 templong = num2cell(SD_Long);
73 [Xu,Zu,Mu,Xw,Zw,Mw,Zwd,Zq,Mwd,Mq,Xde,Zde,Mde,Xth,Zdth,Mdth] = deal(templong{:});
74 clear templong;
75
76
77 % Stability derivatives for lateral motion
78 SD_Lat_dash = aircraft_data(37:50);
79 SD_Lat = LateralFunc(SD_Lat_dash, Ixz, Izz, Ixx, Vto);
80 SD_Lat_final = SD_Lat;
81 templatrel = num2cell(SD_Lat_dash);
82 [Yv,Yb,Lb,Nb,Lp,Np,Lr,Nr,Yda,Ydr,Lda,Nda,Ldr,Ndr] = deal(templatrel{:});
83 clear templatrel;
84
85 Lv=Lb/Vto;
86 Nv=Nb/Vto;
87 Yp=0;
88 Ydr=Ydr*Vto;
89
90 servo= tf(10,[1 10]);
91 integrator=tf(1,[1 0]);
92 differentiator=tf([1 0],1);
93 engine_timelag=tf(0.1,[1 0 1]);
94
95
96 %% Full Longitudinal System
97
98 % Define constants
99 theta_0 = s0(8); wo = s0(3); u_0 = s0(1); wdot=0;
100 long0=[u_0;w_0;q_0;theta_0];
101
102
103 A_longitudinal = [Xu, Xw,-w_0, -g*cos(theta_0);
104                         Zu/(1-Zwd), Zw/(1-Zwd), (Zq + u_0)/(1-Zwd), -g*sin(theta_0)/(1-
105                         Zwd);
106                         Mu + (Zu * Mwd) / (1 - Zwd), Mw + (Zw * Mwd) / (1 - Zwd), Mq +
107                         ((Zq + u_0) * Mwd) / (1 - Zwd), - (g * Mwd * sin(theta_0)) / (1 - Zwd);
108                         0, 0, 1, 0];
109 B_longitudinal = [Xde, Xth;
110                         Zde/(1-Zwd), Zdth/(1-Zwd);
111                         Mde + Mwd*Zde/(1-Zwd), Mdth + Mwd*Zdth/(1-Zwd);
112                         0, 0];
113
114 C_longitudinal = eye(4); % Observing all states
115 D_longitudinal = zeros(4, 2); % No direct feedthrough
116 sys_longitudinal = ss(A_longitudinal, B_longitudinal, C_longitudinal ,
117                         D_longitudinal );
118 tf_full_longitudinal = tf(sys_longitudinal);

```

```

116
117
118 % Transfer function from elevator deflection (De) to each state output
119 De_u = minreal(tf_full_longitudinal(1,1)); % u state
120 De_w = minreal(tf_full_longitudinal(2,1)); % w state
121 De_q = minreal(tf_full_longitudinal(3,1)); % q state
122 De_theta = minreal(tf_full_longitudinal(4,1)); % theta state
123 De_Wd=De_w*diffrentiator;
124 De_az=De_Wd-u_0*De_q;
125 Theta_az=De_az/De_theta;
126 De_alpha=De_w/u_0;
127 De_gamma=De_theta-De_alpha;
128
129 % Transfer function from throttle (Th) to each state output
130 Th_u = minreal(tf_full_longitudinal(1,2)); % u state
131 Th_w = minreal(tf_full_longitudinal(2,2)); % w state
132 Th_q = minreal(tf_full_longitudinal(3,2)); % q state
133 Th_theta = minreal(tf_full_longitudinal(4,2)); % theta state
134 u_dT=tf_full_longitudinal(1,2);
135
136
137 %pitch control
138
139 ol_theta_thetacomm=-servo*De_theta;
140
141 % Velocity Control
142 OL_u_ucom=-servo*engine_timelag*u_dT;

```

9.1.9 MATLAB Code for Autopilot Lateral Control

```

1 % Main Script: Airplane Nonlinear Simulator with RBD Solver
2
3 % Clear workspace
4 clc;
5 close all;
6 global m
7 global I
8 global F M
9 global g
10 %% Load Aircraft Data
11 %read from Excel File
12 % filename_density_L = 'ourflightcondation'; % Path to your excel sheet
13 % aircraft_data = xlsread(filename_density_L, 'B2:B61'); % Read from Excel
14
15 % read Data from CSV
16 filename_density_L = 'ourflightcondation'; % Path to your CSV file
17 aircraft_data = readmatrix(filename_density_L, 'Range', 'B2:B61'); % Read from
    CSV
18
19 % Time vector parameters
20 dt = aircraft_data(1);
21 tfinal = aircraft_data(2);
22 t0 = aircraft_data(3);
23
24
25 % Initial conditions for states
26 s0 = aircraft_data(4:15);
27 sdot0 = zeros(12,1); % Initial derivative of states
28 Vto = sqrt(s0(1)^2 + s0(2)^2 + s0(3)^2); % Compute initial total velocity (Vto)
29 initialstatemodified=[s0(1:3);0;s0(4:6)];
30 % Control actions values
31 dc = [ aircraft_data(57:59) * pi/180 ; aircraft_data(60) ]; % Control inputs in
    radians
32
33 % Gravity, mass, and inertia values from aircraft data
34
35 m = aircraft_data(51);
36 g = aircraft_data(52);
37 Ixx = aircraft_data(53);
38 Iyy = aircraft_data(54);
39 Izz = aircraft_data(55);

```

```

40 Ixx = aircraft_data(56);
41 Ixy = 0; Iyz = 0;
42
43 % Inertia matrix and inverse inertia matrix
44
45 I = [Ixx, -Ixy, -Ixz; -Ixy, Iyy, -Iyz; -Ixz, -Iyz, Izz];
46 invI = inv(I);
47
48 D2R=pi/180;
49 R2D=180/pi;
50
51 %Initial velocities and rates
52 u_0 = s0(1);
53 v_0 = s0(2);
54 w_0 = s0(3);
55 p_0 = s0(4);
56 q_0 = s0(5);
57 r_0 = s0(6);
58 phi_0 = s0(7);
59 theta_0 = s0(8);
60 psi_0 = s0(9);
61 x_0 = s0(10);
62 y_0 = s0(11);
63 z_0 = s0(12);
64 wdot_0 = 0;
65 wdot = 0;
66 mass = m;
67
68 % Stability derivatives for longitudinal motion
69 SD_Long = aircraft_data(21:36);
70 SD_Long_final = SD_Long;
71 templong = num2cell(SD_Long);
72 [Xu,Zu,Mu,Xw,Zw,Mw,Zwd,Zq,Mwd,Mq,Xde,Zde,Mde,Xth,Zdth,Mdth] = deal(templong{:});
73 clear templong;
74
75
76 % Stability derivatives for lateral motion
77 SD_Lat_dash = aircraft_data(37:50);
78 templatrel = num2cell(SD_Lat_dash);
79 [Yv,Yb,Lb,Nb,Lp,Np,Lr,Nr,Yda,Ydr,Lda,Nda,Ldr,Ndr] = deal(templatrel{:});
80 clear templatrel;
81
82 Lv=Lb/Vto;
83 Nv=Nb/Vto;
84 Yp=0;
85 Yr=0;
86 Ydr=Ydr*Vto;
87
88 servo= tf(10,[1 10]);
89 integrator=tf(1,[1 0]);
90 differentiator=tf([1 0],1);
91 engine_timelag=tf(0.1,[1 0 1]);
92
93
94 %% Full Longitudinal System
95
96 % Define constants
97 theta_0 = s0(8); wo = s0(3); u_0 = s0(1); wdot=0;
98
99
100 A_longitudinal = [Xu, Xw,-w_0, -g*cos(theta_0);
101                                     Zu/(1-Zwd), Zw/(1-Zwd), (Zq + u_0)/(1-Zwd), -g*sin(theta_0)/(1-
102                                     Zwd);
103                                     Mu + (Zu * Mwd) / (1 - Zwd), Mw + (Zw * Mwd) / (1 - Zwd), Mq +
104                                     ((Zq + u_0) * Mwd) / (1 - Zwd), - (g * Mwd * sin(theta_0)) / (1 - Zwd);
105                                     0, 0, 1, 0];
106 B_longitudinal = [Xde, Xth;
107                                     Zde/(1-Zwd), Zdth/(1-Zwd);
108                                     Mde + Mwd*Zde/(1-Zwd), Mdth + Mwd*Zdth/(1-Zwd);
109                                     0, 0];

```

```

109 C_longitudinal = eye(4); % Observing all states
110 D_longitudinal = zeros(4, 2); % No direct feedthrough
111 sys_longitudinal = ss(A_longitudinal, B_longitudinal, C_longitudinal, ,
112     D_longitudinal );
113 tf_full_longitudinal = tf(sys_longitudinal);
114
115 % Transfer function from elevator deflection (De) to each state output
116 De_u = minreal(tf_full_longitudinal(1,1)); % u state
117 De_w = minreal(tf_full_longitudinal(2,1)); % w state
118 De_q = minreal(tf_full_longitudinal(3,1)); % q state
119 De_theta = minreal(tf_full_longitudinal(4,1)); % theta state
120 De_Wd=De_w*diffrentiator;
121 De_az=De_Wd-u_0*De_q;
122 Theta_az=De_az/De_theta;
123 De_alpha=De_w/u_0;
124 De_gamma=De_theta-De_alpha;
125
126 % Transfer function from throttle (Th) to each state output
127 Th_u = minreal(tf_full_longitudinal(1,2)); % u state
128 Th_w = minreal(tf_full_longitudinal(2,2)); % w state
129 Th_q = minreal(tf_full_longitudinal(3,2)); % q state
130 Th_theta = minreal(tf_full_longitudinal(4,2)); % theta state
131 u_dT=tf_full_longitudinal(1,2);
132
133
134 %pitch control
135
136 ol_theta_thetacomm=-servo*De_theta;
137
138 % Velocity Control
139 OL_u_ucom=-servo*engine_timelag*u_dT;
140
141 %% Full Lateral Mode System
142 x0_lateral = [v_0; p_0; r_0; phi_0; psi_0];
143
144
145 A_lateral = [Yv, Yp+wo, Yr-u_0, g*cos(theta_0), 0;
146     Lv, Lp, Lr, 0, 0;
147     Nv, Np, Nr, 0, 0;
148     0, 1, tan(theta_0), 0, 0;
149     0, 0, 1/cos(theta_0), 0, 0];
150
151 B_lateral = [Yda, Ydr;
152     Lda, Ldr;
153     Nda, Ndr;
154     0, 0;
155     0, 0];
156
157 C_lateral = eye(5); % Observing all states
158 D_lateral = zeros(5, 2); % No direct feedthrough
159
160 % Create the state-space model for the lateral dynamics
161 sys_lateral = ss(A_lateral, B_lateral, C_lateral, D_lateral);
162 tf_full_lateral = tf(sys_lateral);
163
164 v_da=tf_full_lateral(1,1);
165 p_da=tf_full_lateral(2,1);
166 r_da=tf_full_lateral(3,1);
167 phi_da=tf_full_lateral(4,1);
168 psi_da=tf_full_lateral(5,1);
169 beta_da=v_da/u_0;
170
171
172
173 v_dr=tf_full_lateral(1,2);
174 p_dr=tf_full_lateral(2,2);
175 r_dr=tf_full_lateral(3,2);
176 phi_dr=tf_full_lateral(4,2);
177 psi_dr=tf_full_lateral(5,2);
178 beta_dr=v_da/u_0;

```

```

179
180 ol_r_rcomm=servo*r_dr;
181 load('Yaw_Damper.mat')
182
183 Lat_YawDamper_ss_series=feedback(series(append(1,servo),sys_lateral,[1 2],[1 2]),HPF_YawDamper,2,3,1);
184 Lat_YawDamper_tf_series=tf(Lat_YawDamper_ss_series);
185 phi_da_AfterYawDamper=Lat_YawDamper_tf_series(4,1);
186 ol_phi_phicomm=minreal(servo*phi_da_AfterYawDamper);

```

9.1.10 MATLAB Code for Simulation to Complete Linear and Non-Linear model

```

1 % Main Script
2 clc;
3 %clear all;
4 %close all;
5 global m
6 global I
7 global F M
8 global g
9
10 %% Load Aircraft Data from CSV and assigning them to variables
11 filename_density_L = 'ourflightcondation.csv';
12 aircraft_data = readmatrix(filename_density_L, 'Range', 'B2:B61');
13
14 % Time vector parameters
15 dt = aircraft_data(1);
16 tfinal = aircraft_data(2);
17 time_V = (0:dt:tfinal)';
18
19 % Initial conditions for states
20 s0 = aircraft_data(4:15);
21 sdot0 = zeros(12,1); % Initial derivative of states
22 Vto = sqrt(s0(1)^2 + s0(2)^2 + s0(3)^2); % Compute initial total velocity (Vto)
23 initialstatemodified=[s0(1:3);0;s0(4:6)];
24
25 % Control actions values
26 dc = [ aircraft_data(57:59) * pi/180 ; aircraft_data(60) ]; % Control inputs in radians
27
28 % Gravity, mass, and inertia values from aircraft data
29 m = aircraft_data(51);
30 g = aircraft_data(52);
31 Ixx = aircraft_data(53);
32 Iyy = aircraft_data(54);
33 Izz = aircraft_data(55);
34 Ixz = aircraft_data(56);
35 Ixy = 0; Iyz = 0;
36
37 % Inertia matrix and inverse inertia matrix
38 I = [Ixx, -Ixy, -Ixz; -Ixy, Iyy, -Iyz; -Ixz, -Iyz, Izz];
39 invI = inv(I);
40
41 % Angle rad to deg and vice versa
42 D2R=pi/180;
43 R2D=180/pi;
44
45 % Stability derivatives for longitudinal motion
46 SD_Long = aircraft_data(21:36);
47 SD_Long_final = SD_Long;
48 templong = num2cell(SD_Long);
49 [Xu,Zu,Mu,Xw,Zw,Mw,Zwd,Zq,Mwd,Mq,Xde,Zde,Mde,Xth,Zdth,Mdth] = deal(templong{:});
50 clear templong;
51
52 % Stability derivatives for lateral motion
53 SD_Lat_dash = aircraft_data(37:50);
54 SD_Lat = LateralFunc( SD_Lat_dash, Ixz, Izz, Ixx, Vto);
55 SD_Lat_final = SD_Lat;
56 templatrel = num2cell(SD_Lat);
57 [Yv,Yb,Lb,Nb,Lp,Np,Lr,Nr,Yda,Ydr,Lda,Nda,Ldr,Ndr] = deal(templatrel{:});
58 clear templatrel;

```

```

59 Lv=Lb/Vto;
60 Nv=Nb/Vto;
61 Yp=0; % not found in Nasa data
62 Yr=0; % not found in nasa data
64
65 % Initial gravity force in body frame
66 mg0 = m * g * [sin(s0(8)); -cos(s0(8)) * sin(s0(7)); -cos(s0(8)) * cos(s0(7))];
67 initial_F_M = m * g * [sin(s0(8)); -cos(s0(8)) * sin(s0(7)); -cos(s0(8)) * cos(s0(7)); 0; 0; 0]; % Simulink Input
68 M_0 = [0; 0; 0];
69
70 %Initial velocities and rates
71 u_0 = s0(1);
72 v_0 = s0(2);
73 w_0 = s0(3);
74 p_0 = s0(4);
75 q_0 = s0(5);
76 r_0 = s0(6);
77 phi_0 = s0(7);
78 theta_0 = s0(8);
79 psi_0 = s0(9);
80 x_0 = s0(10);
81 y_0 = s0(11);
82 z_0 = s0(12);
83 wdot_0 = 0;
84 wdot = 0;
85 mass = m;
86
87 %% Matlab Nonlinear Model
88 for i = 1:16
89 SD(i) = SD_Long_final(i);
90 end
91 for j = 1:14
92 SD(j+16) = SD_Lat_final(j); % All stability derivatives in one array
93 end
94
95 n = 1000;
96 velocity_0=s0(1:3);
97 angular_v0=s0(4:6);
98 angles_0=s0(7:9);
99 position_0=s0(10:12);
100 Initial_state=[velocity_0;angular_v0;angles_0;position_0];
101
102 % solve and get the state and data
103 [F,M]=F_M_Cal(SD,s0,Vto,dc,Initial_state,0);
104 [t, states] = RK4_solver(@getstates,Initial_state , 0, tfinal,n, SD,Vto, dc);
105
106 %% Simulink Nonlinear Model
107
108 State_Matrix = [ Xu 0 Xw 0 0 0 0;
109 0 Yv 0 Yp 0 Yr 0;
110 Zu 0 Zw 0 Zq Lr Zwd;
111 0 Lv 0 Lp 0 Lr 0;
112 Mu 0 Mw 0 Mq 0 Mwd;
113 0 Nv 0 Np 0 Nr 0];
114
115 Control_Matrix = [0 Xde Xth 0
116 Yda 0 0 Ydr
117 0 Zde Zdth 0
118 Lda 0 0 Ldr
119 0 Mde Mdth 0
120 Nda 0 0 Ndr];
121
122 % intial struc state
123 so_struct.x = s0(10);
124 so_struct.y = s0(11);
125 so_struct.H = -1*s0(12);
126 so_struct.phi = s0(7);
127 so_struct.theta = s0(8);
128 so_struct.psi = s0(9);

```

```

129 so_struct.p = s0(4);
130 so_struct.q = s0(5);
131 so_struct.r = s0(6);
132 so_struct.u = s0(1);
133 so_struct.v = s0(2);
134 so_struct.w = s0(3);
135 so_struct.alpha = s0(8);
136 so_struct.Beta = 0;
137 so_struct.V_total = Vto;
138 so_struct.W_dot = 0;
139 so_struct.gamma=0;
140
141 % % run the model and get data
142 % modelName = 'Final_Task3_Simulink';
143 % load_system(modelName);
144 % set_param(modelName, 'StartTime', '0', 'StopTime', num2str(tfinal));
145 % simOut = sim(modelName, 'ReturnWorkspaceOutputs', 'on');
146 %
147 % t2 = simOut.tout;
148 % y2 = simOut.simout.Data;
149 % y2 = y2';
150
151 %% Linear Model
152 x0=[u_0;w_0;q_0;theta_0]; %input
153 %% Full Longitudinal System
154 % Define constants
155 theta_0 = s0(8); wo = s0(3); u_0 = s0(1); wdot=0;
156
157 % Define constants and matrices for the longitudinal state-space model
158 u = [dc(3)* ones(size(t)); (dc(4)*ones(size(t)))];
159
160 A_longitudinal = [Xu, Xw,-w_0, -g*cos(theta_0);
161                     Zu/(1-Zwd), Zw/(1-Zwd), (Zq + u_0)/(1-Zwd), -g*sin(theta_0)/(1-
162                     Zwd);
163                     Mu + (Zu * Mwd) / (1 - Zwd), Mw + (Zw * Mwd) / (1 - Zwd), Mq +
164                     ((Zq + u_0) * Mwd) / (1 - Zwd), - (g * Mwd * sin(theta_0)) / (1 - Zwd);
165                     0, 0, 1, 0];
166 B_longitudinal = [Xde, Xth;
167                     Zde/(1-Zwd), Zdth/(1-Zwd);
168                     Mde + Mwd*Zde/(1-Zwd), Mdth + Mwd*Zdth/(1-Zwd);
169                     0, 0];
170 C_longitudinal = eye(4); % Observing all states
171 D_longitudinal = zeros(4, 2); % No direct feedthrough
172 sys_longitudinal = ss(A_longitudinal, B_longitudinal, C_longitudinal,
173                         D_longitudinal );
174 tf_full_longitudinal = tf(sys_longitudinal);
175 [y_full, t, x] = lsim(sys_longitudinal,u, t);
176
177 % Transfer function from elevator deflection (De) to each state output
178 tf_full_longitudinal_De_with_stateu = minreal(tf_full_longitudinal(1,1)); % u
179             state
180 tf_full_longitudinal_De_with_statew = minreal(tf_full_longitudinal(2,1)); % w
181             state
182 tf_full_longitudinal_De_with_stateq = minreal(tf_full_longitudinal(3,1)); % q
183             state
184 tf_full_longitudinal_De_with_state_theta = minreal(tf_full_longitudinal(4,1)); % theta
185             state
186
187 % Transfer function from throttle (Th) to each state output
188 tf_full_longitudinal_Th_with_stateu = minreal(tf_full_longitudinal(1,2)); % u
189             state
190 tf_full_longitudinal_Th_with_statew = minreal(tf_full_longitudinal(2,2)); % w
191             state
192 tf_full_longitudinal_Th_with_stateq = minreal(tf_full_longitudinal(3,2)); % q
193             state
194 tf_full_longitudinal_Th_with_state_theta = minreal(tf_full_longitudinal(4,2)); % theta
195             state
196
197 %% Long Mode For Longitudinal
198 A_longitudinal_long = [Xu, -g*cos(theta_0); -Zu/(Zq+u_0), g*sin(theta_0)/(Zq+u_0)
199 ];

```

```

188 B_longitudinal_long = [Xde, Xth; -Zde/(Zq+u_0), -Zdth/(Zq+u_0)];
189
190 % Assuming the output directly maps to the state (no C and D matrices provided,
191 % use identity matrix for direct mapping)
192 C_longitudinal_long = eye(2); % Direct mapping of state to output
193 D_longitudinal_long = zeros(2, 2); % No direct feedthrough
194
195 % Define state-space model for the long-period longitudinal system
196 sys_longitudinal_long = ss(A_longitudinal_long, B_longitudinal_long,
197 C_longitudinal_long, D_longitudinal_long);
198 tf_long_period = tf(sys_longitudinal_long);
199
200 % Run the simulation for the long-period mode with external input 'u'
201 [y_long, t, x] = lsim(sys_longitudinal_long, u, t);
202
203 % Transfer function from elevator deflection (De) to each state output
204 tf_long_period_De_with_state_u = minreal(tf_long_period(1,1)); % u state
205 tf_long_period_De_with_state_theta = minreal(tf_long_period(2,1)); % theta state
206
207 % Transfer function from throttle (Th) to each state output
208 tf_long_period_Th_with_state_u = minreal(tf_long_period(1,2)); % u state
209 tf_long_period_Th_with_state_theta = minreal(tf_long_period(2,2)); % theta state
210
211 %% Short Mode For Longitudinal
212 A_longitudinal_short = [
213 Zw / (1 - Zwd), (Zq + u_0) / (1 - Zwd);
214 Mw + (Mwd * (Zw / (1 - Zwd))), Mq + (Mwd * ((Zq + u_0) / (1 - Zwd)))
];
215 B_longitudinal_short = [
216 Zde / (1 - Zwd), Zdth / (1 - Zwd);
217 Mde + (Mwd * Zde / (1 - Zwd)), Mdth + (Mwd*Zdth / (1 - Zwd))
];
218 C_longitudinal_short = eye(2); % Direct mapping of state to output
219 D_longitudinal_short = zeros(2, 2); % No direct feedthrough
220
221 % Define state-space model for the short-period longitudinal system
222 sys_longitudinal_short = ss(A_longitudinal_short, B_longitudinal_short,
223 C_longitudinal_short, D_longitudinal_short);
224 tf_short_period = tf(sys_longitudinal_short);
225
226 % Initial state vector for short-period mode ()
227 x0_short = [w_0; q_0]; % Corrected to match the 2-dimensional system
228
229 % Run the simulation for the short-period mode
230 [y_short, t, x] = lsim(sys_longitudinal_short, u, t);
231
232 % Extract and simplify transfer functions with corresponding labels
233 % Transfer function from elevator deflection (De) to each state output
234 tf_short_period_De_with_state_w = minreal(tf_short_period(1,1)); % w state
235 tf_short_period_De_with_state_q = minreal(tf_short_period(2,1)); % q state
236
237 % Transfer function from throttle (Th) to each state output
238 tf_short_period_Th_with_state_w = minreal(tf_short_period(1,2)); % w state
239 tf_short_period_Th_with_state_q = minreal(tf_short_period(2,2)); % q state
240
241 %% Full Lateral Mode System
242 x0_lateral = [v_0; p_0; r_0; phi_0; psi_0];
243
244 A_lateral = [Yv, Yp+wo, Yr-u_0, g*cos(theta_0), 0;
245 Lv, Lp, Lr, 0, 0;
246 Nv, Np, Nr, 0, 0;
247 0, 1, tan(theta_0), 0, 0;
248 0, 0, 1/cos(theta_0), 0, 0];
249
250 B_lateral = [Yda, Ydr;
251 Lda, Ldr;
252 Nda, Ndr;
253 0, 0;
254 0, 0];

```

```

256 C_lateral = eye(5); % Observing all states
257 D_lateral = zeros(5, 2); % No direct feedthrough
258
259 u_lat = [dc(1)* ones(size(t)),1*ones(size(t))]';
260
261 % Create the state-space model for the lateral dynamics
262 sys_lateral = ss(A_lateral, B_lateral, C_lateral, D_lateral);
263 tf_full_lateral = tf(sys_lateral);
264
265 % Initial state vector for the lateral dynamics
266
267 % Run the simulation for the lateral dynamics with the specified input
268 [y_lateral, t, x_lateral] = lsim(sys_lateral, u_lat, t, x0_lateral);
269
270 % Transfer function from aileron deflection (Da) to each state output
271 tf_full_lateral_Da_with_state_v = minreal(tf_full_lateral(1,1));
272 tf_full_lateral_Da_with_state_p = minreal(tf_full_lateral(2,1));
273 tf_full_lateral_Da_with_state_r = minreal(tf_full_lateral(3,1));
274 tf_full_lateral_Da_with_state_phi = minreal(tf_full_lateral(4,1));
275 tf_full_lateral_Da_with_state_epsi = minreal(tf_full_lateral(5,1));
276
277 % Transfer function from rudder deflection (Dr) to each state output
278 tf_full_lateral_Dr_with_state_v = minreal(tf_full_lateral(1,2));
279 tf_full_lateral_Dr_with_state_p = minreal(tf_full_lateral(2,2));
280 tf_full_lateral_Dr_with_state_r = minreal(tf_full_lateral(3,2));
281 tf_full_lateral_Dr_with_state_phi = minreal(tf_full_lateral(4,2));
282 tf_full_lateral_Dr_with_state_epsi = minreal(tf_full_lateral(5,2));
283
284 %% 3-DOF Approximations for Spiral lateral Mode
285 A_lateral_3DOF_spiral = [Lp, Lr, 0;
286                           Np, Nr, 0;
287                           1, tan(theta_0), 0];
288 % B_lateral_3DOF_spiral = [Ldr;Ndr;0];
289 B_lateral_3DOF_spiral = [Lda, Ldr;
290                           Nda, Ndr;
291                           0, 0];
292
293 % Define the output matrix to observe all states (p, r, and v)
294 C_lateral_3DOF_spiral = eye(3); % Observing all three states
295 D_lateral_3DOF_spiral = zeros(3, 2); % No direct feedthrough from input to
296 % output
297
298 % Create the state-space model for the spiral mode approximation
299 sys_lateral_3DOF_spiral = ss(A_lateral_3DOF_spiral, B_lateral_3DOF_spiral,
300                               C_lateral_3DOF_spiral, D_lateral_3DOF_spiral);
301 tf_3DOF_spiral = tf(sys_lateral_3DOF_spiral);
302
303 % Initial state vector for the spiral mode with 3 DOF (initial conditions for p,
304 % r, and v)
305 x0_spiral_3DOF = [p_0; r_0; phi_0]; % Assuming zero initial conditions
306
307 % Run the simulation for the spiral mode with 3 DOF using the specified input
308 [y_spiral_3DOF, t, x_spiral_3DOF] = lsim(sys_lateral_3DOF_spiral, u_lat, t,
309                                              x0_spiral_3DOF);
310
311 % Transfer functions from rudder deflection (Dr) to each state output
312 tf_3DOF_spiral_Dr_with_state_p = minreal(tf_3DOF_spiral(1,1)); % Roll Rate (p)
313 tf_3DOF_spiral_Dr_with_state_r = minreal(tf_3DOF_spiral(2,1)); % Yaw Rate (r)
314 tf_3DOF_spiral_Dr_with_state_phi = minreal(tf_3DOF_spiral(3,1)); % Roll Angle (
315 % phi)
316
317 %% 3-DOF Approximations for Dutch roll lateral Mode
318 A_lateral_3DOF_dutch = [Yv, Yp+wo, Yr-u_0;
319                           Lv, Lp, 0;
320                           Nv, 0, Nr];
321 B_lateral_3DOF_dutch = [Yda, Ydr;
322                           Lda, Ldr;
323                           Nda, Ndr];
324
325 % Output matrix to observe all states (v, p, and r)
326 C_lateral_3DOF_dutch = eye(3); % Observing all three states
327 D_lateral_3DOF_dutch = zeros(3, 2); % No direct feedthrough from input to output

```

```

322 % Create the state-space model for the Dutch Roll mode approximation
323 sys_lateral_3DOF_dutch = ss(A_lateral_3DOF_dutch, B_lateral_3DOF_dutch,
324 C_lateral_3DOF_dutch, D_lateral_3DOF_dutch);
325 tf_3DOF_dutch = tf(sys_lateral_3DOF_dutch);
326
327 % Initial state vector for the Dutch Roll mode with 3 DOF (initial conditions for
328 % v, p, and r)
329 x0_dutch_3DOF = [v_0; p_0; r_0]; % Assuming zero initial conditions
330
331 % Run the simulation for the Dutch Roll mode with 3 DOF using the specified input
332 [y_dutch_3DOF, t, x_dutch_3DOF] = lsim(sys_lateral_3DOF_dutch, u_lat, t,
333 x0_dutch_3DOF);
334
335 % Transfer functions from aileron deflection (Da) to each state output
336 tf_3DOF_dutch_Da_with_state_v = minreal(tf_3DOF_dutch(1,1)); % Side velocity (v)
337 tf_3DOF_dutch_Da_with_state_p = minreal(tf_3DOF_dutch(2,1)); % Roll angle (phi)
338 tf_3DOF_dutch_Da_with_state_r = minreal(tf_3DOF_dutch(3,1)); % Yaw rate (r)
339
340 % Transfer functions from rudder deflection (Dr) to each state output
341 tf_3DOF_dutch_Dr_with_state_v = minreal(tf_3DOF_dutch(1,2));
342 tf_3DOF_dutch_Dr_with_state_p = minreal(tf_3DOF_dutch(2,2));
343 tf_3DOF_dutch_Dr_with_state_r = minreal(tf_3DOF_dutch(3,2));
344
345 %% 2-DOF Approximations for the Dutch roll lateral Mode
346 A_lateral_2DOF_dutch = [Yv, Yr-u_0;
347 % Nv, Nr];
348 B_lateral_2DOF_dutch = [Yda, Ydr;
349 % Nda, Ndr];
350
351 % Output matrix to observe both states (v and r)
352 C_lateral_2DOF_dutch = eye(2); % Observing both states
353 D_lateral_2DOF_dutch = zeros(2, 2); % No direct feedthrough from input to output
354
355 % Create the state-space model for the 2-DOF Dutch Roll mode
356 sys_lateral_2DOF_dutch = ss(A_lateral_2DOF_dutch, B_lateral_2DOF_dutch,
357 C_lateral_2DOF_dutch, D_lateral_2DOF_dutch);
358 tf_2DOF_dutch = tf(sys_lateral_2DOF_dutch);
359
360 % Initial state vector for the 2-DOF Dutch Roll mode (initial conditions for v
361 % and r)
362 x0_dutch_2DOF = [v_0;r_0]; % Assuming zero initial conditions
363
364 % Run the simulation for the Dutch Roll mode with 2 DOF using the specified input
365 [y_dutch_2DOF, t, x_dutch_2DOF] = lsim(sys_lateral_2DOF_dutch, u_lat, t,
366 x0_dutch_2DOF);
367
368 % Transfer functions from aileron deflection (Da) to each state output
369 tf_2DOF_dutch_Da_with_state_v = minreal(tf_2DOF_dutch(1,1)); % Side velocity (v)
370 tf_2DOF_dutch_Da_with_state_r = minreal(tf_2DOF_dutch(2,1)); % Yaw rate (r)
371
372 % Transfer functions from rudder deflection (Dr) to each state output
373 tf_2DOF_dutch_Dr_with_state_v = minreal(tf_2DOF_dutch(1,2));
374 tf_2DOF_dutch_Dr_with_state_r = minreal(tf_2DOF_dutch(2,2));
375
376 %% 1-DOF Approximations for the Roll lateral Mode
377 A_lateral_1DOF = Lp; % Only the roll damping term Lp
378 B_lateral_1DOF = Lda; % Aileron control input affecting roll rate
379 C_lateral_1DOF = 1; % Observe roll rate (p) directly
380 D_lateral_1DOF = 0; % No direct feedthrough
381
382 sys_lateral_1DOF = ss(A_lateral_1DOF, B_lateral_1DOF, C_lateral_1DOF,
383 D_lateral_1DOF);
384 % Calculate the transfer function from aileron deflection (Da) to roll rate (p)
385 tf_1DOF_roll_Da_with_state_p = minreal(tf(sys_lateral_1DOF));
386
387 % Define the input signal (u), representing aileron deflection
388 u_1dof = ones(size(t)); % Constant aileron deflection for demonstration
389
390 % Initial state vector for roll rate
391 x0_roll_1DOF = p_0; % Assuming zero initial roll rate

```

```

386 % Run the simulation for the roll mode with the specified input
387 [y_roll_1DOF, t, x_roll_1DOF] = lsim(sys_lateral_1DOF, u_1dof, t, x0_roll_1DOF);
389
390
391 %% Longitudinal Controller Design
392
393 % Transfer function from elevator deflection (De) to each state output
394 De_u = minreal(tf_full_longitudinal(1,1)); % u state
395 De_w = minreal(tf_full_longitudinal(2,1)); % w state
396 De_q = minreal(tf_full_longitudinal(3,1)); % q state
397 De_theta = minreal(tf_full_longitudinal(4,1)); % theta state
398
399 % Transfer function from throttle (Th) to each state output
400 Th_u = minreal(tf_full_longitudinal(1,2)); % u state
401 Th_w = minreal(tf_full_longitudinal(2,2)); % w state
402 Th_q = minreal(tf_full_longitudinal(3,2)); % q state
403 Th_theta = minreal(tf_full_longitudinal(4,2)); % theta state
404 u_dT= tf_full_longitudinal(1,2);
405
406 % Transfer function used in building the controller
407 servo= tf(10,[1 10]);
408 integrator=tf(1,[1 0]);
409 diffrentiator=tf([1 0],1);
410 engine_timelag=tf(0.1,[1 0 1]);
411
412 De_Wd=De_w*diffrentiator;
413 De_az=De_Wd-u_0*De_q;
414 Theta_az=De_az/De_theta;
415 De_alpha=De_w/u_0;
416 De_gamma=De_theta-De_alpha;
417
418 %pitch control
419 ol_theta_thetacomm=-servo*De_theta;
420
421 % Velocity Control
422 OL_u_ucom=servo*engine_timelag*u_dT;
423
424 load('Velocity_Controller_tf.mat')
425 load('eltaw2am_c.mat')
426 load('Pitch_Design2.mat')
427 load('Altitude_Design.mat')
428
429 %% Lateral Controller Design
430
431 % Transfer function from aileron deflection
432 v_da=minreal(tf_full_lateral(1,1));
433 p_da=minreal(tf_full_lateral(2,1));
434 r_da=minreal(tf_full_lateral(3,1));
435 phi_da=minreal(tf_full_lateral(4,1));
436 psi_da=minreal(tf_full_lateral(5,1));
437 beta_da=v_da/u_0;
438
439 % Transfer function from rudder deflection
440 v_dr=minreal(tf_full_lateral(1,2));
441 p_dr=minreal(tf_full_lateral(2,2));
442 r_dr=minreal(tf_full_lateral(3,2));
443 phi_dr=minreal(tf_full_lateral(4,2));
444 psi_dr=minreal(tf_full_lateral(5,2));
445 beta_dr=v_da/u_0;
446
447 % yaw controller
448 ol_r_rcomm=servo*r_dr;
449 load('Yaw_Damper.mat')
450
451 Lat_YawDamper_ss_series=feedback(series(append(1,servo),sys_lateral,[1 2],[1 2]), ...
    HPF_YawDamper,2,3,1);
452 Lat_YawDamper_tf_series=tf(Lat_YawDamper_ss_series);
453 phi_da_AfterYawDamper=Lat_YawDamper_tf_series(4,1);
454 % phi controller
455 ol_phi_phicomm=minreal(servo*phi_da_AfterYawDamper);

```

```

456
457
458 % %% Ploting
459 % %% MATLAB Plotting
460 % rad_to_deg = 180 / pi; % Conversion from radians to degrees
461 %
462 % % Plot results (e.g., velocities, angles, positions)
463 % figure;
464 % sgttitle('Matlab Code Plots');
465 %
466 % % Plot forward, side, and vertical velocities (u, v, w)
467 % subplot(4,3,1);
468 % plot(t, states(1,:), 'b'); % u (forward velocity)
469 % title('Forward Velocity (u)');
470 % xlabel('Time (s)');
471 % ylabel('Velocity (ft/s)');
472 %
473 % % subplot(4,3,2);
474 % % plot(t2, y2(2,:), 'r'); % v (side velocity)
475 % % title('Side Velocity (v)');
476 % % xlabel('Time (s)');
477 % % ylabel('Velocity (ft/s)');
478 %
479 % % subplot(4,3,3);
480 % % plot(t2, y2(3,:), 'g'); % w (vertical velocity)
481 % % title('Vertical Velocity (w)');
482 % % xlabel('Time (s)');
483 % % ylabel('Velocity (ft/s)');
484 %
485 % subplot(4,3,2);
486 % plot(t, asin(states(2,:)/Vto)*rad_to_deg, 'r'); % bita (side velocity)
487 % title('bita');
488 % xlabel('Time (s)');
489 % ylabel('Velocity (ft/s)');
490 %
491 % subplot(4,3,3);
492 % plot(t, atan(states(3,:)./states(1,:))*rad_to_deg, 'g'); % alpha (vertical
        velocity)
493 % title('Alpa');
494 % xlabel('Time (s)');
495 % ylabel('Velocity (ft/s)');
496 %
497 % % Angular velocities (p, q, r)
498 %
499 % subplot(4,3,4);
500 % plot(t, states(4,:), 'b'); % p (roll rate)
501 % title('Roll Rate (p)');
502 % xlabel('Time (s)');
503 % ylabel('Angular Velocity (rad/s)');
504 %
505 % subplot(4,3,5);
506 % plot(t, states(5,:), 'r'); % q (pitch rate)
507 % title('Pitch Rate (q)');
508 % xlabel('Time (s)');
509 % ylabel('Angular Velocity (rad/s)');
510 %
511 % subplot(4,3,6);
512 % plot(t, states(6,:), 'g'); % r (yaw rate)
513 % title('Yaw Rate (r)');
514 % xlabel('Time (s)');
515 % ylabel('Angular Velocity (rad/s)');
516 %
517 % % Euler angles (phi, theta, psi) in degrees
518 %
519 % subplot(4,3,7);
520 % plot(t, states(7,:) * rad_to_deg, 'b'); % phi (roll angle in degrees)
521 % title('Roll Angle (phi) in degrees');
522 % xlabel('Time (s)');
523 % ylabel('Angle (deg)');
524 %
525 % subplot(4,3,8);

```

```

526 % plot(t, states(8,:)* rad_to_deg, 'r'); % theta (pitch angle in degrees)
527 % title('Pitch Angle (theta) in degrees');
528 % xlabel('Time (s)');
529 % ylabel('Angle (deg)');
530 %
531 % subplot(4,3,9);
532 % plot(t, states(9,:)* rad_to_deg, 'g'); % psi (yaw angle in degrees)
533 % title('Yaw Angle (psi) in degrees');
534 % xlabel('Time (s)');
535 % ylabel('Angle (deg)');
536 %
537 % % Position (x, y, z) in feet
538 %
539 % subplot(4,3,10);
540 % plot(t, states(10,:), 'b');
541 % title('Position X (ft)');
542 % xlabel('Time (s)');
543 % ylabel('Position (ft)');
544 %
545 % subplot(4,3,11);
546 % plot(t, states(11,:), 'r');
547 % title('Position Y (ft)');
548 % xlabel('Time (s)');
549 % ylabel('Position (ft)');
550 %
551 % subplot(4,3,12);
552 % plot(t, round(states(12,:),3), 'g');
553 % title('Position Z (ft)');
554 % xlabel('Time (s)');
555 % ylabel('Position (ft)');
556 %
557 %
558 % % Trajectory (x vs y vs z in feet)
559 % figure;
560 % plot3(states(10,:), states(11,:), round(states(12,:),3), 'b'); % 3D
      trajectory plot
561 % title('Matlab Code Trajectory (ft)', 'FontWeight', 'bold', 'FontSize', 14);
562 % xlabel('X (ft)', 'FontWeight', 'bold', 'FontSize', 12);
563 % ylabel('Y (ft)', 'FontWeight', 'bold', 'FontSize', 12);
564 % zlabel('Z (ft)', 'FontWeight', 'bold', 'FontSize', 12);
565 % grid on;
566 %
567 %
568 % %% Simulink Plot
569 % % Plot results (e.g., velocities, angles, positions)
570 % figure;
571 % sgtitle('Simulink Code Plots');
572 % % Plot forward, side, and vertical velocities (u, v, w)
573 % subplot(4,3,1);
574 % plot(t2, y2(1,:), 'b'); % u (forward velocity)
575 % title('Forward Velocity (u)', 'FontWeight', 'bold', 'FontSize', 12);
576 % xlabel('Time (s)', 'FontWeight', 'bold', 'FontSize', 10);
577 % ylabel('Velocity (ft/s)', 'FontWeight', 'bold', 'FontSize', 10);
578 %
579 % % subplot(4,3,2);
580 % % plot(t2, y2(2,:), 'r'); % v (side velocity)
581 % % title('Side Velocity (v)', 'FontWeight', 'bold', 'FontSize', 12);
582 % % xlabel('Time (s)', 'FontWeight', 'bold', 'FontSize', 10);
583 % % ylabel('Velocity (ft/s)', 'FontWeight', 'bold', 'FontSize', 10);
584 % %
585 % % subplot(4,3,3);
586 % % plot(t2, y2(3,:), 'g'); % w (vertical velocity)
587 % % title('Vertical Velocity (w)', 'FontWeight', 'bold', 'FontSize', 12);
588 % % xlabel('Time (s)', 'FontWeight', 'bold', 'FontSize', 10);
589 % % ylabel('Velocity (ft/s)', 'FontWeight', 'bold', 'FontSize', 10);
590 %
591 %
592 % % plots of alpha and beta
593 % subplot(4,3,2);
594 % plot(t2, y2(13,:)*rad_to_deg, 'r'); % v (side angle beta)
595 % title('Side angle (Beta)', 'FontWeight', 'bold', 'FontSize', 12);

```

```

596 % xlabel('Time (s)', 'FontWeight', 'bold', 'FontSize', 10);
597 % ylabel('Beta (deg)', 'FontWeight', 'bold', 'FontSize', 10);
598 %
599 % subplot(4,3,3);
600 % plot(t2, y2(14,:)*rad_to_deg, 'g'); % w (alpha )
601 % title('angle of attach (Alpha)', 'FontWeight', 'bold', 'FontSize', 12);
602 % xlabel('Time (s)', 'FontWeight', 'bold', 'FontSize', 10);
603 % ylabel('alpha (deg)', 'FontWeight', 'bold', 'FontSize', 10);
604 %
605 %
606 % % Angular velocities (p, q, r)
607 % subplot(4,3,4);
608 % plot(t2, y2(4,:)* rad_to_deg, 'b'); % p (roll rate)
609 % title('Roll Rate (p)', 'FontWeight', 'bold', 'FontSize', 12);
610 % xlabel('Time (s)', 'FontWeight', 'bold', 'FontSize', 10);
611 % ylabel('Angular Velocity (rad/s)', 'FontWeight', 'bold', 'FontSize', 10);
612 %
613 % subplot(4,3,5);
614 % plot(t2, y2(5,:)*rad_to_deg, 'r'); % q (pitch rate)
615 % title('Pitch Rate (q)', 'FontWeight', 'bold', 'FontSize', 12);
616 % xlabel('Time (s)', 'FontWeight', 'bold', 'FontSize', 10);
617 % ylabel('Angular Velocity (rad/s)', 'FontWeight', 'bold', 'FontSize', 10);
618 %
619 % subplot(4,3,6);
620 % plot(t2, y2(6,:)*rad_to_deg, 'g'); % r (yaw rate)
621 % title('Yaw Rate (r)', 'FontWeight', 'bold', 'FontSize', 12);
622 % xlabel('Time (s)', 'FontWeight', 'bold', 'FontSize', 10);
623 % ylabel('Angular Velocity (rad/s)', 'FontWeight', 'bold', 'FontSize', 10);
624 %
625 % % Euler angles (phi, theta, psi) in degrees
626 % subplot(4,3,7);
627 % plot(t2, y2(7,:)* rad_to_deg, 'b'); % phi (roll angle in degrees)
628 % title('Roll Angle (phi) in degrees', 'FontWeight', 'bold', 'FontSize', 12);
629 % xlabel('Time (s)', 'FontWeight', 'bold', 'FontSize', 10);
630 % ylabel('Angle (deg)', 'FontWeight', 'bold', 'FontSize', 10);
631 %
632 % subplot(4,3,8);
633 % plot(t2, y2(8,:)* rad_to_deg, 'r'); % theta (pitch angle in degrees)
634 % title('Pitch Angle (theta) in degrees', 'FontWeight', 'bold', 'FontSize', 12);
635 % xlabel('Time (s)', 'FontWeight', 'bold', 'FontSize', 10);
636 % ylabel('Angle (deg)', 'FontWeight', 'bold', 'FontSize', 10);
637 %
638 % subplot(4,3,9);
639 % plot(t2, unwrap(y2(9,:)) * rad_to_deg, 'g'); % psi (yaw angle in degrees)
640 % title('Yaw Angle (psi) in degrees', 'FontWeight', 'bold', 'FontSize', 12);
641 % xlabel('Time (s)', 'FontWeight', 'bold', 'FontSize', 10);
642 % ylabel('Angle (deg)', 'FontWeight', 'bold', 'FontSize', 10);
643 %
644 % % Position (x, y, z) in feet
645 % subplot(4,3,10);
646 % plot(t2, y2(10,:), 'b');
647 % title('Position X (ft)', 'FontWeight', 'bold', 'FontSize', 12);
648 % xlabel('Time (s)', 'FontWeight', 'bold', 'FontSize', 10);
649 % ylabel('Position (ft)', 'FontWeight', 'bold', 'FontSize', 10);
650 %
651 % subplot(4,3,11);
652 % plot(t2, y2(11,:), 'r');
653 % title('Position Y (ft)', 'FontWeight', 'bold', 'FontSize', 12);
654 % xlabel('Time (s)', 'FontWeight', 'bold', 'FontSize', 10);
655 % ylabel('Position (ft)', 'FontWeight', 'bold', 'FontSize', 10);
656 %
657 % subplot(4,3,12);
658 % plot(t2, round(y2(12,:)), 3, 'g');
659 % title('Position Z (ft)', 'FontWeight', 'bold', 'FontSize', 12);
660 % xlabel('Time (s)', 'FontWeight', 'bold', 'FontSize', 10);
661 % ylabel('Position (ft)', 'FontWeight', 'bold', 'FontSize', 10);
662 %
663 % % Trajectory (x vs y vs z in feet)
664 % figure;
665 % plot3(y2(10,:), y2(11,:), round(y2(12,:)), 3, 'b'); % 3D trajectory plot
666 % title('Simulink Code Trajectory (ft)', 'FontWeight', 'bold', 'FontSize', 14);

```

```

667 % xlabel('X (ft)', 'FontWeight', 'bold', 'FontSize', 12);
668 % ylabel('Y (ft)', 'FontWeight', 'bold', 'FontSize', 12);
669 % zlabel('Z (ft)', 'FontWeight', 'bold', 'FontSize', 12);
670 % grid on;
671 %
672 % %% Step response plots
673 %
674 % %Longitudinal
675 %
676 % % Compare 'u' (velocity) from full and long-period models
677 % subplot(4,1,1);
678 % plot(t, y_full(:,1)+x0(1), 'r', 'DisplayName', 'Fully linearized Model'); hold
679 % on;
680 % plot(t, y_long(:,1)+x0(1), 'b--', 'DisplayName', 'Long-Period Model');
681 % plot(t2, y2(1,:), 'g--', 'DisplayName', 'Non-linear Model');
682 % title('Response of u (velocity)'); xlabel('Time (s)'); ylabel('u (m/s)');
683 % legend;
684 % hold off;
685 %
686 % % Compare 'w' (vertical speed) from full and short-period models
687 % subplot(4,1,2);
688 % plot(t, y_full(:,2)+x0(2), 'r', 'DisplayName', 'Fully linearized Model'); hold
689 % on;
690 % plot(t, y_short(:,1)+x0(2), 'b--', 'DisplayName', 'Short-Period Model');
691 % plot(t, states(3,:), 'g--', 'DisplayName', 'Non-Linear Model');
692 % title('Response of w (vertical speed)'); xlabel('Time (s)'); ylabel('w (m/s)');
693 % legend;
694 % hold off;
695 %
696 % % Compare 'q' (pitch rate) from full and short-period models
697 % subplot(4,1,3);
698 % plot(t, y_full(:,3)+x0(3), 'r', 'DisplayName', 'Fully linearized Model'); hold
699 % on;
700 % plot(t, y_short(:,2)+x0(3), 'b--', 'DisplayName', 'Short-Period Model');
701 % plot(t2, y2(5,:), 'g--', 'DisplayName', 'Non-Linear Model');
702 % title('Response of q (pitch rate)'); xlabel('Time (s)'); ylabel('q (rad/s)');
703 % legend;
704 % hold off;
705 %
706 % % Compare '\theta' (pitch angle) from full and long-period models
707 % subplot(4,1,4);
708 % plot(t, y_full(:,4)+x0(4), 'r', 'DisplayName', 'Fully linearized Model'); hold
709 % on;
710 % plot(t, y_long(:,2)+x0(4), 'b--', 'DisplayName', 'Long-Period Model');
711 % plot(t2, y2(8,:), 'g--', 'DisplayName', 'Non-Linear Model');
712 % title('Response of \theta (pitch angle)'); xlabel('Time (s)'); ylabel('\theta (rad)');
713 % legend;
714 %
715 % %% Ploting Rotloucs and Bodeplot For Longitudinal
716 % % Call the function for each transfer function comparison between full and
717 % % short modes
718 %
719 % % Full longitudinal vs short-period
720 % plotAndSaveSubplots(tf_full_longitudinal_De_with_statew,
721 % tf_short_period_De_with_state_w, 'Short', 'De', 'w');
722 % plotAndSaveSubplots(tf_full_longitudinal_De_with_stateq,
723 % tf_short_period_De_with_state_q, 'Short', 'De', 'q');
724 % plotAndSaveSubplots(tf_full_longitudinal_Th_with_statew,
725 % tf_short_period_Th_with_state_w, 'Short', 'Th', 'w');
726 % plotAndSaveSubplots(tf_full_longitudinal_Th_with_stateq,
727 % tf_short_period_Th_with_state_q, 'Short', 'Th', 'q');
728 %
729 % % Full longitudinal vs long-period
730 % plotAndSaveSubplots(tf_full_longitudinal_De_with_stateu,
731 % tf_long_period_De_with_state_u, 'Long', 'De', 'u');
732 % plotAndSaveSubplots(tf_full_longitudinal_De_with_state_theta,
733 % tf_long_period_De_with_state_theta, 'Long', 'De', 'theta');

```

```

726 % plotAndSaveSubplots(tf_full_longitudinal_Th_with_stateu,
727 % tf_long_period_Th_with_state_u, 'Long', 'Th', 'u');
728 % plotAndSaveSubplots(tf_full_longitudinal_Th_with_state_theta,
729 % tf_long_period_Th_with_state_theta, 'Long', 'Th', 'theta');
730 %
731 %
732 % %% Plot and save Root Locus and Bode plots for each mode
733 % Define the transfer functions and labels for comparisons
734 %
735 % % Aileron Deflection (Da) Comparisons
736 % Da_v = {tf_full_lateral_Da_with_state_v, tf_3DOF_dutch_Da_with_state_v,
737 % tf_2DOF_dutch_Da_with_state_v};
738 % Da_p = {tf_full_lateral_Da_with_state_p, tf_3DOF_dutch_Da_with_state_p,
739 % tf_1DOF_roll_Da_with_state_p};
740 % Da_r = {tf_full_lateral_Da_with_state_r, tf_3DOF_dutch_Da_with_state_r,
741 % tf_2DOF_dutch_Da_with_state_r};
742 % Da_phi = {tf_full_lateral_Da_with_state_phi};
743 % Da_epsi = {tf_full_lateral_Da_with_state_epsi};
744 %
745 % % Rudder Deflection (Dr) Comparisons
746 % Dr_v = {tf_full_lateral_Dr_with_state_v, tf_3DOF_dutch_Dr_with_state_v,
747 % tf_2DOF_dutch_Dr_with_state_v};
748 % Dr_p = {tf_full_lateral_Dr_with_state_p, tf_3DOF_spiral_Dr_with_state_p,
749 % tf_3DOF_dutch_Dr_with_state_p};
750 % Dr_r = {tf_full_lateral_Dr_with_state_r, tf_3DOF_spiral_Dr_with_state_r,
751 % tf_3DOF_dutch_Dr_with_state_r, tf_2DOF_dutch_Dr_with_state_r};
752 % Dr_phi = {tf_full_lateral_Dr_with_state_phi, tf_3DOF_spiral_Dr_with_state_phi};
753 % Dr_epsi = {tf_full_lateral_Dr_with_state_epsi};
754 %
755 % % Mode labels for Aileron Deflection (Da) Comparisons
756 % mode_labels_Da_v = {'Full Mode', '3-DOF Dutch Roll', '2-DOF Dutch Roll'};
757 % mode_labels_Da_p = {'Full Mode', '3-DOF Dutch Roll', '1-DOF Roll'};
758 % mode_labels_Da_r = {'Full Mode', '3-DOF Dutch Roll', '2-DOF Dutch Roll'};
759 % mode_labels_Da_phi = {'Full Mode'};
760 % mode_labels_Da_epsi = {'Full Mode'};
761 %
762 % % Call the function to compare each mode for specific input-output pairs
763 %
764 % % Aileron Deflection (Da) Comparisons
765 % plotAndCompareModesWithSubplots(Da_v, mode_labels_Da_v, 'Da', 'v');
766 % plotAndCompareModesWithSubplots(Da_p, mode_labels_Da_p, 'Da', 'p');
767 % plotAndCompareModesWithSubplots(Da_r, mode_labels_Da_r, 'Da', 'r');
768 % plotAndCompareModesWithSubplots(Da_phi, mode_labels_Da_phi, 'Da', 'phi');
769 % plotAndCompareModesWithSubplots(Da_epsi, mode_labels_Da_epsi, 'Da', 'epsi');
770 %
771 % % Rudder Deflection (Dr) Comparisons
772 % plotAndCompareModesWithSubplots(Dr_v, mode_labels_Dr_v, 'Dr', 'v');
773 % plotAndCompareModesWithSubplots(Dr_p, mode_labels_Dr_p, 'Dr', 'p');
774 % plotAndCompareModesWithSubplots(Dr_r, mode_labels_Dr_r, 'Dr', 'r');
775 % plotAndCompareModesWithSubplots(Dr_phi, mode_labels_Dr_phi, 'Dr', 'phi');
776 % plotAndCompareModesWithSubplots(Dr_epsi, mode_labels_Dr_epsi, 'Dr', 'epsi');
777 %
778 % %% Display Transfer Function For Longitudinal
779 % % Call the function below for each input-output pair comparison
780 %
781 % % Full longitudinal vs short-period
782 % displayTransferFunctionAsFraction(tf_full_longitudinal_De_with_statew,
783 % tf_short_period_De_with_state_w, 'Short', 'De', 'w');
784 % displayTransferFunctionAsFraction(tf_full_longitudinal_De_with_stateq,
785 % tf_short_period_De_with_state_q, 'Short', 'De', 'q');
786 % displayTransferFunctionAsFraction(tf_full_longitudinal_Th_with_statew,
787 % tf_short_period_De_with_state_w, 'Short', 'Th', 'w');
788 % displayTransferFunctionAsFraction(tf_full_longitudinal_Th_with_stateq,

```

```

    tf_short_period_De_with_state_q, 'Short', 'Th', 'q');

785 %
786 % % Full longitudinal vs long-period
787 % displayTransferFunctionAsFraction(tf_full_longitudinal_De_with_stateu,
788 %         tf_long_period_De_with_state_u, 'Long', 'De', 'u');
789 % displayTransferFunctionAsFraction(tf_full_longitudinal_De_with_state_theta,
790 %         tf_long_period_De_with_state_theta, 'Long', 'De', 'theta');
791 % displayTransferFunctionAsFraction(tf_full_longitudinal_Th_with_stateu,
792 %         tf_long_period_Th_with_state_u, 'Long', 'Th', 'u');
793 % displayTransferFunctionAsFraction(tf_full_longitudinal_Th_with_state_theta,
794 %         tf_long_period_Th_with_state_theta, 'Long', 'Th', 'theta');

795 %
796 % %% Display the transfer functions in fraction format
797 % Call the function below for each group of transfer functions
798 %
799 % % Aileron Deflection (Da) Comparisons
800 % displayTransferFunctionGroup(Da_v, mode_labels_Da_v, 'Da', 'v');
801 % displayTransferFunctionGroup(Da_p, mode_labels_Da_p, 'Da', 'p');
802 % displayTransferFunctionGroup(Da_r, mode_labels_Da_r, 'Da', 'r');
803 % displayTransferFunctionGroup(Da_phi, mode_labels_Da_phi, 'Da', 'phi');
804 % displayTransferFunctionGroup(Da_epsi, mode_labels_Da_epsi, 'Da', 'epsi');

805 %
806 % % Rudder Deflection (Dr) Comparisons
807 % displayTransferFunctionGroup(Dr_v, mode_labels_Dr_v, 'Dr', 'v');
808 % displayTransferFunctionGroup(Dr_p, mode_labels_Dr_p, 'Dr', 'p');
809 % displayTransferFunctionGroup(Dr_r, mode_labels_Dr_r, 'Dr', 'r');
810 % displayTransferFunctionGroup(Dr_phi, mode_labels_Dr_phi, 'Dr', 'phi');
811 % displayTransferFunctionGroup(Dr_epsi, mode_labels_Dr_epsi, 'Dr', 'epsi');

812 %
813 % %% Functions
814 %
815 % Define a function to display the transfer function expressions as a large
816 % fraction
817 % function displayTransferFunctionAsFraction(tf_full, tf_mode, mode_name,
818 %     input_name, output_name)
819 %     % Extract numerator and denominator for the full mode transfer function
820 %     [num_full, den_full] = tfdata(tf_full, 'v'); % Get numerator and
821 %     denominator as vectors
822 %     % Convert numerator and denominator to strings
823 %     num_full_str = poly2str(num_full, 's');
824 %     den_full_str = poly2str(den_full, 's');

825 %     % Extract numerator and denominator for the mode transfer function (short/
826 %     long)
827 %     [num_mode, den_mode] = tfdata(tf_mode, 'v'); % Get numerator and
828 %     denominator as vectors
829 %     % Convert numerator and denominator to strings
830 %     num_mode_str = poly2str(num_mode, 's');
831 %     den_mode_str = poly2str(den_mode, 's');

832 %     % Display the formatted transfer functions as a large fraction
833 %     fprintf('Comparison for Transfer Function (%s to %s):\n', input_name,
834 %     output_name);
835 %     fprintf('-----\n');
836 %
837 %     % Display the full mode transfer function in S domain format as a large
838 %     fraction
839 %     fprintf('Full Mode Transfer Function:\n');
840 %     fprintf('%s\n', num_full_str); % Numerator

```

```

841 %     % Add a line break for readability between comparisons
842 %     fprintf('\n\n');
843 % end
844 %
845 % % Define function to display the transfer functions for a group in fraction
846 % format
847 % function displayTransferFunctionGroup(tf_list, mode_labels, input_name,
848 % output_name)
849 %     num_modes = length(tf_list);
850 %     fprintf('Transfer Function Comparisons for %s to %s:\n', input_name,
851 %     output_name);
852 %     fprintf('-----\n');
853 %
854 %     for k = 1:num_modes
855 %         % Extract numerator and denominator
856 %         [num, den] = tfdata(tf_list{k}, 'v');
857 %         num_str = poly2str(num, 's');
858 %         den_str = poly2str(den, 's');
859 %
860 %         % Display transfer function for each mode
861 %         fprintf('%s Mode Transfer Function:\n', mode_labels{k});
862 %         fprintf('    %s\n', num_str); % Numerator
863 %         fprintf('    %s\n', repmat('-', max(length(num_str), length(den_str)), 1)); % Divider line
864 %         fprintf('    %s\n\n', den_str); % Denominator
865 %
866 %     end
867 %     fprintf('\n\n'); % Add extra line spacing between groups for readability
868 % end
869 %
870 % Define function to plot and save Root Locus and Bode plots with subplots for
871 % each mode comparison
872 % function plotAndCompareModesWithSubplots(tf_list, mode_labels, input_name,
873 % output_name)
874 %
875 %     % Ensure 'graphs' directory exists
876 %     if ~exist('graphs', 'dir')
877 %         mkdir('graphs');
878 %     end
879 %
880 %     num_modes = length(tf_list);
881 %
882 %     % Plot Root Locus with each mode in its own subplot
883 %     figure;
884 %     for k = 1:num_modes
885 %         subplot(1, num_modes, k); % Create a subplot for each mode
886 %         rlocus(tf_list{k});
887 %         title([mode_labels{k}]);
888 %         xlabel('Real Axis');
889 %         ylabel('Imaginary Axis');
890 %
891 %     end
892 %     sgtitle(['Root Locus - ', input_name, ' to ', output_name]);
893 %     saveas(gcf, fullfile('graphs', ['RootLocus_Comparison_', input_name, '_to_',
894 %     output_name, '.png']));
895 %
896 %     % Plot Bode Plot with each mode in the same plot for overlay comparison
897 %     figure;
898 %     hold on;
899 %     for k = 1:num_modes
900 %         bode(tf_list{k});
901 %
902 %     end
903 %     hold off;
904 %     title(['Bode Plot Comparison - ', input_name, ' to ', output_name]);
905 %     legend(mode_labels);
906 %     saveas(gcf, fullfile('graphs', ['BodePlot_Comparison_', input_name, '_to_',
907 %     output_name, '.png']));
908 %
909 % Define a function to plot and save root locus and Bode plots with subplots
910 % for each transfer function
911 % function plotAndSaveSubplots(tf_full, tf_short, mode_name, input_name,
912 % output_name)
913 %
914 %     % Ensure 'graphs' directory exists

```

```

902 % if ~exist('graphs', 'dir')
903 % mkdir('graphs');
904 %
905 %
906 % Create figure for Root Locus with two subplots
907 % figure;
908 %
909 % Full Mode Root Locus in the first subplot
910 % subplot(1, 2, 1);
911 % rlocus(tf_full);
912 % title(['Root Locus - Full Mode (', input_name, ' to ', output_name, ')']);
913 % xlabel('Real Axis');
914 % ylabel('Imaginary Axis');
915 %
916 % Short Mode Root Locus in the second subplot
917 % subplot(1, 2, 2);
918 % rlocus(tf_short);
919 % title(['Root Locus - ', mode_name, ' Mode (', input_name, ' to ',
920 % output_name, ')']);
921 % xlabel('Real Axis');
922 % ylabel('Imaginary Axis');
923 %
924 % Save the combined root locus figure
925 % saveas(gcf, fullfile('graphs', ['RootLocus_', input_name, '_to_',
926 % output_name, '_Full_vs_', mode_name, '.png']));
927 %
928 % Bode plot (Separate for Full and Short Mode)
929 % figure;
930 % bode(tf_full);
931 % hold on;
932 % bode(tf_short);
933 % hold off;
934 % title(['Bode Plot - ', input_name, ' to ', output_name, '(Full vs ',
935 % mode_name, ' Mode)']);
936 % legend('Full Mode', [mode_name, ' Mode']);
937 % saveas(gcf, fullfile('graphs', ['BodePlot_', input_name, '_to_',
938 % output_name, '_', mode_name, '.png']));
939 % end
940 airport_name = "Hilo International (PHTO)";
941
942
943 % %% Test_1
944 % %
945 % % Get the folder of the current MATLAB script
946 % current_folder = fileparts(mfilename('fullpath'));
947 % output_folder = fullfile(current_folder, 'Task7_result_graphs'); % Define the
948 % % folder as 'Task7_result_graphs'
949 %
950 % % Figure 1: Pitching Angle Output for Pitch Controller
951 % figure(1)
952 % plot(out.tout, out.theta_states.Data(:, 1), '-.k', 'LineWidth', 2);
953 % grid on
954 % grid minor
955 % hold on
956 % plot(out.tout, out.theta_states.Data(:, 2), 'r', 'LineWidth', 2);
957 % hold on
958 % plot(out.tout, out.theta_states.Data(:, 3), '--b', 'LineWidth', 2);
959 % title('$Pitching$ $Angle$ $Response$ $for$ $Pitch$ $Controller$', ...
960 % 'interpreter', 'latex', 'FontSize', 15);
961 % legend('$\theta$ command', '$\theta$ non$ linear$', '$\theta$ linear',
962 % 'interpreter', 'latex', 'FontSize', 10);
963 % xlabel('Time (s)', 'interpreter', 'latex', 'FontSize', 12); % Added x-axis
964 % ylabel('$\theta$ $(degrees)$', 'interpreter', 'latex', 'FontSize', 12);
965 % % Save Figure

```

```

966 % save_path = fullfile(output_folder, '
967 %     test1_Pitching_Angle_Response_for_Pitch_Controller.png');
968 %
969 % % Figure 2: U Output for Pitch Controller
970 % figure(2)
971 % plot(out.tout, out.u_states.Data(:, 1), '-.k', 'LineWidth', 2);
972 % grid on
973 % grid minor
974 % hold on
975 % plot(out.tout, out.u_states.Data(:, 2), 'r', 'LineWidth', 2);
976 % hold on
977 % plot(out.tout, out.u_states.Data(:, 3), '--b', 'LineWidth', 2);
978 % title('$U$ $Response$ $for$ $Pitch$ $Controller$', ...
979 %     'interpreter', 'latex', 'FontSize', 15);
980 % legend('$Command$', '$non$ $linear$', '$linear$', ...
981 %     'interpreter', 'latex', 'FontSize', 10);
982 % xlabel('Time (s)', 'interpreter', 'latex', 'FontSize', 12);
983 % ylabel('$U$ $(ft/s)$', 'interpreter', 'latex', 'FontSize', 12);
984 % % Save Figure
985 % save_path = fullfile(output_folder, 'test1_U_Response_for_Pitch_Controller.png'
986 % );
987 % exportgraphics(gcf, save_path, 'Resolution', 300);
988 %
989 % % Figure 3: Flight Path Angle for Pitch Controller
990 % figure(3)
991 % plot(out.tout, out.gamma_states.Data(:, 1), 'r', 'LineWidth', 2);
992 % grid on
993 % grid minor
994 % hold on
995 % plot(out.tout, out.gamma_states.Data(:, 2), '--b', 'LineWidth', 2);
996 % title('$\gamma$ $Response$ $for$ $Pitch$ $Controller$', ...
997 %     'interpreter', 'latex', 'FontSize', 15);
998 % legend('$\gamma$ $non$ $linear$', '$\gamma$ $linear$', ...
999 %     'interpreter', 'latex', 'FontSize', 10);
1000 % xlabel('Time (s)', 'interpreter', 'latex', 'FontSize', 12); % Added x-axis
1001 % ylabel('$\gamma$ $(degrees)$', 'interpreter', 'latex', 'FontSize', 12);
1002 % % Save Figure
1003 % save_path = fullfile(output_folder, '
1004 %     test1_Flight_Path_Angle_for_Pitch_Controller.png');
1005 % exportgraphics(gcf, save_path, 'Resolution', 300);
1006 %
1007 % % Figure 4: H Output for Pitch Controller
1008 % figure(4)
1009 % plot(out.tout, out.H_states.Data(:, 2), 'r', 'LineWidth', 2);
1010 % grid on
1011 % grid minor
1012 % hold on
1013 % plot(out.tout, out.H_states.Data(:, 3), '--b', 'LineWidth', 2);
1014 % title('$H$ $Response$ $for$ $Pitch$ $Controller$', ...
1015 %     'interpreter', 'latex', 'FontSize', 15);
1016 % legend('$H$ $non$ $linear$', '$H$ $linear$', ...
1017 %     'interpreter', 'latex', 'FontSize', 10);
1018 % xlabel('Time (s)', 'interpreter', 'latex', 'FontSize', 12); % Added x-axis
1019 % ylabel('$H$ $(ft)$', 'interpreter', 'latex', 'FontSize', 12);
1020 % % Save Figure
1021 % save_path = fullfile(output_folder, 'test1_H_Response_for_Pitch_Controller.png'
1022 % );
1023 % exportgraphics(gcf, save_path, 'Resolution', 300);
1024 % % Plot e (elevator control action)
1025 % figure(5)
1026 % plot(out.tout, out.elevator_controller.Data(:, 1), 'r', 'LineWidth', 2);
1027 % grid on
1028 % grid minor
1029 % hold on
1030 % plot(out.tout, out.elevator_controller.Data(:, 2), '--b', 'LineWidth', 2);

```

```

1031 %     'interpreter', 'latex', 'FontSize', 10);
1032 % xlabel('Time (s)', 'interpreter', 'latex', 'FontSize', 12); % Added x-axis
1033 % label
1034 % % Save Figure
1035 % save_path = fullfile(output_folder, 'Test1_delta_e_for_Pitch_Controller.png');
1036 % exportgraphics(gcf, save_path, 'Resolution', 300);
1037
1038 %
1039 %
1040 % % % Test 2
1041 %%
1042 % % Plot (pitch angle)
1043 % figure(6)
1044 % plot(out.tout, out.theta_states.Data(:, 1), '-.k', 'LineWidth', 2);
1045 % grid on
1046 % grid minor
1047 % hold on
1048 % plot(out.tout, out.theta_states.Data(:, 2), 'r', 'LineWidth', 2);
1049 % hold on
1050 % plot(out.tout, out.theta_states.Data(:, 3), '--b', 'LineWidth', 2);
1051 % title('$\theta$ Response$ $for$ $Pitch$ $\&$ $Velocity$ $Controller$', ...
1052 %       'Interpreter', 'latex', 'FontSize', 15);
1053 % legend('$\theta$ command$', '$\theta$ non$ linear$', '$\theta$ linear$', ...
1054 %       ...
1055 %       'interpreter', 'latex', 'FontSize', 10);
1056 % xlabel('Time (s)', 'interpreter', 'latex', 'FontSize', 12); % Added x-axis
1057 % label
1058 % ylabel('$\theta$ (degrees)', 'interpreter', 'latex', 'FontSize', 12);
1059 % % Save Figure
1060 % save_path = fullfile(output_folder,
1061 %                       'Test2_theta_Response_for_Pitch_Velocity_Controller.png');
1062 % exportgraphics(gcf, save_path, 'Resolution', 300);
1063 %
1064 % % Plot u (forward velocity)
1065 % figure(7)
1066 % plot(out.tout, out.u_states.Data(:, 1), '-.k', 'LineWidth', 2);
1067 % grid on
1068 % grid minor
1069 % hold on
1070 % plot(out.tout, out.u_states.Data(:, 2), 'r', 'LineWidth', 2);
1071 % hold on
1072 % plot(out.tout, out.u_states.Data(:, 3), '--b', 'LineWidth', 2);
1073 % title('$U$ Response$ $for$ $Pitch$ $\&$ $Velocity$ $Controller$', ...
1074 %       'Interpreter', 'latex', 'FontSize', 15);
1075 % legend('$U$ command$', '$U$ non$ linear$', '$U$ linear$', ...
1076 %       'interpreter', 'latex', 'FontSize', 10);
1077 % xlabel('Time (s)', 'interpreter', 'latex', 'FontSize', 12); % Added x-axis
1078 % label
1079 % ylabel('$U$ (ft/s)', 'interpreter', 'latex', 'FontSize', 12);
1080 % % Save Figure
1081 % save_path = fullfile(output_folder,
1082 %                       'Test2_u_Response_for_Pitch_Velocity_Controller.png');
1083 % exportgraphics(gcf, save_path, 'Resolution', 300);
1084 %
1085 % % Plot (flight path angle)
1086 % figure(8)
1087 % plot(out.tout, out.gamma_states.Data(:, 1), 'r', 'LineWidth', 2);
1088 % grid on
1089 % grid minor
1090 % hold on
1091 % plot(out.tout, out.gamma_states.Data(:, 2), '--b', 'LineWidth', 2);
1092 % title('$\gamma$ Response$ $for$ $Pitch$ $\&$ $Velocity$ $Controller$', ...
1093 %       'Interpreter', 'latex', 'FontSize', 15);
1094 % legend('$\gamma$ non$ linear$', '$\gamma$ linear$', ...
1095 %       'interpreter', 'latex', 'FontSize', 10);
1096 % xlabel('Time (s)', 'interpreter', 'latex', 'FontSize', 12); % Added x-axis
1097 % label
1098 % ylabel('$\gamma$ (degrees)', 'interpreter', 'latex', 'FontSize', 12);
1099 % % Save Figure
1100 % save_path = fullfile(output_folder,

```

```

    Test2_gamma_Response_for_Pitch_Velocity_Controller.png');
1095 % exportgraphics(gcf, save_path, 'Resolution', 300);
1096 %
1097 % % Plot h (altitude)
1098 % figure(9)
1099 % plot(out.tout, out.H_states.Data(:, 1), '-.k', 'LineWidth', 2);
1100 % grid on
1101 % grid minor
1102 % hold on
1103 % plot(out.tout, out.H_states.Data(:, 2), 'r', 'LineWidth', 2);
1104 % hold on
1105 % plot(out.tout, out.H_states.Data(:, 3), '--b', 'LineWidth', 2);
1106 % title('$H$ $Response$ $for$ $Pitch$ $Velocity$ $Controller$', ...
1107 %     'Interpreter', 'latex', 'FontSize', 15);
1108 % legend('$H$ $non$ $linear$', '$H$ $linear$', ...
1109 %     'interpreter', 'latex', 'FontSize', 10);
1110 % xlabel('Time (s)', 'interpreter', 'latex', 'FontSize', 12); % Added x-axis
1111 %     label
1112 % ylabel('$H$ $(ft)$', 'interpreter', 'latex', 'FontSize', 12);
1113 % % Save Figure
1114 % save_path = fullfile(output_folder,
1115 %     'Test2_h_Response_for_Pitch_Velocity_Controller.png');
1116 % exportgraphics(gcf, save_path, 'Resolution', 300);
1117 %
1118 % % Plot e (elevator control action)
1119 % figure(10)
1120 % plot(out.tout, out.elevator_controller.Data(:, 1), 'r', 'LineWidth', 2);
1121 % grid on
1122 % grid minor
1123 % hold on
1124 % plot(out.tout, out.elevator_controller.Data(:, 2), '--b', 'LineWidth', 2);
1125 % title('$\delta_e$ $for$ $Pitch$ $Velocity$ $Controller$', ...
1126 %     'Interpreter', 'latex', 'FontSize', 15);
1127 % legend('$\delta_e$ $non$ $linear$', '$\delta_e$ $linear$', ...
1128 %     'interpreter', 'latex', 'FontSize', 10);
1129 % xlabel('Time (s)', 'interpreter', 'latex', 'FontSize', 12); % Added x-axis
1130 %     label
1131 % ylabel('$\delta_e$ $(degrees)$', 'interpreter', 'latex', 'FontSize', 12);
1132 % % Save Figure
1133 % save_path = fullfile(output_folder,
1134 %     'Test2_delta_e_for_Pitch_Velocity_Controller.png');
1135 % exportgraphics(gcf, save_path, 'Resolution', 300);
1136 %
1137 % % Plot th (throttle control action)
1138 % figure(11)
1139 % plot(out.tout, out.Trust_controller.Data(:, 1), 'r', 'LineWidth', 2);
1140 % grid on
1141 % grid minor
1142 % hold on
1143 % plot(out.tout, out.Trust_controller.Data(:, 2), '--b', 'LineWidth', 2);
1144 % title('$\delta_{th}$ $for$ $Pitch$ $Velocity$ $Controller$', ...
1145 %     'Interpreter', 'latex', 'FontSize', 15);
1146 % legend('$\delta_{th}$ $non$ $linear$', '$\delta_{th}$ $linear$', ...
1147 %     'interpreter', 'latex', 'FontSize', 10);
1148 % xlabel('Time (s)', 'interpreter', 'latex', 'FontSize', 12); % Added x-axis
1149 %     label
1150 % ylabel('$\delta_{th}$ ', 'interpreter', 'latex', 'FontSize', 12);
1151 % % Save Figure
1152 % save_path = fullfile(output_folder,
1153 %     'Test2_delta_th_for_Pitch_Velocity_Controller.png');
1154 % exportgraphics(gcf, save_path, 'Resolution', 300);
1155 %
1156 % % Test 3
1157 %
1158 % figure(12)
1159 % plot(out.tout, out.theta_states.Data(:, 1), '-.k', 'LineWidth', 2);
1160 % grid on
1161 % grid minor
1162 % hold on
1163 % plot(out.tout, out.theta_states.Data(:, 2), 'r', 'LineWidth', 2);

```

```

1159 % hold on
1160 % plot(out.tout, out.theta_states.Data(:, 3), '--b', 'LineWidth', 2);
1161 % title('$\theta$ $Response$ $for$ $Altitude$ $Hold$ $Controller$', ...
1162 % 'Interpreter', 'latex', 'FontSize', 15);
1163 % legend('$\theta$ $command$', '$\theta$ $non$ $linear$', '$\theta$ $linear$', ...
1164 % 'interpreter', 'latex', 'FontSize', 10);
1165 % xlabel('Time (s)', 'interpreter', 'latex', 'FontSize', 12);
1166 % ylabel('$\theta$ $(degrees)$', 'interpreter', 'latex', 'FontSize', 12);
1167 % save_path = fullfile(output_folder, ...
1168 %     'Test3_theta_Response_for_Altitude_Hold_Controller.png');
1169 % exportgraphics(gcf, save_path, 'Resolution', 300);
1170 %
1171 % figure(13)
1172 % plot(out.tout, out.u_states.Data(:, 1), '-.k', 'LineWidth', 2);
1173 % grid on
1174 % grid minor
1175 % hold on
1176 % plot(out.tout, out.u_states.Data(:, 2), 'r', 'LineWidth', 2);
1177 % plot(out.tout, out.u_states.Data(:, 3), '--b', 'LineWidth', 2);
1178 % title('$U$ $Response$ $for$ $Altitude$ $Hold$ $Controller$', ...
1179 % 'Interpreter', 'latex', 'FontSize', 15);
1180 % legend('$U$ $command$', '$U$ $non$ $linear$', '$U$ $linear$', ...
1181 % 'interpreter', 'latex', 'FontSize', 10);
1182 % xlabel('Time (s)', 'interpreter', 'latex', 'FontSize', 12);
1183 % ylabel('$U$ $(ft/s)$', 'interpreter', 'latex', 'FontSize', 12);
1184 % save_path = fullfile(output_folder, ...
1185 %     'Test3_u_Response_for_Altitude_Hold_Controller.png');
1186 % exportgraphics(gcf, save_path, 'Resolution', 300);
1187 %
1188 % figure(14)
1189 % plot(out.tout, out.gamma_states.Data(:, 1), 'r', 'LineWidth', 2);
1190 % grid on
1191 % grid minor
1192 % hold on
1193 % plot(out.tout, out.gamma_states.Data(:, 2), '--b', 'LineWidth', 2);
1194 % title('$\gamma$ $Response$ $for$ $Altitude$ $Hold$ $Controller$', ...
1195 % 'Interpreter', 'latex', 'FontSize', 15);
1196 % legend('$\gamma$ $non$ $linear$', '$\gamma$ $linear$', ...
1197 % 'interpreter', 'latex', 'FontSize', 10);
1198 % xlabel('Time (s)', 'interpreter', 'latex', 'FontSize', 12);
1199 % ylabel('$\gamma$ $(degrees)$', 'interpreter', 'latex', 'FontSize', 12);
1200 % save_path = fullfile(output_folder, ...
1201 %     'Test3_gamma_Response_for_Altitude_Hold_Controller.png');
1202 % exportgraphics(gcf, save_path, 'Resolution', 300);
1203 %
1204 % figure(15)
1205 % plot(out.tout, out.H_states.Data(:, 1), '-.k', 'LineWidth', 2);
1206 % grid on
1207 % grid minor
1208 % hold on
1209 % plot(out.tout, out.H_states.Data(:, 2), 'r', 'LineWidth', 2);
1210 % plot(out.tout, out.H_states.Data(:, 3), '--b', 'LineWidth', 2);
1211 % title('$H$ $Response$ $for$ $Altitude$ $Hold$ $Controller$', ...
1212 % 'Interpreter', 'latex', 'FontSize', 15);
1213 % legend('$H$ $command$', '$h$ $non$ $linear$', '$h$ $linear$', ...
1214 % 'interpreter', 'latex', 'FontSize', 10);
1215 % xlabel('Time (s)', 'interpreter', 'latex', 'FontSize', 12);
1216 % ylabel('$H$ $(ft)$', 'interpreter', 'latex', 'FontSize', 12);
1217 % save_path = fullfile(output_folder, ...
1218 %     'Test3_h_Response_for_Altitude_Hold_Controller.png');
1219 % exportgraphics(gcf, save_path, 'Resolution', 300);
1220 %
1221 % figure(16)
1222 % plot(out.tout, out.elevator_controller.Data(:, 1), 'r', 'LineWidth', 2);
1223 % grid on
1224 % grid minor
1225 % hold on
1226 % plot(out.tout, out.elevator_controller.Data(:, 2), '--b', 'LineWidth', 2);

```

```

1225 % title('$\delta_e$ $for$ $Altitude$ $Hold$ $Controller$', ...
1226 %     'interpreter', 'latex', 'FontSize', 15);
1227 % legend('$\delta_e$ $non$ $linear$', '$\delta_e$ $linear$', ...
1228 %     'interpreter', 'latex', 'FontSize', 10);
1229 % xlabel('Time (s)', 'interpreter', 'latex', 'FontSize', 12);
1230 % ylabel('$\delta_e$ $(degrees)$', 'interpreter', 'latex', 'FontSize', 12);
1231 % save_path = fullfile(output_folder, 'Test3_delta_e_for_Altitude_Hold_Controller
1232 % .png');
1233 %
1234 % figure(17)
1235 % plot(out.tout, out.Trust_controller.Data(:, 1), 'r', 'LineWidth', 2);
1236 % grid on
1237 % grid minor
1238 % hold on
1239 % plot(out.tout, out.Trust_controller.Data(:, 2), '--b', 'LineWidth', 2);
1240 % title('$\delta_{th}$ $for$ $Altitude$ $Hold$ $Controller$', ...
1241 %     'interpreter', 'latex', 'FontSize', 15);
1242 % legend('$\delta_{th}$ $non$ $linear$', '$\delta_{th}$ $linear$', ...
1243 %     'interpreter', 'latex', 'FontSize', 10);
1244 % xlabel('Time (s)', 'interpreter', 'latex', 'FontSize', 12);
1245 % ylabel('$\delta_{th}$ $(degrees)$', 'interpreter', 'latex', 'FontSize', 12);
1246 % save_path = fullfile(output_folder,
1247 %     'Test3_delta_th_for_Altitude_Hold_Controller.png');
1248 % exportgraphics(gcf, save_path, 'Resolution', 300);
1249 %
1250 %
1251 % % Plot (sideslip angle)
1252 % figure(18)
1253 % plot(out.tout, out.beta_states.Data(:, 1), 'r', 'LineWidth', 2);
1254 % grid on
1255 % grid minor
1256 % hold on
1257 % plot(out.tout, out.beta_states.Data(:, 2), '--b', 'LineWidth', 2);
1258 % title('$\beta$ $Response$ $for$ $Lateral$ $Controller$', ...
1259 %     'interpreter', 'latex', 'FontSize', 15);
1260 % legend('$\beta$ $non$ $linear$', '$\beta$ $linear$', ...
1261 %     'interpreter', 'latex', 'FontSize', 10);
1262 % xlabel('Time (s)', 'interpreter', 'latex', 'FontSize', 12);
1263 % ylabel('$\beta$ $(degrees)$', 'interpreter', 'latex', 'FontSize', 12);
1264 % % Save Figure
1265 % save_path = fullfile(output_folder, 'Test4_beta_Response_for_Lateral_Controller
1266 % .png');
1267 % exportgraphics(gcf, save_path, 'Resolution', 300);
1268 %
1269 % % Plot (bank angle)
1270 % figure(19)
1271 % plot(out.tout, out.phi_states.Data(:, 1), 'r', 'LineWidth', 2);
1272 % grid on
1273 % grid minor
1274 % hold on
1275 % plot(out.tout, out.phi_states.Data(:, 2), '--b', 'LineWidth', 2);
1276 % title('$\phi$ $Response$ $for$ $Lateral$ $Controller$', ...
1277 %     'interpreter', 'latex', 'FontSize', 15);
1278 % legend('$\phi$ $non$ $linear$', '$\phi$ $linear$', ...
1279 %     'interpreter', 'latex', 'FontSize', 10);
1280 % xlabel('Time (s)', 'interpreter', 'latex', 'FontSize', 12);
1281 % ylabel('$\phi$ $(degrees)$', 'interpreter', 'latex', 'FontSize', 12);
1282 % % Save Figure
1283 % save_path = fullfile(output_folder, 'Test4_phi_Response_for_Lateral_Controller.
1284 % png');
1285 % exportgraphics(gcf, save_path, 'Resolution', 300);
1286 %
1287 % % Plot (heading angle)
1288 % figure(20)
1289 % plot(out.tout, out.psi_states.Data(:, 1), '--k', 'LineWidth', 2);
1290 % grid on
1291 % grid minor
1292 % hold on
1293 % plot(out.tout, out.psi_states.Data(:, 2), 'r', 'LineWidth', 2);

```

```

1292 % hold on
1293 % plot(out.tout, out.psi_states.Data(:, 3), '--b', 'LineWidth', 2);
1294 % title('$\psi$ $Response$ $for$ $Lateral$ $Controller$', ...
1295 %     'interpreter', 'latex', 'FontSize', 15);
1296 % legend('$\psi$ $command$', '$\psi$ $non$ $linear$', '$\psi$ $linear$', ...
1297 %     'interpreter', 'latex', 'FontSize', 10);
1298 % xlabel('Time (s)', 'interpreter', 'latex', 'FontSize', 12); % Added x-axis
1299 %     label
1300 % ylabel('$\psi$ $(degrees)$', 'interpreter', 'latex', 'FontSize', 12);
1301 % % Save Figure
1302 % save_path = fullfile(output_folder, 'Test4_psi_Response_for_Lateral_Controller.
1303 %     png');
1304 % % Plot h (altitude)
1305 % figure(21)
1306 % plot(out.tout, out.H_states.Data(:, 1), '-.k', 'LineWidth', 2);
1307 % grid on
1308 % grid minor
1309 % hold on
1310 % plot(out.tout, out.H_states.Data(:, 2), 'r', 'LineWidth', 2);
1311 % hold on
1312 % plot(out.tout, out.H_states.Data(:, 3), '--b', 'LineWidth', 2);
1313 % title('$H$ $Response$ $for$ $Lateral$ $Controller$', ...
1314 %     'interpreter', 'latex', 'FontSize', 15);
1315 % legend('$H$ $command$', '$h$ $non$ $linear$', '$h$ $linear$', ...
1316 %     'interpreter', 'latex', 'FontSize', 10);
1317 % xlabel('Time (s)', 'interpreter', 'latex', 'FontSize', 12); % Added x-axis
1318 %     label
1319 % ylabel('$H$ $(ft)$', 'interpreter', 'latex', 'FontSize', 12);
1320 % % Save Figure
1321 % save_path = fullfile(output_folder, 'Test4_h_Response_for_Lateral_Controller.
1322 %     png');
1323 % % Plot r (rudder control action)
1324 % figure(22)
1325 % plot(out.tout, out.rudder_controller.Data(:, 1), 'r', 'LineWidth', 2);
1326 % grid on
1327 % grid minor
1328 % hold on
1329 % plot(out.tout, out.rudder_controller.Data(:, 2), '--b', 'LineWidth', 2);
1330 % title('$\delta_r$ $for$ $Lateral$ $Controller$', ...
1331 %     'interpreter', 'latex', 'FontSize', 15);
1332 % legend('$\delta_r$ $non$ $linear$', '$\delta_r$ $linear$', ...
1333 %     'interpreter', 'latex', 'FontSize', 10);
1334 % xlabel('Time (s)', 'interpreter', 'latex', 'FontSize', 12); % Added x-axis
1335 %     label
1336 % ylabel('$\delta_r$ $(degrees)$', 'interpreter', 'latex', 'FontSize', 12);
1337 % % Save Figure
1338 % save_path = fullfile(output_folder, 'Test4_delta_r_for_Lateral_Controller.png')
1339 % ;
1340 % % Plot a (aileron control action)
1341 % figure(23)
1342 % plot(out.tout, out.aileron_controller.Data(:, 1), 'r', 'LineWidth', 2);
1343 % grid on
1344 % grid minor
1345 % hold on
1346 % plot(out.tout, out.aileron_controller.Data(:, 2), '--b', 'LineWidth', 2);
1347 % title('$\delta_a$ $for$ $Lateral$ $Controller$', ...
1348 %     'interpreter', 'latex', 'FontSize', 15);
1349 % legend('$\delta_a$ $non$ $linear$', '$\delta_a$ $linear$', ...
1350 %     'interpreter', 'latex', 'FontSize', 10);
1351 % xlabel('Time (s)', 'interpreter', 'latex', 'FontSize', 12); % Added x-axis
1352 %     label
1353 % ylabel('$\delta_a$ $(degrees)$', 'interpreter', 'latex', 'FontSize', 12);
1354 % % Save Figure
1355 % save_path = fullfile(output_folder, 'Test4_delta_a_for_Lateral_Controller.png')
1356 % ;

```

```

1355 % exportgraphics(gcf, save_path, 'Resolution', 300);
1356 %
1357 % %% Test 5
1358 % % Plot (sideslip angle)
1359 % figure(24)
1360 % plot(out.tout, out.beta_states.Data(:, 1), 'r', 'LineWidth', 2); % Nonlinear
1361 % grid on
1362 % grid minor
1363 % hold on
1364 % plot(out.tout, out.beta_states.Data(:, 2), '--b', 'LineWidth', 2); % Linear
1365 % title('$\beta$ Response$ $for$ $Lateral$ $\&$ $Altitude$ $Hold$ $Controller$', ...
1366 %     'Interpreter', 'latex', 'FontSize', 15);
1367 % legend('$\beta$ non$ $linear$', '$\beta$ linear$', ...
1368 %     'Interpreter', 'latex', 'FontSize', 10);
1369 % xlabel('Time (s)', 'Interpreter', 'latex', 'FontSize', 12); % Added x-axis
1370 %     label
1371 % ylabel('$\beta$ (degrees)', 'Interpreter', 'latex', 'FontSize', 12);
1372 % save_path = fullfile(output_folder, ...
1373 %     'Test5_beta_Response_for_Lateral_Altitude_Hold_Controller.png');
1374 % exportgraphics(gcf, save_path, 'Resolution', 300);
1375 %
1376 % % Plot (bank angle)
1377 % figure(25)
1378 % plot(out.tout, out.phi_states.Data(:, 1), 'r', 'LineWidth', 2); % Nonlinear
1379 % grid on
1380 % grid minor
1381 % hold on
1382 % plot(out.tout, out.phi_states.Data(:, 2), '--b', 'LineWidth', 2); % Linear
1383 % title('$\phi$ Response$ $for$ $Lateral$ $\&$ $Altitude$ $Hold$ $Controller$', ...
1384 %     'Interpreter', 'latex', 'FontSize', 15);
1385 % legend('$\phi$ non$ $linear$', '$\phi$ linear$', ...
1386 %     'Interpreter', 'latex', 'FontSize', 10);
1387 % xlabel('Time (s)', 'Interpreter', 'latex', 'FontSize', 12); % Added x-axis
1388 %     label
1389 % ylabel('$\phi$ (degrees)', 'Interpreter', 'latex', 'FontSize', 12);
1390 % save_path = fullfile(output_folder, ...
1391 %     'Test5_phi_Response_for_Lateral_Altitude_Hold_Controller.png');
1392 % exportgraphics(gcf, save_path, 'Resolution', 300);
1393 %
1394 % % Plot (heading angle)
1395 % figure(26)
1396 % plot(out.tout, out.psi_states.Data(:, 1), '-.k', 'LineWidth', 2); % Command
1397 % grid on
1398 % grid minor
1399 % hold on
1400 % plot(out.tout, out.psi_states.Data(:, 2), 'r', 'LineWidth', 2); % Nonlinear
1401 % hold on
1402 % plot(out.tout, out.psi_states.Data(:, 3), '--b', 'LineWidth', 2); % Linear
1403 % title('$\psi$ Response$ $for$ $Lateral$ $\&$ $Altitude$ $Hold$ $Controller$', ...
1404 %     'Interpreter', 'latex', 'FontSize', 15);
1405 % legend('$\psi$ command$', '$\psi$ non$ $linear$', '$\psi$ linear$', ...
1406 %     'Interpreter', 'latex', 'FontSize', 10);
1407 % xlabel('Time (s)', 'Interpreter', 'latex', 'FontSize', 12); % Added x-axis
1408 %     label
1409 % ylabel('$\psi$ (degrees)', 'Interpreter', 'latex', 'FontSize', 12);
1410 % save_path = fullfile(output_folder, ...
1411 %     'Test5_psi_Response_for_Lateral_Altitude_Hold_Controller.png');
1412 % exportgraphics(gcf, save_path, 'Resolution', 300);
1413 %
1414 % % Plot h (altitude)
1415 % figure(27)
1416 % plot(out.tout, out.H_states.Data(:, 1), '-.k', 'LineWidth', 2); % Command
1417 % grid on
1418 % grid minor
1419 % hold on
1420 % plot(out.tout, out.H_states.Data(:, 2), 'r', 'LineWidth', 2); % Nonlinear
1421 % hold on
1422 % plot(out.tout, out.H_states.Data(:, 3), '--b', 'LineWidth', 2); % Linear

```

```

1417 % title('$H$ $Response$ $for$ $Lateral$ $\\&$ $Altitude$ $Hold$ $Controller$', ...
1418 %     'Interpreter', 'latex', 'FontSize', 15);
1419 % legend('$H$ $command$', '$h$ $non$ $linear$', '$h$ $linear$', ...
1420 %     'Interpreter', 'latex', 'FontSize', 10);
1421 % xlabel('Time (s)', 'Interpreter', 'latex', 'FontSize', 12); % Added x-axis
1422 %     label
1423 % ylabel('$H$ $(ft)$', 'Interpreter', 'latex', 'FontSize', 12);
1424 % save_path = fullfile(output_folder,
1425 %     'Test5_h_Response_for_Lateral_Altitude_Hold_Controller.png');
1426 % exportgraphics(gcf, save_path, 'Resolution', 300);
1427 %
1428 % % Plot r (rudder control action)
1429 % figure(28)
1430 % plot(out.tout, out.rudder_controller.Data(:, 1), 'r', 'LineWidth', 2); %
1431 %     Nonlinear
1432 % grid on
1433 % grid minor
1434 % hold on
1435 % plot(out.tout, out.rudder_controller.Data(:, 2), '--b', 'LineWidth', 2); %
1436 %     Linear
1437 % title('$\\delta_r$ $for$ $Lateral$ $\\&$ $Altitude$ $Hold$ $Controller$', ...
1438 %     'Interpreter', 'latex', 'FontSize', 15);
1439 % legend('$\\delta_r$ $non$ $linear$', '$\\delta_r$ $linear$', ...
1440 %     'Interpreter', 'latex', 'FontSize', 10);
1441 % xlabel('Time (s)', 'Interpreter', 'latex', 'FontSize', 12); % Added x-axis
1442 %     label
1443 % ylabel('$\\delta_r$ $(degrees)$', 'Interpreter', 'latex', 'FontSize', 12);
1444 % save_path = fullfile(output_folder,
1445 %     'Test5_delta_r_for_Lateral_Altitude_Hold_Controller.png');
1446 % exportgraphics(gcf, save_path, 'Resolution', 300);
1447 %
1448 % % Plot a (aileron control action)
1449 % figure(29)
1450 % plot(out.tout, out.aileron_controller.Data(:, 1), 'r', 'LineWidth', 2); %
1451 %     Nonlinear
1452 % grid on
1453 % grid minor
1454 % hold on
1455 % plot(out.tout, out.aileron_controller.Data(:, 2), '--b', 'LineWidth', 2); %
1456 %     Linear
1457 % title('$\\delta_a$ $for$ $Lateral$ $\\&$ $Altitude$ $Hold$ $Controller$', ...
1458 %     'Interpreter', 'latex', 'FontSize', 15);
1459 % legend('$\\delta_a$ $non$ $linear$', '$\\delta_a$ $linear$', ...
1460 %     'Interpreter', 'latex', 'FontSize', 10);
1461 % xlabel('Time (s)', 'Interpreter', 'latex', 'FontSize', 12); % Added x-axis
1462 %     label
1463 % ylabel('$\\delta_a$ $(degrees)$', 'Interpreter', 'latex', 'FontSize', 12);
1464 % save_path = fullfile(output_folder,
1465 %     'Test5_delta_a_for_Lateral_Altitude_Hold_Controller.png');
1466 % exportgraphics(gcf, save_path, 'Resolution', 300);
1467 %
1468 % % Plot e (elevator control action)
1469 % figure(30)
1470 % plot(out.tout, out.elevator_controller.Data(:, 1), 'r', 'LineWidth', 2); %
1471 %     Nonlinear
1472 % grid on
1473 % grid minor
1474 % hold on
1475 % plot(out.tout, out.elevator_controller.Data(:, 2), '--b', 'LineWidth', 2); %
1476 %     Linear
1477 % title('$\\delta_e$ $for$ $Lateral$ $\\&$ $Altitude$ $Hold$ $Controller$', ...
1478 %     'Interpreter', 'latex', 'FontSize', 15);
1479 % legend('$\\delta_e$ $non$ $linear$', '$\\delta_e$ $linear$', ...
1480 %     'Interpreter', 'latex', 'FontSize', 10);
1481 % xlabel('Time (s)', 'Interpreter', 'latex', 'FontSize', 12); % Added x-axis
1482 %     label
1483 % ylabel('$\\delta_e$ $(degrees)$', 'Interpreter', 'latex', 'FontSize', 12);
1484 % save_path = fullfile(output_folder,
1485 %     'Test5_delta_e_for_Lateral_Altitude_Hold_Controller.png');
1486 % exportgraphics(gcf, save_path, 'Resolution', 300);
1487 %

```

```

1474 % % Plot th (throttle control action)
1475 % figure(31)
1476 % plot(out.tout, out.Trust_controller.Data(:, 1), 'r', 'LineWidth', 2); %
    Nonlinear
1477 % grid on
1478 % grid minor
1479 % hold on
1480 % plot(out.tout, out.Trust_controller.Data(:, 2), '--b', 'LineWidth', 2); %
    Linear
1481 % title('$\delta_{th}$ $for$ $Lateral$ $\\&$ $Altitude$ $Hold$ $Controller$', ...
1482 % 'Interpreter', 'latex', 'FontSize', 15);
1483 % legend('$\delta_{th}$ $non$ $linear$', '$\delta_{th}$ $linear$', ...
1484 % 'Interpreter', 'latex', 'FontSize', 10);
1485 % xlabel('Time (s)', 'Interpreter', 'latex', 'FontSize', 12); % Added x-axis
    label
1486 % ylabel('$\delta_{th}$ ', 'Interpreter', 'latex', 'FontSize', 12);
1487 % save_path = fullfile(output_folder,
    'Test5_delta_th_for_Lateral_Altitude_Hold_Controller.png');
1488 % exportgraphics(gcf, save_path, 'Resolution', 300);
1489
1490 % % Test 6
1491 % %
1492 % % Plot (heading angle) for Mission
1493 % figure(32)
1494 % plot(out.tout, out.psi_states.Data(:, 1), '-.k', 'LineWidth', 2); % Command
1495 % grid on
1496 % grid minor
1497 % hold on
1498 % plot(out.tout, out.psi_states.Data(:, 2), 'r', 'LineWidth', 1); % Nonlinear
1499 % hold on
1500 % plot(out.tout, out.psi_states.Data(:, 3), '--b', 'LineWidth', 2); % Linear
1501 % title('$\psi$ $Mission$', 'Interpreter', 'latex', 'FontSize', 15);
1502 % legend('$\psi$ $command$', '$\psi$ $non$ $linear$', '$\psi$ $linear$', ...
1503 % 'Interpreter', 'latex', 'FontSize', 10);
1504 % xlabel('Time (s)', 'Interpreter', 'latex', 'FontSize', 12); % Added x-axis
    label
1505 % ylabel('$\psi$ $(degrees)$', 'Interpreter', 'latex', 'FontSize', 12);
1506 % % Save Figure
1507 % % save_path = fullfile(output_folder, 'Test6_Mission_psi.png');
1508 % % exportgraphics(gcf, save_path, 'Resolution', 300);
1509 % % Plot H (altitude) for Mission
1510 % figure(33)
1511 % plot(out.tout, out.H_states.Data(:, 1), '-.k', 'LineWidth', 2); % Command
1512 % grid on
1513 % grid minor
1514 % hold on
1515 % plot(out.tout, out.H_states.Data(:, 2), 'r', 'LineWidth', 1); % Nonlinear
1516 % hold on
1517 % plot(out.tout, out.H_states.Data(:, 3), '--b', 'LineWidth', 2); % Linear
1518 % title('$H$ $Mission$', 'Interpreter', 'latex', 'FontSize', 15);
1519 % legend('$H$ $command$', '$H$ $non$ $linear$', '$H$ $linear$', ...
1520 % 'Interpreter', 'latex', 'FontSize', 10);
1521 % xlabel('Time (s)', 'Interpreter', 'latex', 'FontSize', 12); % Added x-axis
    label
1522 % ylabel('$H$ $(ft)$', 'Interpreter', 'latex', 'FontSize', 12);
1523 % % Save Figure
1524 % % save_path = fullfile(output_folder, 'Test6_Mission_H.png');
1525 % exportgraphics(gcf, save_path, 'Resolution', 300);

```

9.2 Appendix B Simulink Models

9.2.1 6DOF Euler Angles Simulink Model

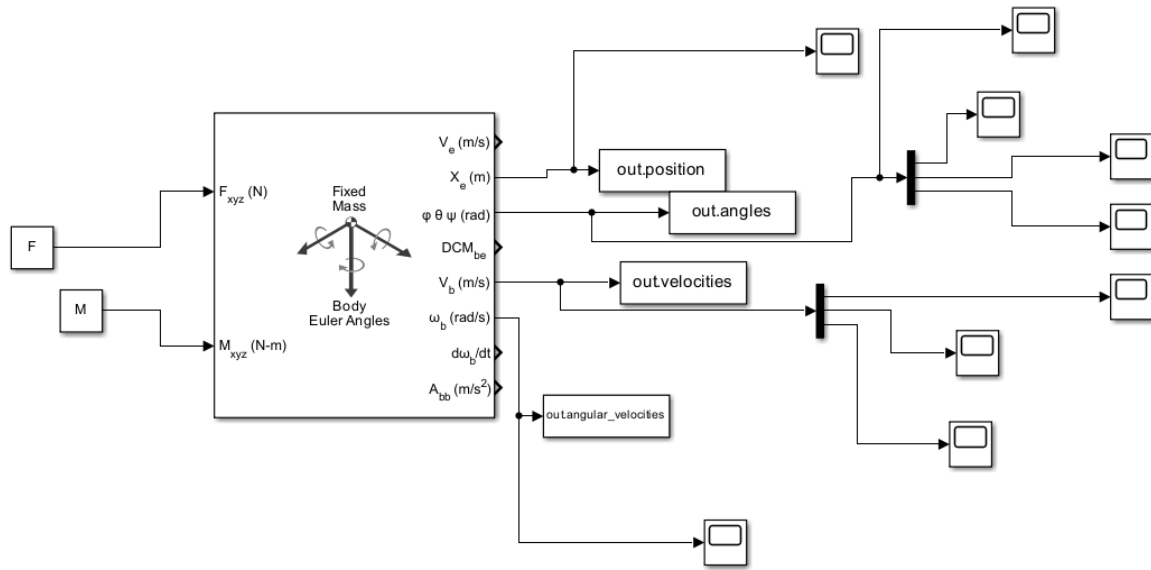


Figure 214: Simulink Model with 6DOF Euler Angles Block for Solving Airplane EOM

9.2.2 Calculation of states Simulink Model

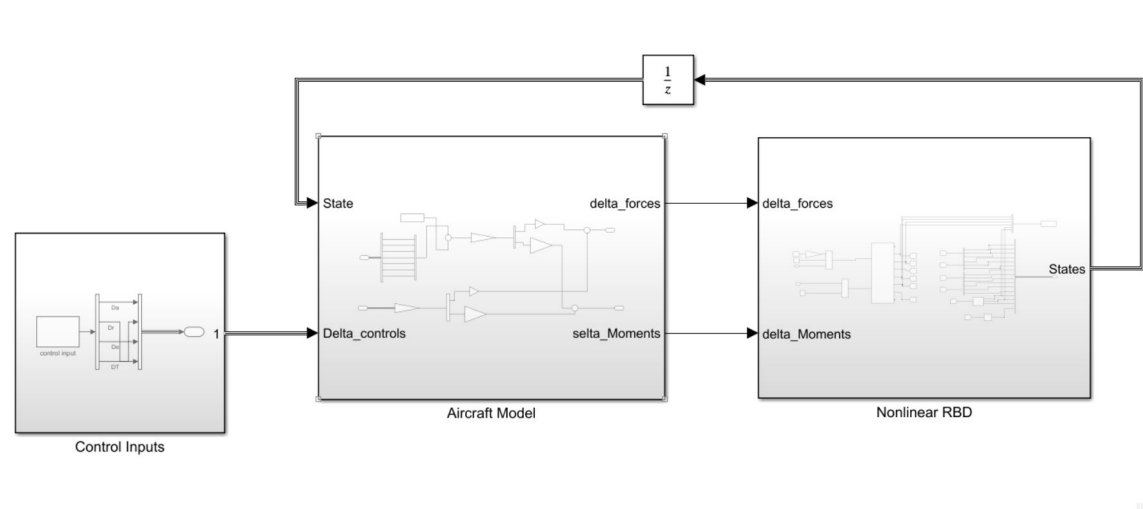
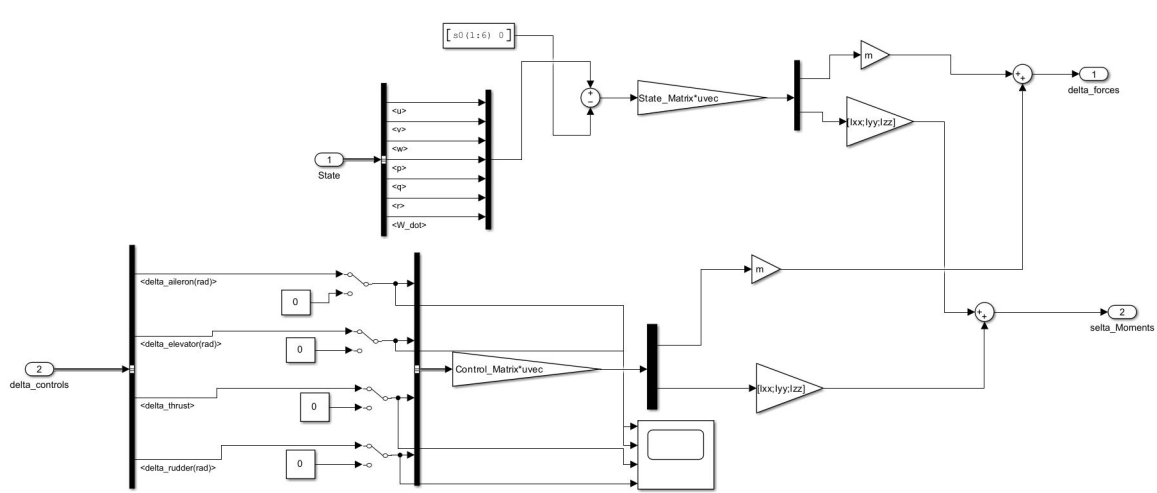
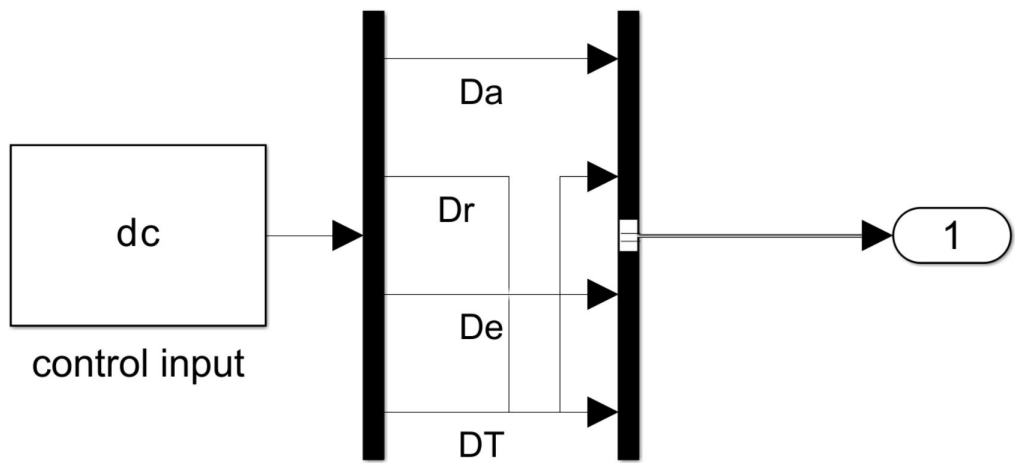


Figure 215: Main Simulink Model with for calculating the states of airplane



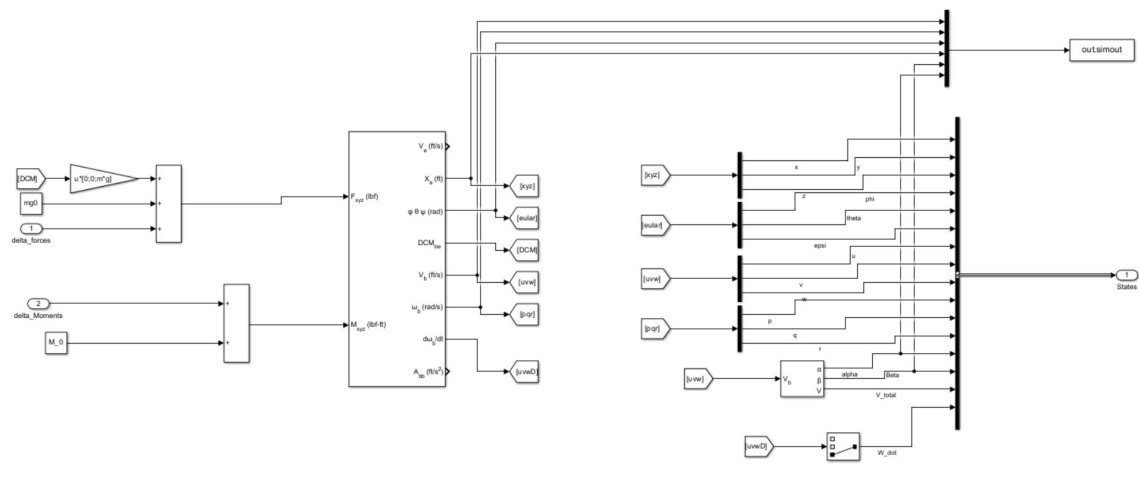


Figure 218: Rigid Body Dynamics Model sub-block

9.2.3 Autopilot Pitch and altitude control

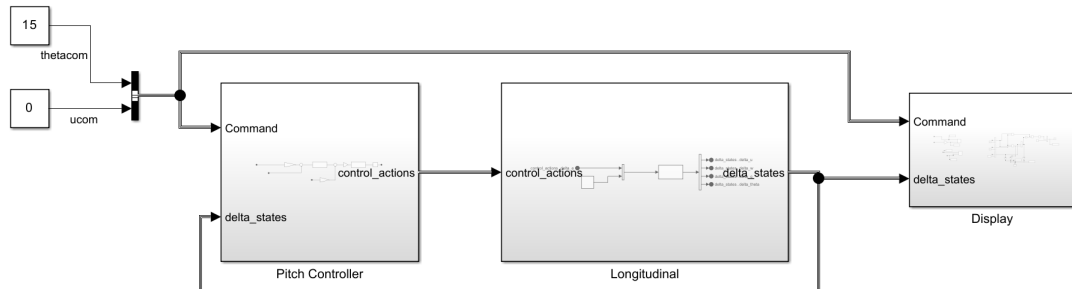


Figure 219: Autopilot pitch control loop

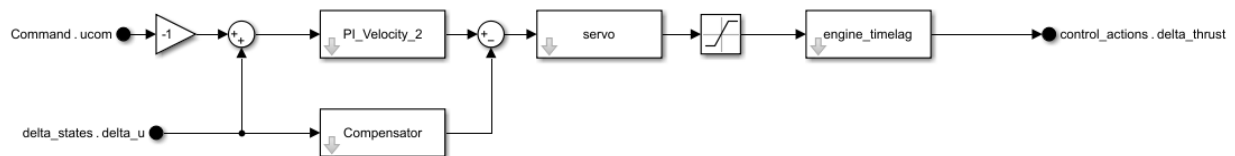


Figure 220: Velocity Controller

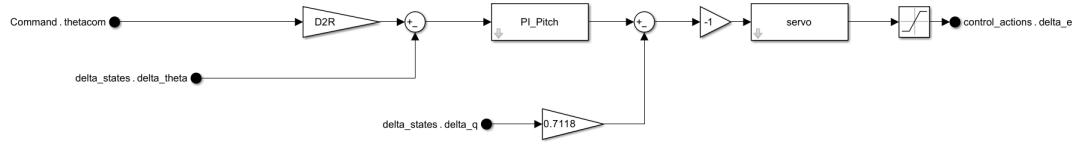


Figure 221: Pitch controller

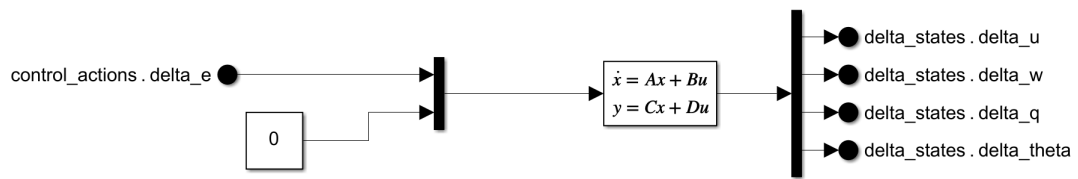


Figure 222: Longitudinal state space

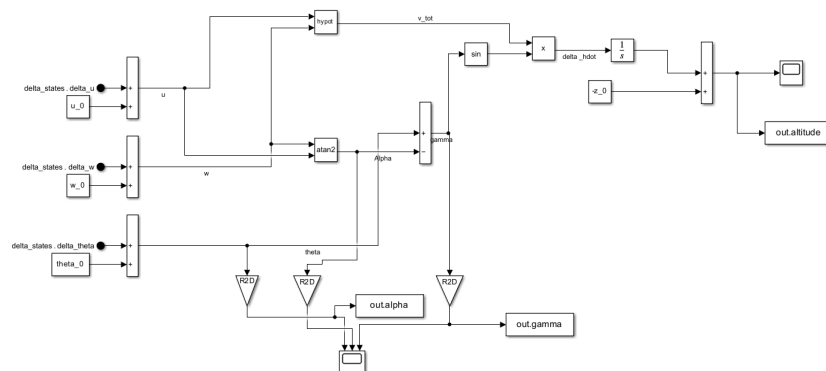


Figure 223: Altitude calculations and display

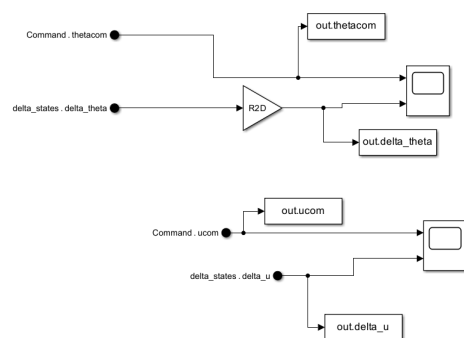


Figure 224: Theta θ and velocity (u) displays

9.2.4 Simulation Model for Linear and Non-Linear

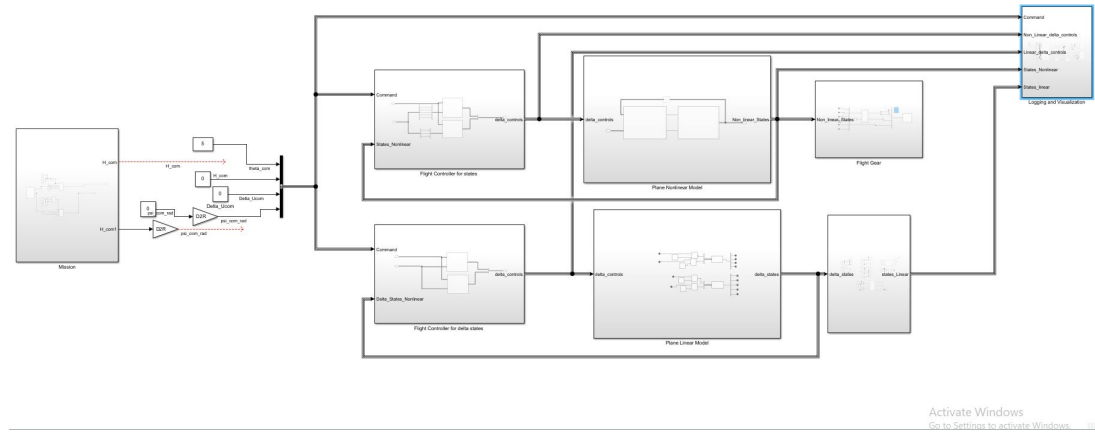


Figure 225: The complete model

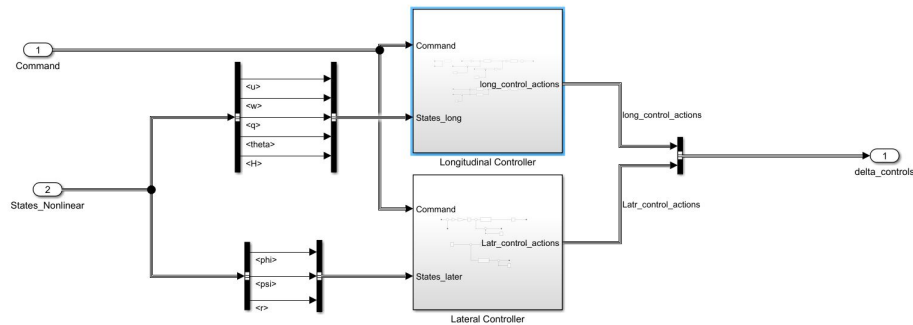


Figure 226: Flight Controller for states

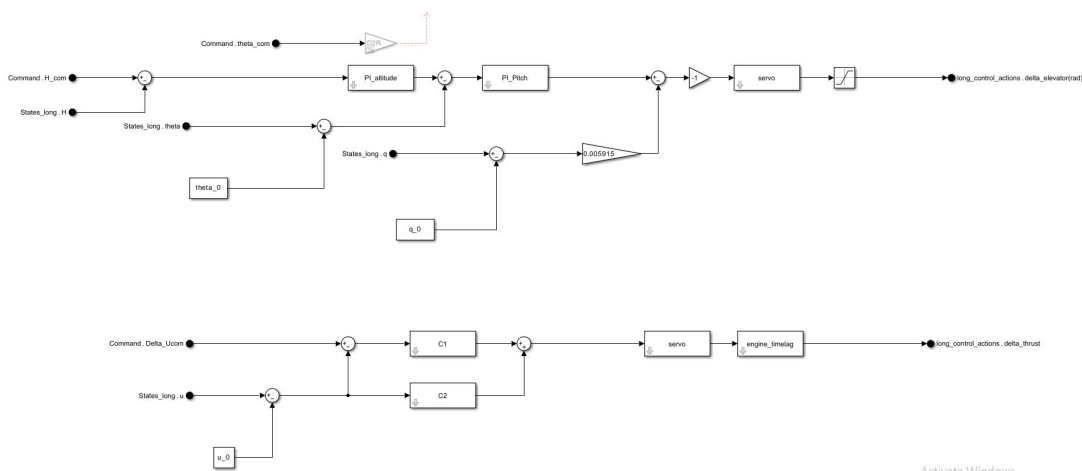


Figure 227: Longitudinal Controller for states

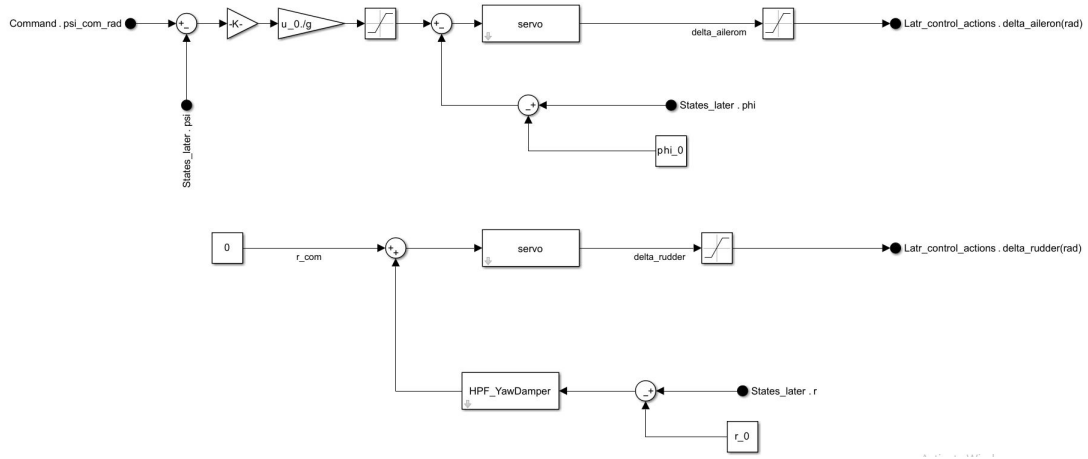


Figure 228: Lateral Controller for states

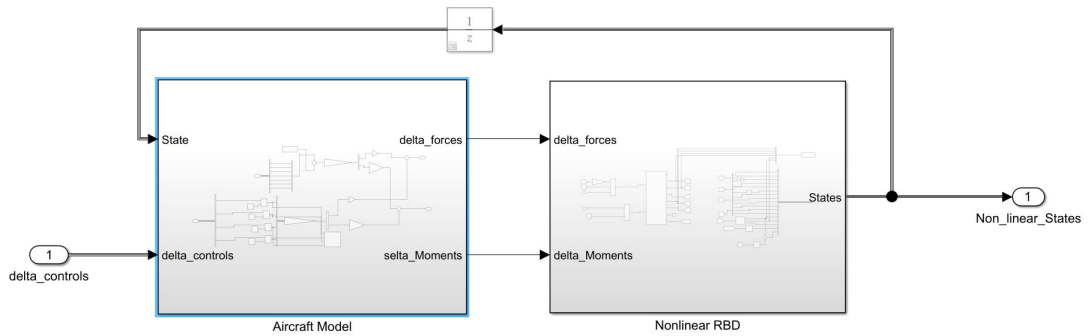


Figure 229: Plane Non-Linear Model

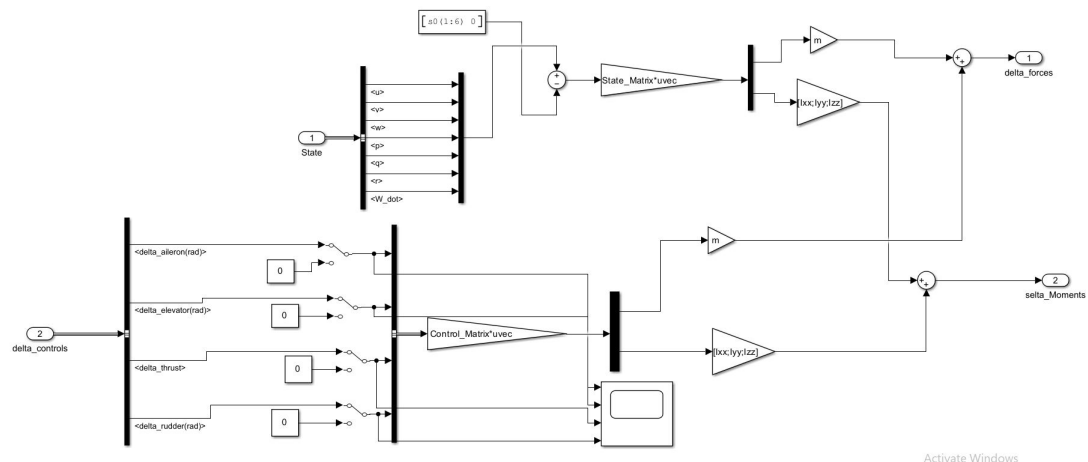


Figure 230: Aircraft Model

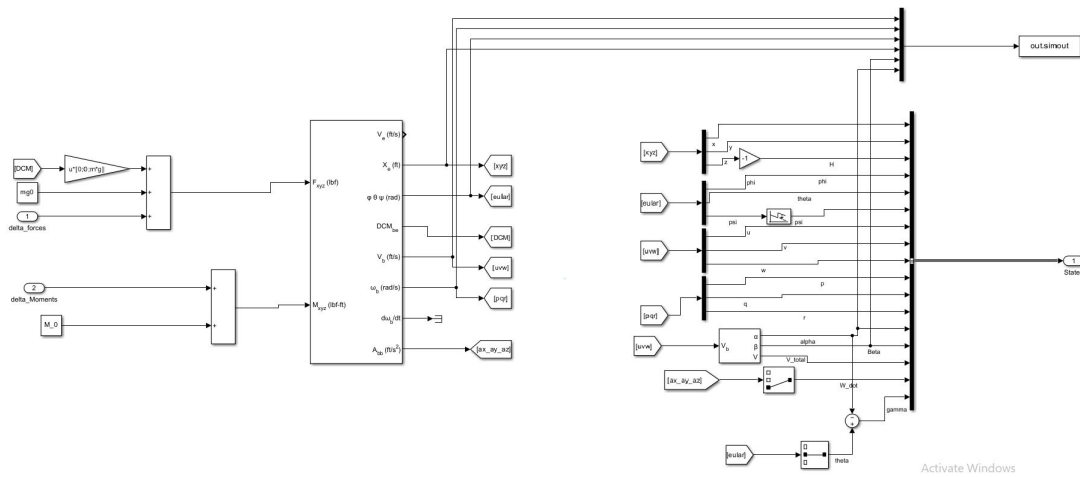


Figure 231: Non-Linear Rigid Body Dynamics

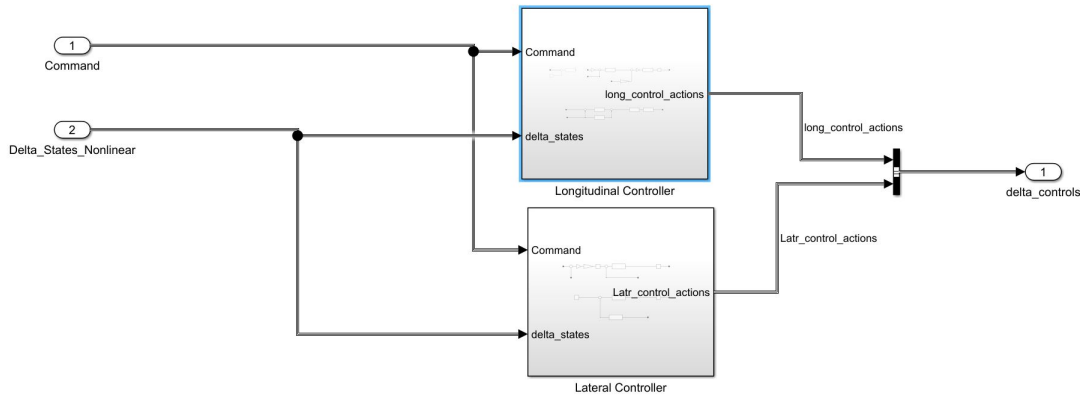


Figure 232: Flight Controller for delta states

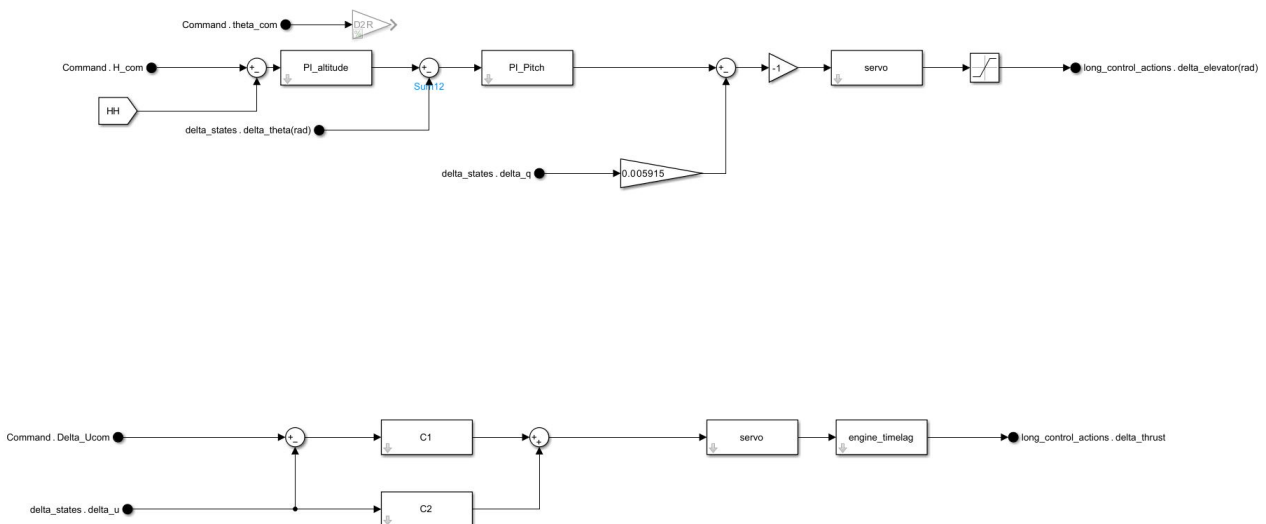


Figure 233: Longitudinal Controller for delta states

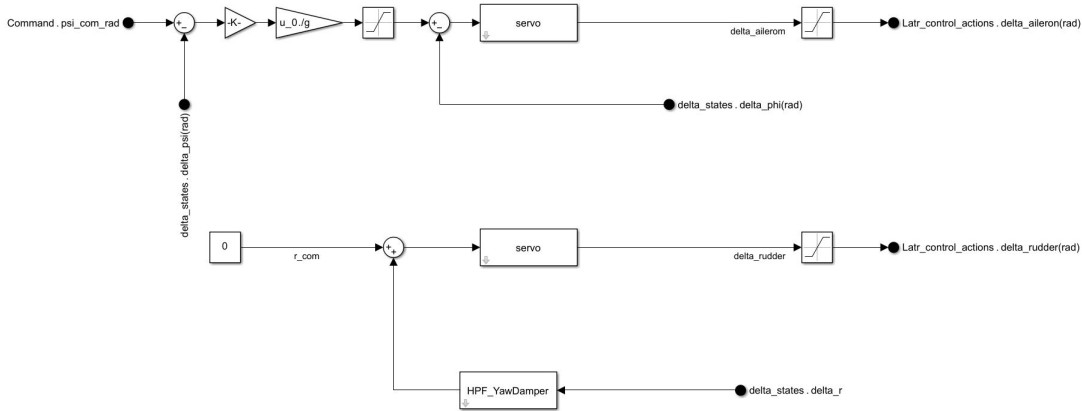


Figure 234: Lateral Controller for delta states

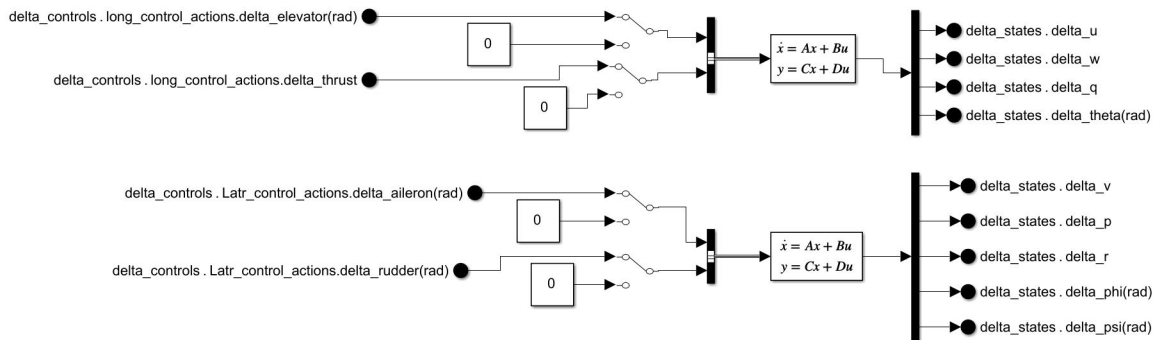


Figure 235: Airplane Linear Model

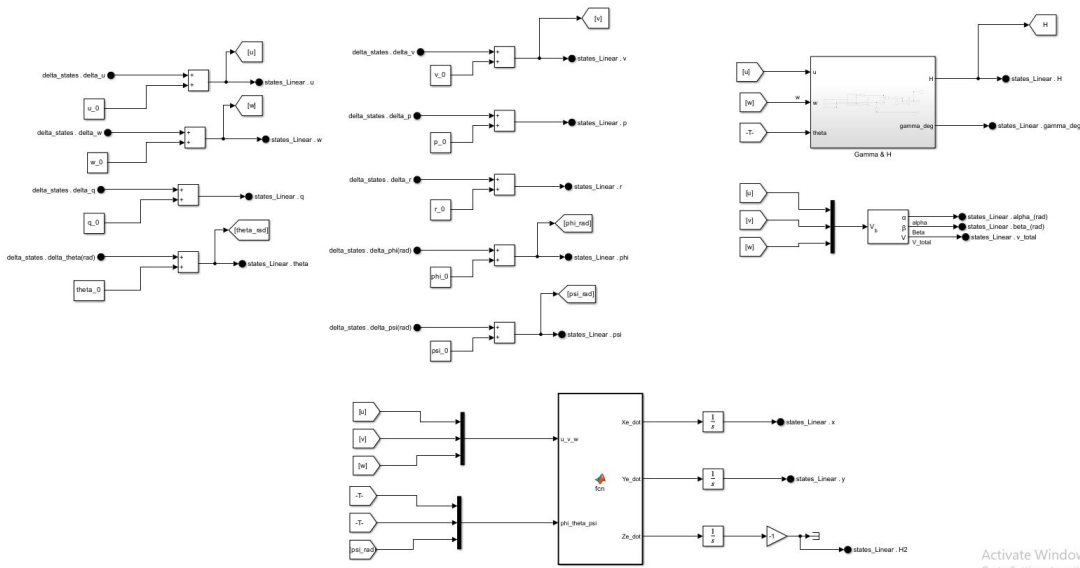


Figure 236: Delta States to States Calculations

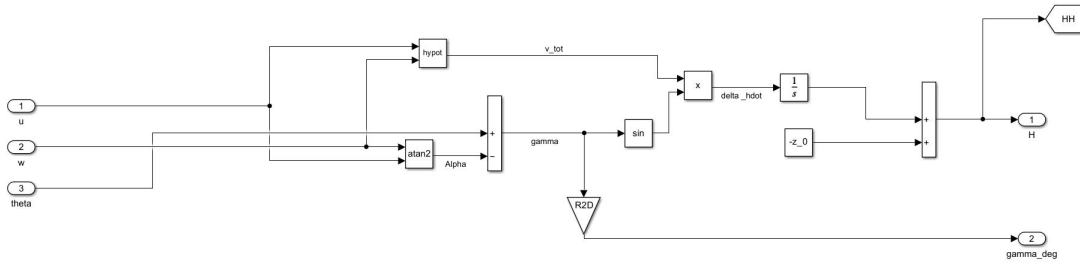


Figure 237: Gamma and H Calculations

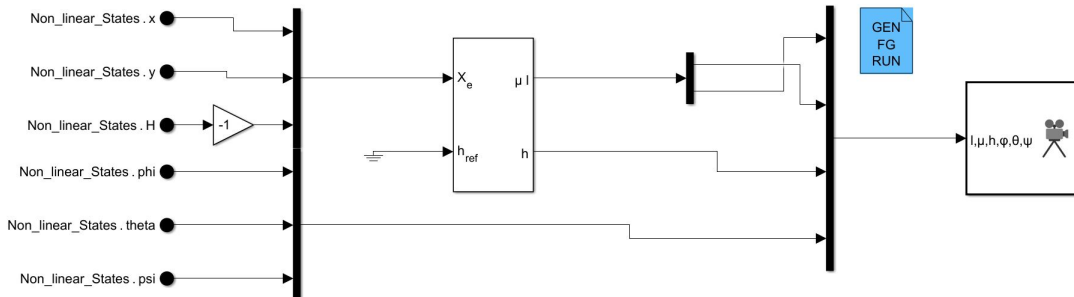


Figure 238: Send Data to Flight Gear

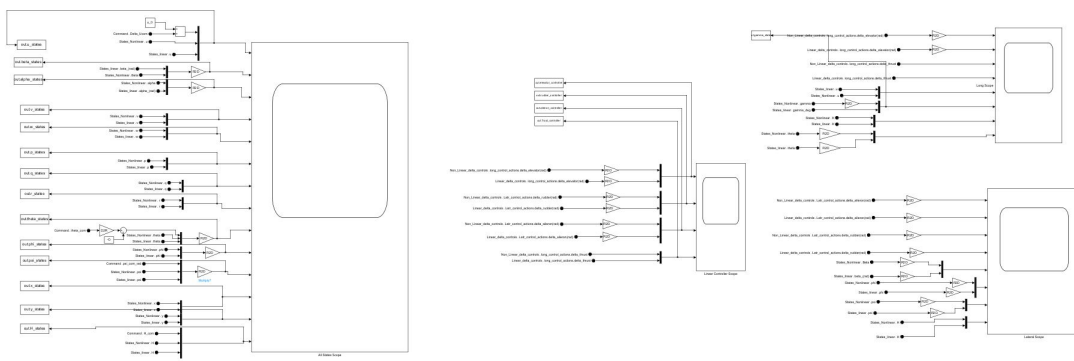


Figure 239: Logging and Visualization

10 Bonus

10.1 Task2 Bonus

Root Mean Squared Error (RMSE)

Root Mean Squared Error (RMSE) is a widely used metric for measuring the differences between values predicted by a model or an estimator and the actual observed values. It quantifies the

magnitude of error in a way that emphasizes larger discrepancies. The RMSE is particularly useful when comparing the accuracy of different models or when assessing the quality of a model's predictions.

The formula for calculating RMSE is given by:

$$\text{RMSE} = \sqrt{\frac{1}{n} \sum_{i=1}^n (x_i - y_i)^2}$$

where:

- x_i represents the predicted values,
- y_i represents the observed values,
- n is the number of data points.

The RMSE value is always non-negative, and a lower RMSE indicates a better fit between the predicted and observed values. RMSE is sensitive to outliers, as larger errors have a disproportionately high influence on the overall metric due to the squaring of the differences.

Normalized Root Mean Squared Error (NRMSE)

Normalized Root Mean Squared Error (NRMSE) extends the RMSE by normalizing the error, allowing for a comparison across different datasets or models with varying scales. Normalization provides a relative measure of error, making it easier to interpret the results in context.

The NRMSE is calculated as follows:

$$\text{NRMSE} = \frac{\text{RMSE}}{\max(y) - \min(y)}$$

In this formula:

- $\max(y)$ and $\min(y)$ represent the maximum and minimum observed values, respectively.
- By normalizing the RMSE, the NRMSE provides a percentage of the total range of the observed data. This metric is especially useful when evaluating models across different datasets, as it accounts for variations in the magnitude of the data. A lower NRMSE indicates a more accurate model, while values closer to 1 suggest a poor fit.

10.2 Task4 Bouns

10.2.1 Model Linearizer for Longitudinal Mode

This section presents the state-space and transfer function representations of the longitudinal mode using the Model Linearizer.

State-Space Representation

The state-space model for the longitudinal mode is structured as follows:

State Variables: $x_1: u - x_2: w - x_3: q - x_4: \theta$

Input Variables: $u_1: \delta_e \quad u_2: \delta_t$

Output Variables: $y_1: q - y_2: \theta - y_3: u - y_4: w$

The complete state-space model for the longitudinal mode is illustrated in Figure 240.

Linearization Result:

$A =$

$$\begin{matrix} & x_1 & x_2 & x_3 & x_4 \\ x_1 & 0 & 0 & -27.15 & -32.13 \\ x_2 & 0 & 0 & 501.3 & -1.74 \\ x_3 & 0 & 0 & 0 & 0 \\ x_4 & 0 & 0 & 1 & 0 \end{matrix}$$

$B =$

$$\begin{matrix} & u_1 & u_2 \\ x_1 & 1.18 & 5.05e-05 \\ x_2 & -21.8 & -2.2e-06 \\ x_3 & -1.4 & 3.02e-07 \\ x_4 & 0 & 0 \end{matrix}$$

$C =$

$$\begin{matrix} & x_1 & x_2 & x_3 & x_4 \\ y_1 & 0 & 0 & 1 & 0 \\ y_2 & 0 & 0 & 0 & 1 \\ y_3 & 1 & 0 & 0 & 0 \\ y_4 & 0 & 1 & 0 & 0 \end{matrix}$$

$D =$

$$\begin{matrix} & u_1 & u_2 \\ y_1 & 0 & 0 \\ y_2 & 0 & 0 \\ y_3 & 0 & 0 \\ y_4 & 0 & 0 \end{matrix}$$

Figure 240: State-space representation of the longitudinal mode using the Model Linearizer

Transfer Function Representation The transfer function of the longitudinal mode, derived from the state-space model, is shown in Figure 241. This representation provides an alternative view of the system dynamics in the frequency domain.

Linearization Result:

From input "u1" to output...

-1.4

y1: ----

s

-1.4

y2: ----

s^2

1.18 s^2 + 38.01 s + 44.98

y3: -----

s^3

-21.8 s^2 - 701.8 s + 2.436

y4: -----

s^3

From input "u2" to output...

3.02e-07

y1: -----

s

3.02e-07

y2: -----

s^2

5.05e-05 s^2 - 8.199e-06 s - 9.702e-06

y3: -----

s^3

-2.2e-06 s^2 + 0.0001514 s - 5.255e-07

y4: -----

s^3

Figure 241: Transfer function of the longitudinal mode using the Model Linearizer

10.2.2 Model Linearizer for Lateral Mode

This section presents the state-space and transfer function representations of the lateral mode using the Model Linearizer.

State-Space Representation

The state-space model for the lateral mode is structured as follows:

State Variables: $x_1: V$ - $x_2: p$ - $x_3: r$ - $x_4: \phi$ - $x_5: \psi$

Input Variables: $u_1: \delta_a$ - $u_2: \delta_r$

Output Variables: $y_1: \psi$ - $y_2: p$ - $y_3: \phi$ - $y_4: r$ - $y_5: V$

The complete state-space model for the lateral mode is illustrated in Figure 242.

Linearization Result:

A =

| | | | | | |
|----|----|-------|---------|-------|---|
| x1 | x2 | x3 | x4 | x5 | |
| x1 | 0 | 27.15 | -501.3 | 32.13 | 0 |
| x2 | 0 | 0 | 0 | 0 | 0 |
| x3 | 0 | 0 | 0 | 0 | 0 |
| x4 | 0 | 1 | 0.05416 | 0 | 0 |
| x5 | 0 | 0 | 1.001 | 0 | 0 |

B =

| | | | |
|----|--------|--------|--|
| | u1 | u2 | |
| x1 | 0 | 11.35 | |
| x2 | 0.229 | 0.254 | |
| x3 | 0.0285 | -0.614 | |
| x4 | 0 | 0 | |
| x5 | 0 | 0 | |

C =

| | | | | | |
|----|----|----|----|----|----|
| | x1 | x2 | x3 | x4 | x5 |
| y1 | 0 | 0 | 0 | 0 | 1 |
| y2 | 0 | 1 | 0 | 0 | 0 |
| y3 | 0 | 0 | 0 | 1 | 0 |
| y4 | 0 | 0 | 1 | 0 | 0 |
| y5 | 1 | 0 | 0 | 0 | 0 |

D =

| | | | |
|----|----|----|--|
| | u1 | u2 | |
| y1 | 0 | 0 | |
| y2 | 0 | 0 | |
| y3 | 0 | 0 | |
| y4 | 0 | 0 | |
| y5 | 0 | 0 | |

Figure 242: State-space representation of the lateral mode using the Model Linearizer

Transfer Function Representation

The transfer function of the lateral mode, derived from the state-space model, is shown in Figure 243. This representation provides an alternative view of the system dynamics in the frequency domain.

Linearization Result:

```
From input "u1" to output...
 0.02854
y1: -----
      s^2

 0.229
y2: -----
      s

 0.2305 s
y3: -----
      s^3

 0.0285
y4: -----
      s

 -8.069 s^2 + 7.407 s
y5: -----
      s^4

From input "u2" to output...
 -0.6149
y1: -----
      s^2

 0.254
y2: -----
      s

 0.2207 s
y3: -----
      s^3

 -0.614
y4: -----
      s

 11.35 s^3 + 314.7 s^2 + 7.092 s + 1.331e-14
y5: -----
      s^4
```

Figure 243: Transfer function of the lateral mode using the Model Linearizer

10.2.3 Comparisons with Manual Linearization

In this section we comparison between the Model Linearizer and manual linearization approaches for both the state-space model and transfer function of the longitudinal and lateral modes. The manual linearization process, detailed in Section 6.

State-Space Model:

In general, the state-space models for both the longitudinal and lateral modes are similar between the Model Linearizer and manual linearization. However, some variations are observed, particularly in the values of the state variables p , q , and r . Notably, the Model Linearizer approximates very small values (e.g., 0.001) as zero, which introduces slight differences in the state variables. These approximations can affect the accuracy of the model, especially in cases where small values are significant.

Transfer Function:

For the transfer functions, both methods yield mostly similar results. However, some differences arise due to the approximations in Simulink, particularly with the values of p , q , and r . The Model Linearizer's tendency to approximate small numbers to zero introduces discrepancies in certain transfer function coefficients, which may impact specific transfer function outputs.

Despite these minor differences, the overall behavior of the system remains consistent across both approaches.